The Application of Radiotracers for Theranostic Use in Breast Cancer

Simone U. Dalm

The Application of Radiotracers for Theranostic Use in Breast Cancer

Simone U. Dalm

The Application of Radiotracers for Theranostic Use in Breast Cancer

De toepassing van radiofarmaca voor
theranostische doeleinden in borstkanker

Proefschrift

ter verkrijging van de graad van doctor aan de
Erasmus Universiteit Rotterdam
op gezag van de rector magnificus

Prof.dr. H.A.P. Pols

en volgens besluit van het College voor Promoties.

De openbare verdediging zal plaatsvinden op
dinsdag 21 februari 2017 om 15:30

door

Simone Ursula Dalm
geboren te Paramaribo, Suriname

Cover design: Ingrid Bakker
Thesis layout: Ingrid Bakker en Ton Everaers
Printing: Ipskamp Printing
ISBN: 978-94-028-0514-7

Erasmus University Rotterdam

PROMOTIECOMMISSIE

Promotoren:	Prof.dr. ing. M. de Jong
Overige leden:	Prof.dr. S. Sleijfer Prof.dr. G.P. Krestin Prof.dr. P.H. Elsinga
Copromotoren:	Dr. C.H.M. van Deurzen Dr. J.W.M. Martens

voor mijn oma

CONTENT

Part 1

Breast Cancer & Nuclear Medicine-based Imaging and Therapy

Chapter 1

General Introduction and Thesis Outline

BREAST CANCER

Breast Cancer Epidemiology

Globally, cancer is a major health problem amongst men and women with incidence rates of 205 and 165 per 100,000 individuals, respectively. In women, breast cancer (BC) is the most common cancer type and is responsible for 25% of the cancer incidence rate with an estimated 1.67 million new cases diagnosed in 2012 worldwide. Concerning mortality, BC is the 5th cause of cancer related death worldwide (1). In 2012, BC incidence and mortality were 13,895 and 3,163, respectively, in the Netherlands (2).

BC Screening and Diagnosis

In view of the high incidence rate of BC and in attempt to decrease mortality rate, mammography was introduced as a screening method for early detection. Mammography applies low energy x-rays to detect abnormal breast lesions. In the Netherlands, women between the age of 50-75 years are invited for screening by mammography biennially since 1988. Multiple studies reported a decrease in BC mortality due to screening mammography programs (3,4). However, mammography has several limitations leading to a significant amount of false positive and false negative findings. False positive and false negative rates ranging from 65.2-121.2 and 1.0-1.5 per 1,000 women depending on age, respectively, were reported (5). Major limiting factors include higher breast density, younger age and pre-menopausal status, which all lead to an increased risk of false positive and particularly false negative findings. Especially high breast density is associated with increased risk of false negative diagnoses. False positive results lead to unnecessary additional tests, which apart from costs may cause psychological harm (6,7). False negative results on the other hand can cause delay in diagnosis and treatment, negatively impacting the course of the disease (6). When a suspicious lesion is detected by mammography, additional imaging is required such as ultrasound (US) and/or magnetic resonance imaging (MRI).

US uses high frequency sound waves to acquire an image of the breast. Previous studies have shown that supplemental US is more sensitive for lesion detection in women with dense breast tissue compared to mammography alone (3-4.6 more lesions are detected per 1000 supplemental US examinations) (8). Furthermore, US is often used to distinguish fluid filled (e.g. cysts) from solid lesions.

MRI uses radiofrequency waves in a strong magnetic field to create a detailed image of tissue structures inside the body, including the breasts. Breast MRI is nowadays incorporated in daily breast radiology. One indication for breast MRI is screening of women with high risk of developing BC, due to a genetic predisposition or due to chest radiation received at young age (9). The sensitivity of MRI is independent of the breast density and about twice as high as the sensitivity of mammography (10).

Although the above imaging methods are used for early detection of BC, diagnosis is based on histopathologic examination. Detected breast lesions are biopsied and the retrieved tissue is examined for the presence of malignancy.

BC Subtypes

BC is a very heterogeneous disease and consists of multiple biological subtypes. Four major BC subtypes are identified based on gene expression patterns: luminal A, luminal B, human epidermal growth factor receptor 2 (HER2)-driven and basal like tumors (11-14). Amongst other molecular factors, these subtypes can to some extent be identified by estrogen receptor (ER), progesterone receptor (PR) and HER2 expression, markers that majorly impact the treatment and prognosis of the disease.

Next to the subtype specific treatments for BC that will be discussed below, local therapies in the form of surgery and radiation therapy are therapeutic methods applied independent of the BC subtypes. Clinically the presence or absence of subtype specific markers, determined by immunostaining and/or in situ hybridization, is used as a surrogate in order to identify BC subtypes after diagnosis.

Luminal BCs account for ±70% of all BCs and are ER- and/or PR-positive, with luminal A tumors having higher ER/PR expression than luminal B tumors. Furthermore, luminal A tumors are HER2-negative, while luminal B tumors have variable HER2 expression. In addition, luminal B tumors have a higher proliferation index rate, assessed by Ki-67, and often have a higher histological grade. In comparison to the other subtypes, this BC subtype has the best prognosis. Luminal A tumors are treated with endocrine treatment, while luminal B tumors may benefit more from a combination of endocrine treatment and chemotherapy (anti-HER2 antibodies such as Trastuzumab in case of HER2-positivity). HER2-driven BCs are usually ER- and/or PR-negative and always HER2-positive. Before the availability of HER2 blocking therapies, this BC subtype had a worse prognosis than that of luminal BCs. However, the prognosis of HER2-driven BCs has improved since the incorporation of anti-HER2 antibodies, resulting in a prognosis similar to that of luminal BCs. Basal-like tumors, accounting for 15% of the BCs, are the most aggressive subtype. These tumors are ER-, PR- and HER2-negative and generally have a high proliferation rate and differentiation grade. Treatment usually consists of chemotherapy, as there are no other (targeted) therapy options. An overview of the BC subtypes is displayed in *Figure 1*.

Despite all available therapy modalities, 20-30% of the patients overall experience relapse which can consist of locoregional recurrence or metastatic disease (15). Unfortunately, metastatic disease is still incurable and an estimated 5-year survival rate of only 25% was reported for advanced disease (16). Approximately 20% of ER-positive BC patients with metastatic disease show intrinsic resistance against first line anti-estrogen treatment and only 30-40% of patients respond to second and third line antihormonal therapy (17). Concerning Trastuzumab treatment, response rates of 11-26% have been reported for trastuzumab monotherapy in metastatic disease (18). Basal-like (or triple negative) BCs are more aggressive than other BCs and have an increased risk of distant recurrence and disease-associated mortality (19). Molecular targets for the latter-mentioned BC subtype are largely lacking and more research is needed to identify potential targets in order to develop more precise treatment strategies (20).

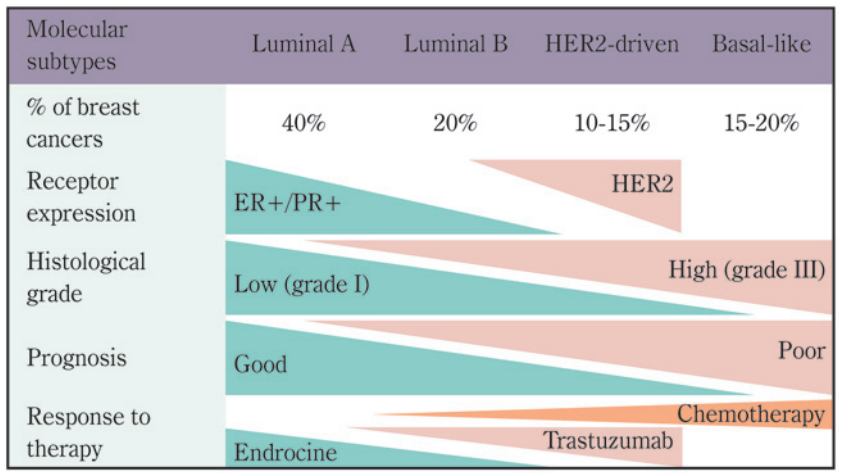

Figure 1. Breast cancer subtypes and associated characteristics. Figure is adapted from (21).

NUCLEAR MEDICINE-BASED IMAGING AND TREATMENT

Concepts Behind Nuclear Imaging and Treatment of Cancer

Since current imaging and therapy options for BC still have limitations, novel options are needed. One of the aims is to improve the survival rate by enhancing BC detection. Within nuclear medicine, systemically administered radiopharmaceuticals are used for imaging and treatment of various cancer types. These radiopharmaceuticals are either radionuclides alone or radionuclides coupled to a targeting molecule. Photons emitted during radioactive decay of radionuclides within in the body can be detected for imaging purposes. For single-photon emission computer tomography (SPECT), single photons from γ-emitting radionuclides are detected at multiple positions around the longitudinal axis of the patients by rotating scintillation cameras, equipped with parallel-hole or pin-hole collimators (22). The acquired data are reconstructed using an appropriate reconstruction algorithm of which several are available (23). Other than SPECT imaging, positron emission tomography (PET) applies positron-emitters. Pairs of photons (with an energy of 511 keV each) generated after annihilation of a positron and an electron are detected and used for image acquisition. These photons travel in opposite direction and are detected by a series of opposing detectors installed in a ring-like pattern (24). This mechanism of PET imaging allows the detection of a higher number of events, resulting in a higher sensitivity and spatial resolution than those retrieved by SPECT imaging (25). The events measured by the detectors during PET imaging are combined and used to reconstruct a 3D image. Both SPECT and PET imaging on their own provide very little information on

anatomical reference and these methods are preferably and widely combined with computed tomography or MRI (26).
For nuclear imaging of BC, dedicated cameras have recently been developed which are currently under investigation (27). These dedicated cameras have a restricted field of view which results in a higher sensitivity, especially for small tumors, compared to whole body scanners (28). Dedicated cameras can however only visualize primary lesions (and in some cases regional lymph node metastases), hence these cameras are not suitable for imaging of distant metastatic disease.
Concerning therapy, in nuclear medicine therapeutic radionuclides can be used to eradicate cancer cells. *Table 1* shows an overview of several radionuclides for SPECT and PET imaging and for radionuclide therapy.

Nuclear Medicine in BC

Concerning nuclear imaging of BC, multiple approaches are being applied. A few of these approaches are based on accumulation of radioactivity in cancer cells because of their high proliferation rate. ^{99m}Tc-Sestamibi, ^{201}Tl and ^{99m}Tc-Tetrofosmin (of which ^{99m}Tc-Sestamibi is studied the most) accumulate in mitochondria, which are abundantly present in BC cells, and ^{18}F-fludeoxyglucose (FDG) is taken up by cancer cells because of their high metabolic rates. These methods lack specificity however, which might lead to false positive scans. In the case of ^{99m}Tc-Sestamibi, false positive scans have e.g. been reported for sites of prior surgical intervention, inflammation and some benign breast diseases (31). ^{18}F-FDG PET scans may show increased uptake in non-cancerous lesions such as inflammatory and infectious lesions, brain, muscle and brown adipose tissue (32). In line with this, clinical studies evaluating the role of ^{99m}Tc-Sestamibi for BC imaging resulted in high sensitivity, but low specificity (33). Concerning ^{18}F-FDG breast scans, studies demonstrated high sensitivity and specificity for pT2 tumors, while a high rate of false negatives was reported for pT1 tumors (34). In agreement with this, sensitivity was low for small, non-invasive, low grade and non-palpable tumors (31,32,35).
A more specific method for cancer imaging is the use of molecular expression patterns for targeting of cancer cells. These targeted imaging methods are already successfully used for other cancer types and may be beneficial for BC as well.

Table 1. Overview of some clinically relevant radionuclides for SPECT, PET and radionuclide therapy

SPECT radionuclides

Radionuclide	$T_{1/2}$ (h)	Decay mode (%)	End-pointis E_γ (keV) (%)	Production Mode
^{99m}Tc	6.02	IT (100), γ	141 (91)	^{99}Mo/^{99m}Tc generator
^{111}In	67.9	EC (100) Auger, γ	171 (90) 245 (94)	Cyclotron
^{67}Ga	78.26	EC (100) Auger, γ	93 (39) 185 (21) 300 (17)	Cyclotron
^{123}I	13.2	EC (100), γ	159 (84) 27 (71) 31 (16)	Cyclotron

PET radionuclides

Radionuclide	$T_{1/2}$ (h)	Decay mode (%)	End-point $E_{\beta+}$ (keV) (%)	Production Mode
^{18}F	1.83	β^+ (97) EC (3)	634 (97)	Cyclotron
^{68}Ga	1.13	β^+ (89) EC (11)	1.899 (88)	^{68}Ge/^{68}Ga generator
^{64}Cu	12.7	β^+ (19) β^- (40) EC (41)	656 (18)	Cyclotron
^{86}Y	14.7	β^+ (33) EC (66)	1.221 (12) 1.314 (17) 1.409 (14) 1.474 (9) 1.545 (6) 1.988 (4) 2.242 (13)	Cyclotron
^{124}I	99.6	EC (77) β^+ (23)	3.160 (24) 2.556 (25) 2.137 (11) 1.535 (12) 866 (11)	Cyclotron

Therapeutic radionuclides
β-emitting radionuclides

Radionuclide	$T_{1/2}$ (h)	Decay mode (%)	End-point $E_{\beta-}$ (keV) (%)	Production Mode
^{90}Y	64.1	β^- (100)	2.280 (99.99)	^{90}Sr/^{90}Y generator
^{177}Lu	161	β^-, γ	498 (79) 385 (9) 177 (12)	Reactor
^{67}Cu	61.9	β^- (100), γ	392 (57) 484 (22) 577 (20)	Accelerator

Table 1. Continued.

Therapeutic radionuclides
α-emitting radionuclides

Radionuclide	$T_{1/2}$ (h)	Decay mode (%)	E_α (keV) (%)	Production Mode
^{213}Bi	0.76	α (2) β^- (98)	5558 (0.18) 5875 (1.96)	^{225}Ac/^{213}Bi Generator
^{225}Ac	240	α (100)	5637 (4.4) 5724 (3.1) 5732 (8.0) 5790.6 (8.6) 5792.5 (18.1) 5830 (50.7)	^{229}Th/^{225}Ac Generator Cyclotron

$T_{1/2}$=half-life, E=energy, IT=isomeric transition, EC=electron capture.
Table is adapted from (29). Information on α radiation is based on (30).

Targeted Nuclear Imaging and Therapy/Theranostics in Oncology

Targeted nuclear imaging and treatment of cancer is based on targeting of biomarkers overexpressed on cancer cells using radioligands. These radioligands consist of a targeting agent (e.g. chemically synthesized peptide analog of a natural ligand, antibodies, nanobodies etc., with high affinity for the biomarker), which can be coupled to a chelator (directly or via a linker) that can stably complex a radionuclide (*Figure 2A*). Depending on the radionuclide that is incorporated in or coupled to the radioligand, targeted imaging and/or therapy can be performed using the same ligand, the so-called theranostic approach. With regard to radionuclides used for theranostic agents, 3 different classes can be used: radionuclides that emit both imaging photons and therapeutic particles, radionuclide pairs consisting of the same element or radionuclide pairs derived from different elements (*Table 2*). The use of theranostic agents offers a personalized approach for disease management by enabling diagnosis/staging, therapy, and monitoring of treatment response (*Figure 2B*). Hereby, only patients that show sufficient accumulation of radioligands in cancer lesions on scans are selected for therapy using the same ligand labeled with a therapeutic radionuclide. Besides, this enables treatment adjustment according to results of interim monitoring. Currently, targeted nuclear imaging and therapy is successfully used in the clinic for imaging and treatment of e.g. neuroendocrine tumors by targeting somatostatin receptors (SSTR) overexpressed on neuroendocrine tumor cells using SSTR-targeting radioligands, which are successfully used for imaging, therapy and response evaluation (36). Since biomarkers for nuclear targeting of BC have been identified, the application of radioligands for theranostic purposes may have the potential to also improve BC patient care.

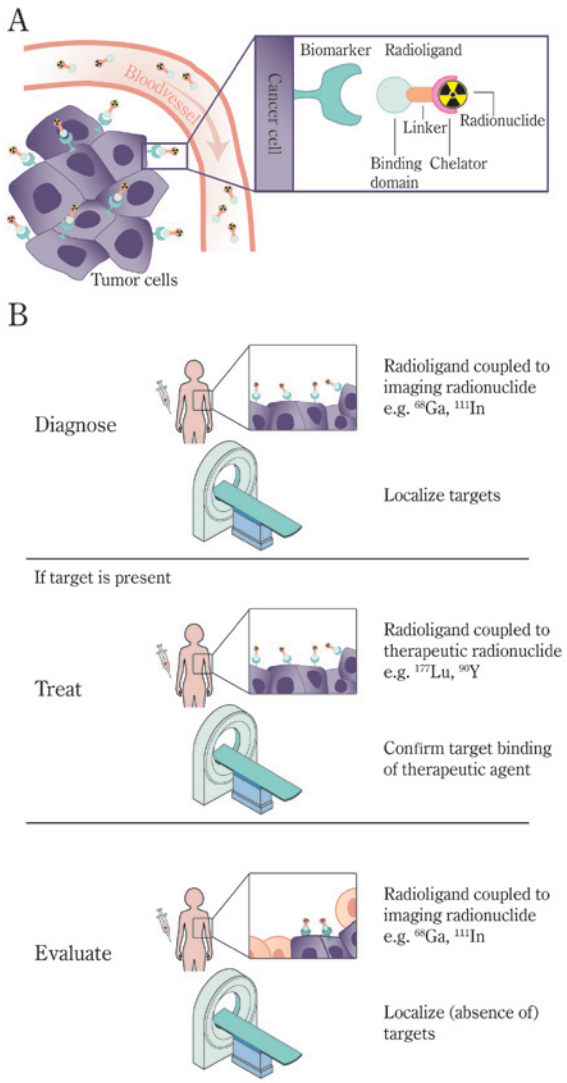

Figure 2. A) Representation of radioligands for targeted nuclear imaging and therapy. Biomarkers overexpressed on tumor cells are targeted using radioligands that contain a binding domain. This binding domain is in some cases coupled to a chelator, often via a linker. The chelator enables stable binding of a radionuclide. Depending on the radionuclide of choice, radioligands can be used for either imaging or treatment. B) The use of radioligands for theranostic purposes. Radiotracers coupled to imaging radionuclides are used to determine target expression and for diagnosis/disease staging. If tumor lesions are visualized, which demonstrates target expression, the same radiotracer coupled to therapeutic radionuclides can be used for therapy. Subsequently, treatment can be adjusted after interim monitoring which can be done by SPECT/PET scanning using the same radioligand coupled to imaging radionuclides.

Table 2. Examples of radionuclide (pairs) used for theranostic purposes

Radionuclides that can be used for both imaging and therapy			
Radionuclide	**$T_{1/2}$ (d)**	**Imaging γ Energy keV (%)**	**Therapy Therapeutic particle(s) (Average keV)**
^{47}Sc	3.35	159 (88)	β⁻ (162)
^{67}Cu	2.58	186 (40)	β⁻ (141)
^{67}Ga	3.26	93 (40) 184 (24) 296 (22)	15 Auger (0.04-9.5 ((572%)) 10 CE (82-291 (30%)
^{111}In	2.80	171 (91) 245 (94)	6 Auger (0.13-25.6 ((407%)) 12 CE (144-245 (21%))
^{131}I	8.0	365 (82)	β⁻ (182)
^{177}Lu	6.71	208 (11) 113 (6.4)	β⁻ (134)
Theranostic pairs consisting of different isotopes of the same element for imaging and therapy			
Radionuclide Pair	**$T_{1/2}$ (d)**	**Imaging β⁺ Energy keV (%)**	**Therapy Therapeutic particle(s) (Average keV)**
^{44}Sc/^{47}Sc	2.4/3.35	511 (94)	β⁻ (162)
^{64}Cu/^{67}Cu	0.53/2.6	511 (35)	β⁻ (141)
^{68}Ga/^{67}Ga	0.05/3.26	511 (176)	15 Auger (0.04-9.5 ((572%)) 10 CE (82-291 (30%)
^{86}Y/^{90}Y	0.61/2.7	511 (66)	β⁻ (935)
^{124}I/^{131}I	4.2/8.0	511 (44)	β⁻ (182)
Theranostic pairs consisting of radionuclides from different elements for imaging and therapy			
Imaging radionuclide		**Therapeutic radionuclide**	
^{68}Ga/^{111}In		^{177}Lu/^{90}Y/^{213}Bi	
^{99m}Tc		$^{186/188}$Re	

$T_{1/2}$=half-life, CE= conversion electrons.
Part of the table is adapted from (37). Data on ^{177}Lu is adapted from (30).

TARGETED NUCLEAR IMAGING OF BC

Molecular Targets

Multiple targets have been identified for nuclear imaging of BC, including the SSTR subtype 2 (SSTR2), the gastrin releasing peptide receptor (GRPR), hormone receptors and HER2. In our review (Chapter 3) we discuss targets currently under investigation for nuclear imaging of BC as well as their potential.

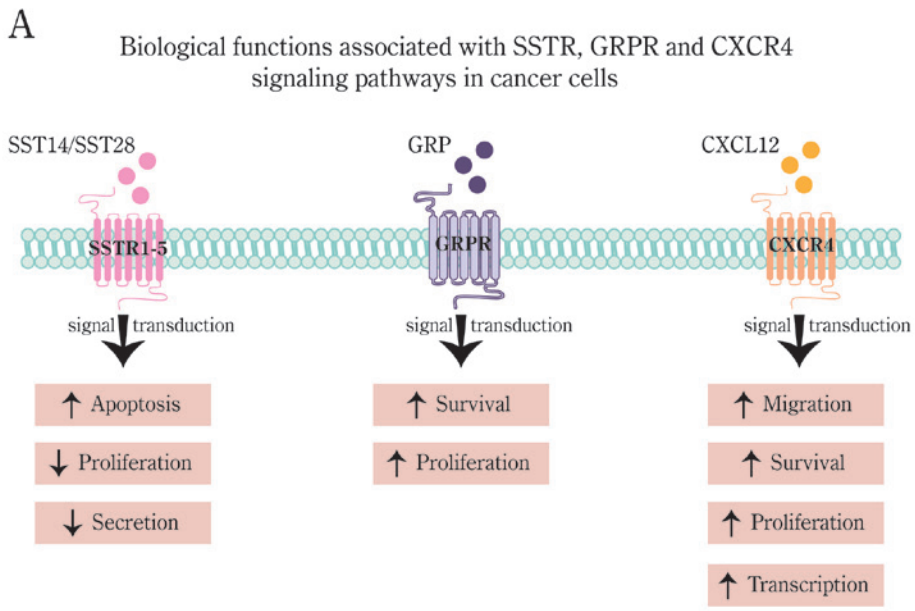

Figure 3. A) Key functions of SSTRs, GRPR and CXCR4 in cancer cells. In contrast to GRPR and CXCR4 that elicit a pro-tumoral response (amongst other factors stimulating proliferation and survival) upon binding of their ligands, activation of SSTRs results in anti-tumoral response by inducing apoptosis and inhibiting proliferation and secretion of hormone such as growth factors. B) Organs in which SSTR, GRPR and CXCR4 malignancies commonly occur.

In this thesis the main focus will be on application of radioligands targeting SSTR2 and GRPR for imaging and treatment of BC. In Chapters 2 and 3 the relevance of a third target, C-X-C chemokine receptor 4 (CXCR4), will be discussed as well.

SSTR

SSTRs are G protein-coupled receptors with 7 transmembrane spanning domains, of which 5 subtypes exist (SSTR1-5). They are differentially expressed throughout the central nervous system and the periphery (including kidneys, pancreas and gastrointestinal tract). Binding of SSTRs to their natural ligands, somatostatin (SST)-14 and SST-28, results in a broad range of biological effects including inhibition of endocrine and exocrine secretions (including growth hormone, thyroid stimulating hormone, gastrointestinal hormones, pancreatic enzymes and neuropeptides), and bowel motility and has an anti-proliferative effect (*Figure 3A*) (38,39). Although all SSTR subtypes can be found in several human cancers, SSTR2 is most widely expressed, followed by SSTR3 and SSTR4. *Figure 3B* shows an overview of the organs in which SSTR-expressing malignancies commonly occur.

Since binding of SST to the SSTR results in an anti-proliferative effect, treatment with SST analogs became interesting for tumor targeting and multiple SST analogs were synthesized for this purpose (40). An example of such a SST analog is octreotide, which is currently approved by the U.S. Food and Drug Administration (FDA) for treatment of acromegaly, carcinoid tumors and vasoactive intestinal peptide tumors. The observation that the success of SST analog treatment was dependent on the density of SSTRs, led to investigations with radiolabeled SST analogs for imaging purposes. The first radiolabeled SST analog tested for imaging in patients was ^{123}I labelled Tyr^3-octreotide (41). Since then, the success of radiolabeled SST analogs has led to major developments with the aim of improving this nuclear medicine based approach. An overview of the developments regarding SST radiotracers is described in a review by Theodoropoulou et al. (42) of which a summary is given here. Following ^{123}I-Tyr^3-octreotide, ^{111}In-DTPA-octreotide (also called ^{111}In-pentetreotide or OctreoScan) was developed and FDA-approved for SPECT imaging of SSTR2-expressing malignancies. ^{99m}Tc-depreotide, a ^{99m}Tc labeled SST analog was also developed for SPECT imaging. The use of ^{99m}Tc labeled SST analogs has a few advantages over ^{111}In labeled SST analogs, since ^{99m}Tc is more ideal for imaging (the lower energy of ^{99m}Tc enables higher dose administration, resulting in an increase in image quality and lesion detection), more readily available and more cost efficient compared to ^{111}In. The next step in the development of SSTR radioligands was the use of the chelator, DOTA, resulting in radiotracers like ^{111}In labeled DOTA-Tyr^3-octreotide (DOTATOC), DOTA-lantreotide and DOTA-Tyr^3-octreotate (DOTATATE). The above-mentioned SST analogs are primarily focused on targeting of SSTR2. ^{111}In-DOTA-1-Nal^3-octreotide (DOTANOC), also used for SPECT imaging, is able to bind to SSTR2, SSTR3 and SSTR5, potentially yielding a higher tumor uptake, but also higher uptake in normal organs. The use of DOTA as a chelator, has offered the opportunity to label SST analogs with different radionuclides, such as ^{68}Ga for PET imaging and ^{90}Y or ^{177}Lu for therapeutic

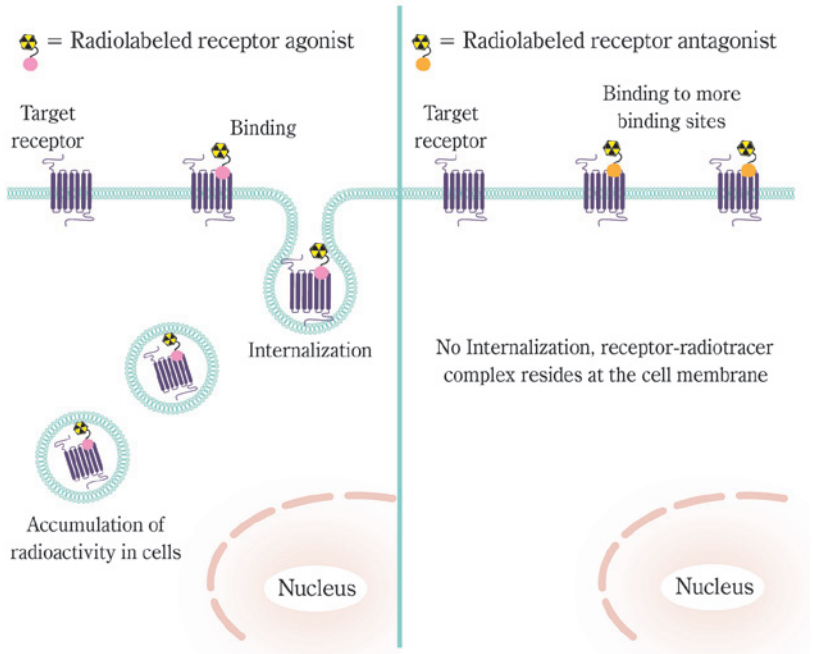

Figure 4. Mechanism of action of radiotracers with agonistic and antagonistic properties. Although radiotracers with agonistic properties are internalized resulting in accumulation of radioactivity in cells, it has been reported that radiotracers with antagonistic properties can target more binding sites resulting in enhanced tumor targeting (47).

purposes. Examples are ^{68}Ga-DOTATATE and ^{177}Lu-DOTATATE/^{90}Y-DOTATOC that are widely used for PET imaging and radionuclide therapy, respectively. SSTR radioligands labeled to other PET radionuclides such as ^{18}F are currently not yet available in the clinic but are being investigated preclinically. The above-mentioned SST analogs are all receptor agonists, which are internalized upon binding to the target receptor. Recently, SST analogs with antagonistic properties have been developed for tumor targeting. Examples include ^{177}Lu-DOTA-JR11 and ^{177}Lu-DOTA-BASS. Only few studies have been performed with these compounds yet, but the SSTR antagonists has been reported to be superior to the clinically used ^{177}Lu-DOTATATE for tumor targeting (43,44). *Figure 4* shows the mechanism of action of radiotracers with agonistic and antagonistic properties.
Overexpression of SSTR, mainly SSTR2, has been reported on 15-75% of BC cells (45). Following the success of SSTR-targeted imaging and treatment of neuroendocrine tumors, studies investigating SSTR-mediated nuclear imaging in BC have been performed in the past. Results of these studies were variable and a summary of these studies is reported in our second review in Chapter 5. To date, SSTR-mediated nuclear imaging is not used clinically in BC patients, because of the limited and variable evidence of clinical utility from clinical studies. However, since our understanding of BC as well as nuclear medicine techniques and radiotracers have improved remarkably over the past decades it is worth

reinvestigating this biomarker as a target for nuclear imaging. Regarding therapy, radiolabeled SST analogs have been tested scarcely in patients with neuroendocrine BCs (neuroendocrine BC is a type of BC with morphologic neuroendocrine features and tumor cells that express neuroendocrine markers) (46), but not in the remaining BC patients.

GRPR

The GRPR or BB2 is a G protein-coupled receptor with 7 transmembrane spanning domains. The receptor is part of the mammalian bombesin receptor family. When bound to its ligands, gastrin releasing peptide (GRP) and to a lesser extent neuromedin B, a signaling cascade is initiated which results in a broad spectrum of biological and pharmacological responses. These include release of neurotransmitters and hormones from various organs, smooth muscle contraction in the gastrointestinal tract and urogenital system, and movement of the digestive system (48). The GRPR can be found widely distributed across the central nervous system and peripheral tissues such as the gastrointestinal tract, the pulmonary, urogenital, reproductive and hematopoietic systems and on endocrine glands, and immune cells (49). Overexpression of the GRPR has been reported on a wide range of cancers such as breast, prostate and lung cancer, head and neck squamous cell carcinoma, cancer of the gastrointestinal tract, and brain and renal cancer (*Figure 3B*) (48). It was reported that activation of the GRPR in cancer cells affects growth and differentiation (*Figure 3A*). With regard to BC, according to literature approximately 62-74% of the breast tumors show high density GRPR expression, making this biomarker an attractive candidate for receptor targeted nuclear imaging and therapy (50-53). A substantial number of different GRPR radioligands with agonistic and antagonistic properties have been developed over the years. These GRPR radioligands have mostly been studied for application in prostate cancer; these investigations expanded knowledge on these radiotracers and led to the development of tracers with improved targeting properties. A review by Sancho et al. (54) provides an overview of studies performed with GRPR radioligands, agonists as well as antagonists. Different structures, linkers, spacers and chelators have been tested in order to develop compounds with optimal tumor targeting properties and optimal tumor to background ratios. Examples of GRPR radioligands that were evaluated clinically include the GRPR agonists and antagonists ^{99m}Tc-Demobesin 4, ^{99m}Tc-HYNIC-[Lys^3]-BN, ^{99m}Tc-RP527, ^{68}Ga-NOTA-Aca-BBN(7-14), ^{64}Cu-CB-TE2A-AR06, ^{68}Ga-RM2/^{68}Ga-BAY 86-7548, ^{68}Ga-SB3 and ^{68}Ga-NeoBOMB1 (55-64) (the latter is a novel GRPR antagonist of which preclinical evaluation is described in Chapter 9 of this thesis). Clinical therapeutic studies using GRPR radioligands are limited but preclinical studies using ^{177}Lu-JMV4168, ^{177}Lu-DOTA-gluBBN and ^{177}Lu-RM2/^{177}Lu-BAY 1017858 (65-67) reported promising results. Concerning therapy, a clinical study using the GRPR agonist ^{177}Lu-AMBA reported side effects and thus for this purpose radiolabeled GRPR antagonists may be a much better choice (68).

CXCR4

CXCR4/fusin or CD184 is an α-chemokine receptor expressed in a variety of organs e.g. lymphatic tissues, thymus, brain, spleen, stomach and the small intestine (69). Upon binding of its ligand, stromal derived factor 1 (SDF1) also called CXCL12, signaling pathways are activated resulting in various biological responses that influence cell survival, migration, proliferation, chemotaxis and adhesion (*Figure 3A*) (69). Overexpression of CXCR4 has been reported on a wide variety of cancers including BC (*Figure 3B*). This overexpression can potentially be attributed to hypoxia or oncoprotein induced transcription, as well as other factors e.g. VEGF induced expression, and altered regulation of CXCR4 independent of effects on transcription or translation such as post-translational ubiquitination (70). High levels of CXCR4 were found in primary breast tumors and regional and distant metastases but not in healthy breast tissue (71). In line with this, expression of CXCR4 and its ligand were positively associated with development of metastatic disease and poor prognosis (69). Based on this knowledge, targeting of CXCR4 with radiotracers for theranostic purposes can potentially benefit BC patients, especially those with aggressive or advanced disease. Multiple CXCR4-targeting radiotracers have been synthesized, including ^{111}In-DTPA-Ac-TZ14011, ^{99m}Tc-O2-AMD3100, ^{67}Ga-AMD3100, ^{11}C-AMD3465, ^{68}Ga-pentixafor and ^{68}Ga-NOTA-NFB (72-77). ^{68}Ga-pentixafor, the CXCR4 radiotracer studied most extensively, has been investigated in preclinical and clinical studies for imaging and therapeutic applications in acute myeloid leukemia, multiple myeloma, glioblastoma and small cell lung cancer patients (78-82).

The Potential of Targeted Nuclear Medicine Techniques in BC

Targeted-nuclear imaging is not suited for nationwide BC screening programs, as the success rate is dependent on sufficient target expression, the relatively high costs and the associated radiation burden. This imaging method, however, can offer a more sensitive and specific option for visualization of primary and metastatic BC lesions in other situations (*Figure 5*). Currently, mammography is the standard imaging method used for follow-up surveillance of BC patients with resected or treated tumors (83). With the knowledge that mammography has several limitations regarding BC detection, there is room for improvement. Tumor material (e.g. from biopsies routinely performed for diagnosis) can be used to determine target expression after which imaging can be performed to monitor disease recurrence. Furthermore, receptor positive tumors can be imaged pre- and post-therapy to select patients for therapy as well as to determine efficacy of treatment. Whole body SPECT or PET imaging can be used for BC staging. Concerning regional lymph node staging, sentinel lymph node biopsy has replaced axillary lymph node dissection in lymph node negative patients. Besides other adverse events, axillary lymph node dissection is still associated with substantial morbidity (84,85). Sentinel lymph node biopsy is associated with less adverse events than axillary lymph node dissection, but this method also has complications (86,87). Targeted nuclear imaging in patients with positive primary tumors might potentially identify malignant lesions in the lymph node in a non-invasive way, sparing sentinel lymph node biopsy and/or axillary lymph node dissection.

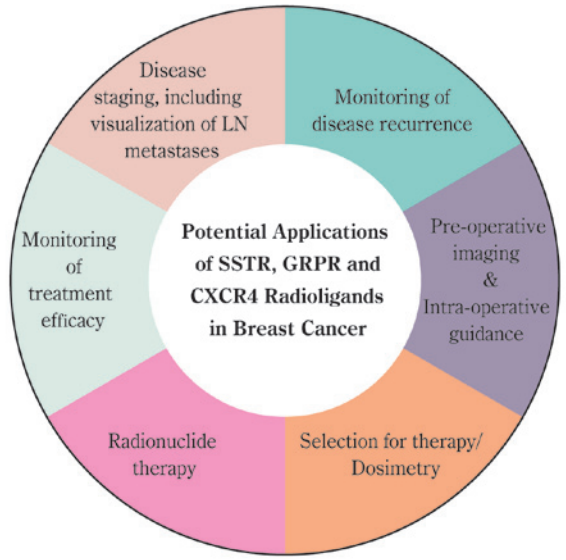

Figure 5. Potential applications for radiotracers targeting the SSTR, GRPR and CXCR4 in breast cancer.

Radiotracers targeting biomarkers on BC can also be used to perform pre-operative imaging for the purpose of surgical planning. Another benefit of the use of radiotracers is the option to use the radiotracers for intra-operative guidance, whether or not in combination with optical imaging. After injection of the radiotracer, γ-probes can be used during surgery to detect radioactivity emitted from the tumor, which guide the surgeon towards the area where the lesion is localized. This can also be of benefit for intra-operative guidance during lymph node dissection, potentially resulting in sparing of unaffected lymph nodes.

Using the theranostic approach, if targeting of a tumor lesion results in a positive SPECT or PET scan, radiotracers labeled with therapeutic radionuclides can be applied for treatment of the disease. In this case expression of biomarkers for tumor targeting can be determined in a non-invasive way and therapy selection takes place in a personalized manner. Targeted radionuclide therapy can especially be beneficial for metastatic disease, since metastases are often not resectable and currently available systemic therapy options can cause severe side effects or are no longer available after multiple lines of therapy. Furthermore, response to therapy can be closely monitored and therapy can be adjusted according to patient needs.

THESIS OUTLINE

This thesis described the application of radiopharmaceuticals for theranostic use in BC with the aim of improving imaging and treatment of the disease. **Chapter 2** reviews the targets currently under investigation for nuclear imaging of BC.

Since BC is a very heterogeneous disease characterized by different subtypes with distinctive molecular patterns, it is important to identify the subtypes of BC that may benefit from application of radiotracers targeting e.g. SSTR2, GRPR or CXCR4. In **Chapter 3** we describe the clinical relevance of targeting SSTR2, GRPR and CXCR4 by measuring mRNA expression in primary breast tumors and correlated this with important clincopathologic and biological factors and prognosis. Since the application of these radiotracers might especially be beneficial for metastatic disease, we also compared *SSTR2*, *GRPR* and *CXCR4* mRNA expression in 60 primary breast tumors and paired regional or distant metastases, as described in **Chapter 4**.

Chapter 5 reviews previous studies on SSTR2-mediated nuclear imaging and the potential benefit of developments in the field of nuclear medicine regarding SSTR-mediated imaging of BC. One such a development is the use of radiolabeled SSTR antagonists that showed enhanced tumor targeting for imaging purposes in neuroendocrine tumors compared to the clinically successfully used agonists. In **Chapter 6** we describe the comparison of a radiolabeled SSTR agonist and antagonist in human BC specimens and a BC mouse model to investigate whether the enhanced binding observed in neuroendocrine tumors can be of benefit for BC targeting as well. As a next step, the use of radiolabeled SSTR agonists and antagonists for therapeutic purposes was compared in an SSTR-expressing lung cancer mouse model to determine whether the observed enhanced binding could also be translated to therapeutic purposes, as described in **Chapter 7**.

In the next section, our research has focused on the application of radioligands targeting the GRPR. In **Chapter 8**, we describe the application of GRPR radioligands for in vivo imaging and in vitro treatment of preclinical BC models. **Chapter 9** describes the study of a novel GRPR radioligand that can be used for both imaging and treatment of GRPR-expressing tumors.

REFERENCES

1. GLOBOCAN 2012: Estimated Cancer Incidence, Mortality and Prevalence Worldwide in 2012. http://globocan.iarc.fr/Pages/fact_sheets_cancer.aspx. Accessed August 17, 2016.
2. EUCAN. http://eco.iarc.fr/eucan. Accessed August 17, 2016.
3. Berry DA, Cronin KA, Plevritis SK, et al. Effect of screening and adjuvant therapy on mortality from breast cancer. N Engl J Med. 2005;353:1784-1792.
4. Lauby-Secretan B, Scoccianti C, Loomis D, et al. Breast-cancer screening -viewpoint of the IARC Working Group. N Engl J Med. 2015;372:2353-2358.
5. Nelson HD, O'Meara ES, Kerlikowske K, Balch S, Miglioretti D. Factors Associated With Rates of False-Positive and False-Negative Results From Digital Mammography Screening: An Analysis of Registry Data. Ann Intern Med. 2016;164:226-235.
6. Brodersen J, Jorgensen KJ, Gotzsche PC. The benefits and harms of screening for cancer with a focus on breast screening. Pol Arch Med Wewn. 2010;120:89-94.
7. Lampic C, Thurfjell E, Bergh J, Sjoden PO. Short- and long-term anxiety and depression in women recalled after breast cancer screening. Eur J Cancer. 2001;37:463-469.
8. Burkett BJ, Hanemann CW. A Review of Supplemental Screening Ultrasound for Breast Cancer: Certain Populations of Women with Dense Breast Tissue May Benefit. Acad Radiol. 2016.
9. Saslow D, Boetes C, Burke W, et al. American Cancer Society guidelines for breast screening with MRI as an adjunct to mammography. CA Cancer J Clin. 2007;57:75-89.
10. Phi XA, Houssami N, Obdeijn IM, et al. Magnetic resonance imaging improves breast screening sensitivity in BRCA mutation carriers age >/= 50 years: evidence from an individual patient data meta-analysis. J Clin Oncol. 2015;33:349-356.
11. Perou CM, Sorlie T, Eisen MB, et al. Molecular portraits of human breast tumours. Nature. 2000;406:747-752.
12. Sorlie T, Perou CM, Tibshirani R, et al. Gene expression patterns of breast carcinomas distinguish tumor subclasses with clinical implications. Proc Natl Acad Sci U S A. 2001;98:10869-10874.
13. Makki J. Diversity of Breast Carcinoma: Histological Subtypes and Clinical Relevance. Clin Med Insights Pathol. 2015;8:23-31.
14. Goldhirsch A, Winer EP, Coates AS, et al. Personalizing the treatment of women with early breast cancer: highlights of the St Gallen International Expert Consensus on the Primary Therapy of Early Breast Cancer 2013. Ann Oncol. 2013;24:2206-2223.
15. Early Breast Cancer Trialists' Collaborative G. Effects of chemotherapy and hormonal therapy for early breast cancer on recurrence and 15-year survival: an overview of the randomised trials. Lancet. 2005;365:1687-1717.
16. Lu J, Steeg PS, Price JE, et al. Breast cancer metastasis: challenges and opportunities. Cancer Res. 2009;69:4951-4953.
17. Murphy CG, Dickler MN. Endocrine resistance in hormone-responsive breast cancer: mechanisms and therapeutic strategies. Endocr Relat Cancer. 2016;23:R337-352.
18. Ahmed S, Sami A, Xiang J. HER2-directed therapy: current treatment options for HER2-positive breast cancer. Breast Cancer. 2015;22:101-116.
19. Dent R, Trudeau M, Pritchard KI, et al. Triple-negative breast cancer: clinical features and patterns of recurrence. Clin Cancer Res. 2007;13:4429-4434.

20. Lehmann BD, Bauer JA, Chen X, et al. Identification of human triple-negative breast cancer subtypes and preclinical models for selection of targeted therapies. J Clin Invest. 2011;121:2750-2767.
21. Wong E, Chanudhry S, Rossi M. http://www.pathophys.org/breast-cancer/. Accessed 23 August, 2016.
22. Patton JA, Turkington TG. SPECT/CT physical principles and attenuation correction. J Nucl Med Technol. 2008;36:1-10.
23. Bruyant PP. Analytic and iterative reconstruction algorithms in SPECT. J Nucl Med. 2002;43:1343-1358.
24. Ziegler SI. Positron Emission Tomography: Principles, Technology, and Recent Developments. Nuclear Physics A. 2005;752:679c-687c.
25. Rahmim A, Zaidi H. PET versus SPECT: strengths, limitations and challenges. Nucl Med Commun. 2008;29:193-207.
26. Maurer AH. Combined imaging modalities: PET/CT and SPECT/CT. Health Phys. 2008;95:571-576.
27. Hsu DF, Freese DL, Levin CS. Breast-Dedicated Radionuclide Imaging Systems. J Nucl Med. 2016;57 Suppl 1:40S-45S.
28. Koolen BB, Vogel WV, Vrancken Peeters MJ, Loo CE, Rutgers EJ, Valdes Olmos RA. Molecular Imaging in Breast Cancer: From Whole-Body PET/CT to Dedicated Breast PET. J Oncol. 2012;2012:438647.
29. Fani M, Maecke HR. Radiopharmaceutical development of radiolabelled peptides. Eur J Nucl Med Mol Imaging. 2012;39 Suppl 1:S11-30.
30. NuDat 2.6. National Nuclear Data Center. http://www.nndc.bnl.gov/nudat2/. Accessed 26 August, 2016.
31. Greene LR, Wilkinson D. The role of general nuclear medicine in breast cancer. J Med Radiat Sci. 2015;62:54-65.
32. Vercher-Conejero JL, Pelegri-Martinez L, Lopez-Aznar D, Cozar-Santiago Mdel P. Positron Emission Tomography in Breast Cancer. Diagnostics (Basel). 2015;5:61-83.
33. Brem RF, Floerke AC, Rapelyea JA, Teal C, Kelly T, Mathur V. Breast-specific gamma imaging as an adjunct imaging modality for the diagnosis of breast cancer. Radiology. 2008;247:651-657.
34. Avril N, Rose CA, Schelling M, et al. Breast imaging with positron emission tomography and fluorine-18 fluorodeoxyglucose: use and limitations. J Clin Oncol. 2000;18:3495-3502.
35. Hodgson NC, Gulenchyn KY. Is there a role for positron emission tomography in breast cancer staging? J Clin Oncol. 2008;26:712-720.
36. Teunissen JJ, Kwekkeboom DJ, Valkema R, Krenning EP. Nuclear medicine techniques for the imaging and treatment of neuroendocrine tumours. Endocr Relat Cancer. 2011;18 Suppl 1:S27-51.
37. Srivastava SC. Paving the way to personalized medicine: production of some promising theragnostic radionuclides at Brookhaven National Laboratory. Semin Nucl Med. 2012;42:151-163.
38. Barbieri F, Bajetto A, Pattarozzi A, et al. Peptide receptor targeting in cancer: the somatostatin paradigm. Int J Pept. 2013;2013:926295.
39. Olias G, Viollet C, Kusserow H, Epelbaum J, Meyerhof W. Regulation and function of somatostatin receptors. J Neurochem. 2004;89:1057-1091.
40. Reubi JC, Laissue JA. Multiple actions of somatostatin in neoplastic disease. Trends Pharmacol Sci. 1995;16:110-115.

41. Lamberts SW, Bakker WH, Reubi JC, Krenning EP. Somatostatin receptor imaging in vivo localization of tumors with a radiolabeled somatostatin analog. J Steroid Biochem Mol Biol. 1990;37:1079-1082.
42. Theodoropoulou M, Stalla GK. Somatostatin receptors: from signaling to clinical practice. Front Neuroendocrinol. 2013;34:228-252.
43. Wild D, Fani M, Fischer R, et al. Comparison of somatostatin receptor agonist and antagonist for peptide receptor radionuclide therapy: a pilot study. J Nucl Med. 2014;55:1248-1252.
44. Cescato R, Waser B, Fani M, Reubi JC. Evaluation of 177Lu-DOTA-sst2 antagonist versus 177Lu-DOTA-sst2 agonist binding in human cancers in vitro. J Nucl Med. 2011;52:1886-1890.
45. Watt HL, Kharmate G, Kumar U. Biology of somatostatin in breast cancer. Mol Cell Endocrinol. 2008;286:251-261.
46. Savelli G, Zaniboni A, Bertagna F, et al. Peptide Receptor Radionuclide Therapy (PRRT) in a Patient Affected by Metastatic Breast Cancer with Neuroendocrine Differentiation. Breast Care (Basel). 2012;7:408-410.
47. Ginj M, Zhang H, Waser B, et al. Radiolabeled somatostatin receptor antagonists are preferable to agonists for in vivo peptide receptor targeting of tumors. Proc Natl Acad Sci U S A. 2006;103:16436-16441.
48. Jensen RT, Battey JF, Spindel ER, Benya RV. International Union of Pharmacology. LXVIII. Mammalian bombesin receptors: nomenclature, distribution, pharmacology, signaling, and functions in normal and disease states. Pharmacol Rev. 2008;60:1-42.
49. Ramos-Alvarez I, Moreno P, Mantey SA, et al. Insights into bombesin receptors and ligands: Highlighting recent advances. Peptides. 2015;72:128-144.
50. Gugger M, Reubi JC. Gastrin-releasing peptide receptors in non-neoplastic and neoplastic human breast. Am J Pathol. 1999;155:2067-2076.
51. Reubi C, Gugger M, Waser B. Co-expressed peptide receptors in breast cancer as a molecular basis for in vivo multireceptor tumour targeting. Eur J Nucl Med Mol Imaging. 2002;29:855-862.
52. Halmos G, Wittliff JL, Schally AV. Characterization of bombesin/gastrin-releasing peptide receptors in human breast cancer and their relationship to steroid receptor expression. Cancer Res. 1995;55:280-287.
53. Reubi JC, Wenger S, Schmuckli-Maurer J, Schaer JC, Gugger M. Bombesin receptor subtypes in human cancers: detection with the universal radioligand (125)I-[D-TYR(6), beta-ALA(11), PHE(13), NLE(14)] bombesin(6-14). Clin Cancer Res. 2002;8:1139-1146.
54. Sancho V, Di Florio A, Moody TW, Jensen RT. Bombesin receptor-mediated imaging and cytotoxicity: review and current status. Curr Drug Deliv. 2011;8:79-134.
55. Mather SJ, Nock BA, Maina T, et al. GRP receptor imaging of prostate cancer using [(99m)Tc] Demobesin 4: a first-in-man study. Mol Imaging Biol. 2014;16:888-895.
56. Santos-Cuevas CL, Ferro-Flores G, Arteaga de Murphy C, Pichardo-Romero PA. Targeted imaging of gastrin-releasing peptide receptors with 99mTc-EDDA/HYNIC-[Lys3]-bombesin: biokinetics and dosimetry in women. Nucl Med Commun. 2008;29:741-747.
57. Van de Wiele C, Dumont F, Dierckx RA, et al. Biodistribution and dosimetry of (99m)Tc-RP527, a gastrin-releasing peptide (GRP) agonist for the visualization of GRP receptor-expressing malignancies. J Nucl Med. 2001;42:1722-1727.
58. Van de Wiele C, Dumont F, Vanden Broecke R, et al. Technetium-99m RP527, a GRP analogue for visualisation of GRP receptor-expressing malignancies: a feasibility study. Eur J Nucl Med. 2000;27:1694-1699.

59. Van de Wiele C, Phonteyne P, Pauwels P, et al. Gastrin-releasing peptide receptor imaging in human breast carcinoma versus immunohistochemistry. J Nucl Med. 2008;49:260-264.

60. Zhang J, Li D, Lang L, et al. 68Ga-NOTA-Aca-BBN(7-14) PET/CT in Healthy Volunteers and Glioma Patients. J Nucl Med. 2016;57:9-14.

61. Wieser G, Mansi R, Grosu AL, et al. Positron emission tomography (PET) imaging of prostate cancer with a gastrin releasing peptide receptor antagonist-from mice to men. Theranostics. 2014;4:412-419.

62. Kahkonen E, Jambor I, Kemppainen J, et al. In vivo imaging of prostate cancer using [68Ga]-labeled bombesin analog BAY86-7548. Clin Cancer Res. 2013;19:5434-5443.

63. Maina T, Bergsma H, Kulkarni HR, et al. Preclinical and first clinical experience with the gastrin-releasing peptide receptor-antagonist [68Ga]SB3 and PET/CT. Eur J Nucl Med Mol Imaging. 2016;43:964-973.

64. Nock BA, Kaloudi A, Lymperis E, et al. Theranostic perspectives in prostate cancer with the GRPR-antagonist NeoBOMB1-Preclinical and first clinical results. J Nucl Med. 2016.

65. Chatalic KL, Konijnenberg M, Nonnekens J, et al. In Vivo Stabilization of a Gastrin-Releasing Peptide Receptor Antagonist Enhances PET Imaging and Radionuclide Therapy of Prostate Cancer in Preclinical Studies. Theranostics. 2016;6:104-117.

66. Lim JC, Cho EH, Kim JJ, et al. Preclinical pharmacokinetic, biodistribution, imaging and therapeutic efficacy of (177)Lu-Labeled glycated bombesin analogue for gastrin-releasing peptide receptor-positive prostate tumor targeting. Nucl Med Biol. 2015;42:234-241.

67. Dumont RA, Tamma M, Braun F, et al. Targeted radiotherapy of prostate cancer with a gastrin-releasing peptide receptor antagonist is effective as monotherapy and in combination with rapamycin. J Nucl Med. 2013;54:762-769.

68. Bodei L, Ferrari M, Nunn AD, et al. 177Lu-AMBA bombesin analogue in hormone refractory prostate cancer patients: a phase I escalation study with single-cycle administrations [abstract]. Eur J Nucl Med Mol Imaging. 2007;34:S221

69. Xu C, Zhao H, Chen H, Yao Q. CXCR4 in breast cancer: oncogenic role and therapeutic targeting. Drug Des Devel Ther. 2015;9:4953-4964.

70. Busillo JM, Benovic JL. Regulation of CXCR4 signaling. Biochim Biophys Acta. 2007;1768:952-963.

71. Muller A, Homey B, Soto H, et al. Involvement of chemokine receptors in breast cancer metastasis. Nature. 2001;410:50-56.

72. Buckle T, van Berg NS, Kuil J, et al. Non-invasive longitudinal imaging of tumor progression using an (111)indium labeled CXCR4 peptide antagonist. Am J Nucl Med Mol Imaging. 2012;2:99-109.

73. Hartimath SV, Domanska UM, Walenkamp AM, Rudi AJOD, de Vries EF. [(9)(9)mTc]O(2)-AMD3100 as a SPECT tracer for CXCR4 receptor imaging. Nucl Med Biol. 2013;40:507-517.

74. Aghanejad A, Jalilian AR, Fazaeli Y, et al. Synthesis and Evaluation of [(67)Ga]-AMD3100: A Novel Imaging Agent for Targeting the Chemokine Receptor CXCR4. Sci Pharm. 2014;82:29-42.

75. Hartimath SV, van Waarde A, Dierckx RA, de Vries EF. Evaluation of N-[(11)C]methyl-AMD3465 as a PET tracer for imaging of CXCR4 receptor expression in a C6 glioma tumor model. Mol Pharm. 2014;11:3810-3817.

76. Herrmann K, Lapa C, Wester HJ, et al. Biodistribution and radiation dosimetry for the chemokine receptor CXCR4-targeting probe 68Ga-pentixafor. J Nucl Med. 2015;56:410-416.

77. Wang Z, Zhang M, Wang L, et al. Prospective Study of (68)Ga-NOTA-NFB: Radiation Dosimetry in Healthy Volunteers and First Application in Glioma Patients. Theranostics. 2015;5:882-889

78. Philipp-Abbrederis K, Herrmann K, Knop S, et al. In vivo molecular imaging of chemokine receptor CXCR4 expression in patients with advanced multiple myeloma. EMBO Mol Med. 2015;7:477-487.

79. Herrmann K, Schottelius M, Lapa C, et al. First-in-Human Experience of CXCR4-Directed Endoradiotherapy with 177Lu- and 90Y-Labeled Pentixather in Advanced-Stage Multiple Myeloma with Extensive Intra- and Extramedullary Disease. J Nucl Med. 2016;57:248-251.

80. Derlin T, Jonigk D, Bauersachs J, Bengel FM. Molecular Imaging of Chemokine Receptor CXCR4 in Non-Small Cell Lung Cancer Using 68Ga-Pentixafor PET/CT: Comparison With 18F-FDG. Clin Nucl Med. 2016;41:e204-205.

81. Lapa C, Luckerath K, Kleinlein I, et al. (68)Ga-Pentixafor-PET/CT for Imaging of Chemokine Receptor 4 Expression in Glioblastoma. Theranostics. 2016;6:428-434.

82. Herhaus P, Habringer S, Philipp-Abbrederis K, et al. Targeted positron emission tomography imaging of CXCR4 expression in patients with acute myeloid leukemia. Haematologica. 2016;101:932-940.

83. Yoon JH, Kim MJ, Kim EK, Moon HJ. Imaging surveillance of patients with breast cancer after primary treatment: current recommendations. Korean J Radiol. 2015;16:219-228.

84. Schijven MP, Vingerhoets AJ, Rutten HJ, et al. Comparison of morbidity between axillary lymph node dissection and sentinel node biopsy. Eur J Surg Oncol. 2003;29:341-350.

85. Ronka R, von Smitten K, Tasmuth T, Leidenius M. One-year morbidity after sentinel node biopsy and breast surgery. Breast. 2005;14:28-36.

86. Wilke LG, McCall LM, Posther KE, et al. Surgical complications associated with sentinel lymph node biopsy: results from a prospective international cooperative group trial. Ann Surg Oncol. 2006;13:491-500.

87. Montgomery LL, Thorne AC, Van Zee KJ, et al. Isosulfan blue dye reactions during sentinel lymph node mapping for breast cancer. Anesth Analg. 2002;95:385-388.

Chapter 2

Review: Targeted Nuclear Imaging of Breast Cancer

S.U. Dalm, J.F. Verzijlbergen and M. de Jong

Dept. of Radiology & Nuclear Medicine, Erasmus MC, Rotterdam, The Netherlands

Submitted to Int J Mol Sci 2016, September 2016, Revised version submitted after peer review in November 2016

ABSTRACT

Targeted nuclear imaging directed against molecular markers overexpressed on breast cancer (BC) cells offers a sensitive and specific method for BC imaging. Currently, a few targets such as estrogen receptor (ER), progesterone receptor (PR), human epidermal growth factor receptor 2 (HER2), somatostatin receptor (SSTR) and the gastrin releasing peptide receptor (GRPR) are being investigated for this purpose. Expression of these targets is BC subtype dependent and information that can be gained from lesion visualization is dependent on the target; ER-targeting radiotracers e.g. can be used to monitor response to anti-estrogen treatment. Here we give an overview of the studies currently under investigation for targeted nuclear imaging of BC. Main findings of imaging studies are summarized and (potential) purposes of lesion visualization by targeting these molecular markers are discussed. Since BC is a very heterogeneous disease and molecular target expression can vary per subtype, but also during disease progression or under influence of treatment, radiotracers for selected imaging purposes should be chosen carefully.

Keywords:
Breast cancer, Targeted Nuclear Imaging, SPECT, PET, GRPR, SSTR, ER, PR, HER2

INTRODUCTION

Breast cancer (BC) is the most common cancer in women worldwide. In 2012, 167 million new BC cases were diagnosed and 522,000 people died of the disease (1). BC is highly heterogenic and comprises of multiple histological subtypes e.g. luminal A, luminal B, human epidermal growth factor 2 (HER2)-driven and basal-like tumors (2). These histological subtypes are characterized by distinctive molecular patterns that play an important role in treatment and prognosis of the disease. The most important molecular tumor characteristics include estrogen receptor (ER), progesterone receptor (PR) and human epidermal growth factor receptor 2 (HER2) expression (2).

Our knowledge of BC has greatly expanded over the past years leading to new diagnostic and therapeutic methods, which positively influenced the mortality rate of the disease. The prognosis of metastatic BC is still poor, the estimated 5-year survival being only 26% (3), and therefore early detection of the disease is essential. Although BC is finally diagnosed by histology, imaging methods are indispensable for detection of the disease. Mammography is used for nationwide screenings, in some cases supplemented with magnetic resonance imaging (MRI) or ultrasound. Unfortunately, these methods have limitations leading to false negatives and false positives (4,5). Concerning mammography, false positive and false negative rates ranging from 65.2-121.2 and 1.0-1.3 cases per 1,000 women per screening round have been reported, respectively (6). MRI and ultrasound have a higher sensitivity than mammography, but a low specificity was reported leading to a significant amount of false positives (7,8).

Imaging techniques that can provide information on molecular characteristics such as biomarker expression can have added value, especially in highly heterogeneous cancer types such as BC. To fulfill this purpose target-mediated nuclear imaging of BC is being investigated.

In nuclear medicine, such target-mediated imaging is successfully used in the clinical setting for imaging of e.g. neuroendocrine tumors (9,10). This approach uses the molecular expression pattern of tumors for targeting. Molecules (e.g. receptors, transporters and enzymes) overexpressed on cancer cells can be targeted with synthesized target ligands (e.g. peptide analogs, antibodies, affibodies and nanobodies) that bind to the target with high affinity and specificity (*Figure 1A*).

Depending on the radionuclide that these peptide analogs are conjugated with, single-photon emission computed tomography (SPECT) or positron emission tomography (PET) can be performed. SPECT and PET are functional, highly sensitive nuclear imaging methods based on the detection of γ-photons directly or indirectly derived from γ-emitting (e.g. ^{111}In) or positron emitting (e.g. ^{68}Ga) radionuclides, respectively (*Figure 1B+C*). Combining SPECT or PET with computed tomography or MRI provides functional imaging information in combination with high resolution imaging of anatomical structures (11,12). In the review by Pattion et al. (13) and the paper by Ziegler et al. (14) the mechanisms of SPECT and PET imaging are described in more detail. With respect to BC imaging, dedicated SPECT and PET imaging devices have been developed that

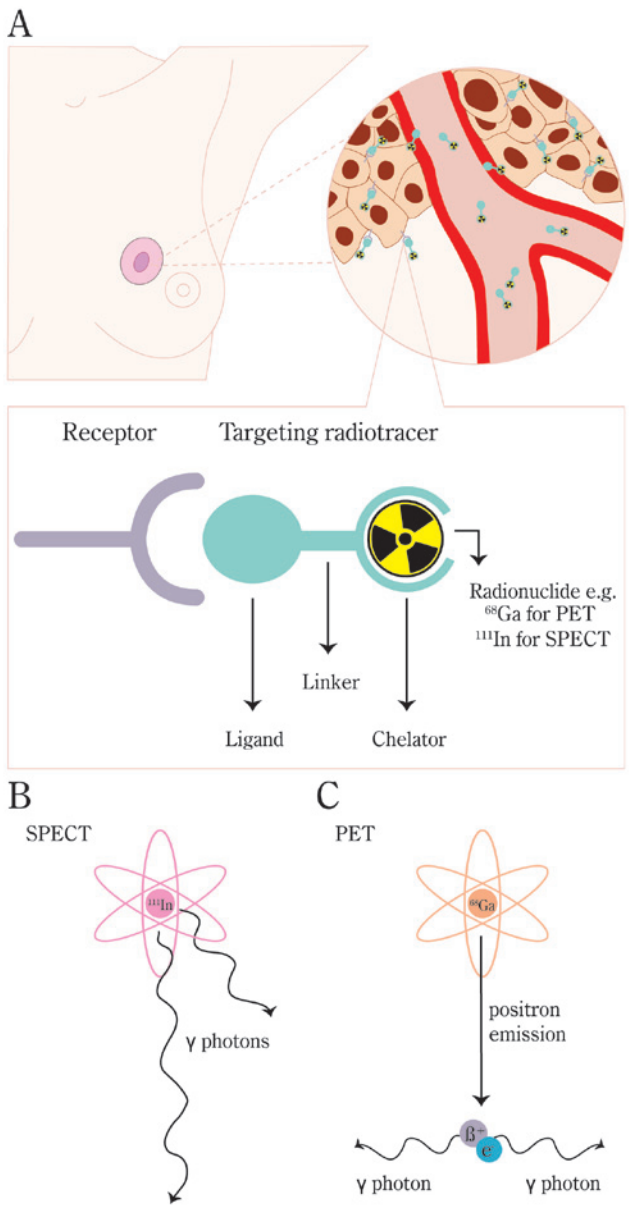

Figure 1. A) Schematic overview of targeted nuclear imaging. Ligands that can bind their targets overexpressed on BC cells can be coupled to a chelator, often via a linker. The chelator enables labeling with radionuclides that can be applied for imaging purposes. B+C) Drawing of the principles of radionuclides for SPECT and PET imaging. For SPECT imaging, γ-photons from radionuclides such as ^{111}In are captured by detectors at multiple angles. For PET imaging positrons emitted from a radionuclide such as ^{68}Ga interact with electrons which results in the production of 2 γ-photons. These photons are picked up at multiple angles by opposing detectors installed in a ring-like pattern.

have a higher resolution and thus better diagnostic accuracy than whole body SPECT and PET systems (15,16).
In the past years a number of molecular targets for targeted nuclear imaging of BC have been identified and are currently under investigation: the somatostatin receptor (SSTR), the gastrin releasing peptide receptor (GRPR), hormone receptors, HER2, folate receptor (FR), C-X-C chemokine receptor type 4 (CXCR4), neuropeptide Y receptor Y1 (NPY1R), vascular endothelial growth factor A (VEGF-A) and vasoactive intestinal polypeptide receptor 1 (VIP-R1). In this review we describe these targets, discuss ongoing investigations and the prospects of BC targeted nuclear imaging.
This review focuses on molecular targets mentioned above. Other radiotracers under investigation for nuclear imaging of BC including radiotracers that accumulate in cells due to (over)expression of functional transporters or higher metabolism in BC cells are beyond the scope of this review.

SSTR-mediated BC Imaging

Receptor-mediated nuclear imaging is successfully used in neuroendocrine tumor patients by targeting SSTRs overexpressed on neuroendocrine tumor cells using SSTR binding radioligands. Next to neuroendocrine tumors, SSTR expression has also been reported on BC cells (17,18). Since radiolabeled peptide analogs targeting these receptors were available, several clinical studies have been performed targeting these receptors for imaging purposes. In our previous review we discussed earlier clinical studies (19-29) on SSTR-mediated imaging, showing very variable sensitivities and specificities ranging from 36-100% and 22-100%, respectively (30). Limiting factors for successful BC targeting were low and heterogeneous SSTR expression, appropriate patient group selection, the use of radiolabeled peptide analogs with suboptimal receptor affinity and imaging equipment with low spatial resolution. For successful receptor-mediated imaging the expression of the target should be sufficient. Since low and heterogeneous SSTR expression was reported as a limiting factor for successful BC imaging, the question is whether SSTR is a suitable target for targeted nuclear BC imaging. However, another limiting factor of the previous studies was non-appropriate patient selection. Since BC is a very heterogeneous disease, SSTR expression between BC subtypes may vary. We and others showed higher SSTR expression in ER-positive BC compared to ER-negative BC, identifying ER-positive BC subtypes as the most suitable subtypes for SSTR-mediated imaging (31-34). If we only focus on these BC subtypes, which account for the majority of the breast tumors, SSTR-mediated BC imaging might be more successful. Furthermore, we studied SSTR expression of primary BCs versus SSTR expression of regional and distant metastases and demonstrated that these expression patterns are similar in the majority of cases (S. Dalm et. al., EANM annual meeting 2016, Barcelona Spain). Previous studies have been performed with radiolabeled octreotide, which has a lower SSTR affinity compared to the currently used radiolabeled somatostatin analogs, including Tyr^3-octreotate (35). In addition, lower spatial resolution planar imaging was used in earlier studies in comparison to currently available whole body and dedicated SPECT and PET techniques (11,15,16). Another

noteworthy recent development is the application of SSTR antagonists that have shown to be superior to SSTR agonists for neuroendocrine tumor targeting (36-40). This enhanced tumor targeting of SSTR antagonists was explained by the ability of receptor antagonists to bind more binding sites/receptors than receptor agonists (40). Since SSTR expression in BC was reported to be low and heterogeneous, the use of antagonists is promising in this respect. Cescato et al. (39) reported 11±4 times higher binding of an SSTR antagonist, ^{177}Lu-DOTA-BASS, vs. the clinically used SSTR agonist ^{177}Lu-DOTA-Tyr^3-octreotate in 7 human BC specimens. We recently reported on enhanced binding of the SSTR antagonist DOTA-JR11 vs. the SSTR agonist DOTA-Tyr^3-octreotate in 40 BC specimens as well as on superior imaging of a patient-derived xenograft mouse model using the radiolabeled receptor agonist vs. the antagonist (S. Dalm et.al., EANM annual meeting 2016, Barcelona Spain).
Thus, previous studies on SSTR-mediated imaging in BC performed under suboptimal conditions were not convincing, but with recent improvements as mentioned above, this outcome might change. Additional studies that benefit from these recent developments are needed to investigate the true potential of SSTR-mediated BC imaging.

GRPR-mediated BC Imaging

The GRPR is a G-protein coupled receptor that is overexpressed on a high percentage of BCs. According to literature 62-96% of primary BCs express GRPR (41-44). Over the past years multiple GRPR targeting radioligands have been described to target GRPR-expressing cancers. Although the majority of these were studied in prostate cancer, these studies expanded our knowledge on preferential radioligand properties and uptake in other/background organs. One example is the preference for radiolabeled GRPR antagonist instead of agonists for tumor targeting, since similar to what was observed for SSTR radioligands, superior binding of GRPR antagonists vs. agonists was reported (45). Several preclinical studies have been performed demonstrating successful GRPR-mediated nuclear imaging using SPECT and PET in BC mouse models (44,46,47). In the study by Prignon et al. (46), GRPR-mediated imaging was compared to ^{18}F-FDG PET for tumor visualization and disease monitoring after endocrine therapy, resulting in a preference for GRPR-mediated imaging. In line with this finding, we reported on high *GRPR* mRNA expression levels to be associated with improved progression free survival after first line tamoxifen (Nolvadex) treatment, indicating that GRPR has predictive value for response to tamoxifen treatment (31). In the same study we reported on higher *GRPR* expression in ER-positive tumors, identifying specific BC patients suited for the application of radiotracers targeting this receptor. Furthermore, we recently reported that BC metastases from GRPR-positive primary BCs also express GRPR, indicating that this imaging method can be applied in both primary and metastatic disease (S.Dalm et.al., EANM annual meeting 2016, Barcelona Spain). Although results obtained from preclinical studies are promising, to date only a few clinical studies have been performed on GRPR-mediated nuclear BC imaging. In a study by Maina et al. (48), 4/8 breast tumors were successfully visualized in patients with advanced

disease using ^{68}Ga-SB3, a radiolabeled GRPR antagonist. Scan outcomes were not related to ER expression in this study. Stoykow et al. (49) showed successful imaging in 13/18 patients with another ^{68}Ga labeled GRPR-antagonist ^{68}Ga-RM2. Positive imaging results were correlated with ER expression in accordance with our findings (31), confirming the potential of GRPR-mediated imaging in ER-positive patients.
Although more clinical studies on the application of GRPR radioligands for BC imaging are needed, current findings suggest that GRPR-targeted imaging might be used successfully for tumor detection and disease monitoring in ER-positive patients.

Targeting of Hormone Receptors for Nuclear Imaging

The ER is not only interesting for therapeutic targeting options, but also for imaging. ^{18}F-FES, a fluorinated estradiol (50), is the most extensively studied ER-targeting PET radioligand in clinical trials. Studies have focused on the potential of ER-mediated nuclear imaging for visualization of ER-positive primary and metastatic BC lesions as well as the ability of the radioligand to predict response to anti-estrogen treatment. Four clinical studies reported on sensitivity and specificity of the radiotracer for tumor visualization; 69-100% and 80-100%, respectively (51-54). Furthermore, ^{18}F-FES imaging was used to predict response to anti-estrogen treatment prior to and in early phases of therapy. High uptake of ^{18}F-FES prior to treatment indicates the presence of ER, which is necessary for a positive therapy response, while a decrease of ^{18}F-FES uptake in early phases of treatment is an indication of successful treatment. Up to now positive and negative predictive values of 65% and 88%, respectively, were reported for pre-therapy scanning in relation to anti-estrogen treatment (55-58). Following these positive results, a substantial number of clinical trials using ^{18}F-FES for BC imaging have started and are still ongoing. Combining current findings, the highest potential for ^{18}F-FES use lies in determining ER expression of BC lesions (offering a less invasive method than immunostaining on biopsy material) and the use of the radiotracer to predict therapy response.
Because expression of the PR is an estrogen-regulated process, primary focus was on the development of ER-targeted radiotracers. However, ER-targeting radiotracers are not always efficient in patients treated with anti-estrogens since these molecules bind to the ER as well, rendering the receptor unavailable for radiotracer binding for e.g. interim monitoring of treatment efficacy. In this case PR-targeted radiotracers might be useful. Furthermore, similar to ER-status, PR-targeting radiotracers offer a less invasive method for determining PR status of breast lesions. A number of PR-targeting radiotracers have been synthesized and investigated in preclinical and clinical studies (59,60). The most successful PR-targeted radiotracer, ^{18}F-FFNP, was used in a clinical pilot study successfully identifying 15/16 PR-positive BCs (61). Previous research reported a decrease in PR expression after successful anti-estrogen treatment as a result of inhibition of ER activated pathways (62) and preclinical studies investigating the potential of ^{18}F-FFNP PET imaging to predict response to anti-estrogen treatment have been performed with promising results (63,64). To date clinical data on PR-targeted nuclear imaging is

limited, but potential application of PR radioligands lies in the determination of PR expression and therapy assessment after endocrine treatment.

HER2-targeted Imaging

Similar to hormone receptors, HER2 expression in BC is not only of interest for therapeutic interventions but also for imaging. HER2 targeted nuclear imaging has been tested in preclinical and clinical studies using both radiolabeled monoclonal antibodies, radiolabeled affibodies and radiolabeled nanobodies. Monoclonal antibodies used for therapy of HER2-expressing BCs were radiolabeled with different radionuclides enabling both SPECT and PET imaging. Following positive results from preclinical studies, radiolabeled Trastuzumab was investigated in clinical studies for its ability to visualize HER2-positive BC lesions (65-71). The main purpose of studying HER2-targeted nuclear imaging was to predict response to treatment with Trastuzumab as well as other types of treatment, and to predict Trastuzumab related toxicity. The results of clinical studies were variable, limiting factors being poor visualization of liver metastases due to high background uptake in the liver and suboptimal imaging of HER2-positive lesions if no unlabeled Trastuzumab was pre-administered. Furthermore, treatment of HER2 positive BC patients with a combination of Trastuzumab and paclitaxel or a heat shock protein 90 inhibitor NVP-AUY922 led to a decrease in uptake of radiolabeled Trastuzumab, indicating that the radiotracer can be used to assess response to these types of treatment (69,70). In contrast to antibodies, the smaller affibody molecules have relatively fast uptake and clearance rates, resulting in a lower radiation burden for patients and offering the opportunity to scan patients at earlier time points after administration of the radiotracer. Two clinical studies have been performed evaluating the use of radiolabeled HER2-targeting affibodies in patients, which resulted in successful imaging of HER2-positive BC lesions (72,73). However, similar to the results with radiolabeled Trastuzumab, imaging of liver metastases was difficult because of high physiological uptake in the liver. Additionally, radiolabeled HER2-targeting nanobodies that can be labeled with different radionuclides (e.g. ^{18}F, ^{68}Ga and ^{99m}Tc) were synthesized and applied for HER2 visualization (74-76). The majority of these nanobodies are still under investigation in a preclinical setting, but a recent clinical study by Keyaerts and Xavier et al. (77) reported on the use of ^{68}Ga-HER2-Nanobody in BC patients. Although not the primary goal of the study, both primary and metastatic BC lesions were successfully visualized. Furthermore, biodistribution was favorable and no toxicity was reported. In addition, radiolabeled HER2 targeting RNA aptamers were synthesized for targeting HER2-positive BC lesions (78). These studies are still in preclinical setting and their advantage to HER2 targeting antibodies, affibodies and nanobodies remains to be established. We conclude that HER2-targeted imaging can be applied to determine HER2 expression of breast tumors and to monitor therapy responses.

Other Targets

Next to the above-mentioned targets there are some other interesting targets that are not extensively studied in BC (yet). Folate targeting radiotracers have been applied for BC imaging. Overexpression of the FR was associated with basal like BCs (79). In a clinical study successful SPECT imaging using a ^{99m}Tc labeled folate tracer was performed in 3/6 BC patients (80). Radiotracers targeting folate receptors are currently in clinical trials mainly focusing on targeting of ovarian cancer.

High expression of CXCR4 and its association with invasive disease was reported on primary and metastatic BC cells (81). Radiotracers targeting this receptor for imaging purposes were investigated in BC in a few preclinical studies and 1 clinical study (82-84). The result of the clinical study using the CXCR4 radiotracer ^{68}Ga-pentixafor was disappointing and ^{18}F-FDG seems superior to ^{68}Ga-pentixafor for BC imaging. However, only few BC patients were included in this study and larger clinical studies are needed to accurately determine the value of CXCR4-mediated BC imaging. Since *CXCR4* mRNA expression was associated with ER-negative tumors (31), successful targeting would offer new imaging opportunities for this patient group.

NPY1R expression has been reported on 85% of breast tumors and radiotracers for BC targeting have been synthesized (85-88). Highest expression of the receptors was reported on triple negative BCs (89). Up to date, proof of successful imaging using these radiotracers is very scarce, but the available data appears promising.

VEGF-A is an important protein involved in tumor angiogenesis. In BC overexpression of VEGF-A was reported and associated with ER-negative tumors (90). Similar to HER2 antibodies, a VEGF-A targeting antibody used for antiangiogenic therapy named Bevacizumab, was radiolabeled for imaging of VEGF-A expression in tumors. To our knowledge one study was performed investigating ^{89}Zr-Bevacizumab PET imaging, resulting in tumor visualization in 25/26 cases (91). In a preclinical setting downregulation of VEGF-A was visualized using ^{89}Zr-Bevacizumab after treating BC cell lines with a heat shock protein 90 inhibitor (92). Although evidence is limited up to now, VEGF-A targeted nuclear imaging might be useful in the selection of patients suitable for VEGF-A targeted therapy and to monitor patients receiving treatment influencing VEGF-A expression.

Furthermore, overexpression of VIP-R on BC cell was reported in multiple studies and radiotracers targeting these receptors were synthesized (93,94). One preclinical and one clinical study described the use of radiolabeled VIP-R radiotracers (^{18}F-dVIP and ^{64}Cu-TP3805, respectively) for imaging purposes in BC patients (95,96). In the clinical study by Thakur et al. (96) 20/20 BCs were successfully imaged. The authors hypothesize that VIP-R type 1-mediated imaging can be used for early and accurate detection of BC because it is overexpressed on all BC cells in early phases of the disease. However, the high uptake of VIP-R type 1 targeted radiotracers in the lungs reported in studies performed in other cancer types should be kept in mind (97).

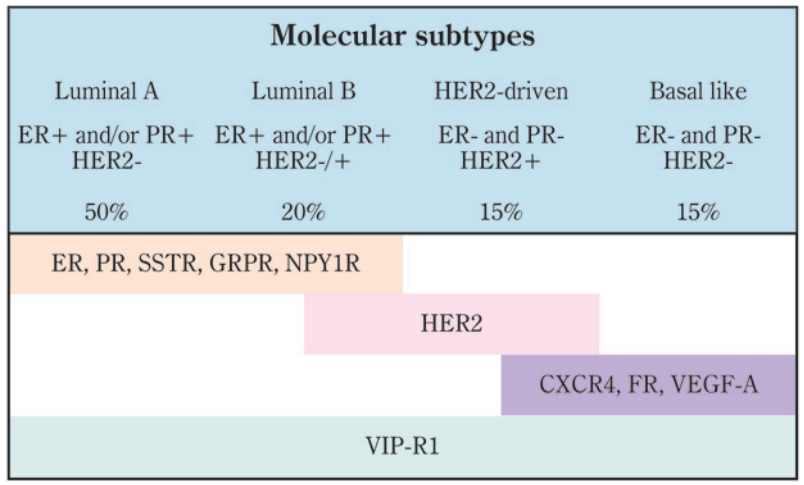

Figure 2. An overview of targets discussed in this review and the BC subtype with highest expression thereof. ER=estrogen receptor, PR=progesterone receptor, SSTR=somatostatin receptor, GRPR=gastrin releasing peptide receptor, NPY1R=Neuropeptide Y receptor Y1, HER2=human epidermal factor receptor 2, CXCR4=C-X-C chemokine receptor type 4, FR=folate receptor, VEGF-A=Vascular endothelial growth factor A and VIP-R1=Vasoactive intestinal polypeptide receptor 1. Details on histological and molecular profiles are derived from (98).

The Use of Targeted Nuclear Imaging in BC

With the different targets discussed above being explored and available for target-mediated nuclear imaging several questions remain. How can targeted nuclear imaging improve BC detection? What is the best target for targeted nuclear BC imaging?

One target does unfortunately not suit all BCs since this tumor type is very heterogeneous. *Figure 2* shows an overview of the targets discussed in this review. Of the targets currently under investigation for targeted nuclear imaging of BC: SSTR, GRPR, ER, PR and NPY1R are best suited for ER-positive luminal A and luminal B BCs, since these targets are only/highest expressed in these BC subtypes. Both ER and PR-targeted radiotracers, but especially ER-targeted radiotracers, are currently studied in clinical trials. These radiotracers can be used for determining ER or PR expression of primary tumors and metastases as well as for evaluation of treatment response to ER-targeted therapy. However, the majority of ER-positive BCs acquire resistance against anti-estrogen treatment and in some cases this is due to loss of ER expression (99). ER status of primary BCs and corresponding metastases may vary (over time) and so visualization of metastases of ER-positive primary tumors is not feasible in all cases (100). ER- and PR-targeted imaging to determine receptor expression is less invasive than immunostaining on biopsy material as is done in current practice. Furthermore, ER and PR-targeted nuclear imaging comprises visualization of the complete tumor lesion, while biopsy material is limited and not always representative for the (heterogeneous) tumor. However, determining hormone receptor expression with nuclear imaging would involve scanning patients several times with (different) radiotracers, which causes a significant radiation burden to the patient that has to be kept in mind. The application of radiotracers to determine hormone receptor status would especially be beneficial for tumors that cannot be biopsied due to an inconvenient location. In cases where ER and/or PR-targeted imaging cannot be applied, SSTR and GRPR-mediated imaging, although not studied as widely as ER and PR-mediated imaging (yet), may be of benefit for imaging of ER-positive primary and metastatic BC lesions. GRPR targeting is preferred because the receptor is expressed more frequently and at higher density (42). Nevertheless, both SSTR and GRPR-mediated imaging can be beneficial in ER-positive tumors that loose ER expression in the course of the disease. For this to be successful the relation between SSTR2 and GRPR, and ER needs to be investigated to make sure that loss of ER expression does not influence GRPR expression. Furthermore, even though SSTR and GRPR expression is higher in ER-positive tumors, ER-negative tumors might also express the receptor and thus radiotracers targeting these receptors might also be applied in other patient groups. NPY1R expression was also associated with ER-positive BCs. To date NPY1R-targeted BC imaging has only been performed in a limited number of studies and more studies are needed to determine the added value of NPY1R in comparison to the above-mentioned targets for imaging of ER-positive BCs.

HER2-targeted BC imaging can be applied in HER2 positive BCs which account for approximately 15% of the BC population (98). This approach can be used to determine HER2 expression and to monitor response to treatment influencing HER2 expression. Similar to ER and PR radiotracers, determining HER2 expression with nuclear imaging can especially be beneficial in cases where biopsies cannot be obtained. Furthermore, as is the case for ER and PR, HER2 expression of primary tumors and metastases may change during the course of the disease (100).

CXCR4, FR and VEGF-A targeted nuclear imaging might be beneficial for basal like tumors, the BC subtype with the worse prognosis (98). CXCR4-mediated imaging in BC has not been successful up to date which might be caused by limited CXCR4 expression at the cell surface (necessary for radiotracer binding) or high CXCR4 expression in cancer stem cells of which only limited numbers are available in different BC subtypes (84). Furthermore, high FR and VEGF-A receptor expression was also associated with basal like tumors. Data on FR targeting in BC is very limited hampering discussion on the value of this radiotracer. VEGF-A is involved in angiogenesis, which explains its high correlation with the more aggressive basal like tumors, and thus VEGF-A radiotracers are applied for monitoring patients after antiangiogenic treatment.

VIP-R1 is expressed on all BCs and thus radiotracers targeting VIP-R1 might be interesting for all BC subtypes. However, VIP-R1 is only expressed in early stage disease limiting the use of this tracer in advanced BC.

A noteworthy option might be the combination of radiotracers directed against different targets, the so called multi-target or “cocktail” approach, with the purpose of enhancing BC visualization. Reubi et al. (42) studied expression of SSTR, GRPR, VIPR-1 and NPY1R in human BC specimens and reported that 60% of the tumors expressed at least 2 of the targets. In this study, GRPR, NPY1R

or both were expressed in almost all (93%) investigated BCs. Studies synthesizing and preclinically testing a hetero-bivalent dual target probe for GRPR and NPY1R were performed (101). Next to these studies, other preclinical studies have investigated the multi-targeting approach (102-104), but to date this was not tested in a clinical setting. A disadvantage of this approach might be enhanced or more extensive uptake in healthy organs which naturally express these targets.
Targeted nuclear imaging can be used for disease visualization (e.g. preoperative scanning) and monitoring of receptor positive tumors, for detection of sentinel lymph nodes containing malignant lesions, visualization of distant metastases and in some cases to evaluate treatment response. It is not the preferred imaging technique for screening, however.
Another benefit of targeted nuclear imaging is the use of radioligands for both imaging and therapy, following the so-called theranostic approach. Most of these radioligands can be labeled with imaging radionuclides (γ- or positron-emitters) as well as therapeutic radionuclides (ß- or α-emitters), enabling the use of the same tracer for both imaging and therapy in different sessions. This is especially interesting for treatment of advanced disease, since distant metastases are often not accessible for resection and most systemic agents are accompanied by severe side effects (3).
Furthermore, the use of dual labeled tracers that are labeled with both radionuclides and optical dyes are interesting for image-guided surgery. This can benefit surgical resection of tumors by offering preoperative imaging (SPECT or PET), intraoperative guidance (by making use of γ-probes detecting the radioactive signal to give an approximate tumor location), and fine guidance and tumor delineation (by detection of the optical signal), ultimately improving success-rate of tumor resection.
Overall, targeted nuclear imaging for BC imaging is promising and has the potential to improve BC care. There is not one appropriate target for all BCs, and thus a personalized approach should be applied. Depending on the BC subtype and the question of the physician, the appropriate target should be selected carefully (either by biopsy or imaging, depending on the availability of biopsy material). More studies are needed to directly compare the value of tracers targeting different receptors in specific patient groups, for example GRPR, SSTR, ER, PR and NPY1R targeted imaging in ER-positive BCs.

REFERENCES

1. Ali S, Coombes RC. Endocrine-responsive breast cancer and strategies for combating resistance. Nat Rev Cancer. 2002;2:101-112.
2. Perou CM, Sorlie T, Eisen MB, et al. Molecular portraits of human breast tumours. Nature. 2000;406:747-752.
3. Lu J, Steeg PS, Price JE, et al. Breast cancer metastasis: challenges and opportunities. Cancer Res. 2009;69:4951-4953.
4. Patlak M, Nass SJ, Henderson IC, Lashof JC, eds. Mammography and Beyond: Developing Technologies for the Early Detection of Breast Cancer: A Non-Technical Summary. Washington (DC): Institute of Medicine (US) and National Research Council Committee on the Early Detection of Breast Cancer. National Academies Press (US); 2001.
5. Mahoney MC, Newell MS. Screening MR imaging versus screening ultrasound: pros and cons. Magn Reson Imaging Clin N Am. 2013;21:495-508.
6. Nelson HD, O'Meara ES, Kerlikowske K, Balch S, Miglioretti D. Factors Associated With Rates of False-Positive and False-Negative Results From Digital Mammography Screening: An Analysis of Registry Data. Ann Intern Med. 2016;164:226-235.
7. Orel SG, Schnall MD. MR imaging of the breast for the detection, diagnosis, and staging of breast cancer. Radiology. 2001;220:13-30.
8. Berg WA, Bandos AI, Mendelson EB, Lehrer D, Jong RA, Pisano ED. Ultrasound as the Primary Screening Test for Breast Cancer: Analysis From ACRIN 6666. J Natl Cancer Inst. 2016;108.
9. Ambrosini V, Campana D, Tomassetti P, Fanti S. 68Ga-labelled peptides for diagnosis of gastroenteropancreatic NET. Eur J Nucl Med Mol Imaging. 2012;39 Suppl 1:S52-60.
10. Bison SM, Konijnenberg MW, Melis M, et al. Peptide receptor radionuclide therapy using radiolabeled somatostatin analogs: focus on future developments. Clin Transl Imaging. 2014;2:55-66.
11. Buck AK, Nekolla S, Ziegler S, et al. SPECT/CT. J Nucl Med. 2008;49:1305-1319.
12. von Schulthess GK, Steinert HC, Hany TF. Integrated PET/CT: current applications and future directions. Radiology. 2006;238:405-422.
13. Patton JA, Turkington TG. SPECT/CT physical principles and attenuation correction. J Nucl Med Technol. 2008;36:1-10.
14. Ziegler SI. Positron Emission Tomography: Principles, Technology, and Recent Developments. Nuclear Physics A. 2005;752:679c-687c.
15. Kalinyak JE, Berg WA, Schilling K, Madsen KS, Narayanan D, Tartar M. Breast cancer detection using high-resolution breast PET compared to whole-body PET or PET/CT. Eur J Nucl Med Mol Imaging. 2014;41:260-275.
16. Hsu DF, Freese DL, Levin CS. Breast-Dedicated Radionuclide Imaging Systems. J Nucl Med. 2016;57 Suppl 1:40S-45S.
17. Reubi JC, Waser B, Foekens JA, Klijn JG, Lamberts SW, Laissue J. Somatostatin receptor incidence and distribution in breast cancer using receptor autoradiography: relationship to EGF receptors. Int J Cancer. 1990;46:416-420.
18. Orlando C, Raggi CC, Bianchi S, et al. Measurement of somatostatin receptor subtype 2 mRNA in breast cancer and corresponding normal tissue. Endocr Relat Cancer. 2004;11:323-332.
19. van Eijck CH, Krenning EP, Bootsma A, et al. Somatostatin-receptor scintigraphy in primary breast cancer. Lancet. 1994;343:640-643.

20. Bajc M, Ingvar C, Palmer J. Dynamic indium-111-pentetreotide scintigraphy in breast cancer. J Nucl Med. 1996;37:622-626.

21. Chiti A, Agresti R, Maffioli LS, et al. Breast cancer staging using technetium-99m sestamibi and indium-111 pentetreotide single-photon emission tomography. Eur J Nucl Med. 1997;24:192-196.

22. Vural G, Unlu M, Atasever T, Ozur I, Ozdemir A, Gokcora N. Comparison of indium-111 octreotide and thallium-201 scintigraphy in patients mammographically suspected of having breast cancer: preliminary results. Eur J Nucl Med. 1997;24:312-315.

23. Alberini JL, Meunier B, Denzler B, et al. Somatostatin receptor in breast cancer and axillary nodes: study with scintigraphy, histopathology and receptor autoradiography. Breast Cancer Res Treat. 2000;61:21-32.

24. Schulz S, Helmholz T, Schmitt J, Franke K, Otto HJ, Weise W. True positive somatostatin receptor scintigraphy in primary breast cancer correlates with expression of sst2A and sst5. Breast Cancer Res Treat. 2002;72:221-226.

25. Skanberg J, Ahlman H, Benjegard SA, et al. Indium-111-octreotide scintigraphy, intraoperative gamma-detector localisation and somatostatin receptor expression in primary human breast cancer. Breast Cancer Res Treat. 2002;74:101-111.

26. Van Den Bossche B, Van Belle S, De Winter F, Signore A, Van de Wiele C. Early prediction of endocrine therapy effect in advanced breast cancer patients using 99mTc-depreotide scintigraphy. J Nucl Med. 2006;47:6-13.

27. Wang F, Wang Z, Wu J, et al. The role of technetium-99m-labeled octreotide acetate scintigraphy in suspected breast cancer and correlates with expression of SSTR. Nucl Med Biol. 2008;35:665-671.

28. Su XH, He XJ, Wu H, et al. Complement of Tc-99m-octreotide scintimammography to mammography in evaluating breast cancers. Nuclear Science and Techniques. 2010;21:24-28.

29. Piperkova E. Somatostatin-receptor scintigraphy-a new diagnostic approach to primary breast cancer. Rentgenol radiol. 1996;35:44-48.

30. Dalm SU, Melis M, Emmering J, Kwekkeboom DJ, de Jong M. Breast cancer imaging using radiolabelled somatostatin analogues. Nucl Med Biol. 2016;43:559-565.

31. Dalm SU, Sieuwerts AM, Look MP, et al. Clinical Relevance of Targeting the Gastrin-Releasing Peptide Receptor, Somatostatin Receptor 2, or Chemokine C-X-C Motif Receptor 4 in Breast Cancer for Imaging and Therapy. J Nucl Med. 2015;56:1487-1493.

32. Kumar U, Grigorakis SI, Watt HL, et al. Somatostatin receptors in primary human breast cancer: quantitative analysis of mRNA for subtypes 1-5 and correlation with receptor protein expression and tumor pathology. Breast Cancer Res Treat. 2005;92:175-186.

33. Van Den Bossche B, D'Haeninck E, De Vos F, et al. Oestrogen-mediated regulation of somatostatin receptor expression in human breast cancer cell lines assessed with 99mTc-depreotide. Eur J Nucl Med Mol Imaging. 2004;31:1022-1030.

34. Rivera JA, Alturaihi H, Kumar U. Differential regulation of somatostatin receptors 1 and 2 mRNA and protein expression by tamoxifen and estradiol in breast cancer cells. J Carcinog. 2005;4:10.

35. Limouris GS, Poulantzas V, Trompoukis N, et al. Comparison of 111In-[DTPA0]Octreotide Versus Non Carrier Added 177Lu- [DOTA0,Tyr3]-Octreotate Efficacy in Patients With GEP-NET Treated Intra-arterially for Liver Metastases. Clin Nucl Med. 2016;41:194-200.

36. Dalm SU, Nonnekens J, Doeswijk GN, et al. Comparison of the Therapeutic Response to Treatment with a 177Lu-Labeled Somatostatin Receptor Agonist and Antagonist in Preclinical Models. J Nucl Med. 2016;57:260-265.

37. Wild D, Fani M, Fischer R, et al. Comparison of somatostatin receptor agonist and antagonist for peptide receptor radionuclide therapy: a pilot study. J Nucl Med. 2014;55:1248-1252.

38. Wild D, Fani M, Behe M, et al. First clinical evidence that imaging with somatostatin receptor antagonists is feasible. J Nucl Med. 2011;52:1412-1417.

39. Cescato R, Waser B, Fani M, Reubi JC. Evaluation of 177Lu-DOTA-sst2 antagonist versus 177Lu-DOTA-sst2 agonist binding in human cancers in vitro. J Nucl Med. 2011;52:1886-1890.

40. Ginj M, Zhang H, Waser B, et al. Radiolabeled somatostatin receptor antagonists are preferable to agonists for in vivo peptide receptor targeting of tumors. Proc Natl Acad Sci U S A. 2006;103:16436-16441.

41. Reubi JC, Wenger S, Schmuckli-Maurer J, Schaer JC, Gugger M. Bombesin receptor subtypes in human cancers: detection with the universal radioligand (125)I-[D-TYR(6), beta-ALA(11), PHE(13), NLE(14)] bombesin(6-14). Clin Cancer Res. 2002;8:1139-1146.

42. Reubi C, Gugger M, Waser B. Co-expressed peptide receptors in breast cancer as a molecular basis for in vivo multireceptor tumour targeting. Eur J Nucl Med Mol Imaging. 2002;29:855-862.

43. Gugger M, Reubi JC. Gastrin-releasing peptide receptors in non-neoplastic and neoplastic human breast. Am J Pathol. 1999;155:2067-2076.

44. Dalm SU, Martens JW, Sieuwerts AM, et al. In vitro and in vivo application of radiolabeled gastrin-releasing peptide receptor ligands in breast cancer. J Nucl Med. 2015;56:752-757.

45. Mansi R, Wang X, Forrer F, et al. Evaluation of a 1,4,7,10-tetraazacyclododecane-1,4,7,10-tetraacetic acid-conjugated bombesin-based radioantagonist for the labeling with single-photon emission computed tomography, positron emission tomography, and therapeutic radionuclides. Clin Cancer Res. 2009;15:5240-5249.

46. Prignon A, Nataf V, Provost C, et al. (68)Ga-AMBA and (18)F-FDG for preclinical PET imaging of breast cancer: effect of tamoxifen treatment on tracer uptake by tumor. Nucl Med Biol. 2015;42:92-98.

47. Parry JJ, Andrews R, Rogers BE. MicroPET imaging of breast cancer using radiolabeled bombesin analogs targeting the gastrin-releasing peptide receptor. Breast Cancer Res Treat. 2007;101:175-183.

48. Maina T, Bergsma H, Kulkarni HR, et al. Preclinical and first clinical experience with the gastrin-releasing peptide receptor-antagonist [68Ga]SB3 and PET/CT. Eur J Nucl Med Mol Imaging. 2016;43:964-973.

49. Stoykow C, Erbes T, Maecke HR, et al. Gastrin-releasing Peptide Receptor Imaging in Breast Cancer Using the Receptor Antagonist (68)Ga-RM2 And PET. Theranostics. 2016;6:1641-1650.

50. Kiesewetter DO, Kilbourn MR, Landvatter SW, Heiman DF, Katzenellenbogen JA, Welch MJ. Preparation of Four Fluorine-18-labeled Estrogens and Their Selective Uptakes in Target Tissues of Immature Rats. J Nucl Med. 1984;25:1212-1221.

51. Mintun MA, Welch MJ, Siegel BA, et al. Breast cancer: PET imaging of estrogen receptors. Radiology. 1988;169:45-48.

52. Peterson LM, Mankoff DA, Lawton T, et al. Quantitative imaging of estrogen receptor expression in breast cancer with PET and 18F-fluoroestradiol. J Nucl Med. 2008;49:367-374.

53. Mortimer JE, Dehdashti F, Siegel BA, Katzenellenbogen JA, Fracasso P, Welch MJ. Positron emission tomography with 2-[18F]Fluoro-2-deoxy-D-glucose and 16alpha-[18F]fluoro-17beta-estradiol in breast cancer: correlation with estrogen receptor status and response to systemic therapy. Clin Cancer Res. 1996;2:933-939.

54. Dehdashti F, Mortimer JE, Siegel BA, et al. Positron tomographic assessment of estrogen receptors in breast cancer: comparison with FDG-PET and in vitro receptor assays. J Nucl Med. 1995;36:1766-1774.

55. Dehdashti F, Mortimer JE, Trinkaus K, et al. PET-based estradiol challenge as a predictive biomarker of response to endocrine therapy in women with estrogen-receptor-positive breast cancer. Breast Cancer Res Treat. 2009;113:509-517.

56. Linden HM, Stekhova SA, Link JM, et al. Quantitative fluoroestradiol positron emission tomography imaging predicts response to endocrine treatment in breast cancer. J Clin Oncol. 2006;24:2793-2799.

57. Mortimer JE, Dehdashti F, Siegel BA, Trinkaus K, Katzenellenbogen JA, Welch MJ. Metabolic flare: indicator of hormone responsiveness in advanced breast cancer. J Clin Oncol. 2001;19:2797-2803.

58. Dehdashti F, Flanagan FL, Mortimer JE, Katzenellenbogen JA, Welch MJ, Siegel BA. Positron emission tomographic assessment of "metabolic flare" to predict response of metastatic breast cancer to antiestrogen therapy. Eur J Nucl Med. 1999;26:51-56.

59. Cunha S, Gano L, Morais GR, Thiemann T, Oliveira MC. Progesterone receptor targeting with radiolabelled steroids: an approach in predicting breast cancer response to therapy. J Steroid Biochem Mol Biol. 2013;137:223-241.

60. Fowler AM, Clark AS, Katzenellenbogen JA, Linden HM, Dehdashti F. Imaging Diagnostic and Therapeutic Targets: Steroid Receptors in Breast Cancer. J Nucl Med. 2016;57 Suppl 1:75s-80s.

61. Dehdashti F, Laforest R, Gao F, et al. Assessment of progesterone receptors in breast carcinoma by PET with 21-18F-fluoro-16alpha,17alpha-[(R)-(1'-alpha-furylmethylidene)dioxy]-19-norpregn- 4-ene-3,20-dione. J Nucl Med. 2012;53:363-370.

62. Waseda N, Kato Y, Imura H, Kurata M. Effects of tamoxifen on estrogen and progesterone receptors in human breast cancer. Cancer Res. 1981;41:1984-1988.

63. Fowler AM, Chan SR, Sharp TL, et al. Small-animal PET of steroid hormone receptors predicts tumor response to endocrine therapy using a preclinical model of breast cancer. J Nucl Med. 2012;53:1119-1126.

64. Chan SR, Fowler AM, Allen JA, et al. Longitudinal noninvasive imaging of progesterone receptor as a predictive biomarker of tumor responsiveness to estrogen deprivation therapy. Clin Cancer Res. 2015;21:1063-1070.

65. Dijkers EC, Oude Munnink TH, Kosterink JG, et al. Biodistribution of 89Zr-trastuzumab and PET imaging of HER2-positive lesions in patients with metastatic breast cancer. Clin Pharmacol Ther. 2010;87:586-592.

66. Perik PJ, Lub-De Hooge MN, Gietema JA, et al. Indium-111-labeled trastuzumab scintigraphy in patients with human epidermal growth factor receptor 2-positive metastatic breast cancer. J Clin Oncol. 2006;24:2276-2282.

67. Tamura K, Kurihara H, Yonemori K, et al. 64Cu-DOTA-trastuzumab PET imaging in patients with HER2-positive breast cancer. J Nucl Med. 2013;54:1869-1875.

68. Mortimer JE, Bading JR, Colcher DM, et al. Functional imaging of human epidermal growth factor receptor 2-positive metastatic breast cancer using (64)Cu-DOTA-trastuzumab PET. J Nucl Med. 2014;55:23-29.

69. Gaykema SB, Schroder CP, Vitfell-Rasmussen J, et al. 89Zr-trastuzumab and 89Zr-bevacizumab PET to evaluate the effect of the HSP90 inhibitor NVP-AUY922 in metastatic breast cancer patients. Clin Cancer Res. 2014;20:3945-3954.

70. Gaykema SB, de Jong JR, Perik PJ, et al. (111)In-trastuzumab scintigraphy in HER2-positive metastatic breast cancer patients remains feasible during trastuzumab treatment. Mol Imaging. 2014;13.

71. Behr T, Behe M, Angerstein C, et al. Does pretherapeutic immunoscintigraphy allow for diagnostic predictions with respect to the toxicity and therapeutic efficacy of cold immunotherapy with trastuzumab (Herceptin)? J Nucl Med. 2000;41:73.

72. Baum RP, Prasad V, Muller D, et al. Molecular imaging of HER2-expressing malignant tumors in breast cancer patients using synthetic 111In- or 68Ga-labeled affibody molecules. J Nucl Med. 2010;51:892-897.

73. Sorensen J, Sandberg D, Sandstrom M, et al. First-in-human molecular imaging of HER2 expression in breast cancer metastases using the 111In-ABY-025 affibody molecule. J Nucl Med. 2014;55:730-735.

74. Vaneycken I, Devoogdt N, Van Gassen N, et al. Preclinical screening of anti-HER2 nanobodies for molecular imaging of breast cancer. Faseb J. 2011;25:2433-2446.

75. Xavier C, Blykers A, Vaneycken I, et al. (18)F-nanobody for PET imaging of HER2 overexpressing tumors. Nucl Med Biol. 2016;43:247-252.

76. Vaidyanathan G, McDougald D, Choi J, et al. Preclinical Evaluation of 18F-Labeled Anti-HER2 Nanobody Conjugates for Imaging HER2 Receptor Expression by Immuno-PET. J Nucl Med. 2016;57:967-973.

77. Keyaerts M, Xavier C, Heemskerk J, et al. Phase I Study of 68Ga-HER2-Nanobody for PET/CT Assessment of HER2 Expression in Breast Carcinoma. J Nucl Med. 2016;57:27-33.

78. Varmira K, Hosseinimehr SJ, Noaparast Z, Abedi SM. An improved radiolabelled RNA aptamer molecule for HER2 imaging in cancers. J Drug Target. 2014;22:116-122.

79. Necela BM, Crozier JA, Andorfer CA, et al. Folate receptor-alpha (FOLR1) expression and function in triple negative tumors. PLoS One. 2015;10:e0122209.

80. Fisher RE, Siegel BA, Edell SL, et al. Exploratory study of 99mTc-EC20 imaging for identifying patients with folate receptor-positive solid tumors. J Nucl Med. 2008;49:899-906.

81. Muller A, Homey B, Soto H, et al. Involvement of chemokine receptors in breast cancer metastasis. Nature. 2001;410:50-56.

82. Nimmagadda S, Pullambhatla M, Stone K, Green G, Bhujwalla ZM, Pomper MG. Molecular imaging of CXCR4 receptor expression in human cancer xenografts with [64Cu]AMD3100 positron emission tomography. Cancer Res. 2010;70:3935-3944.

83. Fu P, Tian L, Cao X, Li L, Xu P, Zhao C. Imaging CXCR4 Expression with (99m)Tc-Radiolabeled Small-Interference RNA in Experimental Human Breast Cancer Xenografts. Mol Imaging Biol. 2016;18:353-359.

84. Vag T, Gerngross C, Herhaus P, et al. First Experience with Chemokine Receptor CXCR4-Targeted PET Imaging of Patients with Solid Cancers. J Nucl Med. 2016;57:741-746.

85. Morgat C, Mishra AK, Varshney R, Allard M, Fernandez P, Hindie E. Targeting neuropeptide receptors for cancer imaging and therapy: perspectives with bombesin, neurotensin, and neuropeptide-Y receptors. J Nucl Med. 2014;55:1650-1657.

86. Reubi JC, Gugger M, Waser B, Schaer JC. Y(1)-mediated effect of neuropeptide Y in cancer: breast carcinomas as targets. Cancer Res. 2001;61:4636-4641.

87. Khan IU, Zwanziger D, Bohme I, et al. Breast-cancer diagnosis by neuropeptide Y analogues: from synthesis to clinical application. Angew Chem Int Ed Engl. 2010;49:1155-1158.

88. Hofmann S, Maschauer S, Kuwert T, Beck-Sickinger AG, Prante O. Synthesis and in vitro and in vivo evaluation of an (18)F-labeled neuropeptide Y analogue for imaging of breast cancer by PET. Mol Pharm. 2015;12:1121-1130.

89. Liu L, Xu Q, Cheng L, et al. NPY1R is a novel peripheral blood marker predictive of metastasis and prognosis in breast cancer patients. Oncol Lett. 2015;9:891-896.

90. Fuckar D, Dekanic A, Stifter S, et al. VEGF expression is associated with negative estrogen receptor status in patients with breast cancer. Int J Surg Pathol. 2006;14:49-55.

91. Gaykema SB, Brouwers AH, Lub-de Hooge MN, et al. 89Zr-bevacizumab PET imaging in primary breast cancer. J Nucl Med. 2013;54:1014-1018.

92. Terwisscha van Scheltinga AG, Berghuis P, Nienhuis HH, et al. Visualising dual downregulation of insulin-like growth factor receptor-1 and vascular endothelial growth factor-A by heat shock protein 90 inhibition effect in triple negative breast cancer. Eur J Cancer. 2014;50:2508-2516.

93. Reubi JC. In vitro identification of vasoactive intestinal peptide receptors in human tumors: implications for tumor imaging. J Nucl Med. 1995;36:1846-1853.

94. Zhang K, Aruva MR, Shanthly N, et al. Vasoactive intestinal peptide (VIP) and pituitary adenylate cyclase activating peptide (PACAP) receptor specific peptide analogues for PET imaging of breast cancer: In vitro/in vivo evaluation. Regul Pept. 2007;144:91-100.

95. Jagoda EM, Aloj L, Seidel J, et al. Comparison of an 18F labeled derivative of vasoactive intestinal peptide and 2-deoxy-2-[18F]fluoro-D-glucose in nude mice bearing breast cancer xenografts. Mol Imaging Biol. 2002;4:369-379.

96. Thakur ML, Zhang K, Berger A, et al. VPAC1 receptors for imaging breast cancer: a feasibility study. J Nucl Med. 2013;54:1019-1025.

97. Virgolini I, Kurtaran A, Raderer M, et al. Vasoactive intestinal peptide receptor scintigraphy. J Nucl Med. 1995;36:1732-1739.

98. Makki J. Diversity of Breast Carcinoma: Histological Subtypes and Clinical Relevance. Clin Med Insights Pathol. 2015;8:23-31.

99. De Marchi T, Foekens JA, Umar A, Martens JW. Endocrine therapy resistance in estrogen receptor (ER)-positive breast cancer. Drug Discov Today. 2016;21:1181-1188.

100. Aurilio G, Disalvatore D, Pruneri G, et al. A meta-analysis of oestrogen receptor, progesterone receptor and human epidermal growth factor receptor 2 discordance between primary breast cancer and metastases. Eur J Cancer. 2014;50:277-289.

101. Shrivastava A, Wang SH, Raju N, Gierach I, Ding H, Tweedle MF. Heterobivalent dual-target probe for targeting GRP and Y1 receptors on tumor cells. Bioorg Med Chem Lett. 2013;23:687-692.

102. Aranda-Lara L, Ferro-Flores G, Ramirez Fde M, et al. Improved radiopharmaceutical based on 99mTc-Bombesin-folate for breast tumour imaging. Nucl Med Commun. 2016;37:377-386.

103. Ji T, Sun Y, Chen B, et al. The diagnostic role of 99mTc-dual receptor targeted probe and targeted peptide bombesin (RGD-BBN) SPET/CT in the detection of malignant and benign breast tumors and axillary lymph nodes compared to ultrasound. Hell J Nucl Med. 2015;18:108-113.

104. Liu Z, Yan Y, Liu S, Wang F, Chen X. (18)F, (64)Cu, and (68)Ga labeled RGD-bombesin heterodimeric peptides for PET imaging of breast cancer. Bioconjug Chem. 2009;20:1016-1025.

Part 2

GRPR, SSTR2 and CXCR4 as Targets for Nuclear Imaging and Therapy of Breast Cancer

Chapter 3

Clinical Relevance of Targeting the Gastrin-Releasing Peptide Receptor, Somatostatin Receptor 2, or Chemokine C-X-C Motif Receptor 4 in Breast Cancer for Imaging and Therapy

S.U. Dalm[1], A.M. Sieuwerts[2], M.P. Look[2], M. Melis[1], C.H.M. van Deurzen[3], J.A. Foekens[2], M. de Jong[1] and J.W.M. Martens[2]

[1]Dept. of Radiology & Nuclear Medicine, Erasmus MC, Rotterdam, The Netherlands; [2]Dept. of Medical Oncology and Cancer Genomics Netherlands, Erasmus MC Cancer Institute, Erasmus MC, Rotterdam, The Netherlands; and [3]Dept. of Pathology, Erasmus MC, Rotterdam, The Netherlands

Adapted from J Nucl Med 2015; 56(10):1487-93

ABSTRACT

Imaging and therapy using radioligands targeting receptors overexpressed on tumor cells is successfully applied in neuroendocrine tumor patients. Because expression of the gastrin-releasing peptide receptor (GRPR), somatostatin receptor 2 (SSTR2), and chemokine C-X-C motif receptor 4 (CXCR4) has been demonstrated in breast cancer (BC), targeting these receptors using radioligands might offer new imaging and therapeutic opportunities for BC patients. The aim of this study was to correlate messenger RNA (mRNA) expression of *GRPR, SSTR2,* and *CXCR4* with clinicopathologic and biologic factors, and with prognosis and prediction to therapy response, in order to identify specific BC patient groups suited for the application of radioligands targeting these receptors.
Methods: First, we studied GRPR and SSTR2 expression in 13 clinical BC specimens by in vitro autoradiography and correlated this with corresponding mRNA levels to investigate whether mRNA levels reliably represent cell surface expression. Next, *GRPR, SSTR2,* and *CXCR4* mRNA levels were measured by quantitative reverse transcriptase polymerase chain reaction in 915 primary BC tissues and correlated with known clinicopathologic and biologic factors, disease-free survival, distant metastasis-free survival, and overall survival (DFS, MFS, and OS, respectively). In 224 adjuvant hormonal treatment-naïve estrogen receptor (ER, *ESR1*)-positive patients who received tamoxifen as first-line therapy for recurrent or metastatic disease, the expression levels of the receptors were correlated with progression-free survival.
Results: Our results showed a significant positive correlation between GRPR and SSTR2 expression analyzed by in vitro autoradiography and by quantitative reverse transcriptase polymerase chain reaction (Spearman's rank correlation coefficient [R_s]=0.94, $P<0.001$, and $R_s=0.73$, $P=0.0042$, respectively). Furthermore, high *GRPR* and *SSTR2* mRNA levels were observed more frequently in *ESR1*-positive specimens, whereas high *CXCR4* expression was associated with *ESR1*-negative specimens. Also, high mRNA expression of *CXCR4* was associated with a prolonged DFS, MFS, and OS (multivariate hazard ratio MFS=0.76 [95% confidence interval, 0.64-0.90], $P=0.001$), whereas high mRNA levels of *GRPR* were associated with a prolonged progression-free survival after the start of first-line tamoxifen treatment (multivariate hazard ratio=0.68 [95% confidence interval, 0.48-0.97], $P=0.031$).
Conclusions: Our data indicates that imaging and therapy using GRPR or SSTR2 radioligands might especially be beneficial for *ESR1*-positive BC and CXCR4 radioligands for *ESR1*-negative BC.

Keywords:
Breast Cancer, GRPR, SSTR2, CXCR4, PRS/PRRT

INTRODUCTION

Breast cancer (BC) is the most common cancer found in women worldwide. An estimated 1.7 million new cases were diagnosed in 2012 worldwide, and 522,000 people died as a consequence of the disease, making it the fifth cause of death by cancer overall (1).
Multiple subtypes of BC exist, with different molecular characteristics such as the absence or presence of estrogen receptor (ER, *ESR1*), progesterone receptor (PR, *PGR*), and human epidermal growth factor 2 (HER2, *ERBB2*) (2). In the case of ER and HER2, these receptors also serve as therapeutic targets. ER-positive patients are treated with either aromatase inhibitors or ER antagonists, most commonly tamoxifen, whereas HER2-positive patients are often treated with the HER2-specific monoclonal antibody trastuzumab (2). However, in the recurrent or metastatic setting nearly all patients acquire resistance against tamoxifen and trastuzumab after an initial response (3,4).
Mammography is the standard method used for BC screening, in some cases supplemented with MR imaging or ultrasound (5). Unfortunately these methods may lead to false-positive and false-negative results (6,7). Because current imaging and the above-mentioned therapy options, in particular, have limitations and are not always successful, new imaging and therapeutic options are urgently needed.
Peptide receptor scintigraphy and peptide receptor radionuclide therapy are methods based on targeting receptors overexpressed on tumor cells using radioligands for diagnostic and therapeutic purposes. Within nuclear medicine, radiolabeled somatostatin (SST) analogs are most widely and successfully used for the localization, treatment, and evaluation of neuroendocrine tumors (8). These SST analogs bind to SST receptors (SSTR, especially SSTR2) overexpressed on tumor cells, enabling imaging when labeled with γ- or positron-emitters and therapy when labeled with β- or α-particle emitters. Currently, multiple radiolabeled SST analogs targeting SSTR2 are available and used in the clinic (9). In the past decade, imaging of BC patients using SSTR2 radioligands has been studied with varying results (10,11). Currently, considerably improved SSTR2-directed radiotracers and imaging equipment are available.
Other promising targeting radioligands for BC comprise of radiolabeled gastrin releasing peptide (GRP) analogs, earlier applied for the visualization and therapy of prostate cancer lesions, because significant GRP receptor (GRPR) levels are present in most primary prostate cancer tissues (12-14). Previous studies by Reubi et al. (15) showed a high expression of both SSTR2 and GRPR in BC. SSTR2 and high-density GRPR expression was found in 75% and 74% of BC cases, respectively.
Moreover, chemokine C-X-C motif receptor 4 (CXCR4) expression has been reported in most BCs. In a study by Salvucci et al. (16), in which 2,022 BC specimens were analyzed for CXCR4 expression using immunohistochemistry, 67% of invasive tumors showed high nuclear staining and 41% of tumors showed cytoplasmic staining (12). Promising radiolabeled peptide derivatives binding to CXCR4 have been synthesized to target these receptors (17,18).

So ^{68}Ga-pentixafor, a CXCR4 radioligand, has successfully been used in a clinical study for the imaging of multiple myeloma patients (19). Thus, these 3 promising categories of radiolabeled compounds could be of promise in BC patients.
Until now, little was known about the correlation between GRPR, SSTR2, and CXCR4 expression levels in BC lesions and important molecular and prognostic characteristics, such as hormone receptor expression, as well as the association of GRPR, SSTR2, and CXCR4 expression with disease-free survival, distant metastasis-free survival, or overall survival (DFS, MFS, and OS, respectively) and with progression-free survival (PFS) after endocrine treatment.
In this study, we first analyzed the correlation between messenger RNA (mRNA) levels and protein expression of GRPR and SSTR2. Subsequently, we analyzed the mRNA expression of *GRPR, SSTR2,* and *CXCR4* in human BC specimens. The aims of this study were to correlate *GRPR, SSTR2,* and *CXCR4* mRNA expression levels with clinicopathologic and biologic factors as well as with prognosis and outcome on tamoxifen therapy, to assess the potential impact of radioligands targeting these receptors for imaging and therapeutic purposes in BC, and to thereby identify patient subgroups that potentially would benefit from application of these radiopharmaceuticals.

MATERIALS AND METHODS

Human BC Cases

The study (MEC02·953) was approved by the Erasmus MC Medical Ethical Committee and adhered to the Code of Conduct of the Federation of Medical Scientific Societies in The Netherlands.
The primary BC tissue of 915 female patients (mean age±SD, 58±13 y) (684 M0 [no metastasis at diagnosis] lymph-node-negative [LNN], 194 M0 lymph-node-positive [LNP], 24 M1 LNP, and 13 patients with unknown nodal status at time of primary treatment) who visited the clinic between 1979 and 2000 were selected from the Erasmus MC fresh-frozen tissue bank as described before (20). The inclusion criteria and the determination of clinicopathologic and biologic factors are described in the supplemental data. GRPR, SSTR2, and CXCR4 expression was initially correlated with clinicopathologic and biologic factors in the LNN M0 patient group (n=194). A representative group of LNP tumors (n=194) was added to study the influence of positive nodal status on the correlation analyses. For prognosis, we focused our analyses on the cohort of 684 systemic treatment-naive patients with LNN disease; for prediction of therapy response, a cohort of 224 hormonal treatment-naive ER-positive patients who received tamoxifen as first-line therapy for recurrent or metastatic disease was analyzed. The clinicopathologic and biologic factors of the LNN M0 tumors are shown in *Table 1*, and clinicopathologic and biologic factors for the LNN and LNP M0 patient group and the ER-positive first-line tamoxifen-treated subcohort are shown in *Supplemental Tables 1A+1B*, respectively. Patients were censored at 120-mo follow-up after surgical removal of the primary tumor in the regression

analysis for DFS (283 events), MFS (241 events), and OS (223 events) and at 36 mo after the start of tamoxifen treatment for analysis of PFS (24 events). The study design is depicted in *Figure 1*.

RNA Isolation, Complementary DNA Synthesis, and Quantitative Reverse Transcriptase Polymerase Chain Reaction (RT-qPCR)

Tissue processing, RNA isolation, complementary DNA synthesis, and RT-qPCR were performed and normalized using the δ Cq method on the average of 3 reference genes (*HMBS*, *HPRT1*, and *TBP*) as described (21). All RNA samples that required more than 25 rounds of real-time PCR for detectable products of our 3 reference genes at a fixed input of 10 ng of total RNA and at a threshold of 0.1 were considered of insufficient quality and were excluded from further analysis. Target genes were quantified using the following intron-spanning Taqman probe-based gene expression assays (Applied BioSystems/Life Technologies): *GRPR*, Hs01055872 m1; *SSTR2*, Hs0099356 m1; and *CXCR4*, Hs00237052 m1, according to the manufacturer's instructions in a MX3000P Real-Time PCR System (Agilent). Genomic grade index (GGI), a gene expression pattern of histologic tumor grade, and *ESR1*, *PGR*, and *ERBB2* levels and status of the samples were already known based on quantification as previously described (22-24).

Radioligands and In Vitro Autoradiography

Peptide analogs targeting the SSTR2 and GRPR, DOTA-Tyr^3-octreotate (Mallinckrodt) and AMBA (BioSynthema), respectively, were radiolabeled with ^{111}In (Covidien), as previously described (25). Quenchers (10 mM methionine, 3.5 mM ascorbic acid, and 3.5 mM gentisic acid) were used to prevent radiolysis (26). Specific activity of both radiotracers was 50 MBq/nmol. Radiometal incorporation (>99%) and radiochemical purity (>90%) were measured by instant thin-layer chromatography on silica gel and high-pressure liquid chromatography as previously described (26).
The CXCR4 radioligand, pentixafor, available to us showed reduced receptor affinity when radiolabeled with ^{111}In, and thus satisfying in vitro autoradiography studies using this compound could not be performed.
In the in vitro autoradiography assay, tissue sections of 13 fresh-frozen BC specimens (10 μm) were incubated with 10^{-9} M ^{111}In-AMBA and ^{111}In-DOTA-Tyr^3-octreoate for 1 h, without and with 10^{-6} M unlabeled tracer as control for nonspecific binding. H69 (SSTR2-positive, GRPR-negative) and PC3 xenografts (GRPR-positive, SSTR2-negative) were used as controls. Results were quantified using OptiQuant software (Perkin Elmer), and the net percentage binding of added dose was calculated. The in vitro autoradiography assay and quantification of the results are described in more detail in the supplemental data.

Statistics

Statistical analyses are described in the supplemental data.

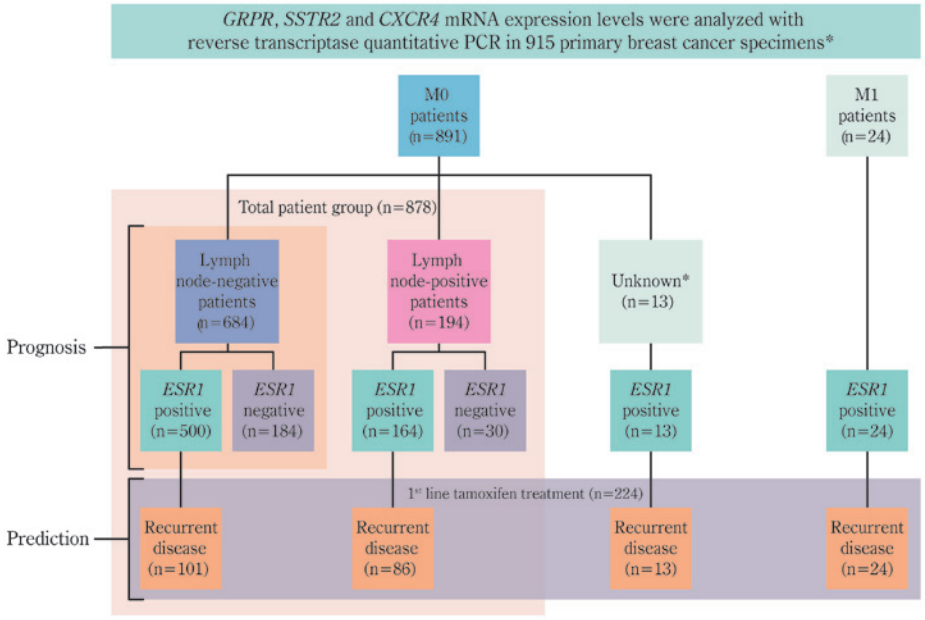

Figure 1. Study design. mRNA expression levels of GRPR, SSTR2, and CXCR4 of 915 primary breast cancer specimens (684 M0 LNN, 194 M0 LNP, 13 with unknown nodal status, and 24 M1) were analyzed using RT-qPCR. LNN and LNP M0 patient groups were used to study association of GRPR, SSTR2, and CXCR4 expression and clinicopathologic and biologic factors, with focus on M0 LNN patient group. Association of GRPR, SSTR2, and CXCR4 with prognostic factors was studied in M0 LNN patients. mRNA levels of ER-positive primary tumors of patients with recurrent breast cancer who received first-line tamoxifen treatment were used to study association of GRPR, SSTR2, and CXCR4 mRNA expression and PFS.

RESULTS

In Vitro Autoradiography and Correlation with mRNA Expression

Specific binding to tumor cells of the GRPR- and SSTR2-mediated radiotracers, ^{111}In-AMBA and ^{111}In-DOTA-Tyr^3-octreotate, respectively, was demonstrated using in vitro autoradiography on 13 selected human BC specimens with varying levels of mRNA receptor expression. Two mouse xenografts served as positive and negative control (*Figure 2A*). Autoradiography results were quantified and correlated with the level of mRNA expression of the respective receptors, resulting in a significant positive correlation for both GRPR (Spearman's rank correlation coefficient [R_s]= 0.94, $P<0.0001$) and SSTR2 ($R_s=0.73$, $P=0.0042$) (*Figure 2B*). Furthermore, binding of the tracers was observed only on tumor cells and not on the surrounding stromal cells. We thus concluded that mRNA expression for *GRPR* and *SSTR2* can be used as a predictor for binding of the radiotracers to tumor tissue.

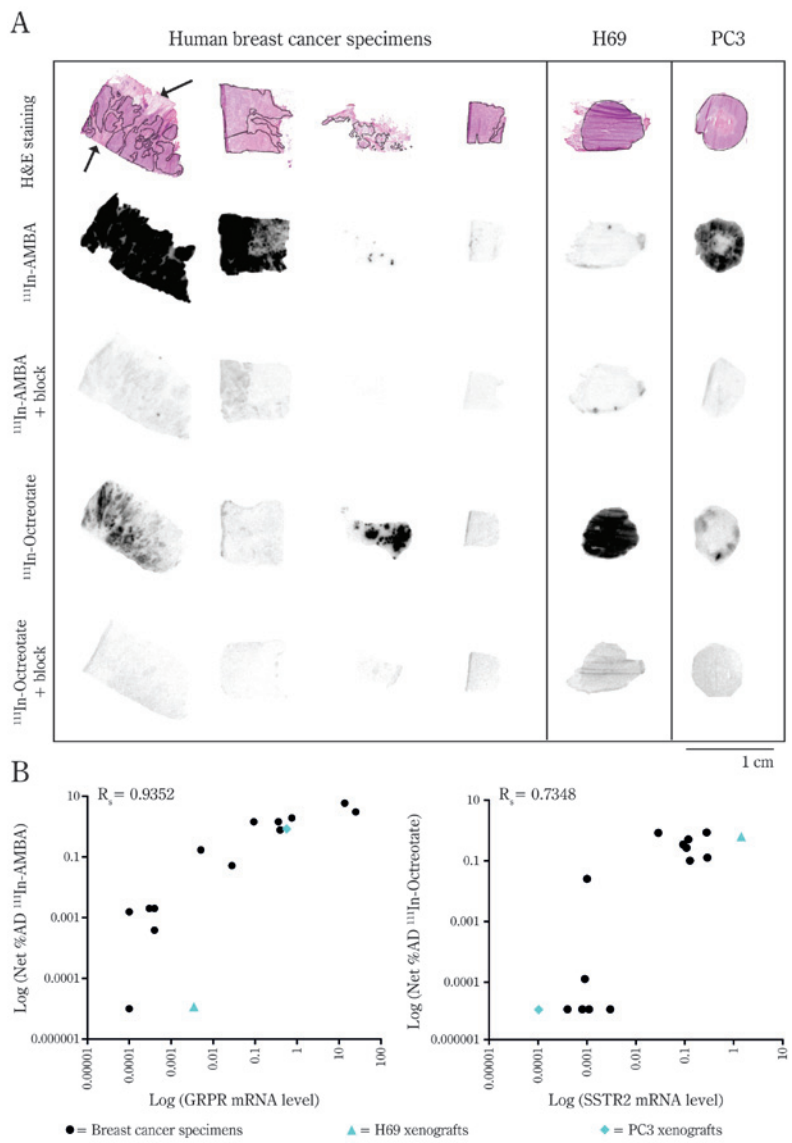

Figure 2. A) In vitro autoradiography of human breast cancer specimens using ^{111}In-AMBA (GRP analog) and ^{111}In-DOTA-Tyr^3-octreotate (SST analog) with and without block, demonstrating specific binding of radiotracers to receptor-positive tumor tissue. H69 (SSTR-positive, GRPR-negative) and PC3 xenografts (SSTR-negative, GRPR-positive) were used as controls. Tumor-containing areas are encircled in hematoxylin and eosin (H&E) stainings. As an example, arrows indicate non-tumor-containing tissue in first H&E staining. (B) Significant correlation between GRPR and SSTR2 mRNA levels and quantification of in vitro autoradiography results analyzed in 13 breast cancer specimens with variable receptor expression, demonstrating that mRNA levels of receptors can be used as predictor for radiotracer binding. %AD=percentage added dose.

Correlation of *GRPR*, *SSTR2*, and *CXCR4* mRNA Expression with Clinicopathologic and Biologic Factors

We focused on the 684 LNN M0 patients to study the correlation between *GRPR, SSTR2,* and *CXCR4* mRNA levels and known clinicopathologic and biologic factors. The results of the correlation analyses are shown in *Table 1*. To study the influence of positive nodal status on the correlation analyses, a representative group of 194 LNP M0 tumors were added to the study. Results of the LNN and LNP M0 patient group are described in *Supplemental Table 1A*.

A significant correlation was observed between *GRPR* mRNA levels and a smaller pathologic tumor size ($P=0.0014$), a positive *ESR1* ($P<0.001$) and *PGR* status ($P<0.001$), a negative *ERBB2* ($P<0.001$) status, and a favorable GGI ($P<0.001$). *SSTR2* mRNA expression showed a significant correlation with a positive *ESR1* ($P<0.001$) and *PGR* mRNA status ($P<0.001$), a negative *ERBB2* status ($P=0.0344$), favorable GGI ($P<0.001$), and 70% or less invasive tumor cells ($P=0.002$).

CXCR4 mRNA expression showed a significant negative correlation with *ESR1* ($P<0.001$) and *PGR* mRNA status ($P<0.001$) and was associated with an unfavorable GGI ($P<0.001$). Furthermore, *CXCR4* mRNA levels were higher in tumors with 70% or less invasive tumor cells ($P<0.001$).

Table 1. Associations of GRPR, SSTR2, and CXCR4 mRNA levels in LNN M0 patients

Characteristic	No of patients*		*GRPR* mRNA (x10^{-2}) Median	*GRPR* mRNA (x10^{-2}) Inter-quartile range	*SSTR2* mRNA (x10^{-2}) Median	*SSTR2* mRNA (x10^{-2}) Inter-quartile range	*CXCR4* mRNA (x10^{-2}) Median	*CXCR4* mRNA (x10^{-2}) Inter-quartile range
All patients in this cohort	**684**	**100%**	**0.72**	**7.07**	**0.58**	**1.75**	**11.78**	**13.13**
Age at surgery (years)								
≤40	60	9%	1.17	12.72	0.90	2.99	14.06	13.75
41-55	252	37%	0.97	9.20	0.61	1.64	11.58	13.18
56-70	218	32%	0.52	5.38	0.52	1.68	12.19	11.34
>70	154	23%	0.72	4.44	0.62	1.61	9.99	12.98
P†			*0.52*		*0.68*		***0.0403***	
Menopausal status								
Premenopausal	273	40%	1.26	10.95	0.62	1.82	11.81	13.73
Postmenopausal	411	60%	0.60	4.87	0.55	1.57	11.76	12.12
P†			*0.13*		*0.53*		*0.39*	
Surgery								
Lumpectomy	378	55%	0.61	7.69	0.57	1.82	11.67	13.15
Ablation	306	45%	0.90	6.79	0.60	1.56	11.90	13.00
P†			*0.69*		*0.59*		*0.65*	

Table 1. Continued

Characteristic	No of patients*		*GRPR* mRNA (x10^{-2}) Median	*GRPR* mRNA (x10^{-2}) Inter-quartile range	*SSTR2* mRNA (x10^{-2}) Median	*SSTR2* mRNA (x10^{-2}) Inter-quartile range	*CXCR4* mRNA (x10^{-2}) Median	*CXCR4* mRNA (x10^{-2}) Inter-quartile range
All patients in this cohort	**684**	**100%**	**0.72**	**7.07**	**0.58**	**1.75**	**11.78**	**13.13**
Pathological tumor size								
pT1	307	45%	1.25	8.54	0.69	1.87	12.03	13.40
pT2+unknown	351	51%	0.41	5.25	0.51	1.65	11.53	12.84
pT3 + pT4	26	4%	0.58	3.05	0.50	1.38	12.19	13.53
P†			***0.0014***		*0.24*		*0.92*	
***ESR1* mRNA status‡**								
Negative <0.2	184	27%	0.09	0.13	0.28	0.42	14.74	13.83
Positive ≥0.2	500	73%	2.46	10.98	0.81	2.59	10.98	12.16
P‡			***<0.001***		***<0.001***		***<0.001***	
***PGR* mRNA status‡**								
Negative <0.1	285	42%	0.12	0.32	0.32	0.56	14.36	14.31
Positive ≥0.1	399	58%	3.67	12.68	1.02	2.98	10.45	11.09
P‡			***<0.001***		***<0.001***		***<0.001***	
***ERBB2* mRNA status‡**								
Negative <18	574	84%	0.99	8.28	0.61	1.92	11.64	12.96
Positive ≥18	107	16%	0.30	1.51	0.49	1.00	13.88	13.32
P§			***<0.001***		***0.0344***		*0.22*	
Grade (GGI)								
1	227	33%	2.42	10.46	0.75	2.11	10.83	11.03
2	229	33%	0.89	6.92	0.63	2.41	11.44	14.59
3	224	33%	0.13	1.42	0.34	0.98	13.83	13.58
P§			***<0.001***		***<0.001***		***<0.001***	
% Invasive tumor cells								
≤ 70%	470	69%	0.81	6.84	0.63	1.88	12.57	13.92
>70%	214	31%	0.64	8.28	0.43	1.28	9.13	10.70
P†			*0.87*		***0.002***		***<0.001***	

* *Because of missing numbers, not all categories add up to 684.*
† *P for Mann-Whitney U or Kruskal-Wallis test when appropriate.*
‡ *ESR1, PGR, and ERBB2 were determined by real-time PCR; cut points were as follows: ESR1=0.2, PGR=0.1, and ERBB2=18.0 (mRNA level relative to reference gene set).*
§ *P for Spearman rank-correlation test.*

Association of *GRPR, SSTR2,* and *CXCR4* mRNA Expression with Prognosis and Efficacy of Tamoxifen Treatment

To exclude the possible confounding effect of adjuvant therapy on prognosis, the association of *GRPR, SSTR2,* and *CXCR4* expression with prognosis was evaluated in the LNN patient group, which did not receive adjuvant systemic therapy. The results of the evaluation of *GRPR, SSTR2,* and *CXCR4* mRNA expression with DFS, MFS, and OS are shown in *Supplemental Table 2*.

No significant associations were observed between *GRPR* and *SSTR2* mRNA expression and DFS, MFS, or OS. For *CXCR4,* however, there was a significant association of its expression with a favorable DFS, MFS, and OS, both when analyzed as a continuous variable and when dichotomized at the median level. For the primary endpoint MFS, the results of the multivariate analysis were hazard ratio (HR)=0.76 (95% confidence interval [CI], 0.64-0.90), P=0.001, when analyzed as a continuous variable, and HR=0.71 (95% CI, 0.55-0.91), P=0.011, when dichotomized at the median level.

To visualize the association of the levels of *CXCR4* mRNA with MFS, Kaplan-Meier analysis was performed as a function of the quartile levels of *CXCR4* mRNA (*Figure 3*). The results show a clear trend of quartiles, with lower expression having a worse MFS time.

In addition, *GRPR, SSTR2,* and *CXCR4* mRNA expression levels were correlated with the efficacy of tamoxifen treatment in *ESR1*-positive patients with recurrent disease (*Supplemental Table 1B*). There was a significant correlation between high *GRPR* mRNA levels and prolonged PFS after the start of first-line

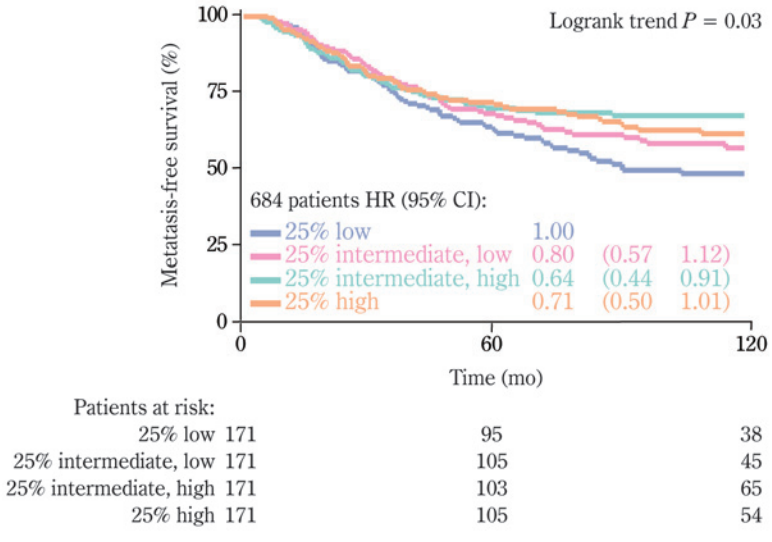

Figure 3. Distant MFS in 684 LNN patients as function of levels of CXCR4. CI=confidence interval; HR=hazard ratio.

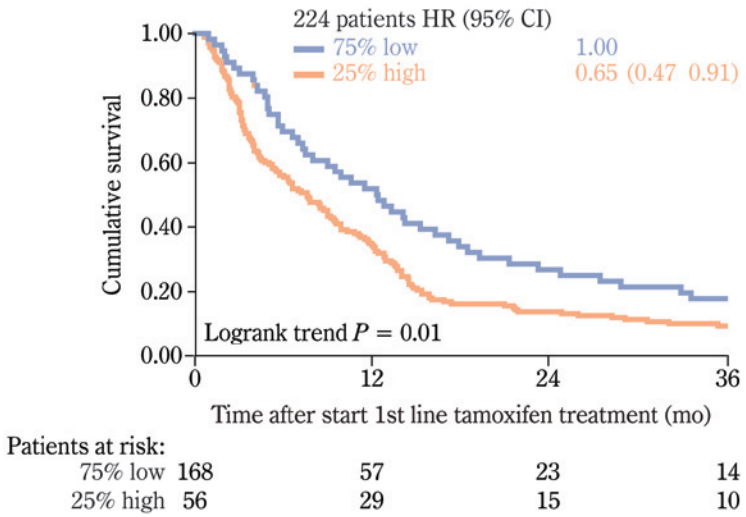

Figure 4. Association of GRPR expression with PFS on first-line tamoxifen treatment. CI=confidence interval; HR= hazard ratio.

tamoxifen treatment, indicating that *GRPR* expression has predictive value for the efficacy of tamoxifen therapy (*Figure 4; Supplemental Table 3*) (25% high vs. 75% low, univariate HR=0.65 [95% CI, 0.47-0.91], P=0.011, and multivariate HR=0.68 [95% CI, 0.48-0.97], P=0.031).

DISCUSSION

We have analyzed *GRPR, SSTR2,* and *CXCR4* mRNA expression in 915 primary BC tissues and correlated mRNA expression of these receptors with clinicopathologic and biologic factors and with prognosis and prediction to therapy response, to study the relevance of the application of radioligands targeting these receptors for imaging and therapy in BC patients. For this, we first successfully demonstrated in vitro binding of radiotracers for GRPR and SSTR2 to tissue sections and showed a significant positive correlation between radiotracer binding and mRNA expression, demonstrating that mRNA levels of these receptors can be used as a predictor for specific radiotracer binding. The CXCR4 radioligand pentixafor, available to us, showed reduced receptor affinity when radiolabeled with ^{111}In for in vitro autoradiography purposes, hampering reliable in vitro autoradiography studies for CXCR4. Thus, studies correlating CXCR4 radiotracer binding and *CXCR4* mRNA expression could not be performed. However, because Philip-Abbrederis et al. (19) reported on detecting *CXCR4* mRNA expression in cell lines and successful in vivo imaging of corresponding xenograft models using ^{68}Ga-pentixafor, we concluded that *CXCR4* mRNA expression can also be used as a predictor for CXCR4 radioligand binding.

Concerning prognosis, we found no association between *GRPR* and *SSTR2* expression and DFS, MFS, and OS in the M0 LNN patients. Surprisingly, we found that high *CXCR4* levels correlated with better prognosis despite its negative correlation with ER, PR, and unfavorable GGI, indicating that a component of CXCR4 expression that is independent of these factors determines good outcome.

Other studies on CXCR4 expression in BC have associated CXCR4 expression with poor patient survival (16). The discrepancy in study outcome might be explained by the fact that in our study we analyzed mRNA expression of the receptors (independent of receptor localization), whereas in the study by Salvucci et al. (16) tissue microarrays were analyzed by immunohistochemistry and nuclear and cytoplasmatic CXCR4 staining were analyzed separately. In agreement with our study, Salvucci et al. (16) reported more cytoplasmic CXCR4 staining in ER-negative (54%) than ER-positive tumors (38%).

Furthermore, we found that high *GRPR* expression was of modest predictive value for increased time to progression on tamoxifen treatment, suggesting GRPR radioligands to be useful in monitoring tumor response to treatment with tamoxifen. Recently, preclinical ^{68}Ga-AMBA PET imaging in a mouse model also demonstrated the feasibility for monitoring tumor response after treatment with tamoxifen (27).

For the association with clinicopathologic and biologic characteristics analyzed in the M0 LNN patients, we observed a significant positive correlation between *GRPR* and *SSTR2* expression and *ESR1*- and *PGR*-positive tumors. In line with our findings, significant positive correlation between SSTR2 and ER expression was reported previously (28), whereas van den Bossche et al. (29) reported estrogen-mediated regulation of SSTR2 expression in BC cell lines. Because *ESR1* and *PGR* positivity correlates with BC of the luminal subtype (2), tumors of this subtype could benefit most from GRPR- or SSTR2-mediated imaging or therapy. Moreover, *ESR1*-negative tumors showed low to no *GRPR* expression, and thus patients with *ESR1*-negative primary tumors are likely not suited for the application of GRPR radioligands. Because *ESR1*- or *PGR*-positive tumors account for 75% of the BC tumors (2), GRPR- and SSTR2-mediated imaging and therapy might be of benefit for the larger part of the BC patient population.

Concerning therapy, GRPR or SSTR2 radioligands can especially be of benefit for patients with *ESR1*-positive tumors who have progressed on various lines of endocrine treatment, because nearly all patients with recurrent disease become resistant against current antiestrogen treatments (4).

Previous studies we performed on GRPR and SSTR2 expression in human BC specimens showed GRPR expression in 48 of 50 (30) and SSTR2 expression in 26 of 53 (SU Dalm, CHM van Deurzen, M Melis, M de Jong, unpublished data, 2014) of the specimens analyzed by in vitro autoradiography, emphasizing that GRPR- and SSTR2-mediated imaging and therapy could be applied in a large group of breast cancer patients.

Contrary to *GRPR* and *SSTR2*, high *CXCR4* mRNA expression was correlated with *ESR1*- and *PGR*-negative tumors, associated with BC of the basal like subtype (2), indicating that these tumors, in particular, might be suitable for CXCR4-mediated imaging or therapy. Patients with triple-negative tumors, especially, might benefit from CXCR4-mediated therapy, because effective therapy options

for this aggressive subtype of BC are scarce. Differences in *CXCR4* expression between *ESR1*- and *PGR*-negative and *ESR1*-and *PGR*-positive patients were less pronounced than for *GRPR* and *SSTR2*. *ESR1*- and *PGR*-positive patients should therefore not be ruled out for CXCR4-mediated imaging or therapy.

Except for the presence of the receptors, for the selection of patients for imaging or treatment with radioligands, also the density of GRPR, SSTR2, and CXCR4 might determine the target of choice. In a study by Reubi et al. (15), among other receptors, GRPR and SSTR2 expression in 77 BC tissues was analyzed using in vitro autoradiography. Results showed that high-density GRPR expression was observed in 50 of 77 tumors, compared with 14 of 77 tumors with high-density SSTR2 expression. Similarly, in our previous work we found homogeneous GRPR expression in 56% of the BC specimens analyzed (30), whereas homogeneous SSTR2 expression was seen in 29% only (SU Dalm, CHM van Deurzen, M Melis, M de Jong, unpublished data, 2014).

One of the benefits of targeted imaging and therapy using GRPR, SSTR2, and CXCR4 radioligands is the possibility to upfront select patients who could benefit from these methods using one of the radioligands. For this, either frozen material from BC biopsies can be used to perform in vitro autoradiography with radioligands or formalin-fixed paraffin-embedded material can be used for immunohistochemistry, or both can be used to perform RT-qPCR, to identify patients suited for imaging or therapy.

There are, however, also limitations to our study. First, mRNA expression was used as a surrogate for radiotracer binding and ER, PGR, and HER2 protein expression, which may, despite our current and previously published data (22,23), turn out not to be entirely equivalent with protein expression. Second, for the prognostic part only, even though our study was relatively large no independent validation was performed. In addition, this is a retrospective study and might not completely represent the current situation in patients.

CONCLUSION

We successfully identified potential BC patient groups for the application of radio-ligands targeting GRPR, SSTR2, or CXCR4 by analyzing associations between receptor expression and clinicopathologic, biologic, and prognostic factors. Our data shows compelling evidence that sensitive and specific nuclear medicine-based imaging and therapy using radioligands might be of great benefit for selected BC patients in a personalized setting. GRPR and SSTR2 radioligands in ER-positive and PR-positive tumors and CXCR4 radioligands in ER-negative patients might offer new, promising tools for imaging and therapy of BC.

Supplemental data

Supplemental data is available online at http://jnm.snmjournals.org.

REFERENCES

1. International Agency on Research for Cancer. GLOBOCAN 2012: estimated cancer incidence, mortality and prevalence worldwide in 2012. International Agency on Research for Cancer website. http://globocan.iarc.fr/Default.aspx. Accessed August 18, 2015.
2. Yersal O, Barutca S. Biological subtypes of breast cancer: prognostic and therapeutic implications. World J Clin Oncol. 2014;5:412-424.
3. Brufsky AM. Current approaches and emerging directions in HER2-resistant breast cancer. Breast Cancer (Auckl). 2014;8:109-118.
4. Milani A, Geuna E, Mittica G, Valabrega G. Overcoming endocrine resistance in metastatic breast cancer: current evidence and future directions. World J Clin Oncol. 2014;5:990-1001.
5. Garcia EM, Storm ES, Atkinson L, Kenny E, Mitchell LS. Current breast imaging modalities, advances, and impact on breast care. Obstet Gynecol Clin North Am. 2013;40:429-457.
6. Mahoney MC, Newell MS. Screening MR imaging versus screening ultrasound: pros and cons. Magn Reson Imaging Clin N Am. 2013;21:495-508.
7. Hubbard RA, Kerlikowske K, Flowers CI, Yankaskas BC, Zhu W, Miglioretti DL. Cumulative probability of false-positive recall or biopsy recommendation after 10 years of screening mammography: a cohort study. Ann Intern Med. 2011;155:481-492.
8. Bison SM, Konijnenberg MW, Melis M, et al. Peptide receptor radionuclide therapy using radiolabeled somatostatin analogs: focus on future developments. Clin Transl Imaging. 2014;2:55-66.
9. Laznicek M, Laznickova A, Maecke HR. Receptor affinity and preclinical biodistribution of radiolabeled somatostatin analogs. Anticancer Res. 2012;32: 761-766.
10. Skånberg J, Ahlman H, Benjegard SA, et al. Indium-111-octreotide scintigraphy, intraoperative gamma-detector localisation and somatostatin receptor expression in primary human breast cancer. Breast Cancer Res Treat. 2002;74: 101-111.
11. Van Den Bossche B, Van Belle S, De Winter F, Signore A, Van de Wiele C. Early prediction of endocrine therapy effect in advanced breast cancer patients using 99mTc-depreotide scintigraphy. J Nucl Med. 2006;47:6-13.
12. Reubi JC, Maecke HR. Peptide-based probes for cancer imaging. J Nucl Med. 2008;49:1735-1738.
13. Wieser G, Mansi R, Grosu AL, et al. Positron emission tomography (PET) imaging of prostate cancer with a gastrin releasing peptide receptor antagonist- from mice to men. Theranostics. 2014;4:412-419.
14. Bodei L, Ferrari M, Nunn AD, et al. 177Lu-AMBA bombesin analogue in hormone refractory prostate cancer patients: a phase I escalation study with singlecycle administrations [abstract]. Eur J Nucl Med Mol Imaging. 2007;34:S221.
15. Reubi C, Gugger M, Waser B. Co-expressed peptide receptors in breast cancer as a molecular basis for in vivo multireceptor tumour targeting. Eur J Nucl Med Mol Imaging. 2002;29:855-862.
16. Salvucci O, Bouchard A, Baccarelli A, et al. The role of CXCR4 receptor expression in breast cancer: a large tissue microarray study. Breast Cancer Res Treat. 2006;97:275-283.
17. Hanaoka H, Mukai T, Tamamura H, et al. Development of a 111In-labeled peptide derivative targeting a chemokine receptor, CXCR4, for imaging tumors. Nucl Med Biol. 2006;33:489-494.
18. Demmer O, Dijkgraaf I, Schumacher U, et al. Design, synthesis, and functionalization of dimeric peptides targeting chemokine receptor CXCR4. J Med Chem. 2011;54:7648-7662.

19. Philipp-Abbrederis K, Herrmann K, Knop S, et al. In vivo molecular imaging of chemokine receptor CXCR4 expression in patients with advanced multiple myeloma. EMBO Mol Med. 2015;7:477-487.
20. Jansen MP, Sieuwerts AM, Look MP, et al. HOXB13-to-IL17BR expression ratio is related with tumor aggressiveness and response to tamoxifen of recurrent breast cancer: a retrospective study. J Clin Oncol. 2007;25:662-668.
21. Sieuwerts AM, Lyng MB, Meijer-van Gelder ME, et al. Evaluation of the ability of adjuvant tamoxifen-benefit gene signatures to predict outcome of hormonenaive estrogen receptor-positive breast cancer patients treated with tamoxifen in the advanced setting. Mol Oncol. 2014;8:1679-1689.
22. Toussaint J, Sieuwerts AM, Haibe-Kains B, et al. Improvement of the clinical applicability of the Genomic Grade Index through a qRT-PCR test performed on frozen and formalin-fixed paraffin-embedded tissues. BMC Genomics. 2009; 10:424.
23. van Agthoven T, Sieuwerts AM, Meijer-van Gelder ME, et al. Relevance of breast cancer antiestrogen resistance genes in human breast cancer progression and tamoxifen resistance. J Clin Oncol. 2009;27:542-549.
24. Sieuwerts AM, Usher PA, Meijer-van Gelder ME, et al. Concentrations of TIMP1 mRNA splice variants and TIMP-1 protein are differentially associated with prognosis in primary breast cancer. Clin Chem. 2007;53:1280- 1288.
25. de Blois E, Schroeder RJ, De Ridder CA, Van Weerden WM, Breeman WP, De Jong M. Improving radiopeptide pharmacokinetics by adjusting experimental conditions for bombesin receptor-mediated imaging of prostate cancer. Q J Nucl Med Mol Imaging. June 19, 2013 [Epub ahead of print].
26. de Blois E, Chan HS, Konijnenberg M, de Zanger R, Breeman WA. Effectiveness of quenchers to reduce radiolysis of 111In- or 177Lu-labelled methionine-containing regulatory peptides: maintaining radiochemical purity as measured by HPLC. Curr Top Med Chem. 2012;12:2677-2685.
27. Prignon A, Nataf V, Provost C, et al. 68Ga-AMBA and 18F-FDG for preclinical PET imaging of breast cancer: effect of tamoxifen treatment on tracer uptake by tumor. Nucl Med Biol. 2015;42:92-98.
28. Kumar U, Grigorakis SI, Watt HL, et al. Somatostatin receptors in primary human breast cancer: quantitative analysis of mRNA for subtypes 1-5 and correlation with receptor protein expression and tumor pathology. Breast Cancer Res Treat. 2005;92:175-186.
29. Van Den Bossche B, D'Haeninck E, De Vos F, et al. Oestrogen-mediated regulation of somatostatin receptor expression in human breast cancer cell lines assessed with 99mTc-depreotide. Eur J Nucl Med Mol Imaging. 2004; 31:1022-1030.
30. Dalm SU, Martens JW, Sieuwerts AM, et al. In-vitro and in-vivo application of radiolabeled gastrin releasing peptide receptor ligands in breast cancer. J Nucl Med. 2015;56:752-757.

Chapter 4

Prospects of Targeting the Gastrin Releasing Peptide Receptor, Chemokine C-X-C Motif Receptor 4 and Somatostatin Receptor 2 for Nuclear Imaging and Therapy in Metastatic Breast Cancer

S.U. Dalm[1], W.A.M.E. Schrijver[2], A.M. Sieuwerts[3], M.P. Look[3], A.C.J. Ziel - van der Made[4], V. de Weerd[3], J.W. Martens[2], P.J. van Diest[2], M. de Jong[1] and C.H.M. van Deurzen[3]

[1]Dept. of Radiology & Nuclear Medicine, Erasmus MC, Rotterdam, The Netherlands;
[2]Dept. of Pathology, University Medical Center Utrecht, Utrecht, The Netherlands;
[3]Dept. of Medical Oncology and Cancer Genomics Netherlands, Erasmus MC Cancer Institute, Erasmus MC, Rotterdam, The Netherlands; and
[4]Dept. of Pathology, Erasmus MC, Rotterdam, The Netherlands

Submitted to PLOS ONE, September 2016
Revised version accepted January 2017

ABSTRACT

The gastrin releasing peptide receptor (GRPR), chemokine C-X-C motif receptor type 4 (CXCR4) and somatostatin receptor 2 (SSTR2) are overexpressed on primary breast cancer (BC), making them ideal candidates for receptor-mediated nuclear imaging and therapy. The aim of this study was to determine whether these receptors are also suitable targets for metastatic BC.

Methods: mRNA expression of human BC samples were studied by in vitro autoradiography and associated with radioligand binding. Next, *GRPR*, *CXCR4* and *SSTR2* mRNA levels of 60 paired primary BCs and metastases from different sites were measured by quantitative reverse transcriptase polymerase chain reaction. Receptor mRNA expression levels were associated with clinicopathologic factors and expression levels of primary tumors and corresponding metastases were compared.

Results: Binding of GRPR and SSTR radioligands to tumor tissue correlated significantly with receptor mRNA expression. High *GRPR* and *SSTR2* mRNA levels were associated with estrogen receptor (*ESR1*)-positive tumors ($P<0.001$ for both receptors). High *GRPR* and *SSTR2* mRNA levels were associated with estrogen receptor (*ESR1*)-positive tumors ($P<0.001$ for both receptors). There was no significant difference in *GRPR* and *CXCR4* mRNA expression of primary tumors versus paired metastases. Regarding *SSTR2* mRNA expression, there was also no significant difference in the majority of cases, apart from liver and ovarian metastases which showed a significantly lower expression compared to the corresponding primary tumors ($P=0.02$ and $P=0.03$, respectively).

Conclusions: Targeting the GRPR, CXCR4 and SSTR2 for nuclear imaging and/or treatment has the potential to improve BC care in primary as well as metastatic disease.

Keywords:
GRPR, CXCR4, SSTR2, Metastatic Breast Cancer, Targeted Nuclear Imaging and Therapy

INTRODUCTION

Breast cancer (BC) is the second most common cancer found in women and the fifth cause of cancer related death (1). The disease is very heterogeneous. Different subtypes with distinctive morphological and molecular characteristics exist. The four major intrinsic BC subtypes are luminal A, luminal B, human epidermal growth factor 2 (HER2)-driven and basal-like BC (2,3). Treatment and prognosis of the disease are highly dependent on these subtypes; luminal A and luminal B tumors have a better prognosis than basal-like BC (2,3). Although multiple therapy options for BC exist, 20-30% of BC patients experience relapse with metastatic disease (4).

Peptide receptor scintigraphy and peptide receptor radionuclide therapy are methods successfully used in the clinic for imaging and treatment of neuroendocrine tumors (5). These methods are based on targeting receptors that are overexpressed on cancer cells using radiolabeled peptide analogues. Regarding BC, multiple studies have demonstrated overexpression of the gastrin releasing peptide receptor (GRPR), chemokine C-X-C motif receptor type 4 (CXCR4) and somatostatin receptor 2 (SSTR2). In line with this, several preclinical as well as clinical studies demonstrated feasibility of imaging and/or treatment of BC with GRPR and SSTR2 radioligands with promising results, and indicated specific BC patient groups that can benefit from the application of these radioligands (6-11).

However, previous studies were solely based on primary BC while BC-related death is largely caused by metastatic disease. Targeting the GRPR, CXCR4 and SSTR2 could thus especially be advantageous for treatment of metastatic BC.

In this study, we examined the *GRPR*, *CXCR4* and *SSTR2* mRNA expression levels of primary tumors and paired metastases, in order to evaluate whether nuclear imaging and therapy might also be beneficial for metastatic BC.

MATERIALS AND METHODS

Human BC Cases

Retrospectively, we selected 74 formalin-fixed paraffin-embedded (FFPE) primary BCs and 77 corresponding metastases from an existing database of the University Medical Center Utrecht and from the pathology archive of the Erasmus Medical Center (12,13). Fresh frozen (FF) tissue of 6 paired primary tumors and regional lymph node metastases were also included. Each specimen was reviewed by a pathologist (CvD) to confirm the presence of malignancy and to determine the percentage of tumor cells (cut-off point of >50% tumor cells). Inclusion criteria were: availability of clinicopathologic data, the presence of enough tumor tissue and good RNA quality to reliably determine Quantitative Reverse Transcriptase Polymerase Chain Reaction (RT-qPCR) levels. After applying these inclusion criteria, 68 primary tumors and 60 metastases remained, resulting in 60 paired primary BCs and metastases from different sites, including brain (n=12), regional lymph nodes (n=20), liver (n=10), ovary

(n=5), lung (n=5) and other sites (n=8, consisting of bone (n=2), uterus (n=1), gastrointestinal tract (n=2) and distant lymph node metastases (n=3)). Clinicopathologic characteristics included age, primary tumor size, histological subtype, histological grade according to Bloom & Richardson (14), estrogen receptor (ER) status, HER2 status, and regional lymph node status.
The use of anonymous or coded left over material for scientific purposes is part of the standard treatment agreement with patients and therefore informed consent was not required according to Dutch law (15,16).

RNA Isolation and RT-qPCR
Ten 10 µm slides were cut from the FFPE and 10×20 µm from the FF primary BCs and paired metastases. The first and last sections (5 µm) were stained with hematoxylin and eosin to guide macro-dissection of the tumor cells for RNA extraction. Total RNA was isolated from the macro-dissected FFPE sections with the AllPrep DNA/RNA FFPE Kit (Qiagen) and from the FF sections with RNA-B (Campro Scientific) according the manufacturer's instructions. Nucleic acid concentrations were measured with a Nanodrop 1000 system. cDNA was generated for 30 min at 48°C with RevertAid H minus (ThermoFisher Scientific) and gene-specific pre-amplified with Taqman PreAmp Master mix (ThermoFisher Scientific) for 15 cycles, followed by Taqman probe-based real time PCRs according the manufacturer's instructions in a MX3000P Real-Time PCR System (Agilent). The following gene expression assays were evaluated (all from ThermoFisher Scientific): *GRPR*, Hs01055872_m1; *CXCR4*, Hs00237052_m1; *SSTR2*, Hs0099356_m1; *ESR1*, Hs00174860_m1; *ERBB2*, Hs01001580_m1, and quantified relative to the average expression of *GUSB*, Hs9999908_m1; *HMBS*, Hs00609297_m1 and *TBP*, Hs00427620_m1 using the δ Cq method (δ Cq=2^(average Cq reference genes-Cq target gene)). Samples that resulted in amplifiable products within 25 cycles for this reference gene set at an input of 50 ng total RNA (91.2% of the samples) were considered to be of good quality to reliably determine RT-qPCR levels. Additional quality and quantity control measurements that were taken to ensure reliable RT-qPCR data analysis are described in the Supplementary text.
In this study, we used *ESR1* and *ERBB2* mRNA expression levels to determine ESR1 and ERBB2 status (using a cut-off δ Cq for *ESR1*>1 and *ERBB2*>3.5 by optimal binning for n=92 and n=87 overlapping samples, respectively. See *Supplemental Figure S1*.

Radioligands and In Vitro Autoradiography
The radiolabeled GRPR antagonist, JMV4168 (17), and the radiolabeled SSTR2 agonist, DOTA-Tyr^3-octreotate (Mallinckrodt) were radiolabeled with ^{111}In (Covidien) using quenchers to prevent radiolysis as previously described (18,19). Specific activity was 80 MBq/nmol for both radiotracers. Radiochemical purity and radiometal incorporation, measured by instant thin-layer chromatography on silica gel and high-pressure liquid chromatography as previously described, were >90% (19).
Slides (10 µM) of FF primary BC and paired metastases (n=6 each) were used for autoradiography experiments. Tissue sections were incubated with 100 µL incubation buffer containing 10^{-9} M of the radiolabeled peptide for 1 h, with and without 10^{-6} M unlabeled tracer to determine specificity of binding. Results of the autoradiography experiments were quantified using Optiquant (Perkin Elmer) and the percentage added dose (%AD) of the radioligand bound to the tumor tissue was used as an indirect measurement for the level of protein expression. Radioligand binding to primary tumors and paired metastasis was compared and correlated with the measured *GRPR* and *SSTR2* mRNA expression levels in corresponding FF tumor material. Furthermore, mRNA receptor expression measured in FF tumor material was correlated with mRNA receptor expression measured from FFPE tumor material of the same tumor. These correlation analyses were performed to demonstrate that mRNA expression of FFPE material could be used as a surrogate for radiotracer binding. The autoradiography experiments and quantification of the results were performed as described in the Supplementary text.
In vitro autoradiography experiments were not performed for CXCR4, since the CXCR4 radioligand available to us, pentixafor, showed reduced receptor affinity when radiolabeled with ^{111}In.

Statistics
For the analysis, the STATA statistical package v14.1 and SPSS version 23 were used. Variables were checked for normality prior to analysis. To compare mean values between two or more groups, the Student t-test or analysis of variance ANOVA were used. To compare values for primary and metastatic disease the paired t-test was applied. Pearson and Spearman correlations were calculated when appropriate. $P \leq 0.05$ were considered statistically significant.

RESULTS

In Vitro Autoradiography
Six pairs of primary BCs and regional lymph node metastases (n=12 samples) with varying mRNA receptor expression were analyzed for their ability to bind the GRPR radioligand, ^{111}In-JMV4168, and the SSTR2 radioligand, ^{111}In-DOTA-Tyr^3-octreotate, using in vitro autoradiography. *Figure 1A* shows the in vitro autoradiography results for four of the paired samples. From the six paired samples analyzed, two cases showed specific binding of the GRPR and SSTR2 radioligands in both the primary tumor and the lymph node metastases. In three cases there was no binding of GRPR and SSTR2 radioligands in both the primary tumors and the lymph node metastases. In one case binding of the GRPR radioligand was observed in the primary tumor but not in the lymph node metastasis, while binding of the SSTR2 radioligand was observed in the lymph node metastasis, but not in the primary tumor.
When the %AD of the radiotracer bound to the FF tumor tissue was correlated with the mRNA receptor expression of the FF tumor material, a significant positive correlation was found for both GRPR (Spearman R_s=0.83, P=0.0008)

and SSTR2 (Spearman R_s=0.87, P=0.0003) (*Figure 1B+D*). Furthermore, correlation analysis of mRNA receptor expression levels quantified in FF and FFPE material of the same tumor, resulted in a significant positive correlation for both *GRPR* (Spearman R_s=0.77, P=0.0034) and *SSTR2* (Spearman R_s=0.72, P=0.0082) (*Figure 1C+E*).

Association of *GRPR, CXCR4* and *SSTR2* mRNA Expression with Clinicopathologic Factors

Table 1 and *Supplemental Table S1* show the patient characteristics, including the association of *GRPR*, *CXCR4* and *SSTR2* mRNA expression of primary BCs with clinicopathologic factors. High *GRPR* mRNA expression levels were significantly associated with low histologic grade, lobular subtype, *ESR1*-positive and *ERBB2*-negative tumors. High *SSTR2* mRNA expression levels were also significantly associated with lobular subtype and *ESR1*-positive tumors. *CXCR4* mRNA expression of the primary BC showed no association with the studied clinicopathologic factors.

GRPR, *CXCR4* and *SSTR2* mRNA expression levels of the metastases were correlated with *ESR1* and *ERBB2* expression of the metastasis itself (*Table 2*). Similar to the primary tumors, high *GRPR* and *SSTR2* mRNA levels were significantly associated with *ESR1*-positive metastases. Furthermore, high *GRPR* mRNA status was significantly associated with *ERBB2*-negative metastases. Unlike the primary tumors, high *SSTR* mRNA levels were significantly associated with *ERBB2*-negative metastatic lesions. In line with the primary BCs studied, *CXCR4* mRNA expression levels of the metastases showed no significant association with *ESR1* and *ERBB2* status.

GRPR, CXCR4 and *SSTR2* mRNA Expression of Primary BC vs. Corresponding Metastases

Figure 2 shows the box plots of *GRPR*, *CXCR4* and *SSTR2* mRNA expression in primary tumors and corresponding metastases.

Comparison of receptor mRNA expression levels of primary tumors and corresponding metastases showed no significant difference in *GRPR* and *CXCR4* mRNA levels between primary tumors and corresponding regional lymph node and distant metastases in the brain, lung, liver and ovaries. However, in the group of metastases from other sites, *GRPR* mRNA expression levels were significantly lower in the metastases compared to the corresponding primary BC (P=0.02).

Regarding *SSTR2* mRNA levels, there were no significant differences in *SSTR2* mRNA expression of the primary tumor and the paired metastasis in regional lymph nodes, brain, lung and other locations. However, *SSTR2* mRNA levels of liver and ovarian metastases were significantly lower compared to the expression in the corresponding primary BC (P=0.02 and P=0.03, respectively).

Next, we compared the receptor mRNA expression levels between distant metastases from various metastatic sites amongst each other. *GRPR* mRNA levels were significantly higher in the ovarian metastases (P=0.03) and *CXCR4* mRNA expression levels were significantly higher in liver metastases (P=0.05).

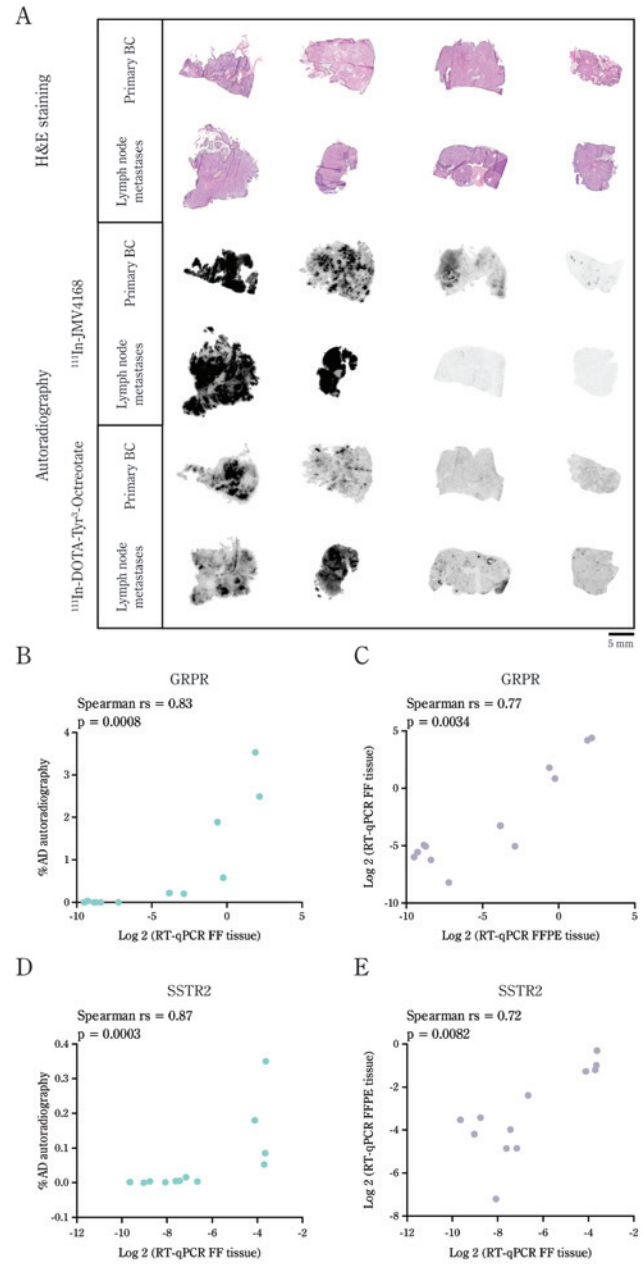

Figure 1. In vitro auto-radiography of primary BC and corresponding regional lymph node metastases. A) Hematoxylin and eosin (H&E) staining and autoradiography results after incubating cells with the GRPR radioligand, ^{111}In-JMV4168, and the SSTR2 radioligand, ^{111}In-DOTA-Tyr^3-Octreotate. B+D) Correlation of quantified auto-radiography results (%AD) with mRNA expression of fresh frozen (FF) tissue. C+E) Correlation of mRNA expression of FF and formalin fixed paraffin embedded (FFPE) tissue of the same tumor.

Table 1. Association of GRPR, CXCR4 and SSTR2 mRNA expression with clinicopathologic factors of primary BC *

Characteristic			*GRPR* mRNA log2		*CXCR4* mRNA log2		*SSTR2* mRNA log2	
	No of patients	Percentage of patients	Mean	SD	Mean	SD	Mean	SD
All patients in this cohort	**68**	**100**	**-2.90**	**3.8**	**0.48**	**0.88**	**-2.51**	**2.15**
Age at surgery (years)								
≤ 40	11	16	-1.63	4.02	0.34	1.10	-2.23	2.13
41-55	27	39	-1.96	3.75	0.53	0.89	-2.08	2.38
56-70	22	32	-4.96	2.85	0.29	0.80	-3.07	1.94
> 70	7	10	-2.72	4.32	1.09	0.67	-2.90	2.04
P†				*0.08*		*0.32*		*0.22*
Tumor size								
≤ 2 cm	25	36	-2.62	3.97	0.34	0.88	-2.61	2.24
2 ≤ 5 cm	29	42	-3.47	3.44	0.53	0.91	-2.32	2.16
> 5 cm	10	14	-2.00	4.22	0.53	0.89	-2.95	2.09
P‡				*0.51*		*0.70*		*0.72*
Histopathologic subtypes								
Ductal	55	80	-3.34	3.76	0.50	0.90	-2.82	2.15
Lobular	11	16	-0..80	3.44	0.49	0.84	-1.04	1.74
Other	2	3	-2.38	3.72	-0.32	0.14	-2.04	1.26
P§				***0.04***		*0.96*		***0.01***
Bloom & Richardson grade								
I + II	15	22	-1.23	3.57	0.18	0.86	-1.80	2.20
III	44	64	-3.66	3.91	0.62	0.89	-2.88	2.18
P¶				***0.04***		*0.10*		*0.12*
***ESR1* status**								
Negative	25	36	-6.52	1.68	0.54	0.90	-3.83	2.09
Positive	42	61	-0.79	3.04	0.41	0.87	-1.79	1.80
P¶				***<0.001***		*0.58*		***<0.001***
***ERBB2* status**								
Negative	46	67	-2.12	3.60	0.50	0.89	-2.44	2.26
Positive	11	16	-5.04	2.62	0.81	0.89	-2.7	2.23
P¶				*0.006*		*0.32*		*0.73*

Table 1. Continued

Characteristic			*GRPR* mRNA log2		*CXCR4* mRNA log2		*SSTR2* mRNA log2	
	No of patients	Percentage of patients	Mean	SD	Mean	SD	Mean	SD
All patients in this cohort	**68**	**100**	**-2.90**	**3.8**	**0.48**	**0.88**	**-2.51**	**2.15**
Regional lymph node status								
Negative	15	22	-4.40	3.06	0.66	1.01	-2.96	2.33
Positive	44	64	-2.67	4.02	0.40	0.82	-2.48	2.01
P¶				*0.13*		*0.33*		*0.44*

* *Due to missing values numbers don't always add up to 68.*
† *Receptor expression of ductal BC and lobular BC was compared using the student t-test.*
‡ *P for Pearson correlation.*
§ *P for variance of ANOVA.*
¶ *P for student t-test.*

There were no significant differences in *SSTR2* mRNA expression levels in distant metastases from different sites.
In some cases studied (n=11), there was a discordance regarding *ESR1* status of primary BCs and corresponding metastases. When studying the effect of change in *ESR1* status on receptor mRNA expression in primary tumors and paired metastasis, *GRPR* and *SSTR2* mRNA expression changed accordingly (higher *GRPR*/*SSTR2* mRNA expression in *ESR1*-positive lesions compared to *ESR1*-negative lesions) in the majority of the tumors. However, this difference was only significant ($P<0.05$) for *ESR1*-positive primary BCs with corresponding *ESR1*-negative metastases (n=6). Discordance regarding *ERBB2* status was seen in 6 paired samples. In these samples a change in *ERBB2* status of primary BCs and corresponding metastases did not have a consistent effect on GRPR mRNA expression levels.

DISCUSSION

Targeting of GRPR, CXCR4 and SSTR2 overexpressed on BC cells with radioligands can offer novel imaging and therapy options for BC. Previous clinical and preclinical studies reported promising results. However, these studies were restricted to primary BC, while metastases are the main cause of BC-related death. In this study, we compared *GRPR*, *CXCR4* and *SSTR2* mRNA expression levels in a unique dataset of primary BC and corresponding metastases to determine whether receptor-based imaging and/or therapy could also be useful for metastatic BC. For this purpose, we selected FFPE material of primary BCs and corresponding metastases from different sites, and compared mRNA

Table 2. Associations of receptor mRNA expression with ESR1 and ERBB2 status in BC metastases

	ER status					ERBB2 status				
	Negative		Positive		*P**	Negative		Positive		*P**
	Mean	SD	Mean	SD		Mean	SD	Mean	SD	
All metastases										
No of patients	24		35			48		11		
GRPR	-6.26	2.76	-1.87	3.90	***<0.001***	-2.67	3.77	-7.98	2.15	***<0.001***
CXCR4	0.27	1.28	0.29	1.07	*0.95*	0.17	1.14	0.74	1.13	*0.15*
SSTR2	-3.95	1.64	-2.89	2.23	***0.04***	-2.91	1.96	-5.11	1.49	***<0.001***
Regional lymph node metastases										
No of patients	4		16			16		4		
GRPR	-7.0	1.96	-1.70	3.53	***0.003***	-1.70	3.54	-7.02	1.84	***0.002***
CXCR4	0.04	0.91	0.14	0.90	*0.85*	0.10	0.88	0.21	1.00	*0.86*
SSTR2	-4.03	0.97	-2.92	2.67	*0.20*	-2.77	2.47	-4.62	1.92	*0.16*
All distant metastases†										
No of patients	20		19			32		7		
GRPR	-6.12	2.92	-2.01	4.27	***0.001***	-3.15	3.84	-8.52	2.26	***<0.001***
CXCR4	0.31	1.36	0.41	1.20	*0.82*	0.21	1.26	1.05	1.14	*0.12*
SSTR2	-3.94	1.76	-2.86	1.85	*0.07*	-2.98	1.69	-5.40	1.26	***0.001***

* *P for student t-test.*
† *Numbers do not add up to 60 because for 1 patient ESR1 and ERBB2 were unknown.*

receptor expression levels of the paired samples. Prior to this, we confirmed that mRNA expression levels of tumor tissue properly represent radioligand binding, by correlating in vitro autoradiography results with mRNA expression levels of selected primary tumors and corresponding metastases with varying mRNA receptor expression. This was only done for GRPR and SSTR2 because our CXCR4 radioligand could not be labelled with a radionuclide suited for in vitro autoradiography. However, based on a previous study by Philipp-Abbrederis et. al. (20), who reported on *CXCR4* mRNA expression in BC cell lines and CXCR4 targeted imaging of corresponding xenograft models, we assumed that *CXCR4* mRNA expression can be used as a surrogate for CXCR4 radioligand binding.
Next, we determined the *GRPR*, *CXCR4* and *SSTR2* mRNA expression of the paired primary BCs and metastases. When we associated receptor mRNA expression levels of primary BCs and metastases with clinicopathologic factors, we observed a significantly higher *GRPR* and *SSTR2* expression in both *ESR1*-

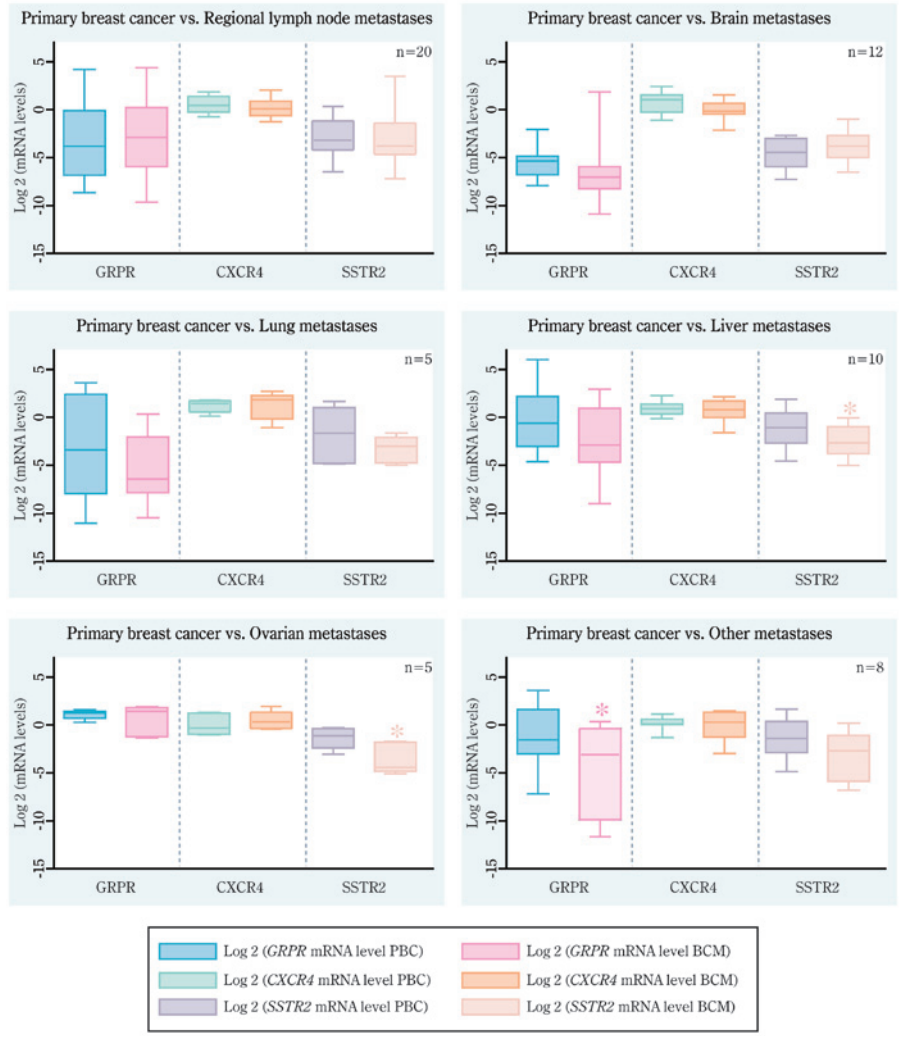

*Figure 2. GRPR, CXCR4 and SSTR2 mRNA levels in primary BC (PBC) and corresponding metastases (BCM). Significant differences are indicated by *.*

positive primary BC and metastases. These findings are in agreement with our previous findings (11) and findings by Kumar et. al. (21) and Stoykow et al. (7). The latter publication describes a clinical study in which the GRPR radioligand, ^{68}Ga-RM2 was successfully used for imaging of BC lesions and imaging success-rate associated positively with ER and PR status. Furthermore, Prignon et al. (22) demonstrated that ^{68}Ga-AMBA, a GRPR agonist, was better suited for monitoring response to hormonal treatment than ^{18}F-FDG PET in an ER-positive BC model. In another study, van den Bossche et al. (23) published data indicating an estrogen-dependent regulation of SSTR expression in BC cell lines. Since ER-positive BC accounts for approximately 75% of the BC population, applying

receptor targeted nuclear imaging and/or therapy using GRPR or SSTR2 radioligands could be beneficial for the majority of the BC population (2).
In contrast to our previous study we did not find a significant association of high *CXCR4* mRNA expression with *ESR1*-negative tumors. A potential explanation for this is the smaller sample size analyzed in this study. Nevertheless, CXCR4 might be a good candidate for targeting of ER-negative BCs, that usually have a poor prognosis (2).
In paired primary tumors and metastases a change in *ESR1* expression from positive to negative resulted in a significant decrease in *GRPR* and *SSTR2* mRNA levels. This may indicate an *ESR1* dependent expression of *GRPR* and *SSTR2,* which is consistent with literature (23,24). Difference in *ERBB2* status in primary tumors and paired metastasis did not show a clear effect on *GRPR* mRNA expression, although these numbers were too small for reliable conclusions.
Comparison of *GRPR*, *CXCR4* and *SSTR2* mRNA levels of primary tumors and corresponding metastasis resulted in similar *GRPR* and *CXCR4* mRNA expression in primary tumors and paired regional lymph nodes and distant metastases of the brain, lung, liver and ovaries. However, *GRPR* mRNA expression was significantly higher in primary tumors compared to corresponding metastases from other sites. Since this group is very diverse, containing metastases from distant lymph nodes, bone, uterus and metastases from the gastrointestinal tract, it is not possible to draw solid conclusions. Regarding *SSTR2*, mRNA expression levels were significantly lower in liver and ovarian metastases compared to the paired primary BC.
Combining our findings, both GRPR and SSTR2 are promising targets for nuclear imaging and/or therapy in primary and metastatic ER-positive BC, but GRPR seems more suitable due to its retained expression in the metastases. This finding is also supported by a previous study by our group, in which we demonstrated GRPR expression in 48/50 BCs (6), while SSTR2 was only expressed in 26/53 BCs (SU Dalm, CHM van Deurzen, M Melis, JW Martens and M de Jong, unpublished data, 2014).
Since a substantial portion of BC patients experience relapse with metastatic disease, it is important to develop new treatment options for this late stage of disease. We showed that receptor mRNA expression levels were similar in primary tumors and corresponding metastases in the majority of the cases, implying that targeting these receptors for disease monitoring or therapy might improve BC patient care.
Biopsy material or excised tumors can be used to determine receptor expression by immunohistochemistry, RNA in situ, in vitro autoradiography or RT-qPCR (25). Disease monitoring of receptor-positive tumors can then be performed by single photon emission computed tomography/computer tomography (SPECT/CT), positron emission tomography (PET)/CT or PET/magnetic resonance imaging using radioligands targeting these receptors. Also, dedicated breast PET cameras can be used. These dedicated cameras have improved sensitivity and specificity compared to whole body PET, because of a restricted field of view, resulting in higher cancer detection (26). Furthermore, tumors can be treated with therapeutic radioligands. Another option is to use GRPR, CXCR4 or SSTR2 radioligands for visualization of sentinel node metastases or as a guide for BC surgery (e.g. preoperative imaging, radioguided surgery) in patients with receptor positive primary tumors (27,28).
The next step would be to perform clinical studies to investigate the feasibility of imaging primary tumors and metastases with radioligands targeting these receptors. One important aspect is to study physiological uptake of the radioligands in other organs, since this is of great importance for successful nuclear imaging and treatment. However, previous studies using radioligands targeting these receptors on other tumor types did not report on any alarming physiological uptake (5,7,29).

CONCLUSION

The presented data indicates that nuclear based imaging and therapy has the potential to improve BC patient care in primary as well as in metastatic disease, by targeting GRPR, CXCR4 and SSTR2. Both GRPR and SSTR2 radioligands, but especially GRPR radioligands, are promising for imaging and treatment of ER-positive primary and metastatic BC. Furthermore, imaging and treatment of metastases derived from CXCR4-positive primary tumors using CXCR4 radioligands seems to be feasible.

Acknowledgements
The authors thank Natalie D. ter Hoeve and Erik de Blois for their technical assistance.

SUPPLEMENTAL DATA

Supplemental Methods

Quality and Quantity Control Measurements for Reliable Quantitative Reverse Transcriptase Polymerase Chain Reaction (RT-qPCR).
For reliable RT-qPCR measurements, only samples that resulted in amplifiable products within 25 cycles for the used reference gene set at an input of 50 ng total RNA (91.2% of the samples) were considered to be of good quality for reliable determination of RT-qPCR levels. Furthermore, a serially diluted fresh frozen (FF) and formalin fixed paraffin embedded (FFPE) breast tumor sample was included in each experiment to evaluate the linear amplification and efficiencies for all genes included in the panel, and absence of amplification in the absence of reverse transcriptase. All gene transcripts were 100% efficient amplified (range 89-113%) and were negative in the absence of reverse transcriptase. To ensure unbiased results from FF and FFPE samples, these 2 data sets were normalized

based on the expression levels measured in a set of n=13 matched FF-FFPE samples.

Estrogen Receptor (ER/*ESR1*) and Receptor Tyrosine-protein Kinase erbB-2 Status/Human Epidermal Growth Factor 2 (*ERBB2*/HER2) Status of the Investigated Samples

Because data regarding ER and HER2 protein expression of our data set was incomplete, *ESR1* and *ERBB2* mRNA expression was used to determine *ESR1* and *ERBB2* mRNA status (using a δ Cq cut-off for *ESR1*>1 and *ERBB2*>3.5 by optimal binning for n=92 and n=87 overlapping samples, respectively (*Figure S1*)). Because ER and HER2 are determined on protein level in daily clinical practice (using a scoring system according to national and international guidelines (30,31)), we investigated whether the *ESR1* and *ERBB2* mRNA status accurately reflected the ER and HER2 protein status as reported in the pathology reports in samples with known receptor protein status. These cut-offs resulted for *ESR1* in a sensitivity of 0.88 and specificity of 0.85 and for *ERBB2* in a sensitivity of 0.89 and specificity of 0.97.

In Vitro Autoradiography

Fresh frozen tumor sections (10 µm) were incubated with 100 µL 10^{-9} M of the radioligands for 1 h, without and with 10^{-6} M unlabeled tracer. Octreotide (Covidien) and Tyr^4-bombesin (Sigma-Aldrich) were used to block the somatostatin receptor and the gastrin releasing peptide receptor, respectively. Subsequently unbound radioligand was removed and slides were exposed to super-resolution phosphor screens (Perkin Elmer) for at least 24 h. Next, screens were read using the cyclone (Perkin Elmer) and the results were quantified using OptiQuant Software (Perkin Elmer). For this tumor containing regions, identified with the help of hematoxylin and eosin staining of adjacent tumor sections, were encircled and the digital light units/mm^2 (DLU/mm^2) were measured. Specific binding was determined by subtracting DLU/mm^2 of blocked tissue sections from the DLU/mm^2 of the unblocked sections ($DLU/mm^2_{unblocked}$ - $DLU/mm^2_{blocked}$ = $DLU/mm^2_{specific}$).

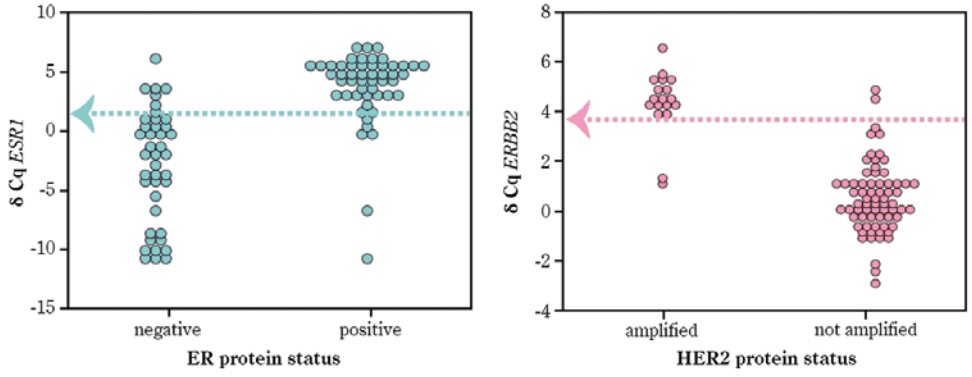

Figure S1. Correlation of ER and HER2 protein status with ESR1 and ERBB2 mRNA levels. Arrows indicate used cut-off value.

Standards containing 1 µL drops of the radiotracer solution were also quantified and used to determine the percentage of added dose that was bound to the tumors (%AD = ($DLU/mm^2_{specific}$ / ($DLU/mm^2_{standard}$ × 100)) × 100%).

*Table S1. Overview of clinicopathologic characteristics of the primary BC associated with the site of the paired metastases**

	RLN n=20		Brain n=12		Lung n=5		Liver n=10		Ovarian n=5		Other n=8			
Characteristic of primary tumor	**№**	**%**	**№**	**%**	**№**	**%**	**№**	**%**	**№**	**%**	**№**	**%**	**№**	**%**
Age at surgery (years)														
≤ 55	34	57	10	50	6	50	3	60	7	70	4	80	4	50
≥ 56	25	42	10	50	6	50	2	40	2	20	1	20	4	50
Tumor size														
< 2 - 5 cm	48	80	18	90	9	75	3	60	8	80	2	40	8	100
> 5 cm	9	15	2	10	1	8	1	20	2	20	3	60		
Histopathologic subtypes														
Ductal	50	83	16	80	11	92	5	100	10	100	2	40	6	75
Lobular	9	15	3	15	1	8					3	60	2	25
Other	1	2	1	5										
Bloom & Richardson grade														
I + II	12	20	3	15	2	17			4	40	2	40	1	13
III	40	67	16	80	10	83	4	80	5	50	2	40	3	38
***ESR1* mRNA status**														
Negative	21	35	9	45	8	67	2	40	1	10			1	13
Positive	38	63	11	55	4	33	3	60	8	80	5	100	7	88
***ERBB2* mRNA status**														
Negative	46	77	14	70	10	83	4	80	6	60	5	100	7	88
Positive	13	22	6	30	2	17	1	20	3	30			1	13

** Due to missing values and rounding off numbers do not add up to 100%.*
RLN = Regional lymphnode metastases.

REFERENCES

1. IACR. GLOBOCAN 2012: Estimated Cancer Incidence, Mortality and Prevalence Worldwide in 2012. http://globocan.iarc.fr/Default.aspx. Accessed 10-07, 2014.
2. Yersal O, Barutca S. Biological subtypes of breast cancer: Prognostic and therapeutic implications. World J Clin Oncol. 2014;5:412-424.
3. Perou CM, Sorlie T, Eisen MB, et al. Molecular portraits of human breast tumours. Nature. 2000;406:747-752.
4. Early Breast Cancer Trialists' Collaborative G. Effects of chemotherapy and hormonal therapy for early breast cancer on recurrence and 15-year survival: an overview of the randomised trials. Lancet. 2005;365:1687-1717.
5. Bison SM, Konijnenberg MW, Melis M, et al. Peptide receptor radionuclide therapy using radiolabeled somatostatin analogs: focus on future developments. Clin Transl Imaging. 2014;2:55-66.
6. Dalm SU, Martens JW, Sieuwerts AM, et al. In vitro and in vivo application of radiolabeled gastrin-releasing peptide receptor ligands in breast cancer. J Nucl Med. 2015;56:752-757.
7. Stoykow C, Erbes T, Bulla S, et al. Gastrin-releasing peptide receptor expression is associated with estrogen receptor status in breast cancer: Findings of a PET/CT pilot study (PW082). Annual Congress of the European Association of Nuclear Medicine. Hamburg, Germany; 2015, October 10-14.
8. Skanberg J, Ahlman H, Benjegard SA, et al. Indium-111-octreotide scintigraphy, intraoperative gamma-detector localisation and somatostatin receptor expression in primary human breast cancer. Breast Cancer Res Treat. 2002;74:101-111.
9. Van Den Bossche B, Van Belle S, De Winter F, Signore A, Van de Wiele C. Early prediction of endocrine therapy effect in advanced breast cancer patients using 99mTc-depreotide scintigraphy. J Nucl Med. 2006;47:6-13.
10. Azad BB, Chatterjee S, Lesniak WG, et al. A fully human CXCR4 antibody demonstrates diagnostic utility and therapeutic efficacy in solid tumor xenografts. Oncotarget. 2016;17:12344-12358.
11. Dalm SU, Sieuwerts AM, Look MP, et al. Clinical Relevance of Targeting the Gastrin-Releasing Peptide Receptor, Somatostatin Receptor 2, or Chemokine C-X-C Motif Receptor 4 in Breast Cancer for Imaging and Therapy. J Nucl Med. 2015;56:1487-1493.
12. Hoefnagel LD, van der Groep P, van de Vijver MJ, et al. Discordance in ERalpha, PR and HER2 receptor status across different distant breast cancer metastases within the same patient. Ann Oncol. 2013;24:3017-3023.
13. Schrijver WA, Jiwa LS, van Diest PJ, Moelans CB. Promoter hypermethylation profiling of distant breast cancer metastases. Breast Cancer Res Treat. 2015;151:41-55.
14. Bloom HJ, Richardson WW. Histological grading and prognosis in breast cancer; a study of 1409 cases of which 359 have been followed for 15 years. Br J Cancer. 1957;11:359-377.
15. FEDERA. Human Tissue and Medical Research: Code of conduct for responsible use (2011). 2011.
16. van Diest PJ. No consent should be needed for using leftover body material for scientific purposes. For. Bmj. 2002;325:648-651.
17. Marsouvanidis PJ, Nock BA, Hajjaj B, et al. Gastrin releasing peptide receptor-directed radioligands based on a bombesin antagonist: synthesis, (111)in-labeling, and preclinical profile. J Med Chem. 2013;56:2374-2384.

18. De Blois E, Schroeder RJ, De Ridder CA, Van Weerden WM, Breeman WP, De Jong M. Improving radiopeptide pharmacokinetics by adjusting experimental conditions for bombesin receptor-mediated imaging of prostate cancer. Q J Nucl Med Mol Imaging [epub]. 2013.
19. De Blois E, Chan HS, Konijnenberg M, de Zanger R, Breeman WA. Effectiveness of quenchers to reduce radiolysis of (111)In- or (177)Lu-labelled methionine-containing regulatory peptides. Maintaining radiochemical purity as measured by HPLC. Curr Top Med Chem. 2012;12:2677-2685.
20. Philipp-Abbrederis K, Herrmann K, Knop S, et al. In vivo molecular imaging of chemokine receptor CXCR4 expression in patients with advanced multiple myeloma. EMBO Mol Med. 2015;7:477-487.
21. Kumar U, Grigorakis SI, Watt HL, et al. Somatostatin receptors in primary human breast cancer: quantitative analysis of mRNA for subtypes 1-5 and correlation with receptor protein expression and tumor pathology. Breast Cancer Res Treat. 2005;92:175-186.
22. Prignon A, Nataf V, Provost C, et al. (68)Ga-AMBA and (18)F-FDG for preclinical PET imaging of breast cancer: effect of tamoxifen treatment on tracer uptake by tumor. Nucl Med Biol. 2015;42:92-98.
23. Van Den Bossche B, D'Haeninck E, De Vos F, et al. Oestrogen-mediated regulation of somatostatin receptor expression in human breast cancer cell lines assessed with 99mTc-depreotide. Eur J Nucl Med Mol Imaging. 2004;31:1022-1030.
24. Nagasaki S, Nakamura Y, Maekawa T, et al. Immunohistochemical analysis of gastrin-releasing peptide receptor (GRPR) and possible regulation by estrogen receptor betacx in human prostate carcinoma. Neoplasma. 2012;59:224-232.
25. Korner M, Waser B, Schonbrunn A, Perren A, Reubi JC. Somatostatin receptor subtype 2A immunohistochemistry using a new monoclonal antibody selects tumors suitable for in vivo somatostatin receptor targeting. Am J Surg Pathol. 2012;36:242-252.
26. Vercher-Conejero JL, Pelegri-Martinez L, Lopez-Aznar D, Cozar-Santiago Mdel P. Positron Emission Tomography in Breast Cancer. Diagnostics (Basel). 2015;5:61-83.
27. Mariani G, Erba P, Villa G, et al. Lymphoscintigraphic and intraoperative detection of the sentinel lymph node in breast cancer patients: the nuclear medicine perspective. J Surg Oncol. 2004;85:112-122.
28. Hindie E, Groheux D, Brenot-Rossi I, Rubello D, Moretti JL, Espie M. The sentinel node procedure in breast cancer: nuclear medicine as the starting point. J Nucl Med. 2011;52:405-414.
29. Lapa C, Luckerath K, Kleinlein I, et al. (68)Ga-Pentixafor-PET/CT for Imaging of Chemokine Receptor 4 Expression in Glioblastoma. Theranostics. 2016;6:428-434.
30. Breast Cancer Guideline, NABON 2012.
31. Wolff AC, Hammond ME, Hicks DG, Dowsett M, McShane LM, Allison KH, et al. Recommendations for human epidermal growth factor receptor 2 testing in breast cancer: American Society of Clinical Oncology/College of American Pathologists clinical practice guideline update. Arch Pathol Lab Med. 2014;138(2):241-56.

Part 3

SSTR-targeted Nuclear Imaging and Therapy

Chapter 5

Breast Cancer Imaging Using Radiolabeled Somatostatin Analogues

S.U. Dalm, M. Melis, J. Emmering, D.J. Kwekkeboom and M. de Jong

Dept. of Radiology & Nuclear Medicine, Erasmus MC, Rotterdam, The Netherlands

Nuclear Medicine and Biology 2016; 43(9):559-65

ABSTRACT

Imaging and therapy using radiolabeled somatostatin analogues are methods successfully used in patients with somatostatin receptor (SSTR)-expressing neuroendocrine tumors. Since these techniques were first introduced, many improvements have been made. SSTR expression has also been reported on breast cancer (BC). Currently mammography, magnetic resonance imaging and ultrasound are the most frequent methods used for BC imaging. Since SSTR expression on BC was demonstrated, clinical studies examining the feasibility of visualizing primary BC using SSTR radioligands have been performed. However, to date SSTR-mediated nuclear imaging is not used clinically in BC patients. The aim of this review is to assess whether recent improvements made within nuclear medicine may enable SSTR-mediated imaging to play a role in BC management. For this we critically analysed results of past studies and discussed the potential of the improvements made within nuclear medicine on SSTR-mediated nuclear imaging of BC.

Methods: Seven databases were searched for publications on BC imaging with SSTR radioligands. The papers found were analysed by 3 individual observers to identify whether the studies met the pre-set inclusion criteria defined as studies in which nuclear imaging using radiolabeled SST analogues was performed in patients with breast lesions. Twenty-four papers were selected for this review including studies on SSTR-mediated nuclear imaging in BC, neuroendocrine BC and other breast lesions.

Results: The analysed studies were heterogeneous with respect to the imaging method, imaging protocol, patient groups and the radiolabeled SST analogues used. Despite the fact that the analysed studies were heterogeneous, sensitivity for primary BC ranged from 36-100%. In a subset of the studies LN lesions were visualized, but sensitivity was lower compared to that for primary tumors. A part of the studies included benign lesions and specificity ranged from 22-100%. Furthermore, false negatives and false positives were reported. In the majority of the studies scan outcome was not associated with BC subtype.

Conclusions: The introduction of better imaging techniques, e.g. hybrid SPECT/CT, PET/CT using ^{68}Ga labelled SSTR radioligands and the development of dedicated breast cameras, have led to major improvements in the field of radionuclide imaging with regard to sensitivity and spatial resolution. Combining the improved imaging techniques with higher receptor affinity somatostatin analogues and careful selection of BC subtypes suited for SSTR-mediated imaging, might greatly improve nuclear imaging of BC using SSTR radioligands and could potentially provide a role for SSTR-mediated imaging in BC management.

Keywords:
Breast cancer, Nuclear Imaging, Somatostatin receptor, Somatostatin Receptor-mediated Imaging

INTRODUCTION

Breast cancer (BC) has the highest incidence and mortality rate of malignancies in women worldwide (1). The disease is highly heterogeneous; subtypes are characterized by molecular properties, such as estrogen receptor (ER) expression, that highly influence treatment and prognosis of the disease (2). BC diagnosis and classification is based on cytology (3). For detection, staging and monitoring of BC lesions several imaging techniques are applied. Mammography is used for nationwide BC screenings. The accuracy of this method is influenced by age and breast density, which may lead to false positive (6-10% per screening round) or false negative (0.1-0.15% per screening round) results (4,5). Other radiology-based methods applied include magnetic resonance imaging (MRI) and ultrasound (US). Both methods have limitations as well, as MRI is labor-intensive and US outcome is operator-dependent. Within nuclear medicine multiple methods have been described for BC imaging e.g. ^{18}F-FDG PET, and ^{99m}Tc-MIBI or ^{201}Th-scintigraphy. These methods vary in sensitivity and are not tumor-specific as they are based on accumulation of radioactive compounds in highly proliferative tissue (4,6).

Receptor-mediated nuclear imaging and therapy using radiolabeled somatostatin (SST) analogues is successfully applied in patients with neuroendocrine tumors (NETs) (7,8). In the late 1980s high somatostatin receptor (SSTR) expression was described on various NETs, after which radiolabeled SST analogues were synthesized to perform imaging and later on radionuclide therapy studies (9). In previous studies, SSTR expression was also demonstrated on BC. In 1990 Reubi et al. (10) demonstrated SSTR expression in 21% of small lesions and 46% of large tumors when BC specimens were analysed by in vitro autoradiography. Furthermore, Orlando et al. (11) reported lower expression of SSTR subtype 2 in normal breast tissue compared to malignant breast lesions. Also, studies have been performed demonstrating that high SSTR expression in BC tissue is positively correlated with ER and progesterone receptor (PR) expression, lymph node (LN) involvement, postmenopausal status and tumor grade (11,12).

From the 1990s several studies have been performed to examine the feasibility of visualization of primary (and metastatic) BC lesions using radiolabeled SST analogues; primarily ^{111}In- or ^{99m}Tc-labelled octreotide. Planar scintigraphy was the standard method of imaging, in some cases compared with single-photon emission computed tomography (SPECT) techniques. These studies showed variable results regarding specificity and sensitivity; and currently SSTR-mediated imaging is not a standard procedure to localize or stage BC. However, major improvements have been made in the field of nuclear imaging; the resolution of γ-imaging equipment has increased, sensitive and multimodal SPECT/computed tomography (CT) and positron emission tomography (PET)/CT platforms have been introduced, including dedicated breast cameras, SST analogues with higher affinity have been developed and new radionuclides for imaging are now available (13-16). Since the expression of SSTR is a prerequisite for successful SSTR-mediated imaging, the above mentioned improvements might especially be beneficial for breast tumors with low density SSTR expression.

Furthermore, our knowledge about BC and its different subtypes and their molecular profiles in association with SSTR expression has expanded, enabling us to better identify patient groups in which SSTR imaging can be of benefit.
The aim of this review is to assess whether the improvements made within the field of nuclear medicine, with respect to imaging modalities, radiolabeled peptide analogues and our knowledge about BC itself, may improve SSTR-mediated imaging of BC. For this, we critically analysed the past studies and their limitations, and discuss the potential influence of recent developments on SSTR-mediated nuclear imaging in BC and the possible role of this imaging method in BC patient care.

LITERATURE SEARCH STRATEGY

Seven databases (Embase, Medline OvidSP, Scopus, Web-of-Science, Cochrane, PubMed publisher and Google Scholar) were searched for publications using the following keywords: "somatostatin OR somatostatin receptor OR somatostatin derivative OR somatostatin analogue OR depreotide OR pentetreotide OR octreotide OR tetraxetan OR 99mTc OR 111In OR 68Ga OR 125I OR 131I OR isotope OR radiolabeled OR breast tumor OR breast cancer OR mamma tumor OR mamma carcinoma OR metastasis OR neoplasm OR carcinoma OR imaging OR radiodiagnosis OR diagnostic imaging equipment OR scintigraphy OR PET OR SPECT OR tomography OR tumor detection". We found a total of 1170 papers (405 papers via Embase, 149 papers via Medline OvidSP, 4 papers via Cochrane, 283 papers via Web-of-Sience, 326 papers via Scopus and 3 papers via PubMed publisher). After removing duplicates 599 papers remained. These papers were analysed by 3 individual researchers based on pre-set inclusion criteria defined by studies in which nuclear imaging using radiolabeled SST analogues was performed in patients with breast lesions.
Figure 1 shows a flowchart of the identified and included studies. From the 599 studies found, 24 studies (17-40), published between 1994 and 2014, fulfilled the criteria and were included in this review. The selected papers included studies in which SSTR-mediated nuclear imaging was performed in patients with suspected or proven breast tumors, patients with neuroendocrine BC and other non-BC related lesions in the breast.

ANALYSIS OF SELECTED LITERATURE

In eleven (17-27) of the selected studies BC patients were included. These studies were published between 1994 and 2010 and included a total of 285 patients (*Table 1*). BC was either detected by physical examination, cytology, mammography, conventional diagnostic methods, clinical findings or histopathologic findings. In 6 of the studies (17-19,22-24) ^{111}In-DTPA-octreotide was the

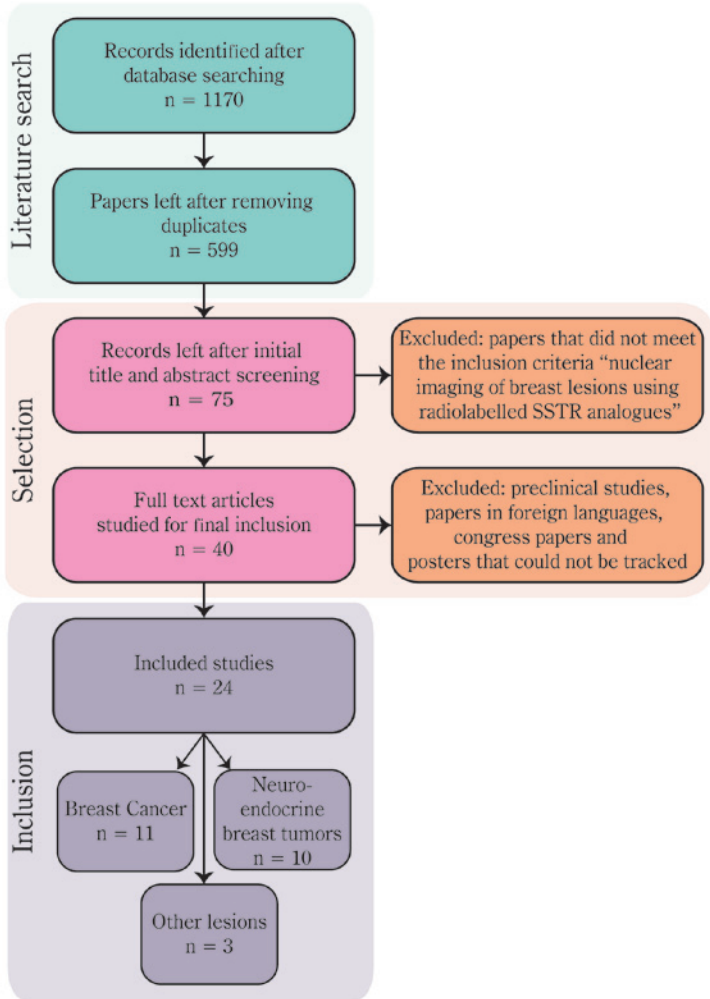

Figure. 1. Flowchart of the studies identified and included in this review

only radiopharmaceutical used. In 1 study (20) both ^{111}In-DTPA-octreotide and ^{99m}Tc-Sestamibi were used, while in another study (21) ^{201}Tl-DTPA-octreotide and ^{111}In-DTPA-octreotide were compared. In the remaining 3 studies ^{99m}Tc labelled SST analogues were used: ^{99m}Tc-depreotide in 1 study (25) and ^{99m}Tc-octreotide in 2 studies (26,27). Reported sensitivity for SSTR-mediated nuclear imaging ranged from 26-100%. Only 6 studies (19,21-23,26,27) included benign lesions, resulting in a specificity ranging from 22-100%. In 5 studies SSTR expression of the tumor lesions was analysed by in vitro autoradiography, immunohisto chemistry (IHC), mRNA analyses or northern blot. Three of these studies reported on SSTR specificity of imaging of 93% (17), 85% (22) and 96% (23). False positive results were reported in 3 studies: one mastopathy (23), multiple fibroadenomas (21,26) and one abscess (21). Non-specific tracer uptake which

was not related to the presence of benign nor malignant breast lesions was observed in 1 study (18). Multiple explanations were given for uptake in non-cancerous breast tissue such as the presence of activated peripheral mononuclear leucocytes or increased blood flow in case of the abscess, biological ^{111}In-DTPA-octreotide distribution, non-specific accumulation due to changed breast tissue permeability, and binding to premalignant cells (18,21). Four studies (18,20,22,27) reported on false negative results in small lesions staged as T1 (<20 mm). Furthermore, van Eijck et al. (17) reported on higher sensitivity for T2 than T1 tumors. Next to tumor size, 3 studies (17,18,22) reported on false negative results in lesions with heterogeneous and/or low density SSTR expression. Thus lesions size and SSTR density were indicated as limiting factors for SSTR-mediated nuclear imaging. Concerning BC subtypes, a significant correlation of BC histological subtype and positive SSTR-mediated nuclear imaging was described in 1 study (van Eijck et al. (17): sensitivity of 85% for invasive ductal carcinomas (IDCs) vs. 56% for invasive lobular carcinomas (ILCs)). This finding was not confirmed in the 4 other studies (18,22,23) that included both IDCs and ILCs. Furthermore, 4 studies (18,20,22,24) determined ER and PR expression of the visualized lesions, but no correlation was found. Detection of axillary lymph nodes (LNs) containing malignant lesions was included in some of the selected studies (17,18,20-22,24,26). LN lesions were successfully visualized in all studies but this was dependent on the size and the number of lesions present. However, in all cases sensitivity was less than in primary tumors. Regarding technical aspects, planar scintigraphy was the main imaging method, in 3 cases (18,20,23) supplemented with SPECT. The studies by Bajc et al. (18) and Chiti et al. (20) reported that SPECT had added value, while this was not discussed in the study by Schulz et al. (23). In the majority of the studies imaging was performed at 4 and/or 24 h post injection (p.i.), but imaging was also performed at other time points e.g. 0.5 h, 1 h, 5 h and 48 h p.i. There seemed to be a preference for later time points (24 h p.i.) e.g. Vural et al. (21) reported on a better tumor to background ratio in late images (24 h p.i.) compared to early images (4 h p.i.). In 1 study (22) subcutaneous local administration and intravenous administration of ^{111}In-DTPA-octreotide was compared, resulting in no significant difference between the two administration routes. In addition we found 10 papers or abstracts (28-37), published between 1995 and 2014, presenting 11 cases of histologically proven primary neuroendocrine BC where SSTR-mediated nuclear imaging successfully identified the primary tumor, metastases or both. In 8 of these studies planar scintigraphy was used (28-35). This was accompanied by SPECT acquisitions in 5 studies (29,32-35), while 1 study (31) also acquired images using scintimammography, presumably with a dedicated camera. ^{111}In-DTPA-octreotide was used as radiopharmacon in 7 papers (28-31,33-35) and ^{99m}Tc-depreotide in 1 paper (32). In a study by Huetteman et al. (36) from 2010, PET was performed, no details on camera or radiopharmacon were provided though. In the most recent study by Mukherjee et al. (37) PET/CT was successfully performed using ^{68}Ga-DOTA-NOC. Main reasons for performing SSTR-mediated nuclear imaging was to identify the primary tumor after presentation with axillary lymphadenopathy (3 patients, 2 of whom afterwards had radio-guided surgery (28,33)

Table 1. Brief summary of the eleven studies in which SSTR-mediated imaging was performed in BC patients.

Author, year	№ of patients included	№ of Lesions Malignant/ Benign	Diagnosed by PE*, Cyto†, Mammo‡, Other§, US¶	Radiolabeled SST analogue	Imaging technique	Sensitivity (%)	Specificity (%)	Specificity for SSTR analyzed by ex vivo SC$, in vitro AR¤, IHC◊, mRNA analysis or Northern blot	Other remarks
Van Eijck, 1994	50	52/0	PE, Cyto, Mammo	^{111}In-DTPA-octreotide	Planar Scintigraphy	69 (39/52)	NA	AR in 30 samples True positives: 22/30 True negatives:6/30 False positive: 1/30 False negative: 1/30 Specificity: 93%	4/13 lymph nodes showed uptake
Bajc, 1996	24	25/0	PE, Cyto, Mammo	^{111}In-DTPA-octreotide	Planar Scintigraphy + SPECT	76 (18/25)	NA	SC in 18 samples True positives:18/18 Specificity: 100%	7/14 lymph nodes showed uptake.
Piperkova, 1996	9	7/2	PE, Other	^{111}In-DTPA-octreotide	Planar Scintigraphy	86 (6/7)	100 (2/2)	ND	
Chiti, 1997	15	16/0	Mammo, Other	^{99m}Tc-Sestamibi and ^{111}In DTPA-octreotide	Planar Scintigraphy + SPECT	94 (15/16)	NA	ND	4/6 lymph nodes showed uptake.
Vural, 1997	21	17/4	Mammo, Other	^{201}Tl-DTPA-octreotide and ^{111}In-DTPA-octreotide	Planar Scintigraphy	94 (16/17)	75 (3/4)	ND	5/6 lymph nodes showed uptake.
Albérini, 2000	13	11/2	Other	^{111}In-DTPA-octreotide	Planar Scintigraphy	36 (4/11)	100 (2/2)	AR in all 13 samples True positives: 4/13 True negatives:7/13 False negatives: 2/13 Specificity: 85%	2/6 lymph nodes showed uptake (4/6 lymph nodes SSTR positive by AR).

Table 1. Continued

Author, year	№ of patients included	№ of Lesions Malignant/ Benign	Diagnosed by PE*, Cyto†, Mammo‡, Other§, US¶	Radiolabeled SST analogue	Imaging technique	Sensitivity (%)	Specificity (%)	Specificity for SSTR analyzed by ex vivo SC$, in vitro AR¤, IHC◊, mRNA analysis or Northern blot	Other remarks
Schulz, 2002	23	20/3	Mammo, US	^{111}In-DTPA-octreotide	Planar Scintigraphy + SPECT	65 (13/20)	67 (2/3)	IHC in 23 samples True positives: 15/23 True negatives: 7/23 False negatives: 1/23 Specificity: 96%	
Skånberg, 2002	12	12/0	Cyto, Mammo	^{111}In-DTPA-octreotide	Planar Scintigraphy	100 (12/12)	NA	No clear correlation with IHC or northern blot analysis performed	3/7 lymph nodes showed uptake.
Bossche van den, 2006	18	18/0	Other	^{99m}Tc-depreotide	Planar Scintigraphy	61 (11/18)	NA	ND	
Wang, 2008	55	37/18	PE, Mammo, Other	^{99m}Tc-octreotide	Planar Scintigraphy	92 (34/37)	22 (4/18)	No clear correlation with IHC or mRNA analysis performed	6/17 lymph nodes showed uptake.
Su, 2010	45	31/14	PE, Mammo	^{99m}Tc-octreotide	Planar Scintigraphy	87 (27/31)	79 (11/14)	ND	

* *PE=Physical examination.*
† *Cyto=cytology.*
‡ *Mammo=mammography.*
§ *Other=conventional diagnostic methods, clinical findings, histopathologic findings.*
¶ *US=ultrasound.*
$ *ex vivo SC=ex vivo scintigraphy.*
¤ *in vitro AR=in vitro autoradiography.*
◊ *IHC=Immunohistochemistry.*
Table was based on the following references (17-27).

and 1 patient who had a biopsy identifying a neuroendocrine BC (30)), work-up for possible peptide receptor radionuclide therapy (3 patients) (34-36) or to exclude local remnant disease and/or distant metastases after surgery (1 patient) (31). In 4 patients described in 3 studies SSTR-mediated nuclear imaging was added to preoperative staging without a stated reason (29,32,37).
Furthermore we found 3 papers (38-40) with 5 case reports of positive SSTR-mediated nuclear scans of the breast for other reasons. Two of these cases visualized NET metastases in the breast, originating from midgut or bronchus carcinoid (40). One case of juvenile fibroadenoma (38) and two cases scanned at 1 and 1.5 month postpartum (39) all showed diffuse high uptake in glandular tissue. It was hypothesized by the authors that post-partum uptake of ^{111}In-DTPA-octreotide could be the result of upregulation of SSTR2 caused by high blood levels of estrogen during pregnancy.

LIMITATIONS OF THE ANALYSED STUDIES

In order to assess whether improvements made within the field of nuclear medicine and our knowledge about BC can improve SSTR-mediated imaging in BC patients, we critically analysed clinical studies on SSTR-mediated nuclear imaging in patients with breast lesions that have been performed over the past decades. The analysed studies demonstrated feasibility of BC imaging with SSTR radioligands and indicated that lesion size and SSTR density are determining factors for successful SSTR-mediated nuclear imaging in BC patients. However, combining the data of the presented studies to come to an overall conclusion was difficult since the studies were performed in heterogeneous BC populations, small patients groups were studied, and various SSTR radioligands and different imaging protocols were used. Furthermore, details on tumor size, SSTR status, BC subset and molecular BC subtype were not reported in many of the investigations. Especially the latter is a major flaw of the performed studies. BC is a very heterogeneous disease that is characterized by molecular properties that influence prognosis as well as treatment of the disease. Examples of the most important molecular properties in BC are ER, PR and human epidermal growth factor receptor 2 (HER2) expression (2). The heterogeneity within the disease is an important factor that cannot be ignored when new imaging and/or therapy options are studied, e.g. SSTR expression between BC subtypes may vary, making SSTR-mediated imaging unsuitable for some BC subtypes. From the 11 studies that included BC patients, only 4 studies (18,20,22,24) correlated SSTR expression with ER and PR expression and no correlation was found. Yet, in another included study treatment with tamoxifen in hormone-sensitive patients resulted in a reduced uptake of ^{99m}Tc-depreotide, whereas non-responders showed increased uptake in the follow-up scan (25), indicating an association between ER expression and SSTR-mediated nuclear imaging. Furthermore, recent preclinical studies by Dalm et al. (12) showed a positive correlation between *SSTR2* mRNA expression and *ER* and *PR* mRNA expression in a cohort of 684 LN-negative

patients, resulting in the identification of ER- and PR-positive BC patients as potential targets for SSTR-mediated nuclear imaging and potentially also therapy. This discrepancy can most likely be explained by the relatively small group size used in the imaging studies and underlines the need for studies with well-chosen homogenous patient groups of sufficient size. Ten of the analysed studies visualized neuroendocrine breast tumors. This type of tumor is characterized by neuroendocrine markers and therefore cannot be compared to other BC subtypes (41).

IMPROVEMENTS WITHIN NUCLEAR MEDICINE AND SSTR-MEDIATED IMAGING IN BC

Over the past decades major improvements have been made in the field of nuclear medicine with respect to nuclear imaging techniques as well as radiolabeled peptide analogues with improved receptor affinity. One such a development is the introduction of multimodal SPECT/CT and PET/CT which led to major improvement of radionuclide imaging regarding resolution and sensitivity. Combining SPECT and PET with anatomical localization by CT increased diagnostic accuracy. The superiority of hybrid SPECT/CT over planar imaging or SPECT has been demonstrated using ^{111}In-DTPA-octreotide for NET detection, as well as for other clinical problems such as head and neck tumors (13). Furthermore SPECT/CT offers quantification of tracer uptake to perform dosimetry and evaluation of therapy response (42). PET/CT is even better suited for reliable quantification and shows higher sensitivity and spatial resolution than SPECT/CT. Several ^{68}Ga-labelled SST analogues are available for PET imaging, which have been studied only sporadically in BC cases (37,43). *Figure 2* illustrates the difference between planar scintigraphy (A) and PET/CT (B) in BC patients. In NET patients multiple studies demonstrated that ^{68}Ga-DOTA-TOC and ^{68}Ga-DOTA-TATE PET/ CT were superior to ^{111}In-based SPECT (14,44,45).

Another noteworthy improvement for nuclear BC imaging is the development of dedicated PET cameras. The advantage of dedicated breast PET cameras is a restricted field of view resulting in an improved spatial resolution to achieve higher cancer detection performance, ultimately leading to better sensitivity and specificity (15). Currently multiple dedicated breast PET devices are available (46). Many studies have been performed comparing full body PET and dedicated PET in BC patients, showing preference for a dedicated PET camera. Kalinyak et al. (47) observed that imaging using a dedicated PET camera visualized more index tumors compared to full body PET and PET/CT. One other welcome advantage of dedicated breast PET cameras is enhanced visualization of axillary lesions, which are of great importance in BC.

Further improvement could be gained by application of radiolabelled SSTR antagonists. Superior images were obtained when SSTR antagonists were compared with SSTR-agonists (such as the currently used octreotide and octreotate), as was shown by Ginj et al. (16) and by Wild et al. (48,49). Preclinical studies by

Cescato et al. (50) examining in vitro binding of an SSTR-agonist and antagonist in BC tissues showed an 11±4 times higher binding of the antagonist compared to the agonist, indicating that the application of radiolabelled SSTR-antagonists might improve detection of BC lesions.

Besides SSTR other targets expressed on BC have been identified for imaging (and therapeutic) purposes. Overexpression of the gastrin releasing peptide receptor (GRPR) was reported on the majority of BC cases (51). Radiolabelled GRPR agonists and antagonists have been described for imaging and therapeutic purposes, primarily aiming at prostate cancer patients (52). However, similar studies using radiolabelled GRPR-analogues have not yet have been performed in BC patients. Furthermore, radiolabelled hormone receptor analogues are studied for PET/CT application in BC. Examples of such are ^{18}F-Fes and ^{89}Zr-bevacizumab targeting ER and HER2, respectively (53). Currently imaging using these radiolabeled hormone receptor analogues are not part of the standard clinical routine, but investigations proving their benefits are ongoing. With a number of other targets being explored for BC imaging, it is important to study the potential of SSTR-mediated imaging of BC patients with the current peptide analogues and imaging techniques available, in order to accurately compare the available compounds.

SSTR-MEDIATED NUCLEAR IMAGING AND BC PATIENT CARE

Taking into account the above described limitations of the past studies and recent developments within nuclear medicine, future well designed studies using the currently available imaging techniques and the best available radiolabelled SST analogues, will better investigate the potential role of SSTR-mediated imaging in BC. The question remains whether and how this will contribute to BC patient care. One option is to use SSTR-mediated imaging as a tool to monitor therapy response after anti-estrogen treatment, since a correlation between ER-positive tumors and SSTR expression was demonstrated (12). Furthermore, SSTR-mediated imaging might be used for the visualization of sentinel node lesions as a guidance for sentinel node biopsy or to exclude the presence of tumor containing lesions, in both cases sparing axial lymph node dissection, and the associated costs and side effects (54). SSTR expression can be determined prior to scanning using IHC of paraffin embedded tissue of biopsy material to determine whether a patient is eligible for SSTR-mediated imaging (in the case of sentinel nodes SSTR expression of primary tumor material can be determined). This prevents unnecessary interventions and can easily be added to routine clinical practice since ER, PR and HER2 expression is currently also determined by IHC. For patients with a positive scan, treatment with ß- or α-labelled SST analogues might be an option. Since about 70% of the total BC population is ER-positive, we consider that a large part of the BC patients might benefit from SSTR-mediated imaging and therapy (2). Focusing on therapeutic possibilities, therapy using radiolabelled

SST analogues can potentially be an option for BC patients that show resistance against anti-estrogen treatment, which is about 40% of the patients that are eligible for this type of treatment (55).

CONCLUSION

From 1990 onward studies were performed showing the feasibility of SSTR-mediated nuclear imaging in BC patients, despite variations in study parameters, imaging agents and imaging techniques used. Since high sensitivity and specificity rates have been found in the reviewed studies, we expect that the recent major improvements in the field of nuclear medicine, including application of radiolabelled SST analogues with higher receptor affinity and/or antagonistic properties, will be of great benefit for this purpose. In future studies, the different subtypes of BC should be taken into account, since BC is a very heterogeneous disease and this might lead to the identification of specific subtypes of BC that can benefit most from the use of radiolabelled SST analogues for targeted imaging and potentially also for therapeutic applications, which might have a significant impact on BC patient care.

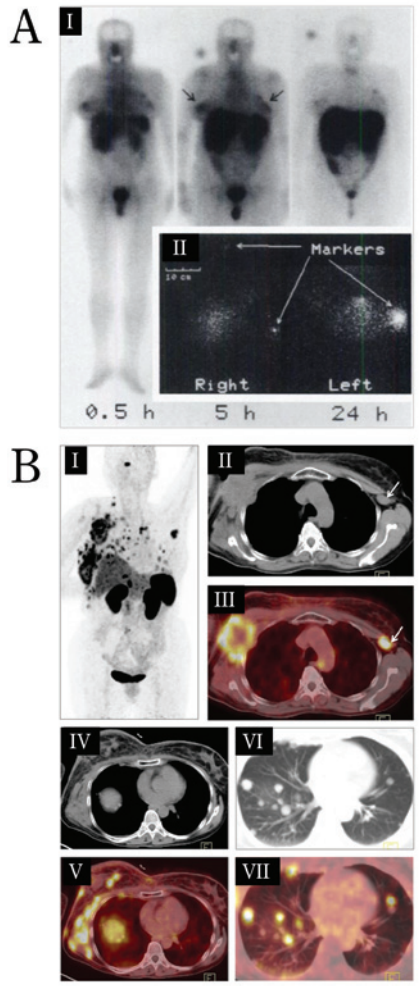

Figure 2. Comparison of a planar whole body scintigram (A) and a PET/CT scan (B). The improvements within nuclear medicine enable SSTR-mediated tumor visualization with a higher sensitivity and resolution, leading to improved diagnostic accuracy. A) Whole-body scintigram of a patient with confirmed bilateral ductal carcinoma (Bajc et al. (18)). Images were obtained 0.5, 5 and 24 h after i.v. injection of 110 MBq ^{111}In-DTPA-octreotide (18). B) ^{68}Ga-DOTA-NOC PET/CT scan of a patient with a NET of the breast (Mukherjee et al. (37)). SSTR-expressing metastatic lesions were found in multiple bilateral axillary and right cervical lymph nodes, bilateral lungs and multiple skeletal sites (I-VII) (37).

REFERENCES

1. Erlay J SI, Ervik M, Dikshit R, Eser S, Mathers C, Rebelo M, Parkin DM, Forman D, Bray F. Cancer Incidence and Mortality Worldwide: IARC CancerBase No. 11. website] http://globocan.iarc.fr. Accessed October 1st, 2014.
2. Yersal O, Barutca S. Biological subtypes of breast cancer: Prognostic and therapeutic implications. World J Clin Oncol. 2014;5:412-424.
3. Arnold L. Sensitivity and Specificity of Digital vs. Film Mammography. The Internet Journal of Academic Physician Assistants. Vol 7; 2009.
4. Garcia EM, Storm ES, Atkinson L, Kenny E, Mitchell LS. Current breast imaging modalities, advances, and impact on breast care. Obstet Gynecol Clin North Am. 2013;40:429-457.
5. Nelson HD, Tyne K, Naik A, et al. Screening for breast cancer: an update for the U.S. Preventive Services Task Force. Ann Intern Med. 2009;151:727-737.
6. Yoon HJ, Kim Y, Lee JE, Kim BS. Background Tc-methoxyisobutylisonitrile uptake of breast-specific gamma imaging in relation to background parenchymal enhancement in magnetic resonance imaging. Eur Radiol. 2015;25:32-40.
7. Kwekkeboom DJ, de Herder WW, Krenning EP. Somatostatin receptor-targeted radionuclide therapy in patients with gastroenteropancreatic neuroendocrine tumors. Endocrinol Metab Clin North Am. 2011;40:173-185.
8. Bodei L, Cremonesi M, Grana CM, et al. Peptide receptor radionuclide therapy with 177Lu-DOTATATE: the IEO phase I-II study. Eur J Nucl Med Mol Imaging. 2011;38:2125-2135.
9. Krenning EP, Bakker WH, Breeman WA, et al. Localisation of endocrine-related tumours with radioiodinated analogue of somatostatin. Lancet. 1989;1:242-244.
10. Reubi JC, Waser B, Foekens JA, Klijn JG, Lamberts SW, Laissue J. Somatostatin receptor incidence and distribution in breast cancer using receptor autoradiography: relationship to EGF receptors. Int J Cancer. 1990;46:416-420.
11. Orlando C, Raggi CC, Bianchi S, et al. Measurement of somatostatin receptor subtype 2 mRNA in breast cancer and corresponding normal tissue. Endocr Relat Cancer. 2004;11:323-332.
12. Dalm SU, Sieuwerts AM, Look MP, et al. Clinical Relevance of Targeting the Gastrin-Releasing Peptide Receptor, Somatostatin Receptor 2, or Chemokine C-X-C Motif Receptor 4 in Breast Cancer for Imaging and Therapy. J Nucl Med. 2015;56:1487-1493.
13. Buck AK, Nekolla S, Ziegler S, et al. Spect/Ct. J Nucl Med. 2008;49:1305-1319.
14. Buchmann I, Henze M, Engelbrecht S, et al. Comparison of 68Ga-DOTATOC PET and 111In-DTPAOC (Octreoscan) SPECT in patients with neuroendocrine tumours. Eur J Nucl Med Mol Imaging. 2007;34:1617-1626.
15. Vercher-Conejero JL, Pelegri-Martinez L, Lopez-Aznar D, Cozar-Santiago Mdel P. Positron Emission Tomography in Breast Cancer. Diagnostics (Basel). 2015;5:61-83.
16. Ginj M, Zhang H, Waser B, et al. Radiolabeled somatostatin receptor antagonists are preferable to agonists for in vivo peptide receptor targeting of tumors. Proc Natl Acad Sci USA. 2006;103:16436-16441.
17. Van Eijck CHJ, Krenning EP, Bootsma A, et al. Somatostatin-receptor scintigraphy in primary breast cancer. Lancet. 1994;343:640-643.
18. Bajc M, Ingvar C, Palmer J. Dynamic indium-111-pentetreotide scintigraphy in breast cancer. J Nucl Med. 1996;37:622-626.
19. Piperkova E. Somatostatin-receptor scintigraphy-a new diagnostic approach to primary breast cancer. Rentgenol radiol. 1996;35:44-48.

20. Chiti A, Agresti R, Maffioli LS, et al. Breast cancer staging using technetium-99m sestamibi and indium-111 pentetreotide single-photon emission tomography. Eur J Nucl Med. 1997;24:192-196.

21. Vural G, Unlu M, Atasever T, Ozur I, Ozdemir A, Gokcora N. Comparison of indium-111 octreotide and thallium-201 scintigraphy in patients mammographically suspected of having breast cancer: Preliminary results. Eur J Nucl Med. 1997;24:312-315.

22. Alberini JL, Meunier B, Denzler B, et al. Somatostatin receptor in breast cancer and axillary nodes: study with scintigraphy, histopathology and receptor autoradiography. Breast Cancer Res Treat. 2000;61:21-32.

23. Schulz S, Helmholz T, Schmitt J, Franke K, Otto HJ, Weise W. True positive somatostatin receptor scintigraphy in primary breast cancer correlates with expression of sst2A and sst5. Breast Cancer Res Treat. 2002;72:221-226.

24. Skanberg J, Ahlman H, Benjegard SA, et al. Indium-111-octreotide scintigraphy, intraoperative gamma-detector localisation and somatostatin receptor expression in primary human breast cancer. Breast Cancer Res Treat. 2002;74:101-111.

25. Van Den Bossche B, Van Belle S, De Winter F, Signore A, Van de Wiele C. Early prediction of endocrine therapy effect in advanced breast cancer patients using 99mTc-depreotide scintigraphy. J Nucl Med. 2006;47:6-13.

26. Wang F, Wang Z, Wu J, et al. The role of technetium-99m-labeled octreotide acetate scintigraphy in suspected breast cancer and correlates with expression of SSTR. Nucl Med Biol. 2008;35:665-671.

27. Su XH, He XJ, Wu H, et al. Complement of Tc-99m-octreotide scintimammography to mammography in evaluating breast cancers. Nuclear Science and Techniques. 2010;21:24-28.

28. Meunier B, Le Cloirec J, Dazord L, et al. Per operative localization of a carcinoid tumour of the breast using indium-111 pentetreotide and a nuclear surgical probe. Eur J Nucl Med. 1995;22:281-283.

29. Chiti A, Agresti R, Savelli G, Giovanazzi R, Greco M, Bombardieri E. Radionuclide imaging of unexpected multifocal breast cancer: surgical implications. Breast. 1997;6:386-387.

30. Lenzi R, Kim EE, Raber MN, Abbruzzese JL. Detection of primary breast cancer presenting as metastatic carcinoma of unknown primary origin by 111In-pentetreotide scan. Ann Oncol. 1998;9:213-216.

31. Rubini G, D'Eredita G. Tc-99m sestamibi and In-111 DTPA octreotide uptake in breast carcinoma with neurendocrine differentiation. Clin Nucl Med. 2000;25:482-483.

32. Montilla-Soler JL, Bridwell RS. Tc-99m depreotide scintigraphy of breast carcinoma. Clin Nucl Med. 2002;27:202-204.

33. Panareo S, Carcoforo P, Lanzara S, et al. Radiolabelled somatostatin analogs for diagnosis and radio-guided surgery of neuroendocrine breast cancer undetectable with conventional imaging procedures. Breast. 2008;17:111-114.

34. Suchak AA, Millo N, MacEwan R, McEwan AJ. Neuroendocrine differentiated breast carcinoma with pleural metastases using indium-111 octreotide. Clin Nucl Med. 2009;34:74-75.

35. Savelli G, Zaniboni A, Bertagna F, et al. Peptide Receptor Radionuclide Therapy (PRRT) in a Patient Affected by Metastatic Breast Cancer with Neuroendocrine Differentiation. Breast Care (Basel). 2012;7:408-410.

36. Heutteman U LE, Neumamm M, Vesper AS, Janni W, Nestle-Kraemling C. Primary metastatic neuroendocrine breast cancer: An extraordinary case report. Arch Gynecol Obstet. 2010;282:S102-S103 [Abstract: 158th Congress of the German Society of Gynecology and Obstetrics, 105-108 October 2010, Munich].

37. Mukherjee A, Karunanithi S, Singla S, Bal C, Kumar R. 68Ga DOTANOC PET/CT in primary neuroendocrine tumor of the breast. Clin Nucl Med. 2014;39:396-398.

38. Won KS, Gayed I, Kim EE, Macapinlac H. Juvenile fibroadenoma of the breast demonstrated on 111in-octreotide SPECT and 18F-FDG PET/CT. Eur J Nucl Med Mol Imaging. 2007;34:440.

39. Van Eeckhoudt SFJ, Teunissen JJM, Kwekkeboom DJ. Increased Mammary Uptake on In-111 Pentetreotide Scintigraphy. Clinical Nuclear Medicine. 2012;37:781-782.

40. Kaltsas GA, Putignano P, Mukherjee JJ, et al. Carcinoid tumours presenting as breast cancer: the utility of radionuclide imaging with 123I-MIBG and 111In-DTPA pentetreotide. Clin Endocrinol (Oxf). 1998;49:685-689.

41. Park YM, Wu Y, Wei W, Yang WT. Primary neuroendocrine carcinoma of the breast: clinical, imaging, and histologic features. AJR Am J Roentgenol. 2014;203:W221-230.

42. Bailey DL, Willowson KP. An evidence-based review of quantitative SPECT imaging and potential clinical applications. J Nucl Med. 2013;54:83-89.

43. Wang L, Tang K, Zhang Q, et al. Somatostatin receptor-based molecular imaging and therapy for neuroendocrine tumors. Biomed Res Int. 2013;2013:102819.

44. Gabriel M, Decristoforo C, Kendler D, et al. 68Ga-DOTA-Tyr3-octreotide PET in neuroendocrine tumors: comparison with somatostatin receptor scintigraphy and CT. J Nucl Med. 2007;48:508-518.

45. Poeppel TD, Binse I, Petersenn S, et al. 68Ga-DOTATOC versus 68Ga-DOTATATE PET/CT in functional imaging of neuroendocrine tumors. J Nucl Med. 2011;52:1864-1870.

46. Koolen BB, Vogel WV, Vrancken Peeters MJ, Loo CE, Rutgers EJ, Valdes Olmos RA. Molecular Imaging in Breast Cancer: From Whole-Body PET/CT to Dedicated Breast PET. J Oncol. 2012;2012:438647.

47. Kalinyak JE, Berg WA, Schilling K, Madsen KS, Narayanan D, Tartar M. Breast cancer detection using high-resolution breast PET compared to whole-body PET or PET/CT. Eur J Nucl Med Mol Imaging. 2014;41:260-275.

48. Wild D, Fani M, Behe M, et al. First clinical evidence that imaging with somatostatin receptor antagonists is feasible. J Nucl Med. 2011;52:1412-1417.

49. Wild D, Fani M, Fischer R, et al. Comparison of somatostatin receptor agonist and antagonist for peptide receptor radionuclide therapy: a pilot study. J Nucl Med. 2014;55:1248-1252.

50. Cescato R, Waser B, Fani M, Reubi JC. Evaluation of 177Lu-DOTA-sst2 antagonist versus 177Lu-DOTA-sst2 agonist binding in human cancers in vitro. J Nucl Med. 2011;52:1886-1890.

51. Reubi C, Gugger M, Waser B. Co-expressed peptide receptors in breast cancer as a molecular basis for in vivo multireceptor tumour targeting. Eur J Nucl Med Mol Imaging. 2002;29:855-862.

52. Yu Z, Ananias HJ, Carlucci G, et al. An update of radiolabeled bombesin analogs for gastrin-releasing peptide receptor targeting. Curr Pharm Des. 2013;19:3329-3341.

53. Oude Munnink TH, Nagengast WB, Brouwers AH, et al. Molecular imaging of breast cancer. Breast. 2009;18 Suppl 3:S66-73.

54. Hindie E, Groheux D, Brenot-Rossi I, Rubello D, Moretti JL, Espie M. The sentinel node procedure in breast cancer: nuclear medicine as the starting point. J Nucl Med. 2011;52:405-414.

55. Droog M, Beelen K, Linn S, Zwart W. Tamoxifen resistance: from bench to bedside. Eur J Pharmacol. 2013;717:47-57.

Chapter 6

Short Communication: Somatostatin Receptor-mediated Breast Cancer Imaging, Is There a Role for Radiolabeled Somatostatin Receptor Antagonists?

S.U. Dalm[1], J. Haeck, G.N. Doeswijk[1], E. de Blois[1], M. de Jong[1] and C.H.M. van Deurzen[2]

[1]Dept. of Radiology & Nuclear Medicine Erasmus MC, Rotterdam, The Netherlands and [2]Dept. of Pathology, Erasmus MC, Rotterdam, The Netherlands

Submitted to J Nucl Med, September 2016
Revised version submitted after peer review in December 2016

ABSTRACT

Recent studies showed enhanced tumor targeting by novel somatostatin receptor (SSTR) antagonists compared to clinically widely used agonists. However, these results have been obtained in neuroendocrine tumors; as yet no data are available for cancer types with lower SSTR expression, including breast cancer (BC). In this preclinical study, we investigated whether application of a SSTR antagonist could improve SSTR-mediated BC imaging.

Methods: ^{111}In-DOTA-Tyr^3-octreotate (SSTR agonist) and ^{111}In-DOTA-JR11 (SSTR antagonist) binding to 40 human BC specimens was compared using in vitro autoradiography. Furthermore, in vivo SPECT/MR imaging was performed in a BC mouse model after injection of ^{177}Lu-DOTA-Tyr^3-octreotate or ^{177}Lu-DOTA-JR11. Also, radioactivity uptake of excised tumors was measured.

Results: ^{111}In-DOTA-JR11 binding to human BC tissue was 6±11 times higher than ^{111}In-DOTA-Tyr^3-octreotate binding. SPECT/MRI resulted in better tumor visualization with the antagonist, corresponding with the measured tumor uptake.

Conclusions: SSTR antagonists are promising candidates for BC imaging.

Keywords:
Breast Cancer, Imaging, Somatostatin Receptor, Somatostatin Receptor Antagonist

INTRODUCTION

Somatostatin receptor (SSTR)-mediated imaging of neuroendocrine tumors using SSTR agonists is successfully applied in the clinic. In 1990, Reubi et al. (1) reported SSTR expression in 21-46% of BC specimens. Since then, multiple studies targeting these receptors were performed. However, due to conflicting results SSTR-mediated imaging is currently not routinely used in BC patients. Low and heterogeneous SSTR expression seems to be the main reason for unsuccessful tumor targeting (2). Therefore, novel developments are needed to improve SSTR-mediated breast cancer (BC) imaging.

A promising development is the application of SSTR antagonists. Enhanced tumor targeting of receptor antagonists vs. agonists is counterintuitive, since agonists can be internalized leading to intracellular accumulation of radioactivity. However, Ginj et al. (3) reported that SSTR antagonists bind to more binding sites. Based on the results of recent studies demonstrating enhanced tumor targeting with SSTR antagonists (3-6), the ability of the antagonist to bind to more binding sites could be more important than internalization. The previous studies are mainly based on neuroendocrine tumors. However, the enhanced binding of antagonists might especially be interesting for targeting of low SSTR-expressing cancers, such as BC.

The aim of this study was to investigate whether the use of SSTR antagonists could improve SSTR-mediated BC imaging. For this purpose, we compared the use of the SSTR agonist (DOTA-Tyr^3-octreotate) and the SSTR antagonist (DOTA-JR11) in 40 human BC specimens and in a BC mouse model.

MATERIALS AND METHODS

Radioligands

The SSTR agonist, DOTA-Tyr^3-octreotate (BioSynthema) and the SSTR antagonist, DOTA-JR11 (kindly provided by Dr. Helmut Maecke) were used. The radiotracers were radiolabeled with ^{111}In (Covidien) or ^{177}Lu (IDB) as previously described (7). Specific activity was 80 and 100 MBq/nmol for the ^{111}In and ^{177}Lu labeled peptide analogs, respectively. Radiometal incorporation and radiochemical purity were >90%.

Human BC Specimens

Fresh frozen tissue specimens from 40 human BCs (31 ductal carcinomas, 4 lobular carcinomas and 5 other subtypes) were selected from the Erasmus MC tissue bank for autoradiography studies comparing SSTR agonist and antagonist binding. The majority of the cases were positive for estrogen receptor (ER: 75%), progesterone receptor (PR: 55%) and human epidermal growth factor 2 (HER2: 18%).

The study adhered to the Code of Conduct of the Federation of Medical Scientific Societies in The Netherlands.

In Vitro Autoradiography

Fresh frozen tissue sections (10 µm) were incubated for 1.5 h with 100 µL 10^{-9} M ^{111}In-DOTA-Tyr^3-octreotate or ^{111}In-DOTA-JR11, with or without 10^{-6} M octreotide as a control for receptor specificity. Following incubation, the excess radiotracer was removed and tissue sections were exposed to super resolution phosphor screens (Perkin Elmer) for 3 d, after which screens were read using the Cyclone (Perkin Elmer). Binding of the radiotracers to tumor containing regions, identified by hematoxylin and eosin (H&E) stainings of adjacent tissue sections, was quantified using OptiQuant software (Perkin Elmer) and expressed as digital lights units per mm^2 (DLU/mm^2). Quantified uptake was corrected for non-specific binding by subtracting DLU/mm^2 of the blocked sections from DLU/mm^2 of the unblocked sections. Drops containing 1 µL 10^{-9} M of the radiotracers were used as standards to determine the added dose (DLU/mm$^2_{standards}$×100). Tumor-bound radiotracer was expressed relative to the added dose (%AD).

Mouse Model, SPECT/MRI and Biodistribution

All animal experiments were approved by the Animal Welfare Committee and conducted in accordance to accepted guidelines.

In order to select an appropriate in vivo mouse model, excised tumor material from 6 BC patient derived tumor xenografts (pdx) were tested for agonist and antagonist binding using autoradiography. Subsequently, one xenograft was used to create an in vivo model for imaging and biodistribution studies.

For the in vivo studies, tumor pieces (~6 mm^3) from a donor animal were transplanted in the 4th mammary fat pad of Balb c *nu/nu* female mice supplemented with 4 mg/L ß-estradiol. When tumors were ~1300 mm^3, animals received an intravenous injection of ~20 MBq/200 pmol ^{177}Lu-DOTA-Tyr^3-octreotate or ^{177}Lu-DOTA-JR11 (n=2 per radiotracer). SPECT/MRI was performed 4 h after radiotracer injection, while animals were anesthetized using isoflurane/O_2 and body temperature was maintained. Focused SPECT images were acquired using a 4-head multipinhole system (NanoScan SPECT/MRI, Mediso Medical Imaging) in 30 min (28 projections, 60 s/projection). Images were reconstructed using the OSEM method with 6 iterations. Concerning MRI, T1 and T2 images were acquired using a gradient echo sequence (TR/TE=12/2 ms) and a spin echo sequence (TR/TE=4500/52 ms). Other scan parameters were: field of view: 70 mm, matrix: 128×128 and slice thickness: 1 mm. The MR images were used to assess tumor composition.

After imaging, animals were euthanized, organs and tumors were excised, weighed and counted in an automatic γ-counter (1480 WIZARD, PerkinElmer) to determine the percentage of injected dose per gram tumor (%ID/g tissue). A radionuclide specific energy window, a counting time of 60 s and a counting error <5% were used for γ-counter measurements.

Fresh frozen tissue from excised tumors was used to perform H&E and SSTR2-immunostaining (SS-8000-RM SSTR2A antibody (BIO-TREND), dilution: 1:50, Ventana Medical System).

Statistics

Grahpad Prism 5 was used for statistical analyses. The Wilcoxon signed rank test was used to compare the %AD of the radiotracers in human BC samples. To compare radioligand binding of ER, PR and HER2 positive vs. negative samples, the Mann Whitney test was used. $P<0.05$ were considered statistically signifcant.

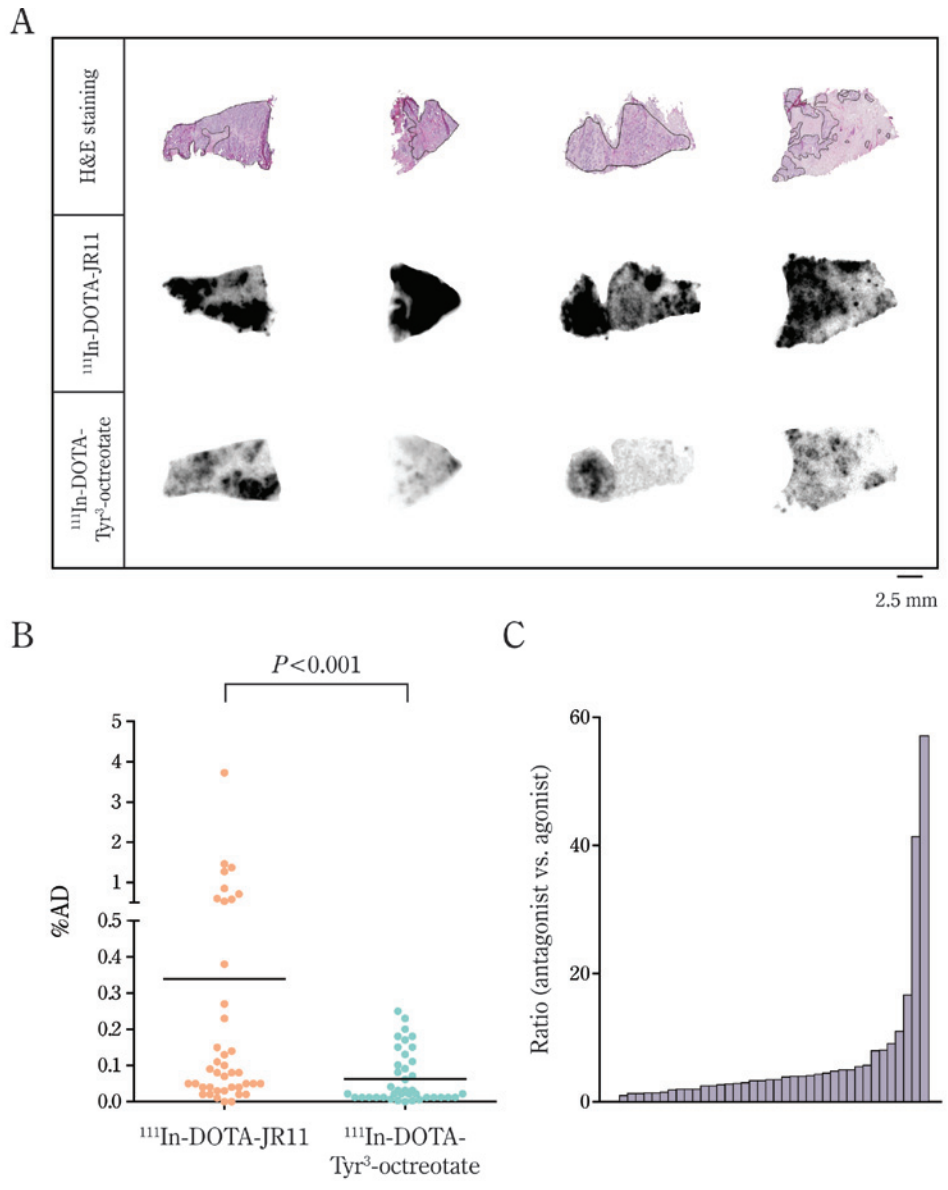

Figure 1. A) Representative autoradiography results performed with ^{111}In-DOTA-JR11 and ^{111}In-DOTA-Tyr^3-octreotate, and H&E stainings indicating tumor cells. B) Quantified uptake (%AD) of the radiotracers. C) Ratio of radiotracer binding (antagonist/agonist).

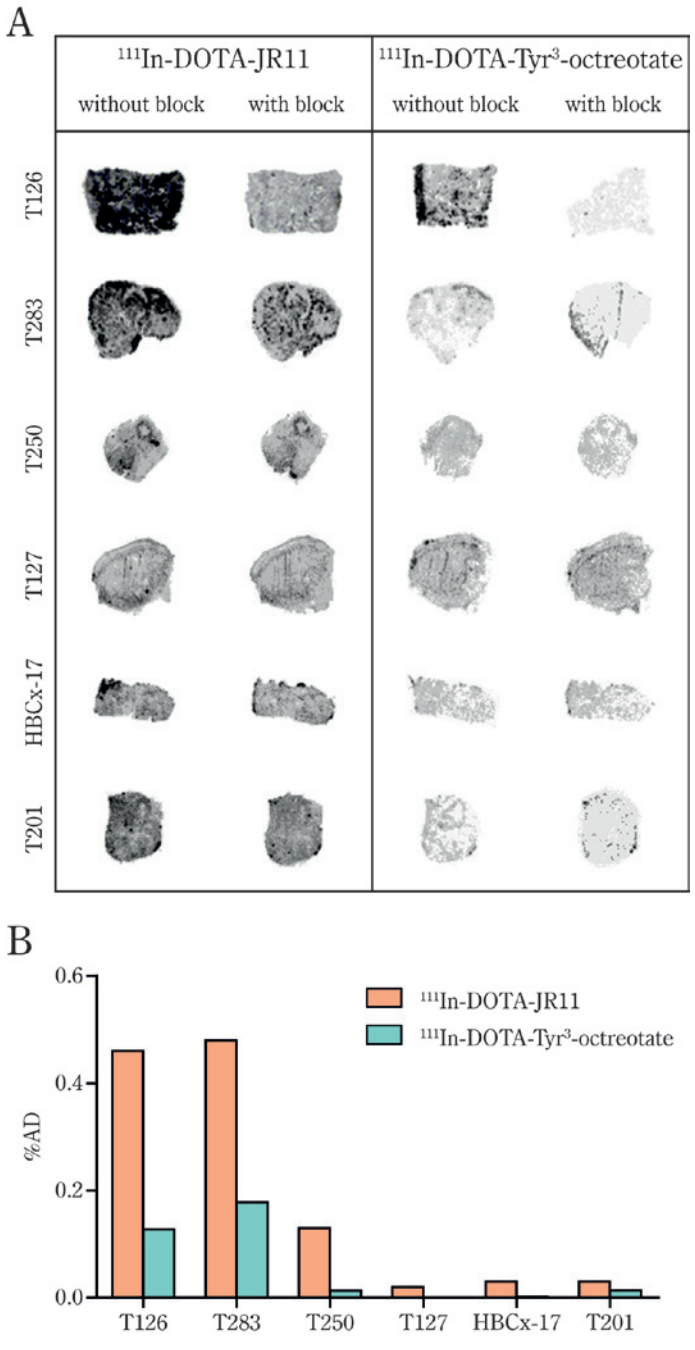

Figure 2. A) Autoradiography results (without and with octreotide to determine specificity of binding) of tumor material from 6 pdx's. B) Quantified uptake (%AD) of ^{111}In-DOTA-JR11 and ^{111}In-DOTA-Tyr^3-octreotate of the autoradiography displayed in A.

RESULTS

In Vitro Autoradiography

The results of the in vitro autoradiography experiment were quantified. The %AD of the antagonist bound to the BC specimens was significantly higher ($P<0.001$) than that of the agonist (*Figure 1*). Amongst the receptor positive tumors (38/40), the ratio %AD antagonist to %AD agonist ranged from 1 (only 1 case) to 57 (average ratio±sd=6±11).

There was no significant association between the %AD of ^{111}In-DOTA-JR11 or ^{111}In-DOTA-Tyr^3-octreotate with ER ($P=0.2$ and 0.8, respectively), PR ($P=0.3$ and 0.1, respectively) and HER2 status ($P=0.2$ and 0.09, respectively).

Six excised tumors from BC pdx's were tested for agonist and antagonist binding (*Figure 2*). Antagonist binding was clearly higher for 3/6 xenografts (T126, T283 and T250), while low binding was observed in the remaining xenografts. Two xenografts showed relatively high ^{111}In-DOTA-JR11 and ^{111}In-DOTA-Tyr^3-octreotate binding (T126 and T283) and were suited for in vivo experiments. Finally, T126 was chosen to create an in vivo mouse model, since this model is ER-positive which seems to be the most promising BC subtype for SSTR-mediated imaging (8).

SPECT/MRI and Biodistribution

The images acquired with ^{177}Lu-DOTA-Tyr^3-octreotate and ^{177}Lu-DOTA-JR11 are displayed in *Figure 3A+B*. The T1 and T2 MR images showed homogenous signal intensity throughout the tumor, indicating viability. SPECT images demonstrated higher uptake of ^{177}Lu-DOTA-JR11 vs. ^{177}Lu-DOTA-Tyr^3-octreotate. H&E and SSTR2-immunostaining demonstrated SSTR2 expression on the tumor (*Figure 3C+D*).

In line with SPECT/MRI results, biodistribution studies resulted in a 1.9 times higher tumor uptake of the antagonist vs. the agonist (*Figure 3E*). High ^{177}Lu-DOTA-JR11 and ^{177}Lu-DOTA-Tyr^3-octreotate uptake was also observed in the pancreas (5.51±0.01 and 0.91±0.06 %ID/g tissue, respectively) and kidneys (12.07±2.42 and 6.30±1.25 %ID/g tissue, respectively). This resulted in a better tumor to pancreas ratio with ^{177}Lu-DOTA-Tyr^3-octreotate vs. ^{177}Lu-DOTA-JR11 (1.02 vs. 0.33), while tumor to kidney ratio was similar.

DISCUSSION

SSTR-mediated nuclear imaging is currently not applied for BC, due to variable results of clinical studies. However, most of these studies were performed over a decade ago, while recently major improvements have been made including the development of SSTR antagonists. Previous research demonstrated that SSTR antagonists bind to more binding sites than agonists (3). Furthermore, antagonists are described to be more chemically stable and hydrophobic, which could result in a longer time of action (3). Therefore, the application of SSTR

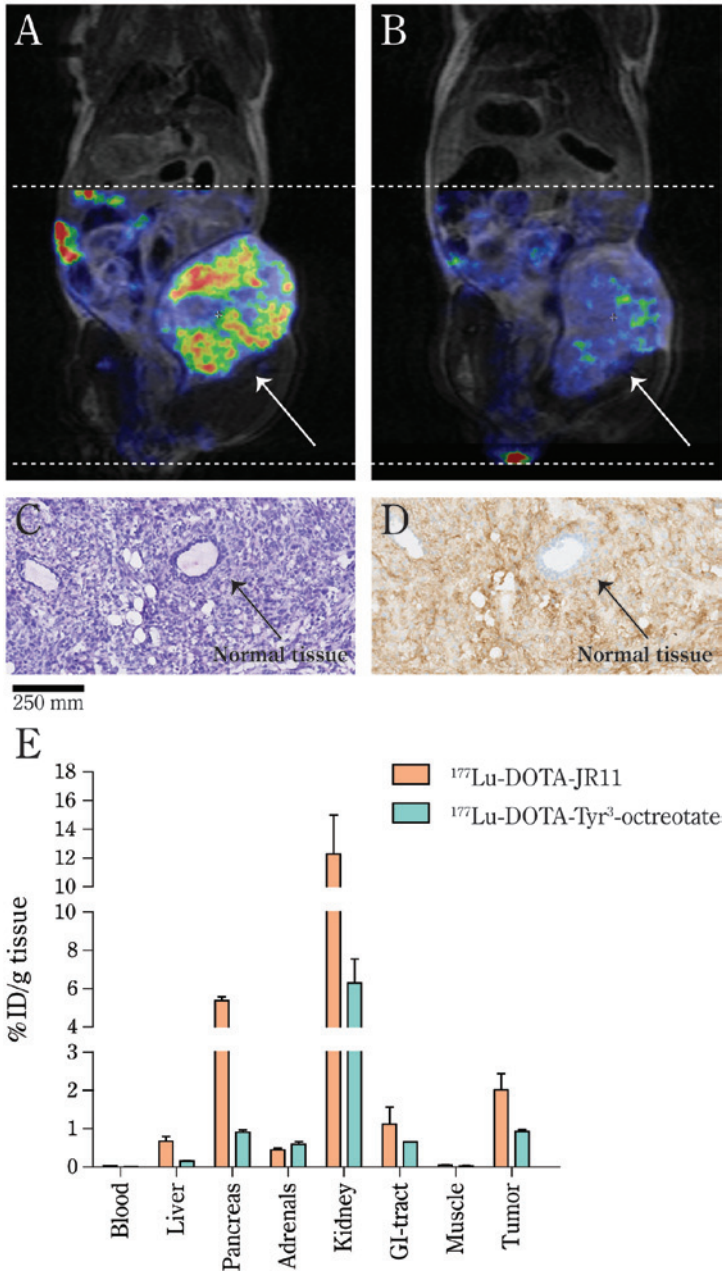

Figure 3. SPECT/MR images acquired post injection of ^{177}Lu-DOTA-JR11 (A) and ^{177}Lu-DOTA-Tyr^3-octreotate (B). Scales are equal for both images. The dotted lines indicate the area scanned with SPECT. Arrows indicate tumor xenografts. C+D) H&E and SSTR2-immunostaining of excised tumors showing SSTR2 expression. Arrows indicate normal tissue without SSTR2 expression. E) Radioactivity uptake (%ID/g tissue) measured in excised tumors and organs.

antagonists might offer novel possibilities for successful BC imaging. In this study, we compared the SSTR agonist ^{111}In-DOTA-Tyr^3-octreotate and the antagonist ^{111}In-DOTA-JR11 in 40 human BC specimens and in a BC mouse model. Since both DOTA-Tyr^3-octreotate and DOTA-JR11 have high affinity for SSTR subtype 2 and low affinity for other SSTR subtypes, the observed difference in binding/uptake is mainly based on interaction with SSTR subtype 2 (9,10).

We found significant higher binding of ^{111}In-DOTA-JR11 vs. ^{111}In-DOTA-Tyr^3-octreotate to the BC specimens. Our findings are in line with results of Cescato et al. (4), who demonstrated higher binding of ^{177}Lu-DOTA-BASS, another SSTR antagonist, compared to ^{177}Lu-DOTA-Tyr^3-octreotate in 7 BCs. The authors also compared ^{177}Lu-DOTA-BASS and ^{177}Lu-DOTA-Tyr^3-octreotate in other tumor types, including pheochromocytoma's. Binding of the antagonist to BCs was as high as binding of the agonist to pheochromocytoma's. Since pheochromocytoma's are successfully targeted with the agonist (4), this indicates the potential of targeting BC with SSTR antagonists.

In our in vivo-model, tumors were visualized better with ^{177}Lu-DOTA-JR11 vs. ^{177}Lu-DOTA-Tyr^3-octreotate, corresponding to the measured ex vivo tumor uptake. High radiotracer uptake was also observed in the kidneys and pancreas. Kidney uptake can be reduced by co-injecting with kidney protectors (6,11). The higher tumor to pancreas ratio with the antagonist has to be taken into account, especially when the radiotracer will be used for therapy. However, radiosensitivity of the pancreas is relatively low (12) and the washout seems to relatively fast (5).

Dude et al. (13) compared the uptake of 2 SSTR agonists (^{68}Ga-DOTATOC and ^{68}Ga-DOTA-Tyr^3-octreotate) and 1 SSTR antagonist (^{68}Ga-NODAGA-JR11) in another BC model. The authors reported a higher uptake of ^{68}Ga-DOTATOC vs. ^{68}Ga-NODAGA-JR11, while similar to our findings ^{68}Ga-NODAGA-JR11 tumor uptake was higher than that of ^{68}Ga-DOTA-Tyr^3-octreotate. These findings could be explained by the different affinity of ^{68}Ga-DOTATOC for SSTR subtypes compared to ^{68}Ga-NODAGA-JR11 and ^{68}Ga-DOTA-Tyr^3-octreotate and indicate that SSTR antagonist might not always be superior for tumor targeting.

Considering that ^{177}Lu is a therapeutic radionuclide, the next step would be to determine whether ^{177}Lu-DOTA-JR11 could also be used for safe and effective BC treatment. In line with our previous study in a human lung cancer model (5), we expect that the enhanced in vivo tumor uptake of the antagonist in BC will also result in a better therapeutic efficacy. Thus, SSTR-mediated BC targeting can offer both imaging and therapy options.

In conclusion, we demonstrated the advantage of radiolabeled SSTR antagonists vs. agonists for BC targeting in a preclinical setting, shedding new light on SSTR-mediated BC imaging. The application of an SSTR antagonist, combined with other recent developments, including dedicated breast cameras (14) and PET radionuclides (15), is very promising and might result in a (more) important role for SSTR-mediated imaging (and treatment) of BC patients.

REFERENCES

1. Reubi JC, Waser B, Foekens JA, Klijn JG, Lamberts SW, Laissue J. Somatostatin receptor incidence and distribution in breast cancer using receptor autoradiography: relationship to EGF receptors. Int J Cancer. 1990;46:416-420.
2. Dalm SU, Melis M, Emmering J, Kwekkeboom DJ, de Jong M. Breast cancer imaging using radiolabelled somatostatin analogues. Nucl Med Biol. 2016;43:559-565.
3. Ginj M, Zhang H, Waser B, et al. Radiolabeled somatostatin receptor antagonists are preferable to agonists for in vivo peptide receptor targeting of tumors. Proc Natl Acad Sci U S A. 2006;103:16436-16441.
4. Cescato R, Waser B, Fani M, Reubi JC. Evaluation of 177Lu-DOTA-sst2 antagonist versus 177Lu-DOTA-sst2 agonist binding in human cancers in vitro. J Nucl Med. 2011;52:1886-1890.
5. Dalm SU, Nonnekens J, Doeswijk GN, et al. Comparison of the Therapeutic Response to Treatment with a 177Lu-Labeled Somatostatin Receptor Agonist and Antagonist in Preclinical Models. J Nucl Med. 2016;57:260-265.
6. Wild D, Fani M, Fischer R, et al. Comparison of somatostatin receptor agonist and antagonist for peptide receptor radionuclide therapy: a pilot study. J Nucl Med. 2014;55:1248-1252.
7. de Blois E, Chan HS, de Zanger R, Konijnenberg M, Breeman WA. Application of single-vial ready-for-use formulation of 111In- or 177Lu-labelled somatostatin analogs. Appl Radiat Isot. 2014;85:28-33.
8. Dalm SU, Sieuwerts AM, Look MP, et al. Clinical Relevance of Targeting the Gastrin-Releasing Peptide Receptor, Somatostatin Receptor 2, or Chemokine C-X-C Motif Receptor 4 in Breast Cancer for Imaging and Therapy. J Nucl Med. 2015;56:1487-1493.
9. Fani M, Braun F, Waser B, et al. Unexpected sensitivity of sst2 antagonists to N-terminal radiometal modifications. J Nucl Med. 2012;53:1481-1489.
10. Reubi JC, Schar JC, Waser B, et al. Affinity profiles for human somatostatin receptor subtypes SST1-SST5 of somatostatin radiotracers selected for scintigraphic and radiotherapeutic use. Eur J Nucl Med. 2000;27:273-282.
11. van Eerd JE, Vegt E, Wetzels JF, et al. Gelatin-based plasma expander effectively reduces renal uptake of 111In-octreotide in mice and rats. J Nucl Med. 2006;47:528-533.
12. Stewart FA, Akleyev AV, Hauer-Jensen M, et al. ICRP publication 118: ICRP statement on tissue reactions and early and late effects of radiation in normal tissues and organs -threshold doses for tissue reactions in a radiation protection context. Ann ICRP. 2012;41:1-322.
13. Dude I, Zhang Z, Hundal N, et al. Preclinical evaluation of somatostatin receptor agonist versus antagonist radioligands for breast cancer imaging. J Nucl Med. 2016;57 (Supplement 2):1175 [abstract]
14. Vercher-Conejero JL, Pelegri-Martinez L, Lopez-Aznar D, Cozar-Santiago Mdel P. Positron Emission Tomography in Breast Cancer. Diagnostics (Basel). 2015;5:61-83.
15. Buchmann I, Henze M, Engelbrecht S, et al. Comparison of 68Ga-DOTATOC PET and 111In-DTPAOC (Octreoscan) SPECT in patients with neuroendocrine tumours. Eur J Nucl Med Mol Imaging. 2007;34:1617-1626.

Chapter 7

Comparison of the Therapeutic Response to Treatment with a ^{177}Lu-labeled Somatostatin Receptor Agonist and Antagonist in Preclinical models

S.U. Dalm[1], J. Nonnekens[1, 2], G.N. Doeswijk[1], E. de Blois[1], D.C. van Gent[2], M.W. Konijnenberg[1] and M. de Jong[1]

[1]Dept. of Radiology & Nuclear Medicine, Erasmus MC, Rotterdam, The Netherlands and [2]Dept. of Genetics, Erasmus MC, Rotterdam, The Netherlands

Adapted from J Nucl Med 2016; 57(2):260-5

ABSTRACT

Peptide receptor scintigraphy and peptide receptor radionuclide therapy using radiolabeled somatostatin receptor (SSTR) agonists are successfully used in the clinic for imaging and treatment of neuroendocrine tumors. Contrary to the paradigm that internalization and the resulting accumulation of radiotracers in cells is necessary for efficient tumor targeting, recent studies have demonstrated the superiority of radiolabeled SSTR antagonists for imaging purposes, despite little to no internalization in cells. However, studies comparing the therapeutic antitumor effects of radiolabeled SSTR agonists versus antagonists are lacking. The aim of this study was to directly compare the therapeutic effect of ^{177}Lu-DOTA-octreotate, an SSTR agonist, and ^{177}Lu-DOTA-JR11, an SSTR antagonist.

Methods: We analyzed radiotracer uptake (both membrane-bound and internalized fractions) and the produced DNA double-strand breaks, by determining the number of p53 binding protein 1 foci, after incubating SSTR2-positive cells with ^{177}Lu-diethylene triamine pentaacetic acid, ^{177}Lu-DOTA-octreotate, or ^{177}Lu-DOTA-JR11. Also, biodistribution studies were performed in tumor-xenografted mice to determine the optimal dose for therapy experiments. Afterward, in vivo therapy experiments comparing the effect of ^{177}Lu-DOTA-octreotate and ^{177}Lu-DOTA-JR11 were performed in this same animal model.

Results: We found a 5 times higher uptake of ^{177}Lu-DOTA-JR11 than of ^{177}Lu-DOTA-octreotate. The major part (88%±1%) of the antagonist uptake was membrane-bound, whereas 74%±3% of the total receptor agonist uptake was internalized. Cells treated with ^{177}Lu-DOTA-JR11 showed 2 times more p53-binding protein 1 foci than cells treated with ^{177}Lu-DOTA-octreotate. Biodistribution studies with ^{177}Lu-DOTA-JR11 (0.5 μg/30 MBq) resulted in the highest tumor radiation dose of 1.8±0.7 Gy/MBq, 4.4 times higher than the highest tumor radiation dose found for ^{177}Lu-DOTA-octreotate. In vivo therapy studies with ^{177}Lu-DOTA-octreotate and ^{177}Lu-DOTA-JR11 resulted in a tumor growth delay time of 18±5 and 26±7 d, respectively. Median survival rates were 43.5, 61, and 71 d for the control group, ^{177}Lu-DOTA-octreotate group, and the ^{177}Lu-DOTA-JR11-treated group, respectively.

Conclusions: On the basis of these results, we concluded that the use of radiolabeled SSTR antagonists such as JR11 might enhance peptide receptor scintigraphy and peptide receptor radionuclide therapy of neuroendocrine tumors and provide successful imaging and therapeutic strategies for cancer types with relatively low SSTR expression.

Keywords:
PRRT, Somatostatin Receptor, Agonist, Antagonist, Therapy

INTRODUCTION

Radiolabeled somatostatin (SST) analogs targeting SST receptors (SSTRs), especially SSTR2, overexpressed on tumor cells are successfully used for imaging and treatment of neuroendocrine tumors. These applications are referred to as peptide receptor scintigraphy (PRS) and peptide receptor radionuclide therapy (PRRT), respectively. PRS using radiolabeled SST analogs was first described in the late 1980s by Krenning et al. (1), and soon after the first studies using radiolabeled SST analogs for PRRT followed. ^{111}In-diethylene triamine pentaacetic acid (DTPA)-octreotide was the first SSTR radioligand used for therapy and although results were positive, partial remissions were uncommon. Over time multiple SST analogs with improved receptor affinity, mostly receptor agonists, have been developed and described. These SST analogs have been coupled to different chelators, enabling labeling of the SST analogs with positron-emitters, such as ^{68}Ga for PET scanning, and β-emitters, such as ^{90}Y and ^{177}Lu for therapeutic purposes, leading to better imaging and therapy results. Concerning therapy, response rates between 10% and 35% have been reported after treatment of gastroenteropancreatic neuroendocrine tumors using ^{90}Y-DOTATOC or ^{177}Lu-DOTA-octreotate (2,3). Although results are positive, there is room for improvement of PRRT using SSTR radioligands. Recent developments to improve therapeutic outcome with SSTR radioligands include the use of a combination of ^{90}Y- and ^{177}Lu-labeled peptide analogs, PRRT using α-emitters, and the combination of PRRT with other anticancer agents (4). Another recent development is the introduction of SST analogs with receptor antagonistic properties. For decades it was believed that radiolabeled receptor agonists would be superior to antagonists, because they are internalized upon receptor binding, resulting in accumulation of radioactivity in tumor cells. However, recent in vitro and human studies surprisingly showed higher tumor uptake of SSTR antagonists than SSTR agonists (5-8). Wild et al. (8) reported a 1.7- to 10.6-fold-higher tumor dose when patients were scanned with ^{177}Lu-DOTA-JR11, an SSTR antagonist, than with ^{177}Lu-DOTA-octreotate, an SSTR agonist. Furthermore, in this same study it was demonstrated that therapy with ^{177}Lu-DOTA-JR11 is feasible (8).

To date, to our knowledge no study, neither preclinical nor clinical, has been performed comparing therapeutic responses between radiolabeled SSTR agonists and SSTR antagonists. The aim of this study was to compare the therapeutic effect of ^{177}Lu-DOTA-octreotate and ^{177}Lu-DOTA-JR11 in vivo in the H69 SSTR-positive mouse xenograft model. We first determined the optimal peptide amount for therapy using these radiotracers by performing biodistribution studies. Also, in vitro experiments were performed studying the uptake and the DNA damage response after treatment with the radiotracers.

MATERIALS AND METHODS

Radioligands

The SSTR agonist DOTA-octreotate (molecular weight: 1,436 g/mol) (BioSynthema) and the SSTR antagonist JR11 (molecular weight: 1,690 g/mol) (9) (kindly provided by Dr. Helmut Maecke) were radiolabeled with ^{177}Lu (IDB), using quenchers to prevent radiolysis, as previously described (8,10,11). Specific activity was 53 MBq/nmol for in vitro studies and 0.5 μg/30 MBq, 1.0 μg/30 MBq, and 2.0 μg/30 MBq for in vivo studies. Instant thin-layer chromatography on silica gel and high-pressure liquid chromatography were used to measure radiometal incorporation (>95%) and radiochemical purity (>90%) as previously described (11).

Cell Lines and Cell Culture

The SSTR2 complementary DNA sequence from image clone 3875163 (Life Technologies) was cloned into the pcDNA3.1 vector (Life Technologies). Human osteosarcoma cells (U2OS) were transfected with the pcDNA3.1-SSTR2 vector using X-treme GENE HP Transfection Reagent (Roche Life Sciences) and selected for 2 wk with Geneticin (Life Technologies). Single cell colonies were grown to obtain a pure SSTR2-positive cell line (U2OS+SSTR2). Cells were cultured in Dulbecco modified Eagle medium (Lonza), supplemented with 10% fetal bovine serum (Biowest) and 5 mL of penicillin (5,000 units/mL) and streptomycin (5,000 μg/mL) (Sigma Aldrich), at 37°C and 5% CO_2.

Uptake Assay

The membrane-bound and internalized fractions of the radiotracers were determined after incubation of the cells with 4 different concentrations of ^{177}Lu-DOTA-octreotate or ^{177}Lu-DOTA-JR11. To demonstrate SSTR specificity of the uptake, cells were also incubated with equal amounts of ^{177}Lu-DTPA.

Cells were seeded in 12-well plates 1 d before the experiment. The next day, adhered cells (8×10^4 cells/well) were incubated with 5×10^{-8} M/2.5 MBq, 2×10^{-8} M/1 MBq, 5×10^{-9} M/0.25 MBq, or 2×10^{-9} M/0.1 MBq of ^{177}Lu-DOTA-octreotate, ^{177}Lu-DOTA-JR11, or equal amounts of ^{177}Lu-DTPA in 1 mL of culture medium for 4 h at 37°C. After incubation, supernatant was removed and cells were washed twice with phosphate-buffered saline (PBS) (Lonza). Membrane-bound radiotracer fraction was separated from the internalized fraction by incubating cells for 10 min with an acid solution (50 mM glycine and 100 mM NaCl, pH 2.8). Subsequently, cells were lysed using 0.1 M NaOH to collect the internalized radiotracer fraction. Membrane-bound and internalized radiotracer fractions were counted in a γ-counter (1480 WIZARD automatic γ-counter; PerkinElmer) using a radionuclide-specific energy window, a counting time of 60 s, and a counting error of 5% or less. Data are expressed as percentage added dose.

DNA Damage Immunofluorescent Staining

DNA double-strand break (DSB) formation was determined by quantifying the number of p53-binding protein 1 (53BP1) foci per nucleus over time in cells treated with the radiotracers. 53BP1 is a key protein that is recruited to DSB

during early repair and is therefore a good marker for DSBs (12). Its accumulation on the DSB is visualized as nuclear foci.

To measure DNA DSBs, cells were seeded on glass coverslips in 6-well plates 1 d before the experiment. The next day, adhered cells were incubated with 5 MBq of ^{177}Lu-DTPA, 7.9×10^{-8} M/5 MBq of ^{177}Lu-DOTA-octreotate, or 7.9×10^{-8} M/5 MBq of ^{177}Lu-DOTA-JR11 in 2 mL culture medium for 4 h at 37°C. Subsequently, cells were washed twice with PBS and incubated for different time points (0, 1, 2, and 3 d) in culture medium without radiotracers. Cells were fixed with 1 mL of 2% paraformaldehyde (Sigma Aldrich) for 15 min at room temperature (RT), permeabilized in PBS containing 0.1% Triton X-100 (Sigma Aldrich) by incubating twice for 10 min at RT, and incubated in blocking buffer (PBS, 0.1% Triton X-100, 2% bovine serum albumin [Sigma Aldrich]) for 30 min at RT. Next, cells were incubated for 90 min at RT with the primary antibody, anti-53BP1 (NB100-304 [Novus Biologicals]; 1/1,000) diluted in blocking buffer. After incubation, cells were washed 3 times for 5 min at RT with PBS and 0.1% Triton X-100 and incubated with the secondary antibody (goat antirabbit Alexa Fluor 594 [Life Technologies]; 1/1,000) in blocking buffer for 60 min at RT. Cells were mounted with Vectashield (Vector Laboratories) containing DAPI (4',6-diamidino-2-phenylindole). Z-stack imaging was performed using a TCS SP5 confocal microscope (Leica), and foci were counted from 30 to 40 cells per condition using Image J software (National Institutes of Health). Foci were considered legitimate when their size was between 20 and 100 squared pixels; foci smaller or bigger were considered background staining.

In Vivo Biodistribution Studies

All animal experiments were approved by the Animal Welfare Committee of the Erasmus MC, and all experiments were conducted in accordance to accepted guidelines.

Balb c *nu/nu* male animals, subcutaneously (right shoulder) inoculated with 4×10^6-4×10^7 cells of the SSTR2-positive human small cell lung cancer cell line H69, were used in this study. Tumors were allowed to grow for 3-4 wk after cell inoculation. Tumor size was 241±151 mm^3 for biodistribution studies and 701±387 mm^3 for in vivo therapy studies.

To determine the optimal radiotracer peptide amount for therapy, biodistribution studies were performed. Because studies determining the optimal dose for ^{177}Lu-DOTA-octreotate were previously performed at our department, biodistribution studies were performed only for ^{177}Lu-DOTA-JR11. For this, animals were injected with 0.5 μg/30 MBq, 1 μg/30 MBq, or 2 μg/30 MBq of ^{177}Lu-DOTA-JR11. At 4 time points (4 h, 2 d, 4 d, and 7 d) after injection, animals (n=4 per peptide amount for each time point) were euthanized, and tumors and organs were collected, weighed, and counted in a γ-counter as previously mentioned. The radioactivity uptake in tumor and organs was determined and expressed as percentage injected dose per gram of tissue (%ID/g).

In Vivo Therapy Studies

In the therapy experiment, 24 Balb c *nu/nu* male mice with subcutaneous H69 xenografts were intravenously injected with 0.5 μg/30 MBq of ^{177}Lu-DOTA-JR11, 0.5 μg/30 MBq of ^{177}Lu-DOTA-octreotate, or 200 μL of injection fluid (sham) (n=8 each group). Animals injected with either one of the radiotracers were pre-injected with 4 mg of modified fluid gelatin (Gelofusin; Braun) to reduce renal uptake (13). Tumor size, weight, and physical well-being of the animals were monitored 3 times per week. Mice were euthanized when tumor size reached 2,000 mm^3 or animal weight decreased by 10% or more.

Dosimetry

Absorbed doses were calculated for both compounds in organs with physiologic uptake and in the tumor xenografts. Organ dosimetry was performed according to the MIRD principle following the equation for absorbed dose in organ j as a summation from all source organs i: $D_j = A\sum_i \tilde{a}_i \times S\,(j \leftarrow i)$.

Time-activity curves were determined by least-squares fitting of single-exponential curves through the data, using Prism software (GraphPad). The time-integrated activity coefficients $\tilde{a}_i$ in each source organ i were determined by integration of the exponential curves folded with the ^{177}Lu decay (half-life, 6.647 d). The S value ^{177}Lu dose factors were taken from the 25-g RADAR stylized mouse phantom (14). The absorbed doses in the tumor xenografts were determined using the spheric node option within the Olinda/EXM software (15).

Statistics

Tumor growth curves were individually determined by least-squares fitting of single-exponential growth curves to the tumor size measurements against time. The growth curves of animals were extrapolated to later times beyond the censoring endpoint due to the maximum tumor volume of 2,000 mm^3. The extrapolated data were combined with the data of the longest surviving animals to obtain a collective growth curve within each group. Group-averaged mean values of tumor size as a function of time were considered only for normally distributed tumor volumes at each time point using the Shapiro-Wilk normality test. A Pearson correlation coefficient $R^2>0.8$ was used for acceptance of the fits. The growth delay time was defined as the difference in time to reach the maximum tumor volume of 2,000 mm^3 between the treatment group and the control. Significant differences were evaluated using the 1-way ANOVA test, after checking for normality by the Shapiro-Wilk normality test. All statistical evaluations were performed with Prism software.

RESULTS

In Vitro Uptake of ^{177}Lu-DOTA-octreotate and ^{177}Lu-DOTA-JR11

In the in vitro assay, tumor cell uptake of both ^{177}Lu-DOTA-octreotate and ^{177}Lu-DOTA-JR11 was observed. Little to no uptake was seen, on the other hand, when cells were incubated with ^{177}Lu-DTPA, demonstrating receptor specificity of the radiotracers. The total uptake of ^{177}Lu-DOTA-JR11 was up to 5 times higher than the ^{177}Lu-DOTA-octreotate uptake (*Figure 1*). Furthermore, the lowest peptide amount added resulted in the highest percentage added dose uptake of both radiotracers. Most radioactivity uptake of ^{177}Lu-DOTA-octreotate, 74±3 %, was internalized, whereas most, 88±1%, of ^{177}Lu-DOTA-JR11 uptake was membrane-bound, in line with the receptor agonistic versus receptor antagonistic properties of the 2 radiotracers.

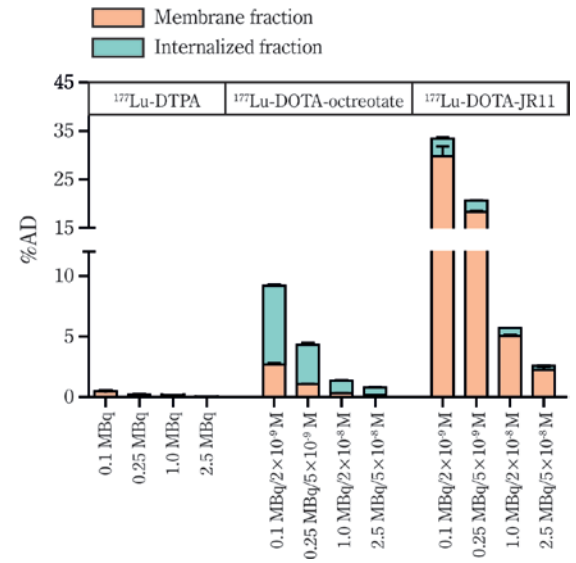

Figure 1. Uptake of SSTR agonist ^{177}Lu-DOTA-octreotate and SSTR antagonist ^{177}Lu-DOTA-JR11 in the SSTR2-transfected U2OS cell line. %AD=percentage added dose.

DNA Damage Response

The timing and level of DNA DSB induction and repair were quantified by counting the number of 53BP1 foci per nucleus over time (*Figure 2*). Initially, DSBs were induced by ^{177}Lu-DTPA, ^{177}Lu-DOTA-octreotate, and ^{177}Lu-DOTA-JR11. However, after unbound radioactivity/radiotracers were removed, the ^{177}Lu-DTPA-induced DSBs were repaired within a day, whereas DSBs caused by ^{177}Lu-DOTA-octreotate and ^{177}Lu-DOTA-JR11 remained present for at least 3 d. In line with the difference in uptake, ^{177}Lu-DOTA-JR11 treatment produced more DSBs than ^{177}Lu-DOTA-octreotate treatment, and this increased level of DSBs remained over time.

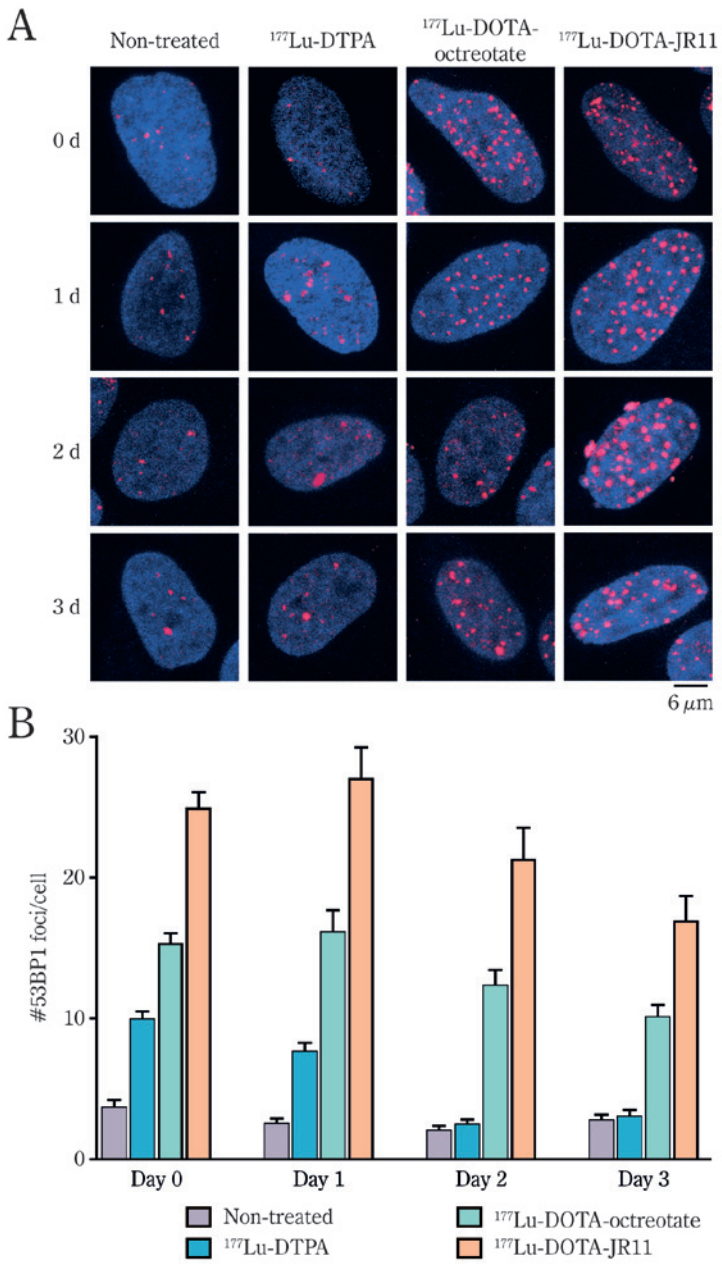

Figure 2. DNA damage response studied by analyzing 53BP1 foci in U2OS+SSTR2 cells after treatment with ^{177}Lu-DOTA-octreotate and ^{177}Lu-DOTA-JR11. Nontreated and ^{177}Lu-DTPA-treated cells were taken along as controls. A) Pictures of 53BP1 and DAPI (nuclear) staining of treated and untreated samples at different time points after treatment. 53BP1 is in red, DAPI is in blue. B) Quantification of 53BP1 foci in 30-40 cells per condition after treatment. Error bars represent SEM.

In Vivo Biodistribution and Dosimetry of ^{177}Lu-DOTA-JR11

Biodistribution studies were performed at 4 different time points after injection of 0.5 μg/30 MBq, 1.0 μg/30 MBq, or 2.0 μg/30 MBq of ^{177}Lu-DOTA-JR11. Injection of 0.5 μg/30 MBq of the radiotracer resulted in the highest tumor uptake, with the lowest variation (20.8±3.4 %ID/g of tissue 4 h after injection). Next to the tumor uptake, high uptake was seen in the kidneys (31.1±5.5 %ID/g of tissue 4 h after injection), as a consequence of urinary excretion and partial reabsorption of the radiotracer, and in the SSTR2-expressing pancreas (9.28±1.22 %ID/g of tissue 4 h after injection) and stomach (7.74±1.00 %ID/g of tissue 4 h after injection). Kidney, stomach, and pancreas radioactivity decreased relatively quickly, with clearance half-lives ranging between 14 and 19 h, whereas tumor uptake remained longer, with a clearance half-life of 30 h. Seven days after injection of 0.5 μg/30 MBq of ^{177}Lu-DOTA-JR11, tumor radioactivity was 6.8±2.5 %ID/g of tissue, whereas kidney, stomach, and pancreas uptake was 1.20±0.26, 0.64±0.20, and 0.32±0.07 %ID/g of tissue, respectively. The results of the biodistribution study are displayed in *Table 1*. Dosimetry calculations resulted in a tumor radiation dose of 1.8±0.7 Gy/MBq using 0.5 μg of the radiotracer. The tumor and highest organ doses for the different peptide amounts are indicated in *Table 2*. The tumor, pancreas, and stomach doses were reduced considerably by higher peptide amount, whereas the dose to the kidney remained constant.

In Vivo Therapy Studies

Balb c *nu/nu* animals with H69 xenografts received either a sham injection, a therapeutic injection of 0.5 μg/30 MBq of ^{177}Lu-DOTA-octreotate, or 0.5 μg/30 MBq of ^{177}Lu-DOTA-JR11, the optimal peptide amount previously reported for ^{177}Lu-DOTA-octreotate and the optimal peptide amount measured in biodistribution studies for ^{177}Lu-DOTA-JR11. Animals treated with ^{177}Lu-DOTA-JR11 showed a decrease in tumor size up to 45±7 d after injection after which tumor regrowth occurred (*Figure 3*). For ^{177}Lu-DOTA-octreotate, tumor regrowth was already observed 41±2 d after injection of the radiotracer. Furthermore, median survival rates were 43.5, 61, and 71 d for the control group, the ^{177}Lu-DOTA-octreotate group, and the ^{177}Lu-DOTA-JR11-treated group, respectively (*Figure 4*).

The mean time to reach 2,000 mm^3 was 45±10 d for control animals, 64±14 d for ^{177}Lu-DOTA-octreotate, and 71±10 d for ^{177}Lu-DOTA-JR11-treated animals. Hence, the growth delay times were 18±5 and 26±7 d for ^{177}Lu-DOTA-octreotate and ^{177}Lu-DOTA-JR11-treated groups, respectively. This was significantly different from the control group but did not show a significant difference between the 2 compounds.

Table 1. Biodistribution of ^{177}Lu-DOTA-JR11 in H69 xenografted mice

Organs	0.5 µg				1.0 µg	
	4 h	2 d	4 d	7 d	4 h	2 d
Blood	0.23±0.04	0.03±0.01	0.02±0.01	0.01±0.00	0.11±0.02	0.01±0.00
Spleen	0.56±0.15	0.35±0.08	0.29±0.05	0.30±0.07	0.55±0.07	0.29±0.09
Pancreas	9.28±1.22	1.32±0.13	0.56±0.08	0.32±0.07	8.22±1.20	0.99±0.11
Adrenals	1.58±0.92	0.49±0.26	0.30±0.04	0.19±0.06	2.04±2.25	0.33±0.13
Kidney	31.13±5.50	7.40±1.04	2.74±0.51	1.20±0.26	30.06±3.80	7.23±1.79
Liver	1.93±0.03	0.68±0.08	0.47±0.01	0.35±0.07	2.36±0.24	0.59±0.11
Stomach	7.71±1.00	2.03±0.52	1.10±0.10	0.64±0.20	5.38±1.17	1.22±0.17
Duodenum	0.98±0.31	0.34±0.20	0.11±0.03	0.08±0.01	0.96±0.26	0.14±0.04
Muscle	0.22±0.20	0.05±0.02	0.04±0.01	0.03±0.01	0.20±0.10	0.04±0.01
Tumor	20.78±3.37	11.21±2.68	10.21±6.49	6.75±2.46	21.44±9.84	13.57±3.25
Tail	1.22±0.28	0.33±0.08	0.38±0.20	0.30±0.22	1.27±0.15	0.38±0.21

Organs	1.0 µg		2.0 µg			
	4 d	7 d	4 h	2 d	4 d	7 d
Blood	0.01±0.01	0.01±0.00	0.10±0.08	0.04±0.04	0.01±0.00	0.00±0.00
Spleen	0.24±0.05	0.25±0.04	0.43±0.21	0.23±0.03	0.18±0.05	0.17±0.04
Pancreas	0.47±0.12	0.28±0.02	3.07±1.06	0.39±0.05	0.20±0.05	0.10±0.01
Adrenals	0.22±0.07	0.19±0.05	0.47±0.09	0.24±0.06	0.15±0.05	0.14±0.07
Kidney	2.58±0.18	1.07±0.51	32.56±13.20	6.27±0.54	2.26±0.53	0.84±0.22
Liver	0.43±0.03	0.25±0.03	1.39±0.59	0.42±0.03	0.33±0.03	0.19±0.03
Stomach	1.01±0.12	0.52±0.04	2.30±0.93	0.58±0.09	0.32±0.05	0.21±0.04
Duodenum	0.11±0.03	0.07±0.02	0.48±0.19	0.08±0.01	0.06±0.02	0.03±0.01
Muscle	0.06±0.02	0.03±0.01	0.18±0.15	0.03±0.00	0.02±0.01	0.03±0.01
Tumor	8.61±2.51	6.25±1.55	13.64±6.15	7.05±1.62	4.32±1.10	3.38±1.05
Tail	0.19±0.04	0.17±0.11	1.07±0.28	0.28±0.12	0.10±0.02	0.09±0.06

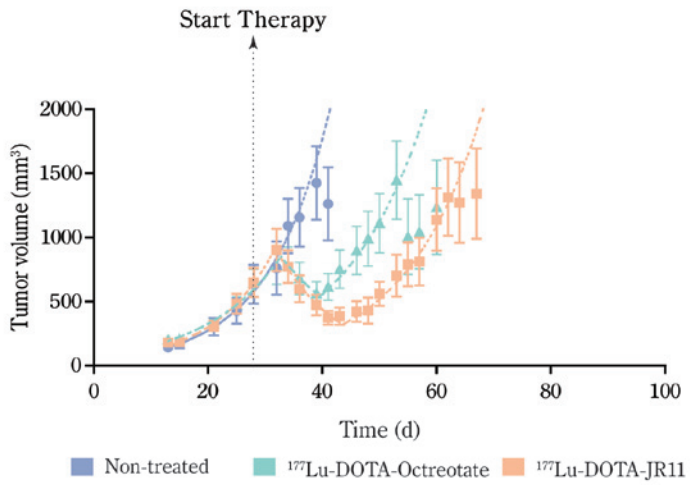

Figure 3. Tumor growth extrapolation of control, ^{177}Lu-DOTA-octreotate, and ^{177}Lu-DOTA-JR11-treated animals. ^{177}Lu-DOTA-octreotate and ^{177}Lu-DOTA-JR11-treated animals were pre-injected with modified fluid gelatin to reduce renal uptake of radiotracers.

Table 2. Absorbed dose per administered activity (Gy/MBq) in 220 mg H69 tumor xenograft and organs for ^{177}Lu-DOTA JR11

Organs	0.5 µg	1.0 µg	2.0 µg
Tumor	1800	1645	936
Kidneys	969	925	886
Stomach	249	189	78
Pancreas	238	202	82

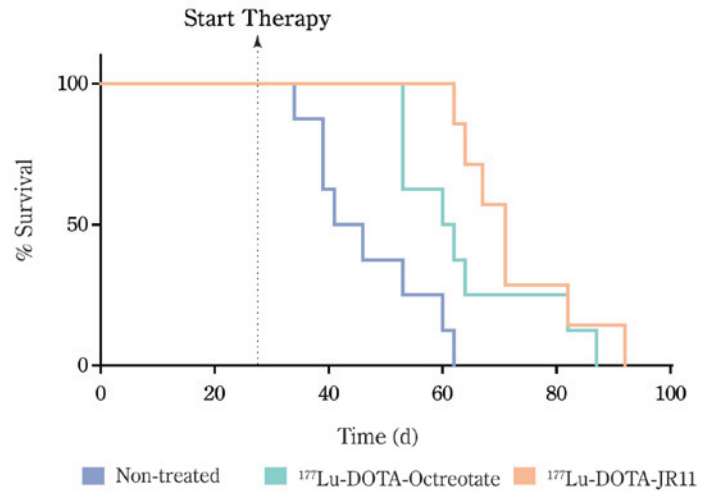

Figure 4. Kaplan-Meier survival curve of control animals, ^{177}Lu-DOTA-octreotate, and ^{177}Lu-DOTA-JR11-treated animals.

DISCUSSION

Previous studies demonstrated SSTR antagonists to be superior to SSTR agonist for tumor targeting, contradicting the paradigm that internalization and accumulation of the radiotracer is necessary for efficient tumor targeting. However, up to now no study has been performed directly comparing the therapeutic effect of radiolabeled SSTR agonists and antagonists. In this study, we compared the therapeutic response of the radiolabeled SSTR agonist ^{177}Lu-DOTA-octreotate and the radiolabeled SSTR antagonist ^{177}Lu-DOTA-JR11 in vitro, in U2OS+SSTR2 cells, and in vivo in H69-xenografted mice.

First, we studied the in vitro uptake of the 2 radiotracers and found uptake to be up to 5 times higher with ^{177}Lu-DOTA-JR11 than with ^{177}Lu-DOTA-octreotate. We saw that the major part of ^{177}Lu-DOTA-octreotate was internalized, whereas the major part of the total uptake of ^{177}Lu-DOTA-JR11 remained membrane-bound, consistent with the receptor agonistic and antagonistic properties of the 2 peptides. These data are in line with previous findings by Fani et al. (9) who demonstrated SSTR2-specific antagonism of Ga-NODAGA-JR11 by immunofluorescence imaging in the presence and absence of the SSTR2 agonist Tyr^3-octreotide.

To compare efficacy of the 2 radiolabeled peptides at the molecular level, we also analyzed the DNA damage response after treating cells with ^{177}Lu-DOTA-octreotate or ^{177}Lu-DOTA-JR11. ^{177}Lu emits β-particles that can induce several types of DNA damage, among which DSBs are the most genotoxic. Unrepaired DSBs can trigger cell cycle arrest, cell death, and chromosomal aberrations. DSB induction initiates a cascade of events, including accumulation of the necessary repair proteins (e.g. 53BP1) (12). Quantification of 53BP1 foci per nucleus is therefore a powerful tool to examine DSB induction and repair (16,17). ^{177}Lu-DTPA produced only transient DSBs comparable to DSBs induced by an external radiation source (16). ^{177}Lu-DOTA-JR11 produced 2 times more DSBs than ^{177}Lu-DOTA-octreotate, even though we observed up to 5 times higher uptake of the radiolabeled antagonist in the uptake assay. This difference might be explained by the different peptide concentrations used in the assays, because radiotracer uptake is dependent on the peptide amount used (2×10^{-9} M of the radiotracers resulted in a 5 times higher uptake of ^{177}Lu-DOTA-JR11 vs. ^{177}Lu-DOTA-octreotate, whereas the uptake was only 3 times higher with 5×10^{-8} M of the radio-tracers). Furthermore, being a receptor antagonist, ^{177}Lu-DOTA-JR11 remained bound to the cell membrane, whereas the receptor agonist ^{177}Lu-DOTA-octreotate is internalized. The ^{177}Lu coupled to JR11, therefore, resides on average at a larger distance from the nucleus and its DNA content. This might reduce the number of β-particles effectively reaching the DNA to induce damage, especially when cells are grown in 2-dimensional cell culture.

^{177}Lu-DOTA-JR11 biodistribution studies in mice with H69 xenografts resulted in the highest tumor uptake with the lowest variation using 0.5 μg/30 MBq of the radiotracer. This was similar to the 22.4±7.6 ID/g of tissue 2 h after injection of 100 pmol ^{68}Ga-DOTA-JR11 reported by Fani et al. (9). Previous biodistribution studies with ^{177}Lu-DOTA-octreotate in the same animal model resulted in

the highest tumor uptake of 4.03±0.83 %ID/g of tissue using 0.5 μg/30 MBq of ^{177}Lu-DOTA-octreotate 2 d after injection of the radiotracer (S Bison, M Konijnenberg, and M de Jong, unpublished data, December 2013). At this time point, 0.5 μg/30 MBq of ^{177}Lu-DOTA-JR11 resulted in an almost 3-times-higher tumor uptake of 11.21±2.68 %ID/g of tissue in our biodistribution studies. This was higher than the 1.2 times higher uptake of ^{68}Ga-DOTA-JR11 compared with ^{68}Ga-DOTA-octreotate 2 h after injection of the radiotracers reported by Fani et al. (9).

The higher tumor uptake after ^{177}Lu-DOTA-JR11 resulted in a tumor radiation dose of 1.8±0.7 Gy/MBq, 4.4-fold higher than the maximum tumor radiation dose for ^{177}Lu-DOTA-octreotate (0.36±0.07 Gy/MBq). Wild et al. (8) reported a 1.7 to 10.6 fold higher tumor dose of ^{177}Lu-DOTA-JR11 in patients, due to higher tumor uptake and longer residence time of the receptor antagonist, indicating the applicability and translational value of our mouse model.

Next to the tumor, high kidney uptake of ^{177}Lu-DOTA-JR11 was found. To reduce the renal uptake in the in vivo therapy studies, animals were pre-injected with modified fluid gelatin. Previous studies showed a decrease in renal uptake of 60% when animals received a pre-injection of modified fluid gelatin (13). Despite the high renal uptake, the treated animals showed no signs of kidney insufficiency. However, in our study animals received only 1 therapeutic injection of ^{177}Lu-DOTA-JR11, and follow-up time was limited. To accurately determine the effect of the radiotracer on the kidneys, additional experiments are needed. In the pilot study by Wild et al. (8), patients were pre-injected with a solution of arginine and lysine to reduce renal uptake, resulting in a 6.2 fold higher tumor-to-kidney ratio for ^{177}Lu-DOTA-JR11 than ^{177}Lu-DOTA-octreotate. Although the patients in this study already had grade 2 or 3 chronic renal failure, no additional decrease in tubular kidney function was reported. Additional studies in larger patient groups without renal problems and studies with longer follow up times are necessary to further investigate potential adverse effects.

Comparing the in vivo therapeutic effect of ^{177}Lu-DOTA-octreotate and ^{177}Lu-DOTA-JR11, we found a longer tumor growth delay time and a longer median survival after ^{177}Lu-DOTA-JR11 treatment. This finding is in line with the higher uptake we found in the in vitro internalization assay and the in vivo biodistribution study. However, the difference in growth delay time between the ^{177}Lu-DOTA-JR11 and ^{177}Lu-DOTA-octreotate-treated animals was not significant. This can be explained by variation in initial tumor size and the fact that animals received only 1 therapeutic injection of the radiotracers. Furthermore, the absorbed dose factor for ^{177}Lu in the cytoplasm (as a consequence of agonist internalization) is 1.5-2 times higher than the absorbed dose factor for ^{177}Lu uptake that is limited to the cell membrane (most of the antagonist uptake) (18).

The superiority of receptor antagonists to receptor agonist has also been reported for other radioligands. So, studies evaluating the use of radiolabeled gastrin releasing peptide receptor agonists and antagonists for targeting of gastrin releasing peptide receptors overexpressed on prostate cancer cells also showed superiority for antagonists (19).

Studies with unlabeled SSTR antagonists BIM-23454 and BIM-23627 in rats showed an increase in growth hormone secretion after administration (20), which

may have a negative effect on tumor therapy. However, the minimal effective concentration, 1 mg/kg for BIM-23454 and 0.02 mg/kg for BIM-23627, necessary to promote growth hormone release was much higher than the dose used for imaging and therapy with radiolabeled SSTR antagonists, for example, 150±20 μg for imaging and 2-3 cycles of 105±35 μg for therapy in the study by Wild et al. (8). The higher uptake of radiolabeled SSTR antagonists might offer possibilities for SSTR-mediated PRS and PRRT to be applied in cancer types with lower SSTR expression, for example, breast cancer. Previous studies by Reubi et al. (21) reported high-density SSTR expression in 21% of the breast tumors analyzed, whereas in total 75% of the tumors expressed the SSTR. Cescato et al. (6) compared binding of the SSTR antagonist ^{177}Lu-DOTA-BASS with the SSTR agonist ^{177}Lu-DOTA-octreotate and reported 11±4-fold-higher binding of the antagonist in 7 breast carcinomas analyzed by in vitro autoradiography. Furthermore, imaging studies in breast cancer patients using SSTR agonists have been performed with varying results (22,23). The use of JR11 may improve these results and provide imaging and therapy options for different tumors.

CONCLUSION

The use of radiolabeled SSTR antagonist such as JR11 may contribute to the improvement of PRS and PRRT in neuroendocrine tumors as well as provide opportunities for SSTR-mediated PRS and PRRT in tumor types with relatively low SSTR expression.

Acknowledgements

We thank Melissa van Kranenburg and Stuart Koelewijn for their technical assistance with the in vitro and in vivo assays and Professor Helmut R. Maecke for providing us with the JR11 peptide.

REFERENCES

1. Krenning EP, Bakker WH, Breeman WA, et al. Localisation of endocrinerelated tumours with radioiodinated analogue of somatostatin. Lancet. 1989;1: 242-244.
2. Kwekkeboom DJ, Mueller-Brand J, Paganelli G, et al. Overview of results of peptide receptor radionuclide therapy with 3 radiolabeled somatostatin analogs. J Nucl Med. 2005;46(suppl 1):62S-66S.
3. Bergsma H, van Vliet EI, Teunissen JJ, et al. Peptide receptor radionuclide therapy (PRRT) for GEP-NETs. Best Pract Res Clin Gastroenterol. 2012;26: 867-881.
4. Bison SM, Konijnenberg M, Melis M, et al. Peptide receptor radionuclide therapy using radiolabeled somatostatin analogs: focus on future developments. Clin Transl Imaging. 2014;2:55-66.
5. Ginj M, Zhang H, Waser B, et al. Radiolabeled somatostatin receptor antagonists are preferable to agonists for in vivo peptide receptor targeting of tumors. Proc Natl Acad Sci USA. 2006;103:16436-16441.
6. Cescato R, Waser B, Fani M, Reubi JC. Evaluation of 177Lu-DOTA-sst2 antagonist versus 177Lu-DOTA-sst2 agonist binding in human cancers in vitro. J Nucl Med. 2011;52:1886-1890.
7. Wild D, Fani M, Behe M, et al. First clinical evidence that imaging with somatostatin receptor antagonists is feasible. J Nucl Med. 2011;52:1412-1417.
8. Wild D, Fani M, Fischer R, et al. Comparison of somatostatin receptor agonist and antagonist for peptide receptor radionuclide therapy: a pilot study. J Nucl Med. 2014;55:1248-1252.
9. Fani M, Braun F, Waser B, et al. Unexpected sensitivity of sst2 antagonists to N-terminal radiometal modifications. J Nucl Med. 2012;53:1481-1489.
10. de Blois E, Chan HS, de Zanger R, Konijnenberg M, Breeman WA. Application of single-vial ready-for-use formulation of 111In- or 177Lu-labelled somatostatin analogs. Appl Radiat Isot. 2014;85:28-33.
11. de Blois E, Chan H, Konijnenberg M, de Zanger R, Breeman W. Effectiveness of quenchers to reduce radiolysis of 111In- or 177Lu-labelled methionine-containing regulatory peptides: maintaining radiochemical purity as measured by HPLC. Curr Top Med Chem. 2012;12:2677-2685.
12. Wyman C, Kanaar R. DNA double-strand break repair: all's well that ends well. Annu Rev Genet. 2006;40:363-383.
13. van Eerd JE, Vegt E, Wetzels JF, et al. Gelatin-based plasma expander effectively reduces renal uptake of 111In-octreotide in mice and rats. J Nucl Med. 2006;47: 528-533.
14. Keenan MA, Stabin MG, Segars WP, Fernald MJ. RADAR realistic animal model series for dose assessment. J Nucl Med. 2010;51:471-476.
15. Stabin MG, Konijnenberg MW. Re-evaluation of absorbed fractions for photons and electrons in spheres of various sizes. J Nucl Med. 2000;41:149-160.
16. Löbrich M, Shibata A, Beucher A, et al. gammaH2AX foci analysis for monitoring DNA double-strand break repair: strengths, limitations and optimization. Cell Cycle. 2010;9:662-669.
17. Barnard S, Bouffler S, Rothkamm K. The shape of the radiation dose response for DNA double-strand break induction and repair. Genome Integr. 2013; 4:1-8.
18. Vaziri B, Wu H, Dhawan AP, Du P, Howell RW, Committee SM. MIRD pamphlet No. 25: MIRDcell V2.0 software tool for dosimetric analysis of biologic response of multicellular populations. J Nucl Med. 2014;55:1557-1564.

19. Schroeder RP, Müller C, Reneman S, et al. A standardised study to compare prostate cancer targeting efficacy of five radiolabelled bombesin analogues. Eur J Nucl Med Mol Imaging. 2010;37:1386-1396.

20. Tulipano G, Soldi D, Bagnasco M, et al. Characterization of new selective somatostatin receptor subtype-2 (sst2) antagonists, BIM-23627 and BIM-23454. Effects of BIM-23627 on GH release in anesthetized male rats after short-term high-dose dexamethasone treatment. Endocrinology. 2002;143:1218-1224.

21. Reubi C, Gugger M, Waser B. Co-expressed peptide receptors in breast cancer as a molecular basis for in vivo multireceptor tumour targeting. Eur J Nucl Med Mol Imaging. 2002;29:855-862.

22. Skånberg J, Ahlman H, Benjegård S, et al. Indium-111-octreotide scintigraphy, intraoperative gamma-detector localisation and somatostatin receptor expression in primary human breast cancer. Breast Cancer Res Treat. 2002; 74:101-111.

23. Van Den Bossche B, van Belle S, de Winter F, Signore A, van de Wiele C. Early prediction of endocrine therapy effect in advanced breast cancer patients using 99mTc-depreotide scintigraphy. J Nucl Med. 2006;47:6-13.

Part 4

GRPR-targeted Nuclear Imaging and Therapy

Chapter 8

In Vitro and In Vivo Application of Radiolabeled Gastrin Releasing Peptide Receptor Ligands in Breast Cancer

S.U. Dalm[1], J.W.M. Martens[2], A.M. Sieuwerts[2], C.H.M. van Deurzen[3], S.J. Koelewijn[1], E. de Blois[1], T. Maina[4], B.A. Nock[4], L. Brunel[5], J. Fehrentz[5], M. de Jong[1] and M. Melis[1]

[1]Dept. of Radiology & Nuclear Medicine, Erasmus MC, Rotterdam, The Netherlands; [2]Dept. of Medical Oncology and Cancer Genomics Netherlands, Erasmus MC Cancer Institute, Erasmus MC, Rotterdam, The Netherlands; [3]Dept. of Pathology, Erasmus MC, Rotterdam, The Netherlands; [4]Molecular Radiopharmacy, INRASTES, NCSR "Demokritos",Athens, Greece; and [5]Institut des Biomolécules Max Mousseron, UMR5247, CNRS-UM1-UM2, Montpellier, France

Adapted from J Nucl Med 2015; 56(5):752-7

ABSTRACT

Breast cancer (BC) consists of multiple subtypes defined by various molecular characteristics, for instance, estrogen receptor (ER) expression. Methods for visualizing BC include mammography, MR imaging, ultrasound, and nuclear medicine-based methods such as ^{99m}Tc-sestamibi and ^{18}F-FDG PET, unfortunately all lacking specificity. Peptide receptor scintigraphy and peptide receptor radionuclide therapy are successfully applied for imaging and therapy of somatostatin receptor-expressing neuroendocrine tumors using somatostatin receptor radioligands. On the basis of a similar rationale, radioligands targeting the gastrin releasing peptide receptor (GRPR) might offer a specific method for imaging and therapy of BC. The aim of this study was to explore the application of GRPR radioligands for imaging and therapy of BC by introducing valid preclinical in vitro and in vivo models.

Methods: GRPR expression of 50 clinical BC specimens and the correlation with ER expression was studied by in vitro autoradiography with the GRPR agonist ^{111}In-AMBA. GRPR expression was also analyzed in 9 BC cell lines applying ^{111}In-AMBA internalization assays and quantitative reverse transcriptase polymerase chain reaction. In vitro cytotoxicity of ^{177}Lu-AMBA was determined on the GRPR-expressing BC cell line T47D. SPECT/CT imaging and biodistribution were studied in mice with subcutaneous and orthotopic ER-positive T47D and MCF7 xenografts after injection of the GRPR antagonist ^{111}In-JMV4168.

Results: Most of the human BC specimens (96%) and BC cell lines (6/9) were found to express GRPR. GRPR tumor expression was positively (P=0.026, $\chi^2(4)$=12,911) correlated with ER expression in the human BC specimens. Treatment of T47D cells with 10^{-7} M/50 MBq of ^{177}Lu-AMBA resulted in 80% reduction of cells in vitro. Furthermore, subcutaneous and orthotopic tumors from both BC cell lines were successfully visualized in vivo by SPECT/CT using ^{111}In-JMV4168; T47D tumors exhibited a higher uptake than MCF7 xenografts.

Conclusions: Targeting GRPR-expressing BC tumors using GRPR radioligands is promising for nuclear imaging and therapy, especially in ER-positive BC patients.

Keywords:
Breast Cancer, PRS/PRRT, GRPR, AMBA, JMV4168

INTRODUCTION

Breast cancer (BC) is a highly heterogeneous disease characterized by multiple molecular features, such as expression of the estrogen receptor (ER), progesterone receptor, and human epidermal growth factor receptor 2 (1). On the basis of molecular characteristics, BC can be divided in 4 subgroups: luminal A and B, human epidermal growth factor receptor 2-like, and triple-negative tumors (2). The treatment and prognosis of BC are highly dependent on this classification. Mammography is the standard imaging technique used during nationwide screening of BC. Additional MR imaging or ultrasound can be performed (3). However, all 3 methods have drawbacks. Mammography lacks sensitivity and specificity, leading to false-positive and false-negative results. Especially in women with dense breast tissue, mammograms are hard to interpret (4). MR imaging and ultrasound also lack specificity. In addition, MR imaging is labor-intensive and expensive, whereas ultrasound is operator-dependent (5).

In nuclear medicine, methods to detect BC lesions and monitor response to treatment include ^{201}Tl-scintigraphy, ^{99m}Tc-sestamibi or ^{99m}Tc-tetrofosmin scintigraphy, and ^{18}F-FDG PET (6). Unfortunately, these methods also lack specificity. Peptide receptor scintigraphy applies specific in vivo targeting of tumor lesions overexpressing a receptor of interest. This method was first described by Krenning et al. (7), using a radioactive somatostatin receptor (SSTR) ligand to image neuroendocrine tumors (NETs) overexpressing the SSTR subtype 2. To date, imaging with SSTR radioligands is routinely applied to characterize and evaluate (tumor localization, staging, monitoring) NETs (8). Furthermore, SSTR radioligands labeled with therapeutic radionuclides are successfully used for treatment of NET patients, using so-called peptide receptor radionuclide therapy (PRRT) (9).

Following the same principle, the gastrin-releasing peptide receptor (GRPR) can be targeted. GRPRs are expressed on most BC cases; autoradiography studies by Reubi et al. (10) showed that 65% of the breast tumors analyzed expressed the GRPR. Moreover, also lymph node metastases from primary tumors expressing GRPR were positive (10-12). GRPR binds a family of peptides, including the gastrin-releasing peptide; its C-terminal fragment neuromedin C, both endogenous in humans; and the amphibian tetradecapeptide bombesin.

The application of GRPR radioligands, analogs of the above native peptides, might offer a sensitive and specific method for imaging of GRPR overexpressing BC. In addition, PRRT with radiolabeled GRPR ligands might be feasible. Recently, multiple GRPR radioligands, receptor agonists and antagonists, have been described that can be labeled with positron and γ-emitters, for example, ^{68}Ga and ^{111}In, for imaging and with β- and α-emitters, for example, ^{177}Lu and ^{213}Bi, for therapeutic purposes, as yet primarily aiming at application in prostate cancer (13). Preclinical studies evaluating the potential of targeting the GRPR in BC using GRPR radioligands are limited. The aim of this study was to further characterize the GRPR as a potential target for the visualization of BC lesions and for PRRT. For this purpose, we analyzed GRPR expression in human clinical BC specimens and correlated this with ER expression. In addition, we used selected GRPR-

/ER-expressing human-derived BC cells to perform in vitro cytotoxicity assays and to develop suitable xenograft-bearing animal models for preclinical imaging studies.

MATERIALS AND METHODS

Radiolabeled GRPR Ligands

For in vitro studies, the GRPR agonist AMBA (BioSynthema) was used (14). Because radiolabeled AMBA exhibits high uptake in the gastrointestinal tract that potentially interferes with orthotopic tumor visualization, the GRPR antagonist JMV4168 (University of Montpellier) was used for in vivo studies (14,15). The GRPR ligands were radiolabeled with ^{111}In (Covidien) or ^{177}Lu (IDB), using quenchers (10 mM methionine, 3.5 mM ascorbic acid, and 3.5 mM gentisic acid) to prevent radiolysis (16). Radiolabeling was performed for 20 min at 80°C as previously described (17), with a specific activity of 100 MBq/nmol (for in vitro studies, both ^{111}In and ^{177}Lu) or 150 MBq/nmol (in vivo studies). Radiometal incorporation and radiochemical purity, measured by instant thin-layer chromatography on silica gel and high-pressure liquid chromatography as previously described (16), were greater than 95% and greater than 90%, respectively.

In Vitro Autoradiography on Human BC Specimens

In vitro autoradiography was performed on 50 human BC specimens with known ER protein status. Specimens were selected from the Erasmus MC fresh frozen tissue bank. The study (MEC02·953) was approved by the Erasmus MC Medical Ethical Committee and adhered to the Code of Conduct of the Federation of Medical Scientific Societies in The Netherlands.

Frozen sections (10 μm) of the BC specimens were incubated with 10^{-9} M/0.1 MBq of ^{111}In-AMBA, without or with 10^{-6} M unlabeled Tyr^4-bombesin (Sigma-Aldrich), to determine nonspecific binding, for 1 h and exposed to super resolution phosphor screens (PerkinElmer) for at least 24 h and read using the Cyclone (PerkinElmer). Adjacent tissue sections were stained with hematoxylin and eosin to determine tumor content. Autoradiography results were scored visually by 3 independent observers. Among the positive tumors, a division was made between tumors that were 1-25%, 26-50%, 51-75%, and 76-100% positive.

Cell Culture, Internalization Assay, and Quantitative Reverse Transcriptase Polymerase Chain Reaction

Nine human-derived BC cell lines, obtained from the Department of Medical Oncology, Erasmus MC, with different molecular properties (*Supplemental Table 1*) were screened for GRPR expression using internalization assays and Quantitative Reverse Transcriptase Polymerase Chain Reaction (RT-qPCR). Cell lines, authenticated by short tandem repeat profiling using the Powerplex STR kit (Promega), were cultured as described by Riaz et al. (18).

In the internalization assay, cells were incubated for 1 h at 37°C with 10^{-9} M/0.1 MBq of ^{111}In-AMBA (without or with 10^{-6} M unlabeled Tyr^4-bombesin). In addition, assays were performed using 10^{-7} M/10 MBq, 10^{-8} M/1 MBq, and 10^{-9} M/0.1 MBq of ^{111}In-AMBA with incubation times of 1, 2, and 4 h to select the optimal conditions for the in vitro cytotoxicity studies. The internalization assay protocol is described in the supplemental materials.

To measure *GRPR* mRNA levels of the BC cell lines, RNA was isolated using RNA-Bee (Campro Scientific) according to the manufacturer's instructions. Subsequently, complementary DNA synthesis and RT-qPCR were performed and normalized using the δ Cq method on the average of 2 reference genes (*HMBS* and *HPRT1*) as previously described (19). The quantification of target genes was performed using the Taqman probe-based gene expression assay, *GRPR*: Hs01055872_m (Applied BioSystems/Life Technologies), according to the manufacturer's instructions.

In Vitro Cytotoxicity Studies

Cells (12.5×10^6/5 mL in a T25 culture flask, seeded 1 d before the experiment) were treated with 10^{-7} M/50 MBq, 5×10^{-8} M/25 MBq, or 10^{-8} M/5 MBq of ^{177}Lu-AMBA in 5 mL of internalization medium for 4 h. Untreated cells, ^{177}Lu-diethylenetriaminepentaacetic acid (DTPA)-treated, and unlabeled AMBA-treated cells served as controls. After incubation, cells were washed twice with phosphate-buffered saline (GIBCO/Life Technologies) and detached using 0.1 mM ethylenediaminetetraacetic acid. Cells were resuspended in medium, counted, and seeded in 3 wells of 12-well plates (12,500 cells/well/1 mL). Seven days after treatment, cells were fixed using 1 mL of 10% trichloroacetic acid (Sigma-Aldrich), and a sulforhodamine B colometric assay was performed to determine cell density. Results are expressed as percentages relative to untreated controls. The sulforhodamine B colometric assay protocol is described in the supplemental materials.

In Vivo Imaging, Biodistribution, and In Vitro Autoradiography of BC Xenografts

All animal studies were in agreement with the Animal Welfare Committee requirements of Eramus MC and conducted in accordance with accepted guidelines. Balb c *nu/nu* female mice (6-8 wk) (Janvier), supplemented with β-estradiol (4 mg/L; Sigma-Aldrich) in drinking water, were subcutaneously (between the shoulders) and orthotopically (left fourth mammary fat pad) inoculated with 8×10^6 T47D cells or 7×10^6 MCF7 cells (n=6 for each cell line).

A 40-min SPECT/CT scan was acquired at 2 time points after inoculation (time point 1 [t1], 40±3 d, and time point 2 [t2], 103±3 d), using the NanoSPECT/CT scanner (Bioscan) 4 h after intravenous injection of approximately 35 MBq/200 pmol of ^{111}In-JMV4168, co-injected with 300 μg of phosphoramidon (Peptides International Inc.) to inhibit in vivo enzymatic degradation of the peptide. During the scan acquisition, the animals were anesthetized with isoflurane/O_2 and body temperature was maintained. Bladder uptake was masked after reconstruction of the images. After the second scan, animals were euthanized, and tumors and organs were collected, weighed, and counted in a γ-counter. Data obtained were expressed as percentage injected dose per gram of tissue (%ID/g). In addition, in

vitro autoradiography was performed on the excised tumors, using ^{111}In-JMV4168 without or with 10^{-6} M unlabeled Tyr^4-bombesin, to demonstrate receptor specificity of the tracer. Scanning, reconstruction, and counting details are described in the supplemental materials. *Supplemental Figure 1* depicts the time line of the in vivo experiments.

Statistics
Statistical analyses are described in the supplemental materials.

RESULTS

GRPR Expression in Clinical BC Specimens
The autoradiography results of 50 human BC tissue specimens with known ER protein status were scored for GRPR expression. Hematoxylin and eosin staining of adjacent tissue sections was used to discriminate between malignant and healthy tissue (*Figure 1A*). Most (48/50 [96%]) of the BC specimens analyzed were positive for GRPR. The majority (56%) of the samples showed greater than 75% positivity, indicating a homogeneous GRPR expression. Of the remaining samples, 29% was 1-25% positive, 8% was 26-50% positive, and 6% was 51-75% positive (*Figure 1B*). In addition, a significant, positive (P=0.026, $\chi^2(4)$=12,911) correlation was found between ER status and extent of GRPR expression.

GRPR Expression in Human-Derived BC Cell Lines and In Vitro Cytotoxicity Studies
Most of the BC cell lines examined (6/9) selectively bound and internalized ^{111}In-AMBA, although to a variable extent (*Figure 2A*). This process was GRPR specific, because binding and internalization were significantly decreased when an excess of unlabeled GRPR ligand was added. The extent of ^{111}In-AMBA binding and internalization seemed higher in ER-positive BC cell lines than in the ER-negative BC cell lines. However, the observed difference was not statistically significant (P=0.757), probably because of the lower power of the cell line study than the clinical BC specimen study. Also, no clear correlation with progesterone receptor (P=0.209) and human epidermal growth factor receptor 2 status (P=0.192) of the BC cell lines was found.
To confirm that internalization levels correlated with GRPR expression and were not attributed to, for example, receptor recycling efficiency, GRPR expression was independently quantified by RT-qPCR (*Supplemental Table 1*). A significant positive correlation (P=0.0108, R_s=0.8167) was found between mRNA levels of *GRPR* and ^{111}In-AMBA uptake (*Figure 2B*).
The ER-positive cell lines T47D and MCF7 showed the highest uptake of ^{111}In-AMBA. T47D was therefore selected for in vitro cytotoxicity experiments, and both T47D and MCF7 were used for inoculation in mice to create relevant in vivo models.

To determine the optimal incubation time and radioligand concentration for in vitro cytotoxicity studies, taking into account potential GRPR saturation, T47D cells were incubated with 3 different concentrations of ^{111}In-AMBA (10^{-7} M/10 MBq, 10^{-8} M/1 MBq, and 10^{-9} M/0.1 MBq) for 3 different incubation times (1, 2, and 4 h). The highest absolute amount of ^{111}In-AMBA (counts per minute) was observed after 4 h of incubation with 10^{-7} M ^{111}In-AMBA, both in the membrane-bound and in the internalized fraction (*Figure 3A*).

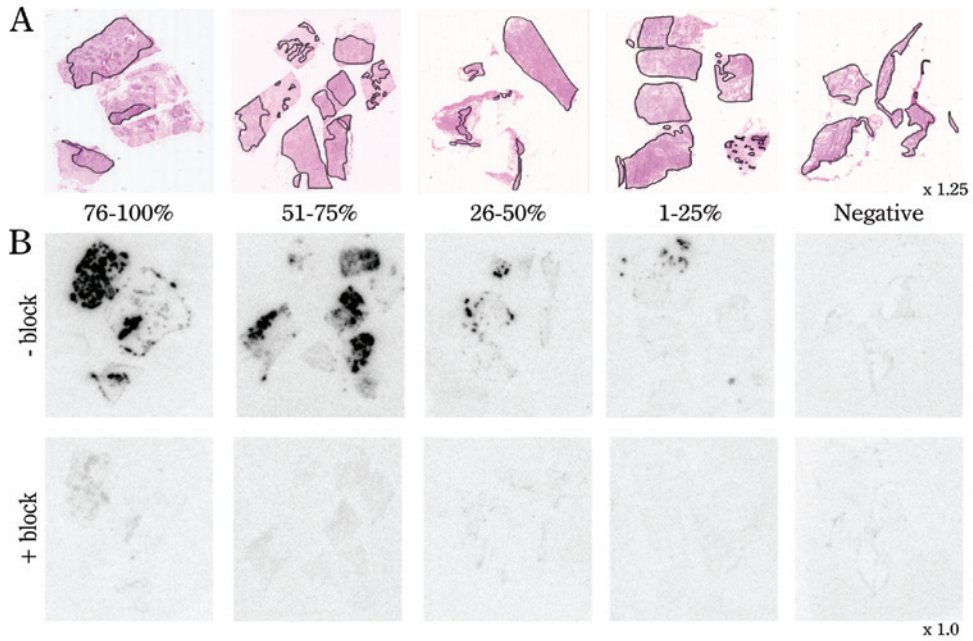

Figure 1. A) Hematoxylin and eosin staining of sections indicating tumor-containing regions, corresponding to autoradiography results in B. B) Representative examples of ^{111}In-AMBA binding to human BC specimens, without (-block) and with (+block) 10^{-6} M Tyr^4-bombesin. Binding was GRPR-specific because no binding was observed when the GRPR was blocked by Tyr^4-bombesin. Among GRPR-positive tumors, a subdivision was made between tumors that were 1-25%, 26-50%, 51-75%, and 76-100% GRPR-positive.

When T47D cells were treated for 4 h with ^{177}Lu-AMBA, a significant reduction in cell number of 20%, 50%, and 80% was observed after incubation with 10^{-8} M/5 MBq, 5×10^{-8} M/25 MBq, or 10^{-7} M/50 MBq of ^{177}Lu-AMBA, respectively (*Figure 3B*). Treatment with the same amount of ^{177}Lu-DTPA for 4 h, which is not actively internalized, did not inhibit cell proliferation, similarly to incubation with unlabeled AMBA. Therefore, the therapeutic effect of ^{177}Lu-AMBA can be associated to the combination of specific GRPR-mediated uptake and retention of ^{177}Lu within the cells over time.

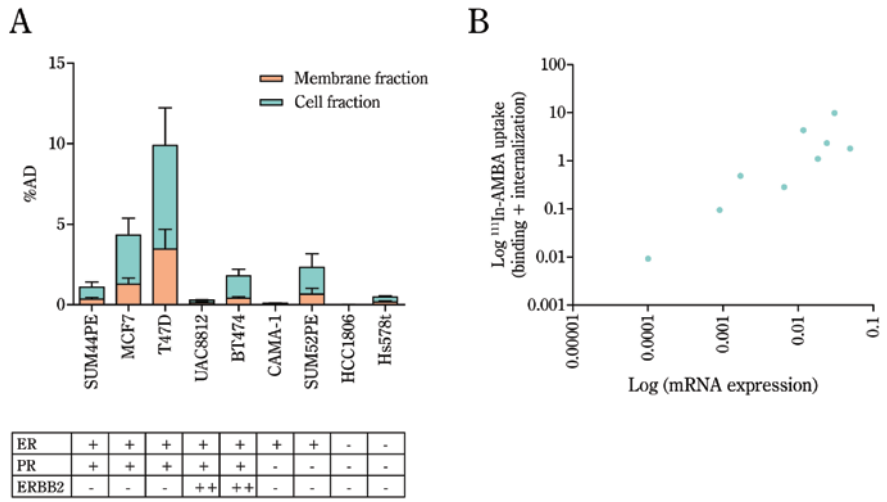

Figure 2. A) Selective binding and internalization after 1 h of incubation with 10^{-9} M/0.1 MBq of ^{111}In-AMBA, a GRPR agonist. Nine human-derived BC cell lines with different molecular properties (18) were screened. Both membrane- and internalized/cell fraction are displayed. Results shown are average of 3 independent experiments, each performed in triplicate (mean±SD). B) Significant correlation ($P=0.0108$, $R_s=0.8167$) between GRPR mRNA expression and level of ^{111}In-AMBA uptake (membrane plus cell fraction).

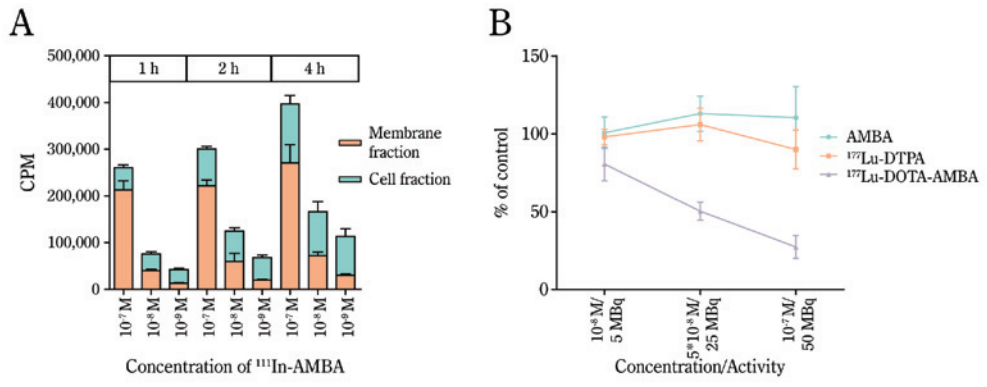

Figure 3. A) Uptake of ^{111}In-AMBA by GRPR-expressing human-derived BC cell line T47D, at 1, 2, and 4 h after incubation with 10^{-7} M/10 MBq, 10^{-8} M/1 MBq, or 10^{-9} M/0.1 MBq of ^{111}In-AMBA. Results shown are average of 2 independent experiments, each performed in triplicate (mean±SD). B) Treatment of T47D cells with 3 different concentrations of AMBA, ^{177}Lu-DTPA, and ^{177}Lu-AMBA for 4 h. Significant reduction of 80% in cell viability was reached when cells were treated with 10^{-7} M/50 MBq of ^{177}Lu-AMBA, whereas no significant effects were observed when cells were similarly treated with AMBA or ^{177}Lu-DTPA. Results shown are average of 3 independent experiments, each performed in triplicate (mean±SD).

In Vivo Visualization of GRPR Expression in BC Xenografts

We successfully obtained T47D and MCF7 xenografts in immune-deficient female mice orally supplemented with estrogen.

At 2 time points after tumor cell inoculation, T47D and MCF7 xenografts were visualized using in vivo SPECT/CT imaging after an injection of approximately 35 MBq/200 pmol of ^{111}In-JMV4168 + 300 µg of phosphoramidon. T47D xenografts had a significantly ($P<0.0001$) higher uptake than MCF7 xenografts (748-1,706 vs. 169-658 kBq/g for subcutaneous tumors and 1,151-2,127 vs. 189-672 kBq/g for orthotopic tumors). Therefore, T47D xenografts were visualized with higher contrast than MCF7 xenografts (*Figure 4*). No significant difference in

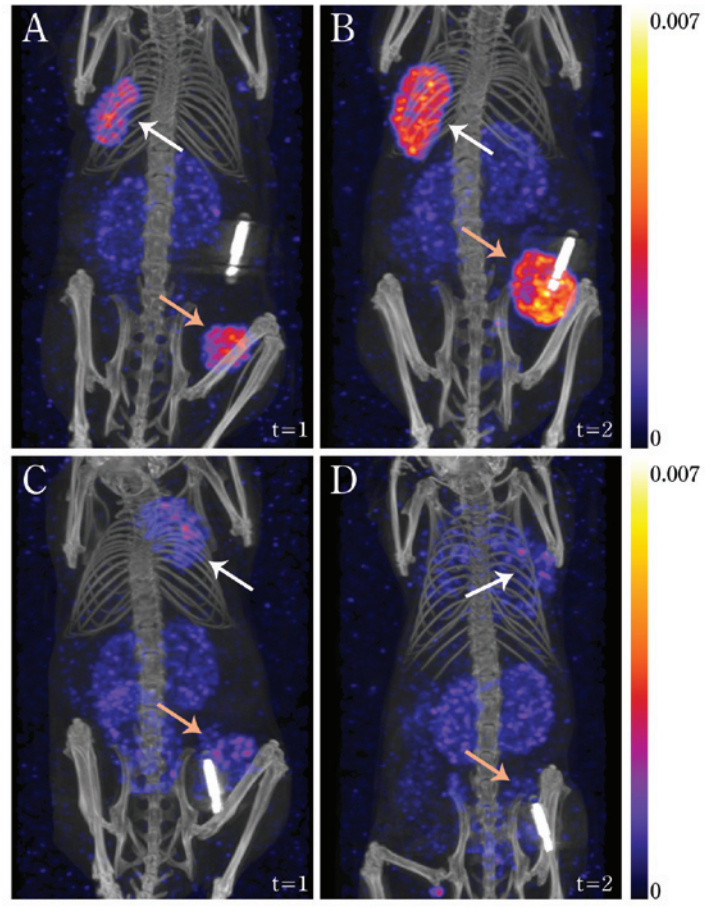

Figure 4. SPECT/CT scans indicating orthotopic (orange arrows) and subcutaneous (white arrows) tumors of T47D and MCF7 xenograft-bearing mice at 4 h after injection of approximately 35 MBq (200 pmol) of ^{111}In-JMV4168 + 300 µg of phosphoramidon. T47D xenografts were scanned at t1=43 d (A) and t2=100 d (B). MCF7 xenografts were scanned at t1=37 d (C) and t2=106 d (D). Bladder uptake is masked. Mice were provided with a chip for identification purposes. T47D xenografts were visualized with higher contrast than MCF7 xenografts.

uptake between orthotopic and subcutaneous tumors of both T47D ($P=0.92$) and MCF7 xenografts ($P=0.95$) was determined. Biodistribution results obtained at t2 confirmed higher radiotracer uptake and a better tumor-to-kidney ratio (2.1 vs. 0.4) in T47D than MCF7 xenografts (*Figure 5*). In vitro autoradiography of the excised tumors demonstrated specific binding of ^{111}In-JMV4168 (*Supplemental Figure 2*). However, the proliferation of MCF7 xenografts was faster than that of T47D xenografts; orthotopic tumors ranged from 178 to 390 mm^3 for T47D xenografts and from 755 to 1,830 mm^3 for MCF7 xenografts at t1. At that time point, subcutaneous T47D xenografts ranged from 11 to 630 mm^3, compared with 532-2,095 mm^3 for MCF7 xenografts. As yet, we cannot exclude the effect of tumor size on radiotracer uptake. Two of 6 T47D subcutaneous tumors were small (12.3 and 4.0 mm^3) and were therefore excluded from the biodistribution study.

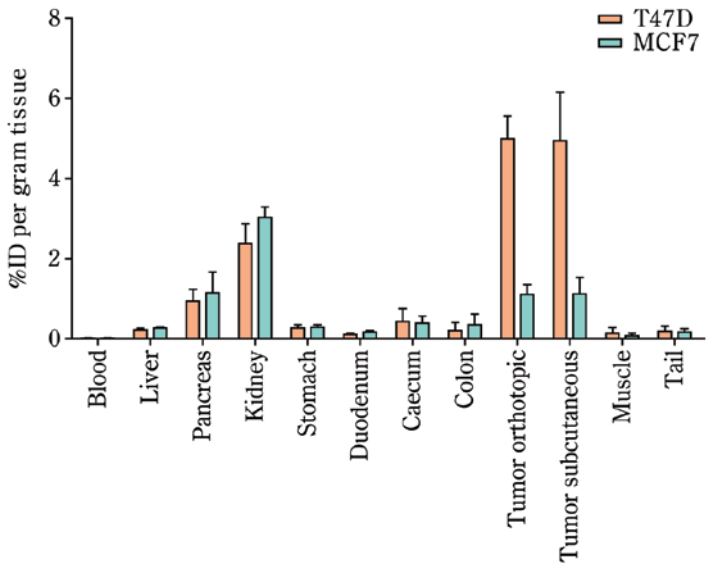

Figure 5. Quantification of ^{111}In-JMV4168 uptake in tumors and organs collected after last scan (t2); n=6 for each mouse model (2 small subcutaneous T47D xenografts were excluded). Significantly ($P<0.0001$) higher uptake of ^{111}In-JMV4168 was determined in T47D than in MCF7 xenografts.

DISCUSSION

To gain more insight into the feasibility of diagnostic imaging and therapeutic applications of GRPR radioligands in BC patients, we aimed to develop reliable preclinical models expressing the GRPR based on well-characterized human-derived BC cell lines. We first confirmed GRPR expression on clinical BC specimens and found that most (96%) indeed expressed the GRPR, which was higher than the

65% of GRPR-expressing BC specimens reported by Reubi et al. (10). In the latter study, GRPR, analyzed by in vitro autoradiography, was more frequently and more densely expressed than any other of the investigated targets, including neuropeptide Y receptor subtype 1, SSTR, and vasoactive intestinal peptide receptor. We observed a homogeneous GRPR expression in more than half (56%) of the tumors, supporting the conclusion that GRPR is a suitable target for radioligands in BC patients.

Furthermore, a significant correlation was found between GRPR and ER expression in the clinical BC specimens analyzed. ER-positive tumors were associated with higher GRPR expression, indicating BC patients with ER-positive tumors as a potential target group for imaging or therapy with GRPR radioligands. Our findings were in accordance with studies by Halmos et al. (12), showing a significant positive correlation between ER expression and GRPR binding affinity examined on isolated cell membranes from BC samples. Because ER-positive tumors account for 75% of all breast tumors, GRPR-based imaging could offer new imaging and therapeutic possibilities for most BC patients (2,20). In addition, because current treatments with antihormonal agents, such as tamoxifen and aromatase inhibitors, are ineffective in about 40% of the ER-positive metastatic BC patients (20,21), GRPR ligands radiolabeled with particle emitters might offer new therapeutic options for these patients.

Furthermore, we found that most of the examined BC cell lines expressed the GRPR. T47D was selected for in vitro therapy and, together with MCF7, for in vivo imaging studies.

Treatment of T47D cells with ^{177}Lu-AMBA resulted in a significant decrease in cell viability, proving this cell line to be suitable as a model for future in vivo therapy studies in xenograft-bearing mice. An 80% decrease in cell viability was established using 10^{-7} M/50 MBq of ^{177}Lu-AMBA. The uptake of ^{177}Lu by the tumor cells appeared to be a prerequisite, because the same amounts of ^{177}Lu-DTPA, which does not bind or internalize, showed no significant effect on cell viability after 4 h exposure. Müller et al. (22) also studied the effect of ^{177}Lu-DTPA on cell viability, next to $^{177}LuCl_3$. In line with our results, treatment with $^{177}LuCl_3$, which is also internalized by cells, resulted in a larger decrease in cell viability than treatment with ^{177}Lu-DTPA. In the study by Müller et al. (22), a decrease in cell viability was measured after treatment with ^{177}Lu-DTPA as well, but cells were treated for 4 d with ^{177}Lu-DTPA in contrast to the 4 h treatment in our study, which can explain the discrepancy.

On the basis of our in vitro cytotoxicity studies with ^{177}Lu-AMBA, we expect a similar effect of GRPR antagonists on cell viability, because binding of the radioligand to the receptor results in cell membrane-bound accumulation of ^{177}Lu, enabling radiation-induced DNA damage and thus cytotoxicity, despite the lack of internalization. A recent study by Wild et al. (23) comparing the application of ^{177}Lu-labeled SSTR agonist and antagonist for PRRT in NET patients showed a higher tumor dose for the SSTR antagonist than for the agonist and therefore successful therapeutic effects, providing evidence that treatment with receptor antagonists is feasible.

According to previous studies, adverse effects have been reported during the clinical evaluation of ^{177}Lu-AMBA in prostate cancer patients (24). Such undesirable

effects can be evaded with GRPR antagonists instead of agonists (25). For this reason and to prevent interference with orthotopic tumor visualization, the GRPR antagonist JMV4168 was used for in vivo imaging studies.

With the aim of inhibiting the in vivo enzymatic degradation of ^{111}In-JMV4168, which may potentially interfere with GRPR targeting and tumor uptake, ^{111}In-JMV4168 was co-injected with the neutral endopeptidase inhibitor phosphoramidon (26). Recent studies by Nock et al. (27) have shown significantly prolonged survival of several radioligands in the circulation when phosphoramidon was administered simultaneously. In the current study, ^{111}In-JMV4168 + phosphoramidon was successfully applied to visualize both orthotopic and subcutaneous BC tumors in mice, approximately 100 mm^3 in size, indicating that GRPR expression was sufficiently high to discriminate tumor lesions. Already approximately 1 %ID/g uptake of MCF7 xenografts resulting in approximately 200 kBq of ^{111}In/g enabled visualization of tumor lesions, which was even higher for T47D xenografts, showing about 5 %ID/g uptake. Parry et al. (28) reported a similar tumor uptake in subcutaneous T47D xenografts using different GRPR radioligands. Thus, these mouse models will now be used for future studies to examine the therapeutic potential of ^{177}Lu-labeled GRPR radioligands.

Recently several imaging studies using ^{99m}Tc-labeled bombesin analogs in BC patients were performed with promising results (29-32), identifying tumor lesions in patients suspected for BC based on mammography. In the most recent study by Shariati et al. (32), a sensitivity of 61% and specificity of 100% were reported, indicating that imaging with bombesin analogs is promising and deserves further investigation. Interestingly, 2 of these imaging studies described the identification of lymph node metastases, demonstrating the presence of the GRPR on lymph node metastases next to primary tumor tissue (31,32). However, the capacity to visualize distant metastases still needs to be established. In a study by Bergsma et al. (33), 50% of the disseminated BC lesions studied were successfully visualized using the ^{68}Ga-labeled GRPR antagonist Sarabesin 3 without adverse effects, once more showing the successful application of radiolabeled GRPR antagonists in BC patients. None of these studies reported on correlation of positive scintigraphy with BC subtype and molecular markers.

Up to now, GRPR-based PRRT has been performed targeting prostate cancer, either in xenograft-bearing animals, with GRPR agonists or antagonists (14,34), or in patients during a pilot study using ^{177}Lu-AMBA (24). However, GRPR-based PRRT is not yet being applied in BC animal models or patients. When GRPR radioligands will be used for therapeutic purposes, the physiologic uptake in the pancreas should be considered regarding safety. Yet, the radiosensitivity of the pancreas is relatively low, and the fast pancreatic washout of radiolabeled GRPR antagonists is favorable in this respect (35).

The results obtained in the current study together with the positive first experience with ^{99m}Tc and ^{68}Ga labeled GRPR radioligands to localize BC are encouraging for future application of the so-called theranostic approach in BC, using, for example DOTA-coupled receptor ligands radiolabeled with ^{111}In and ^{68}Ga for imaging or with ^{177}Lu, ^{90}Y, or ^{213}Bi for therapeutic purposes.

CONCLUSION

We confirmed GRPR expression in clinical BC specimens, correlating with ER expression. Hence, ER-positive BC patients are potential candidates for imaging and PRRT using GRPR radioligands. In addition, we successfully developed BC xenograft mouse models by inoculation of the selected ER- and GRPR-positive BC cell lines T47D and MCF7 and visualized the generated tumors using ^{111}In-JMV4168, co-injected with phosphoramidon. These mouse models will be used to study the therapeutic effects of ^{177}Lu-labeled GRPR radioligands, such as ^{177}Lu-JMV4168.

Supplemental data

Supplemental data is available online at http://jnm.snmjournals.org.

REFERENCES

1. Perou CM, Sorlie T, Eisen MB, et al. Molecular portraits of human breast tumours. Nature. 2000;406:747-752.
2. Yersal O, Barutca S. Biological subtypes of breast cancer: prognostic and therapeutic implications. World J Clin Oncol. 2014;5:412-424.
3. Garcia EM, Storm ES, Atkinson L, Kenny E, Mitchell LS. Current breast imaging modalities, advances, and impact on breast care. Obstet Gynecol Clin North Am. 2013;40:429-457.
4. Humphrey LL, Helfand M, Chan BK, Woolf SH. Breast cancer screening: a summary of the evidence for the U.S. Preventive Services Task Force. Ann Intern Med. 2002;137:347-360.
5. Mahoney MC, Newell MS. Screening MR imaging versus screening ultrasound: pros and cons. Magn Reson Imaging Clin N Am. 2013;21:495-508.
6. Schillaci O, Buscombe JR. Breast scintigraphy today: indications and limitations. Eur J Nucl Med Mol Imaging. 2004;31(suppl 1):S35-S45.
7. Krenning EP, Bakker WH, Breeman WA, et al. Localisation of endocrine-related tumours with radioiodinated analogue of somatostatin. Lancet. 1989;1: 242-244.
8. Kim KW, Krajewski KM, Nishino M, et al. Update on the management of gastroenteropancreatic neuroendocrine tumors with emphasis on the role of imaging. AJR. 2013;201:811-824.
9. Bodei L, Pepe G, Paganelli G. Peptide receptor radionuclide therapy (PRRT) of neuroendocrine tumors with somatostatin analogues. Eur Rev Med Pharmacol Sci. 2010;14:347-351.
10. Reubi C, Gugger M, Waser B. Co-expressed peptide receptors in breast cancer as a molecular basis for in vivo multireceptor tumour targeting. Eur J Nucl Med Mol Imaging. 2002;29:855-862.
11. Gugger M, Reubi JC. Gastrin-releasing peptide receptors in non-neoplastic and neoplastic human breast. Am J Pathol. 1999;155:2067-2076.
12. Halmos G, Wittliff JL, Schally AV. Characterization of bombesin/gastrin-releasing peptide receptors in human breast cancer and their relationship to steroid receptor expression. Cancer Res. 1995;55:280-287.
13. Reubi JC, Maecke HR. Peptide-based probes for cancer imaging. J Nucl Med. 2008;49:1735-1738.
14. Lantry LE, Cappelletti E, Maddalena ME, et al. 177Lu-AMBA: synthesis and characterization of a selective 177Lu-labeled GRP-R agonist for systemic radiotherapy of prostate cancer. J Nucl Med. 2006;47:1144-1152.
15. Marsouvanidis PJ, Nock BA, Hajjaj B, et al. Gastrin releasing peptide receptordirected radioligands based on a bombesin antagonist: synthesis, 111In-labeling, and preclinical profile. J Med Chem. 2013;56:2374-2384.
16. de Blois E, Chan HS, Konijnenberg M, de Zanger R, Breeman WA. Effectiveness of quenchers to reduce radiolysis of 111In- or 177Lu-labelled methionine-containing regulatory peptides: maintaining radiochemical purity as measured by HPLC. Curr Top Med Chem. 2012;12:2677-2685.
17. De Blois E, Schroeder RJ, De Ridder CA, Van Weerden WM, Breeman WP, De Jong M. Improving radiopeptide pharmacokinetics by adjusting experimental conditions for bombesin receptor-mediated imaging of prostate cancer. Q J Nucl Med Mol Imaging. June 19, 2013 [Epub]

18. Riaz M, van Jaarsveld MT, Hollestelle A, et al. miRNA expression profiling of 51 human breast cancer cell lines reveals subtype and driver mutation-specific miRNAs. Breast Cancer Res. 2013;15:R33.
19. Sieuwerts AM, Meijer-van Gelder ME, Timmermans M, et al. How ADAM-9 and ADAM-11 differentially from estrogen receptor predict response to tamoxifen treatment in patients with recurrent breast cancer: a retrospective study. Clin Cancer Res. 2005;11:7311-7321.
20. Droog M, Beelen K, Linn S, Zwart W. Tamoxifen resistance: from bench to bedside. Eur J Pharmacol. 2013;717:47-57.
21. Williams C, Lin CY. Oestrogen receptors in breast cancer: basic mechanisms and clinical implications. Ecancermedicalscience. 2013;7:370.
22. Müller C, Reber J, Haller S, et al. Direct in vitro and in vivo comparison of 161Tb and 177Lu using a tumour-targeting folate conjugate. Eur J Nucl Med Mol Imaging. 2014;41:476-485.
23. Wild D, Fani M, Fischer R, et al. Comparison of somatostatin receptor agonist and antagonist for peptide receptor radionuclide therapy: a pilot study. J Nucl Med. 2014;55:1248-1252.
24. Bodei L, Ferrari M, Nunn AD, et al. 177Lu-AMBA bombesin analogue in hormone refractory prostate cancer patients: a phase I escalation study with single-cycle administrations [abstract]. Eur J Nucl Med Mol Imaging. 2007;34(suppl 2):S221.
25. Cescato R, Maina T, Nock B, et al. Bombesin receptor antagonists may be preferable to agonists for tumor targeting. J Nucl Med. 2008;49:318-326.
26. Suda H, Aoyagi T, Takeuchi T, Umezawa H. Letter: a thermolysin inhibitor produced by actinomycetes-phospholamidon. J Antibiot (Tokyo). 1973;26:621-623.
27. Nock BA, Maina T, Krenning EP, de Jong M. "To serve and protect": enzyme inhibitors as radiopeptide escorts promote tumor targeting. J Nucl Med. 2014;55:121-127.
28. Parry JJ, Andrews R, Rogers BE. MicroPET imaging of breast cancer using radiolabeled bombesin analogs targeting the gastrin-releasing peptide receptor. Breast Cancer Res Treat. 2007;101:175-183.
29. Scopinaro F, Di Santo GP, Tofani A, et al. Fast cancer uptake of 99mTc-labelled bombesin (99mTc BN1). In Vivo. 2005;19:1071-1076.
30. Soluri A, Scopinaro F, De Vincentis G, et al. 99MTC [13LEU] bombesin and a new gamma camera, the imaging probe, are able to guide mammotome breast biopsy. Anticancer Res. 2003;23:2139-2142.
31. Van de Wiele C, Phonteyne P, Pauwels P, et al. Gastrin-releasing peptide receptor imaging in human breast carcinoma versus immunohistochemistry. J Nucl Med. 2008;49:260-264.
32. Shariati F, Aryana K, Fattahi A, et al. Diagnostic value of 99mTc-bombesin scintigraphy for differentiation of malignant from benign breast lesions. Nucl Med Commun. 2014;35:620-625.
33. Bergsma HKH, Meuller D, Maina T, et al. PET/CT imaging with a novel 68Ga-labelled GRP-receptor antagonist, "Sarabesin 3": first clinical data in patients with prostate and breast cancer [abstract]. J Nucl Med. 2013;54(suppl 2):280.
34. Dumont RA, Tamma M, Braun F, et al. Targeted radiotherapy of prostate cancer with a gastrin-releasing peptide receptor antagonist is effective as monotherapy and in combination with rapamycin. J Nucl Med. 2013;54:762-769.
35. Stewart FA, Akleyev AV, Hauer-Jensen M, et al. ICRP publication 118: ICRP statement on tissue reactions and early and late effects of radiation in normal tissues and organs-threshold doses for tissue reactions in a radiation protection context. Ann ICRP. 2012;41:1-322

Chapter 9

^{68}Ga/^{177}Lu-NeoBOMB1, a Novel Radiolabeled GRPR Antagonist for Theranostic Use in Oncology

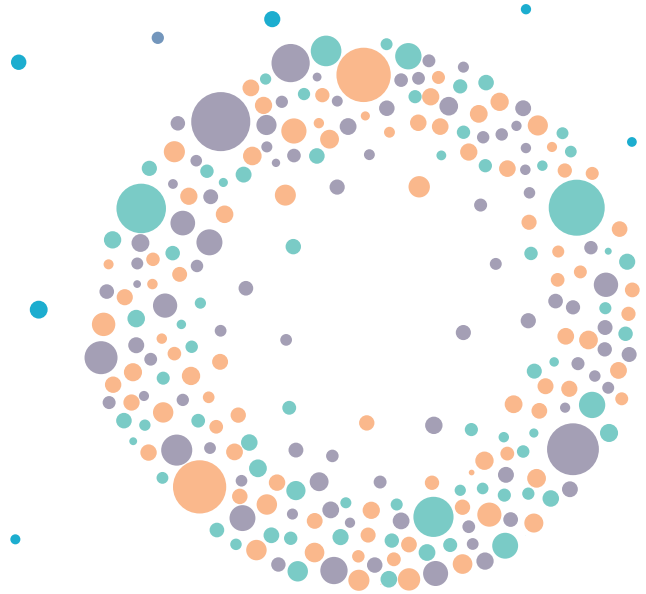

S.U. Dalm[1*], I.L. Bakker[1*], E. de Blois[1], G.N. Doeswijk[1], M.W. Konijnenberg[1], F. Orlandi[2], D. Barbato[2], M. Tedesco[2], T. Maina[3], B.A. Nock[3] and M. de Jong[1]

*Authors equally contributed to the work

[1]Dept. of Radiology & Nuclear Medicine, Erasmus MC, Rotterdam, The Netherlands; [2]Advanced Accelerator Applications, Colleretto Giacosa, Italy; and [3]Molecular Radiopharmacy, INRASTES, NCSR "Demokritos", Athens, Greece

Adapted from J Nucl Med 2016 Sep. 8 [epub ahead of print]

ABSTRACT

Since overexpression of the gastrin releasing peptide receptor (GRPR) has been reported on various cancer types, e.g. prostate cancer and breast cancer, targeting this receptor with radioligands might have significant impact on staging and treatment of GRPR-expressing tumors. NeoBOMB1 is a novel DOTA-coupled GRPR antagonist with high affinity for GRPR and excellent in vivo stability. The purpose of this preclinical study was to further explore the use of NeoBOMB1 for theranostic application by determining the biodistribution of ^{68}Ga-NeoBOMB1 and ^{177}Lu-NeoBOMB1.

Methods: PC-3 tumor-xenografted Balb c *nu/nu* mice were injected with either ~13 MBq/250 pmol ^{68}Ga-NeoBOMB1, or a low (~1 MBq/200 pmol) vs. high (~1 MBq/10 pmol) peptide amount of ^{177}Lu-NeoBOMB1 after which biodistribution and imaging studies were performed. At 6 time points (15, 30, 60, 2 h, 4 h and 6 h for ^{68}Ga-NeoBOMB1 and 1, 4, 24, 48, 96 and 168 h for ^{177}Lu-NeoBOMB1) post injection (p.i.) tumor and organ uptake was determined. To assess receptor-specificity additional groups of animals were co-injected with an excess of unlabeled NeoBOMB1. Results of the biodistribution studies were used to determine pharmacokinetics and dosimetry. Furthermore, positron emission tomography/computed tomography (PET/CT) and single photon emission computed tomography/magnetic resonance imaging (SPECT/MRI) was performed.

Results: Injection of ~250 pmol ^{68}Ga-NeoBOMB1 resulted in a tumor and pancreas uptake of 12.4±2.3 and 22.7±3.3 %ID/g tissue 120 min p.i., respectively. ^{177}Lu-NeoBOMB1 biodistribution studies revealed a higher tumor uptake (17.9±3.3 vs. 11.6±1.3 %ID/g tissue 4 h p.i.) and a lower pancreatic uptake (19.8±6.9 vs. 105±13 %ID/g tissue 4 h p.i.) with the higher peptide amount injected, leading to a significant increase in the absorbed dose to the tumor vs. the pancreas (200 pmol: 570 vs. 265 mGy/MBq, 10 pmol: 435 vs. 1393 mGy/MBq). Using this data to predict patient dosimetry we found a kidney, pancreas and liver exposure of 0.10, 0.65 and 0.06 mGy/MBq, respectively. Imaging studies resulted in good visualization of the tumor with both ^{68}Ga-NeoBOMB1 and ^{177}Lu-NeoBOMB1.

Conclusions: Our findings indicate that ^{68}Ga/^{177}Lu-NeoBOMB1 is a very promising radiotracer with excellent tumor uptake and favorable pharmacokinetics for imaging and therapy of GRPR-expressing tumors.

Keywords:
Cancer Theranostics, Gastrin Releasing Peptide Receptor, GRPR Antagonist, Biodistribution, Dosimetry

INTRODUCTION

The gastrin releasing peptide receptor (GRPR), also known as bombesin receptor subtype 2, is a G-protein coupled receptor expressed in various organs, including those of the gastrointestinal tract (GI-tract) and the pancreas (1,2). Upon binding of a suitable ligand, the GRPR is activated, eliciting multiple physiological processes, such as regulation of exocrine and endocrine secretion (1,2). In the past decades, GRPR expression has been reported in various cancer types, including prostate cancer and breast cancer (3,4). Therefore, the GRPR became an interesting target for receptor mediated tumor imaging and treatment, such as peptide receptor scintigraphy and peptide receptor radionuclide therapy (2). Following the successful use of radiolabeled somatostatin peptide analogs in neuroendocrine tumors for nuclear imaging and therapy (5,6), multiple radiolabeled GRPR radioligands have been synthesized and studied in preclinical as well as in clinical studies, mostly in prostate cancer patients. Examples of such peptide analogs include AMBA, the Demobesin-series and MP2653 (7-11). Recent studies have shown a preference for GRPR antagonists compared to GRPR agonists (12,13). Receptor antagonists often show higher binding and favorable pharmacokinetics compared to agonists (14). Also, clinical studies with radiolabeled GRPR agonists reported unwanted side effects in patients caused by activation of the GRPR after binding of the peptide to the receptor (15).

Although, imaging and treatment with radiolabeled GRPR peptide analogs is not yet approved for routine clinical practice, progress made over the years led to new diagnostic radiotracers which are most promising. On the route to developing a new successful imaging and treatment strategy for GRPR-expressing tumors, the development of radiotracers with favorable pharmacokinetics that can be labeled with different radionuclides is an essential step. Further studies are now needed to optimize the use of GRPR radioligands for imaging and treatment of GRPR-expressing tumors to determine the clinical value of GRPR-targeting radiotracers.

In this study, we explored the use of a novel DOTA-coupled GRPR antagonist, NeoBOMB1, derived from a previously reported GRPR antagonist, SB3 (16). The peptidic part of NeoBOMB1 however is based on a different GRPR-antagonist first described by Heimbrook et al. (17) and generated by modification of the C-terminal Leu^{13}-Met^{14}-NH_2 and the replacement of Asn^6 by DPhe^6 of native bombesin(6-14). NeoBOMB1 was chosen for further studies because of its improved affinity for the GRPR (18,19). Coupling of the antagonist to a DOTA chelator enables labeling with different radionuclides such as ^{68}Ga (for positron emission tomography (PET)), ^{111}In (for single photon emission computed tomography (SPECT)) and ^{177}Lu (for radionuclide therapy), which makes theranostic use of NeoBOMB1 possible. In a preliminary communication on NeoBOMB1, a GRPR-affinity in the low nanomolar range for ^{nat}Ga-NeoBOMB1 and excellent in vivo stability of ^{67}Ga-NeoBOMB1 was reported (18).

The aim of our study was to further explore the perspectives of ^{68}Ga-NeoBOMB1 and ^{177}Lu-NeoBOMB1 for clinical translation by performing biodistribution studies in PC-3-xenografted mice. Two peptide amounts of ^{177}Lu-NeoBOMB1

were studied in order to define the optimal peptide amount for increasing tumor targeting while minimizing background radioactivity levels. Data of the ^{177}Lu-NeoBOMB1 biodistribution studies were used to determine dosimetry in mice and to predict dosimetry in humans.

MATERIALS AND METHODS

Radiotracer and Radiolabeling Procedure

NeoBOMB1 (Advanced Accelerator Applications) (*Figure 1*) (20) was diluted in ultra-pure water and concentration and chemical purity were monitored with an in-house developed titration method (21). Labeling of NeoBOMB1 was based on a previously published kit approach by Castaldi et. al. (22). Radioactivity was added (60 MBq/nmol ^{68}Ga or 100 MBq/nmol ^{177}Lu) to a vial containing all the necessary excipients, e.g. buffer, anti-oxidants and peptide, subsequently this was heated at 85°C for 7 and 20 min, respectively. To measure radiometal incorporation, quality control was performed by instant thin layer chromatography on silica gel using 0.1 M citrate (pH 5) or 1 M ammonium acetate/methanol (30/70 v/v) as buffers. High-performance liquid chromatography was performed with a gradient of methanol and 0.1% trifluoroacetic acid to determine radiochemical purity. Both ^{68}Ga-NeoBOMB1 and ^{177}Lu-NeoBOMB1 were diluted in phosphate-buffered saline plus a tensioactive agent to prevent sticking of the peptide, before injection in animals.

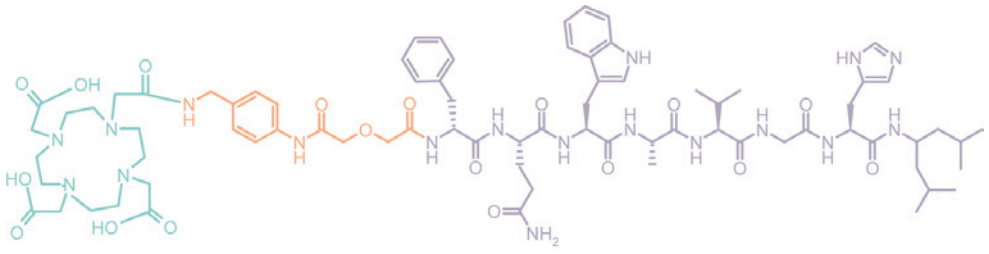

Figure 1. Chemical structure of NeoBOMB1. Green=DOTA chelator, Orange=spacer, Purple=binding domain.

Animal Model

All animal studies were conducted in agreement with the Animal Welfare Committee requirements of Erasmus MC and in accordance with accepted guidelines. Male Balb c *nu/nu* animals (6-8 wks) (Janvier) were subcutaneously (right shoulder) injected with 150 µL inoculation medium (1/3 Matrigel high concentration (Corning) and 2/3 HBSS (Thermofisher scientific)) containing 5×10^6 cells of the GRPR-expressing human derived prostate cancer cell line, PC-3 (American Type Culture Collection). In vivo imaging and biodistribution studies were performed 3-4 weeks post tumor cell inoculation, when tumor size was 340±114 mm^3.

Imaging Studies

Mice (n=2 per radiotracer) were injected with 50 µL ~11.5 MBq/230 pmol ^{68}Ga-NeoBOMB1 or 200 µL 20 MBq/200 pmol ^{177}Lu-NeoBOMB1 after which PET/computed tomography (CT) or SPECT/magnetic resonance imaging (MRI) was performed.

The PET/CT scans were performed 1 h post injection (p.i.) of ^{68}Ga-NeoBOMB1 in a small animal SPECT/PET/CT scanner (VECTor/CT, Milabs) under isoflurane/O_2 anesthesia. Whole body scans were acquired for 120 min (48 projections, 38 sec/projection) using a special collimator with clustered-pinholes for high-energy photons. The collimator contains 162 pinholes with a diameter of 0.7 mm grouped in clusters of 4. Reconstruction was performed using a pixel-based Ordered Subset Expectation Maximization method (4 subsets, 30 iterations) and visualized with Vivoquant (InVicro). A post reconstruction 3D Gaussian filter was applied (1.2 mm full width half maximum).

Whole body SPECT images were obtained 4 h p.i. of ^{177}Lu-NeoBOMB1 under isoflurane/O_2 anesthesia, using a 4-head multipinhole system (NanoScan SPECT/MRI, Mediso Medical Imaging). The images were acquired using 28 projections (40 sec/projection) and reconstructed using the Ordered Subset Expectation Maximization method and a voxel size of 0.25×0.25×0.25 mm and a scan time of 47 min. Coronal T2 weighted images were acquired with a 2D fast spin echo sequence on a 1 tesla permanent magnet (Mediso) with a 35 mm transmit/receive solenoid coil. Scan parameters used were: TE/TR: 4500/39 ms; number of signals averaged: 4; field of view: 70 mm; resolution: 0.4×0.4×0.8 mm, with 0.1 mm spacing between slices and a scan time of 10 min.

Biodistribution Studies

Biodistribution studies were performed to determine tumor and organ uptake of ^{68}Ga-NeoBOMB1. Animals (n=4 for each time point) were injected intravenously with an average of 13 MBq/250 pmol ^{68}Ga-NeoBOMB1 (injected volume: 50 µL) at t=0. At 6 selected time points (15 min, 30 min, 1 h, 2 h, 4 h and 6 h) p.i. animals were euthanized, organs and tumors were excised and their radioactivity uptake was determined. For the ^{177}Lu-NeoBOMB1 biodistribution studies, animals were injected with either 1 MBq/200 pmol or 1 MBq/10 pmol ^{177}Lu-NeoBOMB1 (injected volume: 200 µL) to determine the peptide amount with optimal tumor to background ratio. Four hours, 24 h, 48 h, 96 h and 168 h p.i. animals were euthanized, organs were collected and radiotracer uptake was determined (n=4 for each concentration per time point). For both the ^{68}Ga-NeoBOMB1 and ^{177}Lu-NeoBOMB1 biodistribution studies the following organs were collected: blood, lungs, spleen, pancreas, kidneys, liver, organs of the GI-tract (stomach, intestine, caecum and colon), muscle, tail and tumor. To confirm receptor specificity of radiotracer uptake PC-3-xenografted mice were co-injected with either ^{68}Ga-NeoBOMB1 or ^{177}Lu-NeoBOMB1 plus an excess (40 nmol) of unlabeled NeoBOMB1 (n=2 and n=4, respectively), after which tumor and organ uptake was determined 2 h and 4 h p.i., respectively.

After collecting tumor and organs, the samples were weighed and counted in a γ-counter (1480 WIZARD automatic γ-counter, PerkinElmer) to determine the

percentage of injected dose per gram tissue (%ID/g tissue). For γ-counter measurements an isotope specific energy window, a counting time of 60 sec and a counting error ≤5% was used.
Radioactivity uptake in tumor and organs was corrected for the percentage of radioactivity measured in the tail.

Dosimetry
Kinetic analysis of the biodistribution data was performed to determine uptake and clearance characteristics of the radiotracers. For ^{177}Lu-NeoBOMB1, the resulting time-activity concentration curves through the uptake data were used to calculate the absorbed doses to the organs and tumor. The mouse dosimetry was performed using the RAdiation Dose Assessment Resource realistic mouse model (23). The absorbed dose to an organ D_{organ} was calculated according to the Medical Internal Radiation Dose scheme (24):

$D_{organ} = m_{organ} \times \sum_{src} TIAC_{src} \times S(organ \leftarrow src)$, with $TIAC_{src}$ the time-integrated activity concentration $TIAC_{src} = \int_0^{\infty} \frac{\%IA_{src}}{g}(t)dt$, S(organ←src) the absorbed dose rate per unit activity in the source src for all source and organ combinations. The organ mass m_{organ} is taken from a reference mouse phantom of 25 g to obtain invariance to the measured organ weights. Tumor dosimetry was performed in the same way with the S-values from Stabin et al. (25).
Extrapolation of the mouse biodistribution data to estimate human dosimetry was performed according to the methods by M. Stabin (26). Only organ uptake values were extrapolated and time-scaling was not applied. Two methods were applied for translation of the mice TIAC to human TIAC for each organ:

$TIAC_{human} = TIAC_{mouse} \times \frac{M_{mouse}}{M_{human}}$, by the ratio in body weights: M_{mouse}=25 g and M_{human}=70 kg

$TIAC_{human} = TIAC_{mouse} \times \frac{m_{mouse}}{m_{human}}$, by the ratio in organ weights of mouse and human, e.g. for pancreas: m_{mouse}=0.305 g and m_{human}=94.3 g.
The extrapolated $TIAC_{human}$, multiplied by the reference man organ weight, was used as input to the dosimetry software OLINDA/EXM (27). Absorbed doses to the organs were derived for the reference male phantom. Fifty percent of the activity was considered to be distributed in the whole body (remainder) and the dynamic bladder model was used to derive the urinary bladder dose with 5 voids per day.

Statistics
Least-square fits with exponential curves were performed with the Graphpad Prism software (version 5.01). Decisions on the number of exponentials and plateau values were based on the Aikake information criterion, thereby balancing

better fit correlation and degrees of freedom for the fit. A correlation coefficient R^2>0.7 was used as lowest allowable goodness of fit criterion. Time-activity curves below this criterion were piece-wise integrated by the trapezoidal method.

RESULTS

Biodistribution of ^{68}Ga-NeoBOMB1
The results of the biodistribution studies with ~13 MBq/250 pmol ^{68}Ga-NeoBOMB1 are presented in *Figure 2*. The highest tumor uptake of 12.4±2.3 %ID/g tissue was measured at 120 min p.i. (*Figure 2A*). At that time point uptake in the pancreas was 22.7±3.3 %ID/g tissue. As a consequence of renal and hepatobiliary excretion, uptake values in the kidney and liver were 5.7±2.4 %ID/g tissue and 8.3±1.8 %ID/g tissue, respectively. When receptors were blocked by co-injection with an excess of unlabeled NeoBOMB1, uptake in GRPR-expressing tissues, such as tumor and pancreas decreased to 1.0±0.1 %ID/g tissue and 0.7±0.1 %ID/g tissue, respectively. Pharmacokinetic calculations resulted in a tumor clearance half-life of 6.9±2.8 h and a pancreas clearance half-life of 12.9±4.0 h (*Figure 2B+C*). Clearance from blood proceeded according to a bi-phasic pattern: 66±9% with $T_{1/2}$=8±5 min and 34% with $T_{1/2}$=50±15 min.
PET/CT scans of animals injected with 11.5 MBq/230 pmol resulted in good visualization of the tumor tissue. As expected, uptake was also seen in the abdominal area as a consequence of uptake in the GI-tract and/or pancreas. Images are presented in *Figure 2D*.

Biodistribution of ^{177}Lu-NeoBOMB1
Injection of 1 MBq/10 pmol or 1 MBq/200 pmol ^{177}Lu-NeoBOMB1 in PC-3-xenografted mice resulted in a higher tumor uptake with 200 pmol ^{177}Lu-NeoBOMB1 compared to that obtained after injection of 10 pmol ^{177}Lu-NeoBOMB1 (17.9±3.3 %ID/g tissue 4 h. p.i. vs. 11.6±1.3 %ID/g tissue 4 h p.i.). *Figure 3* shows the results of the ^{177}Lu-NeoBOMB1 biodistribution studies with 200 pmol (*Figure 3A*) and with 10 pmol (*Figure 3B*). Next to the tumor, high uptake was seen in the pancreas. However, in contrast to the tumor uptake, pancreas uptake was lower after injection of 200 pmol ^{177}Lu-NeoBOMB1 (19.8±6.9 %ID/g tissue 4 h p.i.) compared to injection of 10 pmol ^{77}Lu-NeoBOMB1 (105±13 %ID/g 4 h p.i.), resulting in a significant increase of the tumor to pancreas ratio with the higher peptide amount. Apart from the tumor and pancreas, the difference in peptide amount injected did not affect uptake in other non-GRPR-expressing organs (e.g. kidney uptake was 2.8±0.4 vs. 2.5±0.6 %ID/g tissue 4 h p.i. of 200 pmol and 10 pmol ^{177}Lu-NeoBOMB1, respectively).
Uptake in tumor and pancreas was receptor-specific, since co-injection with an excess of unlabeled NeoBOMB1 resulted in a significant decrease of both tumor uptake (0.50±0.02 %ID/g tissue and 0.39±0.06 %ID/g tissue using 200 pmol and 10 pmol ^{177}Lu-NeoBOMB1 respectively) and pancreas uptake (0.13±0.01 %ID/g tissue and 0.10±0.01 %ID/g tissue using 200 pmol and 10 pmol ^{177}Lu-NeoBOMB1

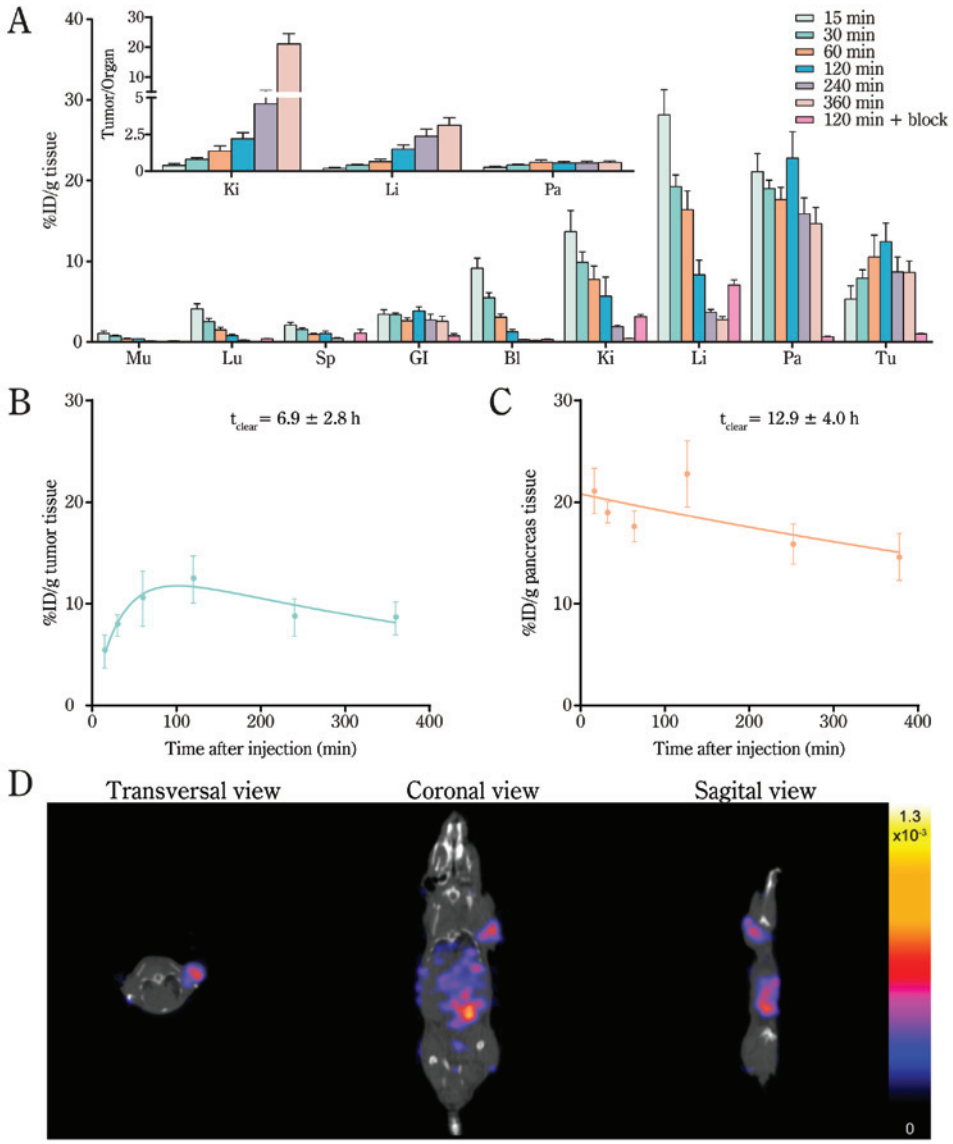

Figure. 2. ^{68}Ga-NeoBOMB1 biodistribution and imaging. A) Biodistribution of ~13 MBq/250 pmol ^{68}Ga-NeoBOMB1. Tumor to organ ratios are displayed in the upper bar graph. B+C) Pharmacokinetic modeling of the ^{68}Ga-NeoBOMB1 tumor and pancreas uptake, respectively. D) PET/CT images acquired 1 h post injection of 11.5 MBq/230 pmol ^{68}Ga-NeoBOMB1. Tumor is located on the right shoulder. Mu=muscle, Lu=lungs, Sp=spleen, GI=GI-tract, Bl=blood, Ki=kidney, Li=liver, Pa=pancreas and Tu=PC-3 tumor.

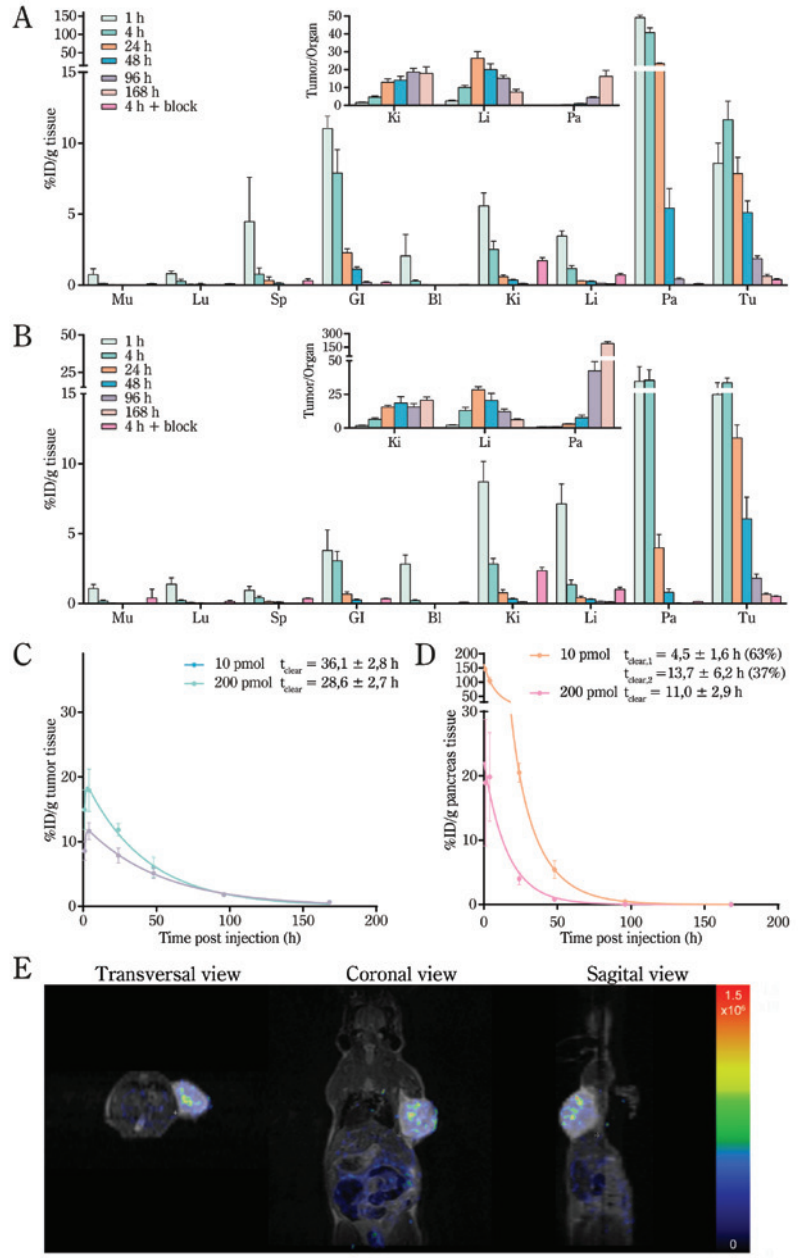

Figure 3. ^{177}Lu-NeoBOMB1 biodistribution and imaging. A+B) Biodistribution of 200 pmol and 10 pmol ^{177}Lu-NeoBOMB1 in PC-3-xenografted animals, respectively. Tumor to organ ratios are displayed in the upper bar graph. C) Pharmacokinetic modeling of the ^{177}Lu-NeoBOMB1 tumor uptake. D) Pharmacokinetic modeling of the ^{177}Lu-NeoBOMB1 pancreas uptake. E) SPECT/MR images 4 h post injection of 20 MBq/200 pmol ^{177}Lu-NeoBOMB1. Tumor is located on the right shoulder. Mu=muscle, Lu=lungs, Sp=spleen, GI=GI-tract, Bl=blood, Ki=kidney, Li=liver, Pa=pancreas and Tu=PC-3 tumor.

respectively), independent of the peptide amount used. Although initial radioactivity uptake in the pancreas was high, pancreas uptake decreased relatively rapidly, while tumor radioactivity was retained longer. The pharmacokinetic calculations resulted in a tumor clearance half-life of 28.6±2.7 h and in a pancreas clearance half-life of 11.0±2.9 h when animals were injected with 200 pmol ^{177}Lu-NeoBOMB1 (*Figure 3C+D*). The tumor clearance half-life was 36.1±2.8 h after injection of 10 pmol of the radiotracer. The clearance from the pancreas showed a bi-exponential pattern after injection of 10 pmol ^{177}Lu-NeoBOMB1: 63% with a half-life of 4.5±1.6 h and 37% with 13.7±6.2 h. After injection of 200 pmol ^{177}Lu-NeoBOMB1, only a single-exponential curve could be fitted. Clearance from blood proceeded according to a single-phase pattern with $T_{1/2}$=63±32 min after injection of 10 pmol ^{177}Lu-NeoBOMB1 and with$T_{1/2}$=48±12 min after injection of 200 pmol of the radiotracer.
SPECT/MR images acquired 4 h p.i. of ~20 MBq/200 pmol of ^{177}Lu-NeoBOMB1 resulted in good visualization of the tumor (*Figure 3E*). In line with the results of the biodistribution study minimal uptake was observed in the GI-tract.

Dosimetry

Dosimetry calculations resulted in a higher tumor dose (581 mGy/MBq vs. 435 mGy/MBq) and a lower dose to the pancreas (265 mGy/MBq vs. 1393 mGy/Mbq) after injection of 200 pmol ^{177}Lu-NeoBOMB1 vs. 10 pmol ^{177}Lu-NeoBOMB1 (*Table 1*). When animal data were used to predict human dosimetry according to method 2 (ratio of organ weights), we found a kidney, pancreas and liver exposure of 0.10, 0.65 and 0.06 mGy/MBq respectively (*Table 2*). Method 1 (ratio of body weights) yielded lower absorbed dose estimates.

Table 1. Absorbed dose per administered activity (mGy/MBq) in 340±100 mm³ PC-3-tumor xenografts and organs for ^{177}Lu-NeoBOMB1

Organs	10 pmol	200 pmol	D (tumor)/D (organ)	
			10 pmol	**200 pmol**
Tumor	435	570	-	-
Kidneys	58	57	7.5	10
Pancreas	1393	265	0.31	2.15

Table 2. Extrapolated human dosimetry (mGy/MBq) for ^{177}Lu-NeoBOMB1

	10 pmol		200 pmol	
Organs	**Method 1**	**Method 2**	**Method 1**	**Method 2**
Lower large intestine wall	0.18	0.32	0.17	0.18
Small intestine	0.17	0.19	0.15	0.16
Stomach wall	0.16	0.19	0.15	0.17
Upper large intestine wall	0.23	0.34	0.17	0.21
Heart wall	0.02	0.02	0.01	0.01
Kidneys	0.03	0.09	0.03	0.10
Liver	0.15	0.03	0.03	0.06
Lungs	0.02	0.01	0.01	0.01
Muscle	0.01	0.01	0.01	0.01
Pancreas	0.54	3.37	0.11	0.65
Red Marrow	0.11	0.10	0.11	0.11
Osteogenic cells	0.44	0.42	0.45	0.44
Spleen	0.02	0.03	0.01	0.02
Urinary bladder wall	0.75	0.74	0.75	0.75
Total Body	0.15	0.14	0.15	0.15

DISCUSSION

Since overexpression of the GRPR is reported in various cancer types, targeting this receptor with radiolabeled peptide analogs for imaging and therapy might have a significant impact on patient care. In this study we explored the use of a novel radiolabeled GRPR antagonist, NeoBOMB1, for tumor targeting by performing imaging and biodistribution studies in a prostate cancer mouse model. NeoBOMB1 is linked to a DOTA-chelator and can be labeled with different radionuclides enabling the theranostic use of the peptide analog. We evaluated the biodistribution of both ^{68}Ga-NeoBOMB1, for imaging purposes, and ^{177}Lu-NeoBOMB1, for therapy purposes in a mouse model in order to generate information for theranostic use of the radiotracer.
Biodistribution studies with ^{68}Ga-NeoBOMB1 resulted in high tumor uptake, leading to clear visualization of the tumor on PET/CT scans. Furthermore, relatively high uptake of ^{68}Ga-NeoBOMB1 was observed in the GRPR-expressing pancreas, resulting in a tumor to pancreas ratio of 0.6 (1 h p.i.). Clearance half-lives demonstrated a lower clearance half-life for the tumor (6.9±2.8 h) compared to the pancreas (12.9±4.0 h). Presumably, this is a consequence of the limited time points studied in the ^{68}Ga-NeoBOMB1 biodistribution studies. Furthermore, tumor uptake was slower than pancreas uptake. Because of the short half-life of ^{68}Ga in combination with the slower tumor kinetics, biodistribution studies could

not be performed at later time points. Nevertheless, the presented data indicates that NeoBOMB1 has excellent pharmacokinetic properties for imaging.

In the ^{177}Lu-NeoBOMB1 biodistribution studies, we compared organ and tumor uptake of 2 different peptide amounts, 1 MBq/10 pmol and 1 MBq/200 pmol. Injection of 1 MBq/200 pmol ^{177}Lu-NeoBOMB1 resulted in a higher tumor uptake and a lower pancreatic uptake compared to the uptake observed after administration of 1 MBq/10 pmol ^{177}Lu-NeoBOMB1, resulting in a favorable tumor to pancreas ratio (0.9 vs. 0.11, based on radioactivity uptake 4 h p.i.) with the high peptide amount used. In contrast to the GRPR-positive pancreas, the uptake in other organs was not influenced by the injected peptide amount. The observed peptide amount dependent uptake in the pancreas is likely due to partial receptor saturation of the pancreas when 200 pmol of the radiotracer is administered. Our results are in line with previous observations (8,28) for the GRPR agonist AMBA, and emphasize the need for careful optimization of protocols for nuclear imaging and therapy.

Furthermore, dosimetry calculations resulted in a 1.3 times higher tumor dose and a 5 times lower pancreas dose with 200 pmol ^{177}Lu-NeoBOMB1 compared to 10 pmol ^{177}Lu-NeoBOMB1. When comparing dosimetry data with other radiolabeled GRPR antagonists, such as ^{177}Lu-JMV4168 (29), estimated absorbed radiation doses to the tumor were higher for ^{177}Lu-NeoBOMB1 (29 Gy/50 MBq vs. 11 Gy/50 MBq) even when ^{177}Lu-JMV4168 was stabilized by co-injection of an enzyme inhibitor (29 Gy/50 MBq vs. 20 Gy/MBq). When we compared the dose to the kidneys and pancreas of the radiotracers, we found a more favorable tumor to kidney ratio for ^{177}Lu-NeoBOMB1 (10 vs. 1.5) and a similar tumor to pancreas ratio (2.2 vs. 2.5).

As expected, comparing the biodistribution of the ^{68}Ga-NeoBOMB1 or ^{177}Lu-NeoBOMB1, with the uptake of radiolabeled GRPR agonists, e.g. ^{99m}Tc-Demobesin4 or ^{177}Lu-AMBA, a lower uptake was observed in GRPR-expressing organs, namely the pancreas and the gastrointestinal tract (8,13).

Comparing uptake and dosimetry of radiolabeled NeoBOMB1 with other radiolabeled GRPR antagonists mentioned in literature is difficult because of the differences between experimental conditions, such as the peptide amount used and the radionuclide bound to the peptide. However, we can report that in vivo tumor to pancreas ratio in mouse models are more favorable for ^{68}Ga-NeoBOMB1 (0.6) compared to other GRPR antagonists such as ^{67}Ga-SB3 (0.2) reported by Maina et al. (16) and ^{99m}Tc-Demobesin 1 (0.2) reported by Cescato et al. (13) (numbers are based on biodistribution results 1 h p.i. of the radiotracers). However, lower peptide amounts were used in these studies which could lead to less favorable results as demonstrated in the ^{177}Lu-NeoBOMB1 biodistribution studies. Nevertheless, the mentioned radiotracers have successfully been used in clinical trials for the visualization of both breast and newly diagnosed prostate cancer lesions, emphasizing the potential of ^{68}Ga-NeoBOMB1 for tumor visualization in humans.

Comparing extrapolated human dosimetry data of ^{177}Lu-NeoBOMB1 with extrapolated dosimetry data of ^{177}Lu-DOTA-Tyr^3-octreotate, which is currently successfully used for treatment of patients with neuroendocrine tumors, we found similar values (*Table 3*). This was expected since excretion patterns of

Table 3. Comparison between extrapolated and determined absorbed doses per injected activity for ^{177}Lu-DOTA-Tyr^3-octreotate

Organs	Method 1*	Method 2†	^{177}Lu-DOTA-Tyr^3-octreotate in patients†
Kidneys	0.06	0.16	0.62 (0.49-0.75)
Liver	0.01	0.01	0.29 (0.21-0.49)
Red Marrow	0.11	0.11	0.016 (0.012-0.022)
Spleen	0.01	0.02	0.68 (0.51-0.92)
Total Body	0.14	0.14	

** Data based on published data by S. Bison et al. (32).*
† Data published by Sandström et al. (33).

the two radiotracers are comparable. Although the extrapolated dosimetry data of ^{177}Lu-DOTA-Tyr^3-octreotate does not completely fit the dosimetry values obtained from patients studies (*Table 3*), based on the extrapolated data of ^{177}Lu-NeoBOMB1 we expect similar values.

Concerning imaging, patient studies by Maina et al. (16) in which prostate cancer lesions were successfully visualized using a GRPR radioligand showed a biodistribution pattern in physiological organs similar to what was found in mice. Although the authors did not report on limitations of their imaging studies, more clinical studies are needed.

Very promising prostate-specific membrane antigen (PSMA)-targeting ligands are currently also under investigation for the same purpose. In a recent study Minamimoto et al. (30) compared PSMA and GRPR-targeted imaging in prostate cancer and found no significant differences. Furthermore, Perera et al. (31) reported on a relatively low sensitivity of PSMA-targeted imaging in patients with low prostate-specific antigen levels and patients with primary disease (40% and 50%, respectively). Especially in these patient groups the application of GRPR radioligands may be of benefit.

Based on the presented data we conclude that both ^{68}Ga-NeoBOMB1 and ^{177}Lu-NeoBOMB1 have excellent tumor uptake and favorable pharmacokinetics for theranostic use. Clinical studies using this radiotracer in GRPR-expressing cancer, e.g. prostate cancer and breast cancer, have yet to be performed, but expectations are high.

REFERENCES

1. Guo M, Qu X, Qin XQ. Bombesin-like Peptides and their Receptors: Recent Findings in Pharmacology and Physiology. Curr Opin Endocrinol Diabetes Obes. 2015;22:3-8.
2. Gonzalez N, Moody TW, Igarashi H, Ito T, Jensen RT. Bombesin-related Peptides and their Receptors: Recent Advances in their Role in Physiology and Disease States. Curr Opin Endocrinol Diabetes Obes. 2008;15:58-64.
3. Gugger M, Reubi JC. Gastrin-releasing Peptide Receptors in Non-neoplastic and Neoplastic Human Breast. Am J Pathol. 1999;155:2067-2076.
4. Markwalder R, Reubi JC. Gastrin-releasing Peptide Receptors in the Human Prostate: Relation to Neoplastic Transformation. Cancer Res. 1999;59:1152-1159.
5. Brabander T, Kwekkeboom DJ, Feelders RA, Brouwers AH, Teunissen JJ. Nuclear Medicine Imaging of Neuroendocrine Tumors. Front Horm Res. 2015;44:73-87.
6. Kwekkeboom DJ, Krenning EP. Peptide Receptor Radionuclide Therapy in the Treatment of Neuroendocrine Tumors. Hematol Oncol Clin North Am. 2016;30:179-191.
7. Yu Z, Ananias HJ, Carlucci G, et al. An Update of Radiolabeled Bombesin Analogs for Gastrin-releasing Peptide Receptor Targeting. Curr Pharm Des. 2013;19:3329-3341.
8. Lantry LE, Cappelletti E, Maddalena ME, et al. 177Lu-AMBA: Synthesis and Characterization of a Selective 177Lu-labeled GRP-R Agonist for Systemic Radiotherapy of Prostate Cancer. J Nucl Med. 2006;47:1144-1152.
9. Schroeder RP, Muller C, Reneman S, et al. A Standardised Study to compare Prostate Cancer Targeting Efficacy of Five Radiolabelled Bombesin Analogues. Eur J Nucl Med Mol Imaging. 2010;37:1386-1396.
10. Nock B, Nikolopoulou A, Chiotellis E, et al. [99mTc]Demobesin 1, a Novel Potent Bombesin Analogue for GRP Receptor-targeted Tumour Imaging. Eur J Nucl Med Mol Imaging. 2003;30:247-258.
11. Mather SJ, Nock BA, Maina T, et al. GRP Receptor Imaging of Prostate Cancer using [(99m)Tc]Demobesin 4: a First-In-Man Study. Mol Imaging Biol. 2014;16:888-895.
12. Mansi R, Wang X, Forrer F, et al. Development of a Potent DOTA-conjugated Bombesin Antagonist for targeting GRPr-positive Tumours. Eur J Nucl Med Mol Imaging. 2011;38:97-107.
13. Cescato R, Maina T, Nock B, et al. Bombesin Receptor Antagonists may be preferable to Agonists for Tumor Targeting. J Nucl Med. 2008;49:318-326.
14. Ginj M, Zhang H, Waser B, et al. Radiolabeled Somatostatin Receptor Antagonists are Preferable to Agonists for in vivo Peptide Receptor Targeting of Tumors. Proc Natl Acad Sci U S A. 2006;103:16436-16441.
15. Bodei L, Ferrari M, Nunn AD, et al. 177Lu-AMBA Bombesin Analogue in Hormone Refractory Prostate Cancer Patients: a Phase I Escalation Study with Single-cycle Administrations [abstract]. Eur J Nucl Med Mol Imaging. 2007;34:S221
16. Maina T, Bergsma H, Kulkarni HR, et al. Preclinical and First Clinical Experience with the Gastrin-releasing Peptide Receptor-antagonist [Ga]SB3 and PET/CT. Eur J Nucl Med Mol Imaging. 2016;43:964-973.
17. Heimbrook DC, Saari WS, Balishin NL, et al. Gastrin Releasing Peptide Antagonists with Improved Potency and Stability. J Med Chem. 1991;34:2102-2107.

18. Nock B, Kaloudi A, Lymperis E, et al. [68Ga]NeoBomb1, a New Potent GRPR-antagonist for PET Imaging-Preclinical and First Clinical Evaluation in Prostate Cancer. J Nucl Med. 2016;57 (Suppl 2):583.
19. Dalm S, Bakker I, de Blois E, et al. 68Ga/177Lu-NeoBOMB1, a Novel Radiolabeled GRPR Antagonist for Theranostic Use. J Nucl Med. 2016;57 (Suppl 2):331.
20. Maina-Nock T, Nock BA, de Jong M. Grpr-antagonists for detection, diagnosis and treatment of grpr-positive cancer. Google Patents; 2014.
21. Breeman WA, de Zanger RM, Chan HS, de Blois E. Alternative Method to Determine Specific Activity of (177)Lu by HPLC. Curr Radiopharm. 2015;8:119-122.
22. Castaldi E, Muzio V, D'Angeli L, Fugazza L. 68GaDOTATATE lyophilized Ready to use Kit for PET Imaging in Pancreatic Cancer Murine Model. J Nucl med. 2014;(Supplement 1):55.
23. Keenan MA, Stabin MG, Segars WP, Fernald MJ. RADAR Realistic Animal Model Series for Dose Assessment. J Nucl Med. 2010;51:471-476.
24. Bolch WE, Eckerman KF, Sgouros G, Thomas SR. MIRD Pamphlet No. 21: a Generalized Schema for Radiopharmaceutical Dosimetry -Standardization of Nomenclature. J Nucl Med. 2009;50:477-484.
25. Stabin MG, Konijnenberg MW. Re-evaluation of Absorbed Fractions for Photons and Electrons in Spheres of Various Sizes. J Nucl Med. 2000;41:149-160.
26. Stabin MG. Fundamentals of Nuclear Medicine Dosimetry. 1 ed: Springer-Verlag New York; 2008.
27. Stabin MG, Sparks RB, Crowe E. OLINDA/EXM: the Second-generation Personal Computer Software for Internal Dose Assessment in Nuclear Medicine. J Nucl Med. 2005;46:1023-1027.
28. De Blois E, Schroeder RJ, De Ridder CA, Van Weerden WM, Breeman WP, De Jong M. Improving Radiopeptide Pharmacokinetics by adjusting Experimental Conditions for Bombesin Receptor-mediated Imaging of Prostate Cancer. Q J Nucl Med Mol Imaging. 2013 [epub].
29. Chatalic KL, Konijnenberg M, Nonnekens J, et al. In Vivo Stabilization of a Gastrin-Releasing Peptide Receptor Antagonist Enhances PET Imaging and Radionuclide Therapy of Prostate Cancer in Preclinical Studies. Theranostics. 2016;6:104-117.
30. Minamimoto R, Hancock S, Schneider B, et al. Pilot Comparison of 68Ga-RM2 PET and 68Ga-PSMA-11 PET in Patients with Biochemically Recurrent Prostate Cancer. J Nucl Med. 2016;57:557-562.
31. Perera M, Papa N, Christidis D, et al. Sensitivity, Specificity, and Predictors of Positive 68Ga-Prostate-specific Membrane Antigen Positron Emission Tomography in Advanced Prostate Cancer: A Systematic Review and Meta-analysis. Eur Urol. 2016 [epub].
32. Bison SM, Konijneberg MW, Koelewijn SJ, Melis ML, de Jong M. Influence of Specific Activity on Tumour Dosimetry and Response to Therapy in a Nude Mouse Small Cell Lung Cancer Model. 2014;41 (Suppl 2):S151-S705.
33. Sandstrom M, Garske-Roman U, Granberg D, et al. Individualized Dosimetry of Kidney and Bone Marrow in Patients undergoing 177Lu-DOTA-octreotate Treatment. J Nucl Med. 2013;54:33-41.

Part 5

Epilogue

Summary, Discussion and Future Perspectives

SUMMARY

Breast cancer (BC) is the 2nd most common cancer worldwide and the most frequent cancer type occurring in women. The disease is highly heterogeneous consisting of various subtypes; and therapy and prognosis varies dependent on the BC subtype (1,2). Over the years different detection techniques and novel therapies for BC have been introduced, which had a positive impact on BC care and outcome (3). However, the currently used imaging methods still have limitations and current treatments for metastatic disease are unfortunately not associated with cure. As a result the mortality rate is still too high. The aim of the studies described in this thesis was to investigate radiotracers for theranostic purposes in BC. *Figure 1* shows an overview of the main findings.

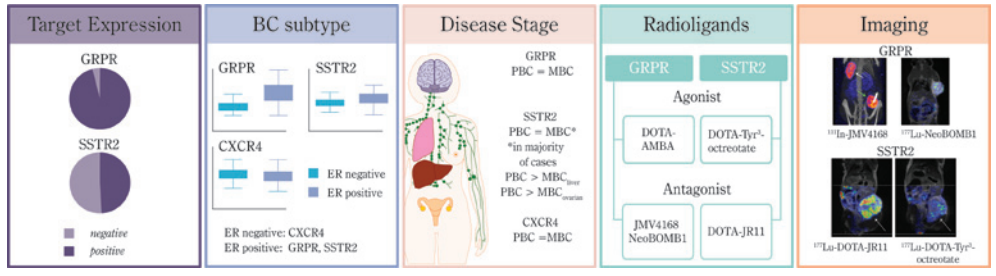

Figure 1. Overview of the main findings of the studies described in this thesis. PBC=primary breast cancer, MBC=metastatic breast cancer.

Chapter 1 of this thesis provides an introduction on BC characteristics and current imaging and therapy options. Next, nuclear medicine-based imaging techniques and therapeutic options are explained, and examples of commonly used radionuclides for these purposes are mentioned. Subsequently, the currently used nuclear medicine-based imaging methods for BC and their limitations are portrayed, followed by an introduction of a more specific approach for nuclear medicine based imaging, in which biomarkers overexpressed on cancer cells are targeted with radiotracers. These radiotracers can also be used for therapeutic purposes when labeled with therapeutic radionuclides. In this regard, the concept of theranostics is explained including a list of radionuclides suitable for this purpose. Three biomarkers, SSTR, GRPR and CXCR4, interesting for targeting of BC for theranostic purposes are described. Finally, the potential benefits of targeted nuclear imaging and treatment of BC are discussed. **Chapter 2** provides an overview of all biomarkers currently under investigation in preclinical and/or clinical studies for targeted nuclear imaging. These biomarkers are differentially expressed in the different BC subtypes and information gained from nuclear imaging is dependent on the biomarker targeted. The heterogeneity of BC requires a more personalized approach of the disease; one size does not fit all, and thus careful selection of the right radiotracer for the right purpose and the right patient is needed. In order to achieve a successful personalized approach, important benefits and limitations of the radiotracers should be considered.

The second part of the thesis focuses on the clinical relevance of targeting SSTR2, GRPR and CXCR4 in BC with the goal of identifying patient groups and applications of radiotracers targeting these receptors. In **Chapter 3,** we describe measurements of *SSTR2*, *GRPR* and *CXCR4* mRNA expression levels of 915 primary BCs by RT-qPCR and correlation with known clinicopathologic factors, biological factors and prognosis. First, in vitro autoradiography was performed using both a GRPR and a SSTR2 radioligand on a small panel of BC specimens to determine whether mRNA expression of the 2 receptors could be used as a surrogate for radiotracer binding; this resulted in a significant positive correlation. Although autoradiography studies with CXCR4 radioligands could not be performed, prior studies reported that *CXCR4* mRNA and protein expression correlated significantly as well. Associating *SSTR2*, *GRPR* and *CXCR4* mRNA expression levels with BC characteristics identified ER-positive tumors (luminal A and B BCs) as potential candidates for SSTR2 and GRPR-mediated imaging and therapy, while targeting of CXCR4 might be more suited for ER-negative tumors (including basal-like tumors). Moreover, high *CXCR4* mRNA levels were associated with a prolonged prognosis in terms of disease-free, metastases-free and overall survival. This finding was unexpected, because high *CXCR4* mRNA expression levels were associated with ER-negative tumors, which are usually more aggressive. This could be explained by a factor independent of ER expression that determines good outcome in this patient group. *SSTR2* expression showed no significant association with prognosis, while high *GRPR* mRNA expression levels were associated with prolonged progression-free survival after first-line tamoxifen treatment.

Since metastatic BC is incurable and the main reason for BC-related death, better detection and better treatment of advanced disease is very important. Therefore, we studied the expression of *SSTR2*, *GRPR* and *CXCR4* mRNA expression in 60 paired primary BCs as well as in the corresponding locoregional or distant metastases as described in **Chapter 4.** The comparison of matched primary tumors and metastases demonstrated that there were no significant differences in *GRPR* and *CXCR4* mRNA levels between primary tumors and corresponding metastases. Regarding *SSTR2*, the mRNA expression was lower in liver and ovarian metastases compared to the matched primary tumor ($P=0.02$ and $P=0.03$, respectively). Furthermore, similar to data reported in Chapter 3 high *GRPR* and *SSTR2* mRNA expression was mainly associated with ER-positive tumors. In only few tumors ER status between primary tumors and metastases was discordant, which also affected *GRPR* and *SSTR2* expression in the majority of these lesions: in ER-negative metastases that had matched ER-positive primary breast tumors, a significant lower expression of GRPR and SSTR2 was observed as well. A switch in ER expression between primary tumors and metastases is observed in approximately 14% of BCs (4), and hence the associated change in *GRPR* and *SSTR2* expression should be kept in mind if GRPR- and SSTR2-targeting is considered. Based on these findings we concluded that targeting of SSTR2, GRPR and CXCR4 for theranostic purposes might be beneficial for both primary and advanced disease.

In the next section of the thesis the focus is on SSTR-mediated imaging of BC. **Chapter 5** is a review of all previously performed clinical studies on SSTR-mediated nuclear imaging, of which the majority was performed over a decade ago. The aim of the review was to critically assess the methods, findings and limitations of the clinical studies in order to determine whether recent developments made in the field of nuclear medicine, both related to better imaging methods as well as improved radiotracers, could improve SSTR2 radiotracer-based BC imaging. A sensitivity and specificity ranging between 36-100% and 22-100%, respectively, was reported from the different studies. Low and heterogeneous target expression were identified as the main limiting factors. In the performed studies, planar imaging was the main imaging method, octreotide or depreotide were the SST analogs applied, and no discrimination between different BC subtypes was made. With the currently available and approved nuclear medicine imaging techniques (SPECT, PET and dedicated breast imaging platforms), the novel SST analogs (receptor agonists as well as antagonist) with higher receptor affinity available, as well as the knowledge of SSTR-expression in relation to BC subtypes, it seems worth to reinvestigate the value of SSTR-mediated imaging of BC, both in primary and advanced disease. In case imaging is successful, SSTR2 radioligands coupled to therapeutic radionuclides might be considered for therapeutic purposes.

One recent development is the use of SSTR2 antagonists for tumor targeting. It has been reported in preclinical and clinical studies that radiolabeled SSTR2 antagonists are superior to SSTR2 agonists for imaging purposes in neuroendocrine tumors, despite the accumulation of radioactivity in tumor cells as a consequence of radio-agonist internalization. The enhanced binding of the antagonist was explained by the ability to bind more binding sites/receptors than the agonist. Since low and heterogeneous SSTR2 expression was identified as a limiting factor for SSTR-mediated BC imaging, application of radiolabeled SSTR2 antagonists might increase radiotracer accumulation and as a consequence result in better tumor targeting. In **Chapter 6** we compared the binding of a radiolabeled SSTR2 agonist, DOTA-Tyr^3-octreotate, and an SSTR2 antagonist, DOTA-JR11, in 40 human BC specimens as well as the biodistribution of the 2 compounds in a patient-derived orthotopic BC xenograft mouse model. Binding of ^{111}In-DOTA-Tyr^3-octreotate and ^{111}In-DOTA-JR11 to the BC specimens analyzed by in vitro autoradiography was significantly higher ($P<0.001$) for the receptor antagonist compared to the agonist. The ratio of antagonist to agonist binding ranged from 1 (in only 1 case) -57 (median (interquartile range)=3.39 (2-5)). SPECT/MR imaging in a patient-derived orthotopic BC mouse model (T126) resulted in much better visualization of the tumor after injection of ^{177}Lu-DOTA-JR11 vs. ^{177}Lu-DOTA-Tyr^3-octreotate. Biodistribution studies performed after imaging confirmed the higher tumor uptake of the antagonist. It was concluded that the use of SSTR2 antagonists such as DOTA-JR11, could improve BC targeting, shedding new light on SSTR-targeted nuclear imaging and potentially also SSTR-targeted therapy.

Since the superiority of SSTR2 radiotracers was only demonstrated for imaging purposes and a major benefit of radiotracers is the application for treatment as

well, we compared ^{177}Lu-DOTA-JR11 and ^{177}Lu-DOTA-Tyr^3-octreotate for therapeutic purposes in a preclinical setting (both in vitro and in vivo) in **Chapter 7.** To deliver proof of principle these experiments were performed in vitro in cells transfected with SSTR2 (U2OS+SSTR2) and in vivo in mice bearing SSTR-expressing H69 xenografts. In vitro, tracer uptake and DNA damage (indirectly measured by 53BP1 foci) were determined after incubation with ^{177}Lu-DOTA-JR11 and ^{177}Lu-DOTA-Tyr^3-octreotate. This resulted in a 5 times higher uptake and 2 times more DNA damage after incubation with the radio-antagonist vs. the radio-agonist. In vivo therapy studies, performed after determining the optimal peptide amount for tumor targeting in biodistribution studies, resulted in a longer growth delay and a better median survival time after ^{177}Lu-DOTA-JR11 treatment compared to those observed after ^{177}Lu-DOTA-Tyr^3-octreotate treatment. These findings led to the conclusion that the use of SSTR2 antagonists is not only superior for imaging, but also for therapeutic purposes and could thus improve the theranostic use of SSTR2 radiotracers. This is especially interesting for tumor types with lower SSTR2 expression, including BC

The last section of the thesis focusses on the use of GRPR radiotracers for tumor targeting. In **Chapter 8** the application of GRPR radioligands in BC was studied in a preclinical setting. First, in vitro autoradiography using a radiolabeled GRPR agonist, ^{111}In-AMBA, was used to determine GRPR expression in 50 human BC specimens. The majority of the tumors (96%) expressed the receptor and GRPR expression was positively associated with ER expression. Next, a panel of BC cell lines was screened for their ability to bind ^{111}In-AMBA and the cell lines with the highest uptake, T47D and MCF7 (both ER-positive cell lines), were used for further studies. In vitro therapy of T47D cells with ^{177}Lu-AMBA resulted in a significant reduction (up to 80%) of viable cells compared to untreated cells, while treatment with ^{177}Lu-DTPA and unlabeled AMBA had no significant effect on cell viability. Mice with subcutaneous and orthotopic T47D or MCF7 xenografts scanned by SPECT after injection of an in situ stabilized radiolabeled GRPR antagonist, ^{111}In-JMV4168 + phosphoramidon (an enzyme inhibitor preventing degradation of the peptide), showed good visualization of the tumors. In line with the in vitro studies, T47D xenografts were visualized better than MCF7 xenografts. This was also confirmed in the biodistribution studies. The application of GRPR radioligands proofed to be promising for nuclear imaging and treatment of GRPR-positive breast lesions. Since high GRPR expression is associated with ER-positive BC and ~70% of BCs are ER-positive, targeting the GRPR for theranostic purposes holds promise for the majority of BCs.
In the final chapter (**Chapter 9**) a novel GRPR radiotracer, NeoBOMB1 was investigated for theranostic use. In vivo studies were performed comparing the use of ^{177}Lu and ^{68}Ga labeled NeoBOMB1 in vivo in a prostate cancer (PC3) xenograft mouse model. Biodistribution and imaging studies (SPECT and PET) were performed at different time points after injection of the radiotracers. Data was used to determine pharmacokinetics, dosimetry and to predict patient dosimetry. For the ^{177}Lu-NeoBOMB1 studies, two different peptide amounts (10 pmol vs. 200 pmol) were compared to find the best tumor to background ratio for tumor targeting. Both ^{68}Ga-NeoBOMB1 and ^{177}Lu-NeoBOMB1 uptake in tumors was high and tumors were successfully visualized in SPECT and PET imaging studies. Notable uptake was also observed in the GRPR-expressing pancreas and the kidneys, the latter due to renal excretion and partial reabsorption of the radiotracers. However, clearance from the pancreas and kidneys was relatively fast, while in the tumor the radiotracer was retained better. When 2 peptide amounts of ^{177}Lu-NeoBOMB1 were compared, the highest peptide amount appeared to be the preferred one, as higher tumor uptake and a lower background uptake were observed. As expected, this resulted in a higher tumor dose and lower dose in normal organs that showed radiotracer uptake after the highest amount, 200 pmol NeoBOMB1 labeled with ^{177}Lu, was injected. Concerning the predicted patient dosimetry, the calculated values were similar to those reported for the clinically successfully used SSTR2 radiotracer ^{177}Lu-DOTA-Tyr^3-octreotate. Based on the acquired data it was concluded that both ^{68}Ga-NeoBOMB1 and ^{177}Lu-NeoBOMB1 had excellent tumor uptake and pharmacokinetics for theranostic use. Although these studies were performed in a prostate cancer mouse model, our findings indicate the potential of this radiotracer for theranostic purposes in BC as well.

DISCUSSION AND FUTURE PERSPECTIVES

The studies described in this thesis demonstrated the potential of SSTR, GRPR and CXCR4 (with the majority of studies focused on SSTR2 and GRPR) as targeting radiotracers for theranostic use in BC. Application of targeted nuclear medicine can potentially offer a non-invasive, sensitive, specific and personalized method for imaging and treatment of the disease. Based on the results of the preclinical studies, it is suggested that there are specific BC patient groups that may benefit from SSTR2, GRPR or CXCR4 targeting. There are still many challenges, however, that need to be addressed.

BC Subtypes

ER-positive BC subtypes were identified as the most suitable BCs for GRPR- and SSTR2-targeting, while ER-negative BC showed higher expression of CXCR4, making the latter target more suitable for ER-negative tumors. However, it is necessary to mention that GRPR, SSTR2 and CXCR4 expression was not limited to ER-positive and -negative tumors, respectively, and thus in some cases radiotracers targeting these receptors might also be applied to the other BC subtypes. The other way around, although the majority of ER-positive BCs express the GRPR, not all tumors showed (sufficient) expression for targeting. This was also the case for SSTR2 and CXCR4, the latter in the case of ER-negative tumors. Furthermore, the difference in target expression observed between ER-positive and ER-negative tumors was less pronounced for CXCR4 than for GRPR and SSTR2.
The high correlation between ER expression and GRPR and SSTR2 expression suggests a connection between the receptors. Various studies reported an

estrogen dependent regulation of SSTR2 expression via ER in human derived BC cell lines (5-7). In some studies it was reported that incubation with tamoxifen led to an increase in SSTR2 expression, while incubation with "pure" anti-estrogens caused a decrease in SSTR2 expression. Concerning GRPR expression, to our knowledge there are no studies describing a connection between ER signaling and GRPR expression or vice versa. If SSTR2 and GRPR-mediated imaging and/or treatment is to be used in patients treated with anti-estrogen treatment, it is important to be aware of the potential effect of anti-estrogens on SSTR2 and GRPR expression and to understand the mechanisms underlying SSTR2 and GRPR expression in relation to ER. The latter is also important in tumors that show resistance against anti-estrogen treatment. In the metastatic setting, in which response can be assessed, approximately 20% of patients show intrinsic resistance against first line anti-estrogen treatment, and only 30-40% of patients respond to second and third line endocrine therapy (8). Especially in patients who have been treated with multiple lines of endocrine treatment, the use of SSTR2 or GRPR radioligands for therapeutic purposes might be considered, if SSTR2 and GRPR expression in these patients is retained. There are a few mechanisms described regarding anti-estrogen resistance including down regulation of ER, genetic mutations in *ESR1*, loss of ER, impaired co-activator signaling and activation of the growth factor signaling pathway (9-11). The question remains whether and how these factors negatively influence SSTR2 and GRPR expression. In a substantial percentage of breast tumors hormone receptor expression and/or HER2 expression changes during disease progression, resulting in discordance of receptor expression between primary BC and metastases (12). In one of the described studies (Chapter 4) we investigated the effect of ER and HER2 discordance on *SSTR2*, *GRPR* and *CXCR4* expression in a small number of primary tumors and metastatic lesions. Although we found preliminary evidence that a change in ER expression influenced *GRPR* and *SSTR2* expression as well, the studied sample size was too small for reliable conclusions and larger studies are needed.

It is currently recommended by both the national and international societies to biopsy metastatic disease as much as possible to determine hormone receptor and HER2 expression of the metastatic lesions in order to administer the appropriate therapy, and to prevent ineffective treatment when considering biomarker expression of the primary tumor only (13). On the other hand, it is not always possible to biopsy all the metastatic lesions, and it is theoretically possible that biomarker expression varies with the location of the metastases. With regard to SSTR2, GRPR and CXCR4, the theranostic use of radiotracers offers the opportunity to evaluate target expression of metastases or recurrent disease in a non-invasive way by performing imaging studies and therefore biopsy is not necessary. The results of these imaging studies might indicate whether targeted radionuclide treatment is recommended in a specific patient.

Targets and Radioligands

A number of targets are currently under investigation for BC imaging. If we limit our discussion to the targets investigated in this thesis, both SSTR2 and GRPR seem to be suitable for application in ER-positive BCs. However, according to our studies and other published papers, SSTR2 expression was reported to be less frequent, of low density and heterogeneously distributed over the tumor, while GRPR was found to be expressed frequently, abundantly and homogenously in the majority of breast tumors (14). Based on this information targeting of GRPR seems more promising for ER-positive BC than targeting of SSTR2. Nevertheless, BC is a very heterogeneous disease; there is not one specific target suitable for all ER-positive BCs and when GRPR targeting is not possible, targeting of SSTR2 might be a good second option. In order to select the best biomarker for tumor targeting, expression of potential targets should be determined on biopsy material (as is currently done for ER, PR and HER2 expression) or by performing SPECT or PET imaging studies using radioligands targeting these biomarkers, which is less invasive but comes with the cost of radiation burden. Furthermore, physiological uptake of radiotracers in healthy organs might be dose-limiting when radiotracers are applied for therapeutic purposes, and dosimetry calculations should be performed based on imaging and pharmacokinetic data. So, high SSTR2 radiotracer uptake was reported in spleen, adrenals, liver, kidneys and the bladder of patients with neuroendocrine tumors (15,16). Furthermore, next to the kidneys, bone marrow has been identified as the dose-limiting organ because of the high exposure of this organ to radioactivity that is in the blood (17). For GRPR radiotracers, high uptake was reported in the pancreas, kidneys, bladder and gastrointestinal sphincters (18,19).

Furthermore, as was described in our second chapter, other biomarkers are currently under investigation for targeting with radiotracers mainly for imaging purposes, including ER and PR. Limitations of these biomarkers include difficulty to target lesions when treated with anti-estrogens that bind to the ER since this makes the receptor unavailable for radiotracer binding. Besides, down regulation or loss of the ER/PR has been observed during anti-estrogen resistance, which also hampers the use of ER-targeted radiotracers.

Concerning CXCR4, ER-negative tumors showed the highest expression. In view of the limited therapeutic options for this BC subtype, the use of radiotracers targeting this receptor might offer new options for this patient group, particularly in patients progressing on standard of care therapies (usually only chemotherapy). However, studies using CXCR4 radiotracers for BC targeting are scant. A recent clinical study by Vag et al. (20) reported low to moderate uptake of ^{68}Ga-pentixafor in BC lesions. Multiple explanations were given for this observation, such as low cell surface expression of the receptor (even though CXCR4 expression in BC cells is high, the majority of the receptors might be present inside the cell where they are inaccessible for the radiotracer) and high expression of CXCR4 on cancer stem cells of which the number present in a tumor seems to differ between BC subtypes. Only 3 BC patients were included in this study and no information regarding hormone receptor status was provided. More investigations are therefore needed to determine the true value of targeting CXCR4 for theranostic purposes.

Once a suitable target has been selected, the question remains which radioligand to choose. Although the studies in this thesis did not primarily focus on selecting the best radioligand for targeting the studied biomarkers, it is worthwhile to

make a few remarks. A successful radioligand should have high affinity for its target, good in vivo stability, good tumor retention, as well as low uptake in and fast clearance from healthy organs. SSTR2 radioligands have been tested widely in the clinic for their application in neuroendocrine tumors. Currently several SSTR2 ligands, including DOTATATE, DOTANOC, DOTATOC and DTPA-octreotide, that can be labeled with different radionuclides are being applied (21). Concerning BC, our studies demonstrated that SSTR2 radioligands with antagonistic properties are more suitable, but these radioligands are not approved for clinical use yet. DOTATATE has the highest affinity for SSTR2 and can be labeled with ^{68}Ga for PET imaging (Somakit). Since PET imaging is currently the most sensitive nuclear based imaging method and high sensitivity is necessary to increase the chance of detecting tumors with low and heterogeneous target expression, ^{68}Ga-DOTATATE is the best radiotracer for SSTR2 targeted imaging. Furthermore, DOTATATE can also be labeled with ^{177}Lu for therapeutic purposes. For GRPR radioligands the situation is more complicated. Even though a number of radioligands are being explored, currently no GRPR radioligand is approved for clinical use. In this thesis 3 GRPR radioligands were used: radio-labeled AMBA, JMV4168 and NeoBOMB1. AMBA is a GRPR agonist, while JMV4168 and NeoBOMB1 are receptor antagonists. Since radiolabeled agonists might cause side effects when used for therapeutic purposes, it was reported that GRPR antagonists are more suited for therapy and theranostic purposes. In Chapter 9, we described the use of a novel GRPR antagonist, NeoBOMB1, which has excellent tumor targeting capacity, good tumor to background ratio and favorable pharmacokinetics making this radiopharmaceutical promising for theranostic applications. Application of this GRPR radioligand in BC patients has not been described, but results obtained in prostate cancer patients are promising (22). When results of preclinical studies using ^{177}Lu-NeoBOMB1 and ^{177}Lu-JMV4168 were compared, tumor dose and tumor to kidney ratio were more favorable for NeoBOMB1. Recently, another radiolabeled GRPR antagonist, ^{68}Ga-RM2, was applied for imaging purposes in BC patients, which resulted in successful visualization of primary tumors, lymph node lesions and bone metastasis (23).

Prospects Regarding Targeted Radionuclide Therapy of BC

The studies described in this thesis highlight the potential of targeted radionuclide therapy for treatment of BC in a preclinical setting. According to our studies GRPR and SSTR2 are expressed in 96% and 49% of breast tumors, respectively, emphasizing that targeting these receptors with radiotracers might be beneficial for a large group of BC patients in specific settings.

Targeted radionuclide therapy has not been studied in patients with BC yet. However, studies on treatment of neuroendocrine tumors treated with SSTR-targeting radiotracers reported stable disease and partial remissions in the majority of cases (24). Radionuclide therapy should first be tested in BC patients with refractory disease and if successful this method can also be considered for other patient groups. Also, the combination of targeted radionuclide therapy with another form of systemic therapy (either endocrine therapy, HER2-targeted therapy, or chemotherapy) might be beneficial. Although, combination treatment with SSTR2 or GRPR radiotracers and endocrine therapy, HER2-targeted or chemotherapy has not been investigated yet, studies in other cancer types showed promising results. One example is treatment with a combination of ^{177}Lu-DOTATATE and Capecitabine or Temozolomide, which resulted in an enhanced anti-tumor effect in neuroendocrine tumors (25).

Also, studies on radioresistance of BC cells have identified a few key players in this mechanism such as HER2 and the EGFR/PI3K/Akt pathways (26). These molecules exhibit at least a part of their radioresistance by facilitating DNA repair, enabling cells to survive DNA damage caused by radiation. These studies were mostly based on external beam radiation, but the acquired knowledge can be used in an attempt to avoid resistance against radionuclide therapy by combining the use of radiotracers with radiosensitizers such as lapatinib, a dual inhibitor of EGFR and HER2. A recent study by Nonnekens et al. (27) successfully combined ^{177}Lu-DOTATATE therapy with a DNA repair inhibitor, Olaparib, demonstrating the potential of this approach.

Concluding Remarks

To summarize, the studies described in this thesis identified BC subtypes suited for targeting of GRPR, SSTR2 and CXCR4, showed feasibility of targeting SSTR2 and GRPR in BC with radioligands in a preclinical setting and demonstrated the potential of radiolabeled SSTR2 antagonists for theranostic use of cancer including low SSTR-expressing cancers such as BC. Moreover, important in vivo characteristics of a novel GRPR radioligand were studied preclinically, delivering a basis for future clinical studies using this radiotracer.

In the section above we discussed that GRPR might be the more suitable target for ER-positive BC, since receptor expression is seen more frequently, at higher density, and more homogenously compared to that of SSTR2. One target does not serve all however and thus SSTR-targeting can still be beneficial in BC cases that lack GRPR. More studies are needed to determine whether there is sufficient cell surface expression of CXCR4 for tumor targeting, but if so this method can best be applied in ER-negative BCs. Since biomarker expression may change during treatment and disease progression, more research is needed to investigate the role of these events on target expression. Except for the studied biomarkers, other targets are being investigated for targeted-nuclear imaging and treatment. These radiotracers are suited for targeting of different BC subtypes and can be used for different purposes (e.g. disease monitoring and assessing of treatment response), depending on the target. A critical evaluation is needed to select the best target for a specific BC subtype and a specific purpose. Concerning therapy, future research should explore the use of therapeutic radioligands alone, as well as in combination with other treatment modalities currently used (e.g. endocrine treatment or chemotherapy) or radiosensitizers.

Using the theranostic approach in a personalized setting, targeting of GRPR, SSTR2 and CXCR4 with radioligands has the potential to play an important role in BC care, offering new possibilities for disease monitoring, pre-operative imaging, monitoring of therapy response, visualization of regional and distant metastases, intra-operative guidance and radionuclide therapy.

REFERENCES

1. Sorlie T, Perou CM, Tibshirani R, et al. Gene expression patterns of breast carcinomas distinguish tumor subclasses with clinical implications. Proc Natl Acad Sci U S A. 2001;98:10869-10874.
2. Perou CM, Sorlie T, Eisen MB, et al. Molecular portraits of human breast tumours. Nature. 2000;406:747-752.
3. Berry DA, Cronin KA, Plevritis SK, et al. Effect of screening and adjuvant therapy on mortality from breast cancer. N Engl J Med. 2005;353:1784-1792.
4. Yeung C, Hilton J, Clemons M, et al. Estrogen, progesterone, and HER2/neu receptor discordance between primary and metastatic breast tumours-a review. Cancer Metastasis Rev. 2016.
5. Kimura N, Takamatsu N, Yaoita Y, Osamura RY, Kimura N. Identification of transcriptional regulatory elements in the human somatostatin receptor sst2 promoter and regions including estrogen response element half-site for estrogen activation. J Mol Endocrinol. 2008;40:75-91.
6. Xu Y, Song J, Berelowitz M, Bruno JF. Estrogen regulates somatostatin receptor subtype 2 messenger ribonucleic acid expression in human breast cancer cells. Endocrinology. 1996;137:5634-5640.
7. Rivera JA, Alturaihi H, Kumar U. Differential regulation of somatostatin receptors 1 and 2 mRNA and protein expression by tamoxifen and estradiol in breast cancer cells. J Carcinog. 2005;4:10.
8. Murphy CG, Dickler MN. Endocrine resistance in hormone-responsive breast cancer: mechanisms and therapeutic strategies. Endocr Relat Cancer. 2016;23:R337-352.
9. Ali S, Coombes RC. Endocrine-responsive breast cancer and strategies for combating resistance. Nat Rev Cancer. 2002;2:101-112.
10. Wiebe VJ, Osborne CK, Fuqua SA, DeGregorio MW. Tamoxifen resistance in breast cancer. Crit Rev Oncol Hematol. 1993;14:173-188.
11. Clemons M, Danson S, Howell A. Tamoxifen ("Nolvadex"): a review. Cancer Treat Rev. 2002;28:165-180.
12. Yao ZX, Lu LJ, Wang RJ, et al. Discordance and clinical significance of ER, PR, and HER2 status between primary breast cancer and synchronous axillary lymph node metastasis. Med Oncol. 2014;31:798.
13. Theriault RL, Carlson RW, Allred C, et al. Breast cancer, version 3.2013: featured updates to the NCCN guidelines. J Natl Compr Canc Netw. 2013;11:753-760; quiz 761.
14. Reubi C, Gugger M, Waser B. Co-expressed peptide receptors in breast cancer as a molecular basis for in vivo multireceptor tumour targeting. Eur J Nucl Med Mol Imaging. 2002;29:855-862.
15. Sandstrom M, Velikyan I, Garske-Roman U, et al. Comparative biodistribution and radiation dosimetry of 68Ga-DOTATOC and 68Ga-DOTATATE in patients with neuroendocrine tumors. J Nucl Med. 2013;54:1755-1759.
16. Moradi F, Jamali M, Barkhodari A, et al. Spectrum of 68Ga-DOTA TATE Uptake in Patients With Neuroendocrine Tumors. Clin Nucl Med. 2016;41:e281-287.
17. Forrer F, Krenning EP, Kooij PP, et al. Bone marrow dosimetry in peptide receptor radionuclide therapy with [177Lu-DOTA(0),Tyr(3)]octreotate. Eur J Nucl Med Mol Imaging. 2009;36:1138-1146.
18. Maina T, Bergsma H, Kulkarni HR, et al. Preclinical and first clinical experience with the gastrin-releasing peptide receptor-antagonist [(6)(8)Ga]SB3 and PET/CT. Eur J Nucl Med Mol Imaging. 2016;43:964-973.
19. Minamimoto R, Hancock S, Schneider B, et al. Pilot Comparison of (6)(8)Ga-RM2 PET and (6)(8)Ga-PSMA-11 PET in Patients with Biochemically Recurrent Prostate Cancer. J Nucl Med. 2016;57:557-562.
20. Vag T, Gerngross C, Herhaus P, et al. First Experience with Chemokine Receptor CXCR4-Targeted PET Imaging of Patients with Solid Cancers. J Nucl Med. 2016;57:741-746.
21. Mikolajczak R, Maecke HR. Radiopharmaceuticals for somatostatin receptor imaging. Nucl Med Rev Cent East Eur. 2016;19:126-132.
22. Nock BA, Kaloudi A, Lymperis E, et al. Theranostic perspectives in prostate cancer with the GRPR-antagonist NeoBOMB1-Preclinical and first clinical results. J Nucl Med. 2016.
23. Stoykow C, Erbes T, Maecke HR, et al. Gastrin-releasing Peptide Receptor Imaging in Breast Cancer Using the Receptor Antagonist (68)Ga-RM2 And PET. Theranostics. 2016;6:1641-1650.
24. Horsch D, Ezziddin S, Haug A, et al. Effectiveness and side-effects of peptide receptor radionuclide therapy for neuroendocrine neoplasms in Germany: A multi-institutional registry study with prospective follow-up. Eur J Cancer. 2016;58:41-51.
25. Claringbold PG, Turner JH. Pancreatic Neuroendocrine Tumor Control: Durable Objective Response to Combination 177Lu-Octreotate-Capecitabine-Temozolomide Radiopeptide Chemotherapy. Neuroendocrinology. 2016;103:432-439.
26. Kaidar-Person O, Lai C, Kuten A, Belkacemi Y. "The Infinite Maze" of breast cancer, signaling pathways and radioresistance. Breast. 2013;22:411-418.
27. Nonnekens J, van Kranenburg M, Beerens CE, et al. Potentiation of Peptide Receptor Radionuclide Therapy by the PARP Inhibitor Olaparib. Theranostics. 2016;6:1821-1832.

Samenvatting

SAMENVATTING

Borstkanker is op één na de meest voorkomende kanker in de wereld en de meest voorkomende kankersoort bij vrouwen. De ziekte is erg heterogeen en bestaat uit verschillende subtypen, die bepalend zijn voor de behandeling en prognose. Verschillende beeldvormingstechnieken (zoals mammografie) en behandelingsmethoden (zoals chirurgie, radiotherapie, hormoon behandeling en chemotherapie) voor borstkanker zijn ontwikkeld en beschikbaar, deze hebben een positief effect gehad op het ziekteverloop. De beeldvormingstechnieken en behandelingsmethoden die momenteel gebruikt worden in de kliniek hebben echter nog steeds een aantal beperkingen en het sterftecijfer als gevolg van de ziekte is helaas nog steeds hoog. Het doel van de studies beschreven in dit proefschrift is het bestuderen van het gebruik van nieuwe radiofarmaca (radiotracers) voor beeldvorming (imaging) en behandeling (radionuclidentherapie) van borstkanker.

In **Hoofdstuk 1** van het proefschrift wordt borstkanker beschreven, inclusief de karakteristieken van de ziekte en de momenteel toegepaste beeldvormingstechnieken en behandelingsmethoden. Vervolgens worden nucleair geneeskundige beeldvormingstechnieken en therapieën beschreven. De nucleaire beeldvormingstechnieken die momenteel klinisch worden toegepast voor het in beeld brengen van borstkanker (bijvoorbeeld ^{18}F-FDG PET) worden eerst genoemd, gevolgd door de introductie van een specifiekere methode die toegepast kan worden voor borstkanker imaging. Deze specifiekere methode is gebaseerd op het gebruik van radiogelabelde tracers die specifiek gericht zijn tegen moleculaire eiwitten die tot (over)expressie komen op kankercellen en niet of in veel mindere mate op gezonde/normale cellen. Afhankelijk van het radionuclide waarmee deze tracers gelabeld zijn, kunnen de radiotracers ook gebruikt worden voor therapeutische doeleinden. Met betrekking tot het laatstgenoemde, wordt het theranostisch concept (het gebruik van dezelfde tracer voor zowel beeldvorming als therapie) uitgelegd en wordt er een lijst gegeven van radionucliden die hiervoor gebruikt kunnen worden. Moleculaire eiwitten die kunnen dienen als doelwitten voor radiotracers worden besproken met de nadruk op de “somatostatine receptor subtype 2 (SSTR2)”, de “gastrin releasing peptide receptor (GRPR)” en de “C-X-C chemokine receptor type 4 (CXCR4)”. Tenslotte worden de potentiele voordelen van deze doelwit-gemedieerde nucleaire beeldvormingstechnieken en radionuclidentherapie besproken. **Hoofdstuk 2** geeft een overzicht van de moleculaire eiwitten die momenteel worden onderzocht in preklinische en klinische studies voor doelwit-gemedieerde nucleaire beeldvorming en bespreekt de (potentiele) voordelen van de verschillende benaderingen. Een aantal moleculaire eiwitten wordt bestudeerd als potentieel doelwit, inclusief de eerder genoemde SSTR2, GRPR en CXCR4, maar ook hormoonreceptoren en de “human epidermal growth factor receptor 2”. Deze doelwitten komen niet voor op alle borstkanker subtypen en radiotracers gericht tegen deze moleculaire eiwitten kunnen gebruikt worden voor verschillende doeleinden. De heterogeniteit van borstkanker vraagt om een persoonsgerichte benadering, waarbij indien doelwit-gemedieerde nucleaire middelen hun toepassing vinden in de dagelijkse

praktijk er een zorgvuldige afweging moet worden gemaakt voordat een radiotracer gericht tegen een specifiek doelwit wordt gekozen. Hierbij moeten de voordelen en beperkingen van de verschillende methoden goed in acht worden genomen.

In het tweede gedeelte van het proefschrift ligt de focus op de klinische relevantie van SSTR2, GRPR en CXCR4-gemedieerde imaging en therapie bij borstkanker patiënten met als voornaamste doel het identificeren van borstkanker patiëntengroepen en doeleinden geschikt voor de applicatie van deze methoden. In **Hoofdstuk 3** worden *SSTR2*, *GRPR* en *CXCR4* mRNA expressie levels van 915 primaire borsttumoren gecorreleerd aan klinisch-pathologische factoren, biologische factoren en prognose. Om aan te tonen dat mRNA expressie representatief is voor radiotracer binding aan tumor celen, is voorafgaand in een kleine set borsttumoren eiwitexpressie van SSTR2 en GRPR gemeten door middel van autoradiografie studies. De resultaten van de autoradiografie studies zijn gecorreleerd aan mRNA expressie, resulterend in significante correlaties. Hieruit hebben wij geconcludeerd dat *SSTR2* en *GRPR* mRNA expressie representatief was voor SSTR2 en GRPR eiwitexpressie. Helaas was het voor CXCR4 niet mogelijk een dergelijke correlatie aan te tonen door gebrek aan een geschikte radiotracer, maar eerder gepubliceerde studies toonden aan dat *CXCR4* mRNA expressie ook representatief is voor CXCR4 eiwitexpressie. De correlatie van *SSTR2*, *GRPR* en *CXCR4* mRNA expressie met borstkanker karakteristieken toonde aan dat oestrogeen receptor (ER)-positieve tumoren het meest geschikt zijn voor SSTR2 en GRPR-gerichte imaging en therapie, terwijl CXCR4 juist in ER-negatieve tumoren een toepassing zal hebben omdat het in deze borstkanker subgroep op mRNA niveau het hoogst tot expressie komt. Met betrekking tot prognose, was een hoge *CXCR4* expressie geassocieerd met een betere ziektevrije- , metastasevrije- en totale overleving. Deze laatste bevinding was onverwacht omdat hoge CXCR4 expressie geassocieerd is met ER-negatieve tumoren, de meeste agressieve borsttumoren. Een mogelijke verklaring is dat er een andere factor is, onafhankelijk van ER expressie, die bepalend is voor een goede prognose van deze patiënten groep. *SSTR2* expressie was niet significant geassocieerd met prognose terwijl hoge *GRPR* mRNA expressie levels waren geassocieerd met een verlengde progressie vrije overleving na behandeling met hormoon therapie met tamoxifen. Uitgezaaide borstkanker is ongeneeslijk, de uitzaaiingen vormen de voornaamste reden voor sterfte als gevolg van de ziekte. Derhalve zijn betere visualisatie en betere behandelingsopties van borstkankermetastasen heel belangrijk om de kwaliteit van leven ten gevolge van de ziekte te verbeteren. In **Hoofdstuk 4** hebben wij *SSTR2*, *GRPR* en *CXCR4* mRNA expressie van 60 primaire borsttumoren en bijbehorende metastasen (zowel metastasen in regionale lymfeklieren als afstandsmetastasen in onder andere de hersenen, longen, lever en eierstokken) onderzocht. mRNA expressie levels van primaire tumoren en gepaarde metastasen zijn met elkaar vergeleken, wat resulteerde in vergelijkbare *GRPR* en *CXCR4* mRNA expressie niveaus van primaire tumoren en bijbehorende metastasen. Echter, *SSTR2* mRNA expressie in lever- en eierstok metastasen was significant lager dan dat in de primaire tumoren ($P=0.02$ en $P=0.03$, respectievelijk). Bovendien was hoge *SSTR2* en *GRPR* expressie geassocieerd met ER-positieve tumoren en hoge *CXCR4* expressie met ER-negatieve tumoren. Dit is in overeenstemming met hetgeen gevonden in Hoofdstuk 3. In een enkele gevallen was ER-status van de primaire tumor niet gelijk aan de ER-status van de gepaarde metastase. Dit verschil in ER-status was van invloed op de *SSTR2* en *GRPR* expressie, waarbij de *SSTR2* en *GRPR* expressie de ER-status van de metastase lijkt te volgen. Een discrepantie in ER-expressie tussen primaire tumoren en metastasen komt in ongeveer 14% van de borstkanker patiënten voor en de daarmee gepaarde verandering in *GRPR* expressie moet in gedachte worden gehouden als GRPR als doelwit wordt gebruikt voor imaging en/of therapie. Op basis van deze bevindingen hebben wij geconcludeerd dat SSTR2, GRPR en CXCR4 goede doelwitten zijn voor theranostische doeleinden in zowel primaire als uitgezaaide borstkankers, waarbij gezegd moet worden dat het borstkankersubtype in acht moet worden genomen bij de keuze van het doeleiwit.

In het volgende gedeelte van het proefschrift ligt de focus op SSTR2-gemedieerde imaging van borstkanker. **Hoofdstuk 5** is een review van eerder gepubliceerde klinische studies over SSTR2-gemedieerde imaging van borstkanker, waarvan het merendeel van de studies meer dan 10 jaar geleden is uitgevoerd. Het doel van de review was het kritisch analyseren van de methoden, bevindingen en beperkingen van deze klinische studies, om zodoende te bepalen of de recentere ontwikkelingen op het gebied van nucleaire geneeskunde kunnen leiden tot verbetering van de resultaten. Samenvoeging van de resultaten van de geanalyseerde studies resulteerde in een sensitiviteit van 36-100% en een specificiteit van 22-100% voor SSTR2-gemedieerde borstkanker imaging. De voornaamste beperking van eerder gerapporteerde studies was een lage en heterogene SSTR2-expressie in de tumoren. Planaire beeldvorming was de voornaamste beeldvormingstechniek gebruikt in deze vroege studies, octreotide of depreotide werd gebruikt als somatostatine analoog en er werd geen onderscheid gemaakt tussen de verschillende borstkanker subtypen. Er is veel ontwikkeling geweest op het gebied van beeldvormingstechnieken (bijvoorbeeld SPECT, PET of de daarvan afgeleide toegewijde mamma camera's) en somatostatine-analoga (receptor-agonisten en receptor-antagonisten met hogere affiniteit voor de SSTR2). Voorts is de kennis over SSTR2-expressie in relatie tot de verschillende borstkanker subtypen toegenomen. Deze ontwikkelingen kunnen SSTR2-gemedieerde borstkanker-imaging gunstig beïnvloeden. Derhalve is nieuw onderzoek nodig met toepassing van de nu beschikbare kennis en technieken. Als SSTR2-gemedieerde imaging van borstkanker succesvol blijkt, kan deze methode ook gebruikt worden voor therapie. Één van de ontwikkelingen op het gebied van SSTR2-gemedieerde imaging is het gebruik van SSTR2 antagonisten. Uit recente preklinische en klinische studies blijkt dat SSTR2 antagonisten beter zijn dan SSTR2 agonisten voor het in beeld brengen van SSTR2-positieve tumoren, ondanks de accumulatie van SSTR2 agonisten in kankercellen. Dit verschijnsel wordt verklaard door het vermogen van de antagonist om te binden aan meer bindingsplaatsen/receptoren dan de agonist. Omdat lage en heterogene SSTR2 expressie een beper-

kende factor is voor succesvolle SSTR2-gemedieerde imaging kan de applicatie van radiogelabelde SSTR2 antagonisten gunstig zijn. In **Hoofdstuk 6** hebben we het gebruik van een SSTR2-agonist, Tyr^3-DOTA-octreotate, en een SSTR2-antagonist, DOTA-JR11, vergeleken in 40 humane borstkankerweefsels en in een orthotoop borstkankermuismodel. Binding van ^{111}In-DOTA-JR11 aan de borstkankerweefsels was significant hoger ($P<0.001$) dan dat van ^{111}In-DOTA-Tyr^3-octreotaat. De verhouding antagonist- vs. agonist-binding verhield zich van 1 (slechts in 1 geval aangetoond) staat tot 57. SPECT/MR imaging studies in het muismodel resulteerde in een betere tumor visualisatie na injectie van de antagonist ^{177}Lu-DOTA-JR11 vs. de agonist ^{177}Lu-DOTA-Tyr^3-octreotaat. De resultaten van biodistributie studies, uitgevoerd na het scannen, bevestigde een hogere opname van de antagonist in de tumorweefsel. Deze resultaten leidden tot de conclusie dat SSTR2 antagonisten zoals DOTA-JR11, SSTR2-gemedieerde borstkanker-imaging kunnen verbeteren en potentieel ook gebruikt kunnen worden voor therapie doeleinden. Studies hebben bewezen dat radiogelabelde SSTR2-antagonisten beter zijn voor imaging doeleinden, maar over de toepassing van SSTR2-antagonisten voor therapie is nog weinig bekend. Een groot voordeel van deze radiotracers is dat ze voor zowel imaging en therapie gebruikt kunnen worden. Daarom hebben wij in **Hoofdstuk 7** het gebruik van ^{77}Lu-DOTA-JR11 en ^{177}Lu-DOTA-octreotaat voor therapie doeleinden vergeleken in een preklinische setting. Hiervoor hebben wij in vitro opname studies en DNA schade-analyses (53BP1 is gebruikt als indirecte meting voor DNA schade) gedaan in een cellijn getransfecteerd met de SSTR2 (U2OS+SSTR2). Verder hebben wij in vivo therapie experimenten gedaan in Balb c muizen met H69 (een SSTR2-positieve long kanker cellijn) xenograft tumoren. De gemeten opname van de antagonist in U2OS+SSTR2 cellen was 5 keer hoger dan die van de agonist en de DNA schade veroorzaakt door ^{177}Lu-DOTA-JR11 was 2 keer hoger dan die veroorzaakt door ^{177}Lu-DOTA-Tyr^3-octreotaat. In vivo therapie studies na injectie van de optimale peptide hoeveelheid van de radiotracers resulteerde in een langere tijd tussen de start van de therapie en tumor hergroei. Voorts was er een betere mediane overleving na therapeutische injectie van^{177}Lu-DOTA-JR11 in vergelijking met ^{177}Lu-DOTA-Tyr^3-octreotaat. De bovengenoemde bevindingen leidden tot de conclusie dat SSTR2-antagonisten beter zijn dan SSTR2-agonisten voor zowel imaging als behandeling. Dit is vooral interessant voor kankersoorten met een relatief lage SSTR2-expressie zoals borstkanker.

De laatste sectie van het proefschrift heeft als focus de applicatie van GRPR-radiotracers voor theranostische doeleinden. In **Hoofdstuk 8** is de applicatie van GRPR-radioliganden voor imaging en therapie van borstkanker bestudeerd in een preklinische setting. Allereerst is de binding van een radiogelabeld GRPR-agonist, ^{11}In-AMBA, aan 50 humane borstkanker weefsels geanalyseerd en geassocieerd met ER-expressie van de tumoren. De radiotracer kon aan de meerderheid (96%) van de tumoren binden, wat impliceert dat deze tumoren GRPR tot expressie brengen. De binding van de radiotracer was positief gecorreleerd met ER-expressie. Vervolgens is dezelfde radiotracer gebruikt in in vitro opname studies voor het bepalen van GRPR-expressie van 10 borstkankercellijnen. De meerderheid van de cellijnen lieten opname van de radiotracer zien. De 2 cellijnen met de hoogste radiotracer opname, T47D en MCF7 (beide ER positief) zijn gebruikt voor vervolg studies. T47D is gebruik voor in vitro studies, waarbij de cellijn is behandeld met verschillende concentraties ^{177}Lu-AMBA, resulterend in een significante vermindering (tot aan 80%) van het aantal cellen na behandeling. Dit effect van de radiotracer op de cellen werd niet waargenomen na incubatie met het radionuclide alleen of met het niet radiogelabeld ligand. Ook zijn er in vivo biodistributie- en imaging studies gedaan bij muizen na subcutane en orthotope inoculatie met T47D- of MCF7-cellen. Na tumorvorming zijn de muizen geïnjecteerd met een GRPR antagonist, ^{111}In-JMV4168 + phosphoramidon (een enzymremmer die afbraak van het radioligand tegen gaat), en is een SPECT scan gemaakt. Zowel T47D- als MCF7-tumoren waren duidelijk zichtbaar op de scan, maar opname was hoger in T47D- ten opzichte van MCF7-tumoren. De hogere opname in T47D-xenografts werd bevestigd in biodistributie studies. Op basis van bovengenoemde resultaten concluderen wij dat GRPR radioliganden veelbelovend zijn voor nucleaire beeldvorming en therapie van GRPR-positieve borsttumoren. In het laatste hoofdstuk (**Hoofdstuk 9**) is het gebruik van een nieuwe GRPR-radiotracer, NeoBOMB1, getest voor theranostische doeleinden. In 2 in vivo studies, uitgevoerd in een prostaatkanker (PC3) xenograft muismodel, is de biodistributie van ^{177}Lu- en ^{68}Ga-gelabeld NeoBOMB1 getest. Ook zijn er imaging studies (zowel SPECT en PET) uitgevoerd na injectie van de radiotracers. De verworven data zijn gebruikt om de farmacokinetiek, muizendosimetrie en patiëntendosimetrie te voorspellen. In het geval van ^{177}Lu-NeoBOMB1 is het gebruik van 2 verschillende peptiden hoeveelheden (10 pmol en 200 pmol) met elkaar vergeleken om de peptide hoeveelheid te vinden met de ideale verhouding tussen tumor opname ten opzichte van opname in andere organen. De opname van zowel ^{68}Ga-NeoBOMB1- als ^{177}Lu-NeoBOMB1 in tumoren was goed. Radiotracer-opname was ook te zien in de GRPR-positieve pancreas en in de nieren. Het laatste als gevolg van renale uitscheiding van de radiotracers. Radiotracer klaring uit de pancreas en de nieren verliep relatief snel, terwijl de tumor-opname langer behouden bleef. Met betrekking tot de 2 verschillende hoeveelheden ^{177}Lu-NeoBOMB1 die getest werden, resulteerde de hogere peptide dosis in een betere biodistributie (een hogere tumor opname en een lagere opname in andere organen) dan de lage peptidemassa. Zoals verwacht op basis van bovenstaande resultaten, resulteerde dit in een hoge radionuclidedosis in de tumor en een lagere dosis in overige organen. De waarden verkregen na voorspelling van de patiëntendosimetrie waren vergelijkbaar met de waarden gerapporteerd voor de klinisch succesvol gebruikte ^{177}Lu-DOTA-Tyr^3-octreotaat. De SPECT en PET imaging studies resulteerden in goed zichtbare tumoren op de scans. Gebaseerd op de verkregen data concluderen we dat zowel ^{68}Ga-NeoBOMB1 en ^{177}Lu-NeoBOMB1 uitstekende tumor-opname en goede farmacokinetische eigenschappen hebben voor theranostisch gebruik. Hoewel deze studies in een prostaatkanker-model zijn uitgevoerd, zijn de bevindingen ook veelbelovend voor applicatie van de radiotracer voor imaging en therapie van borstkanker.

Curriculum Vitae

Simone Ursula Dalm was born on February 26, 1987 in Paramaribo, Suriname. At the age of 15 she moved to The Netherlands with her parents, where she completed her pre-university secondary education at the Baken Park Lyceum in Almere in 2006. Afterwards she started her Bachelor studies in Biomedical Sciences at the VU University in Amsterdam. During this period she did a 3-month internship focused on targeting of 14-3-3 proteins expressed in cancer cells using an organic compound called Fusicoccin. During her bachelor studies and in particular during the above-mentioned internship, her interest in cancer research grew. In 2009 she obtained her Bachelor's degree and started her Master studies titled Master in Oncology also at the VU University in Amsterdam.
During the first year of her Masters education she did a master research training at the department of Otoloryngology-Head and Neck surgery at the Cancer Center Amsterdam which is part of the VU Medical Center. This research, supervised by Prof.dr. Ruud Brakenhoff, was focused on the identification of genes responsible for sensitization to and accumulation of cisplatin in head and neck cancer cell lines. To combine her interest for travelling and research she did her second master internship abroad at the Northern Institute for Cancer Research, Newcastle University. For a period of 6 months she worked on a project titled "Studies on the mechanism of cisplatin potentiation by NU2058, a potent cdk2 inhibitor" at the Department of Drug Discovery and Imaging under supervision of Prof.dr. Herbie Newell. Early 2012 she completed her Master's degree.
To continue her passion for research, especially cancer research, she started a PhD study in 2012 at the department of Nuclear Medicine (now Radiology & Nuclear Medicine) of the Erasmus MC, Rotterdam. Here she learned about nuclear medicine research and successfully combined her knowledge of and previous experience with oncology related research with this interesting discipline. Her PhD project, which was focused on the application of radiotracers for breast cancer imaging and treatment, was performed in collaboration with the department of Pathology and the department of Medical Oncology. This interdisciplinary project was carried out under supervision of Prof.dr. Marion de Jong, Dr. Marleen Melis, Dr. Carolien van Deurzen and Dr. John Martens. During her PhD studies she obtained 2 Alavi-Mandell Publication Awards from the Society of Nuclear Medicine and a 2nd place poster prize at the Pathology Days, organized by the Dutch Pathology Association.

List of Publications

Publications Relevant To This Thesis

Dalm SU, Schrijver WAME, Sieuwerts AM, Look MP, Ziel-van der Made ACJ, de Weerd M, Martens JW, van Diest PJ, de Jong M, Deurzen CHM. **Prospect of Targeting the Gastrin Releasing Peptide Receptor, Chemokine C-X-C Motif Receptor 4 and Somatostatin Receptor 2 for Nuclear Imaging and Therapy in Metastatic Breast Cancer.** PLOS ONE, Accepted: January 2017

Dalm SU, Bakker IL, de Blois E, Doeswijk GN, Konijnenberg MW, Orlandi F, Barbato D, Tedesco M, Maina T, Nock BA, de Jong M. **^{68}Ga/^{177}Lu-NeoBOMB1, a Novel Radiolabeled GRPR Antagonist for Theranostic Use in Oncology.** J Nucl Med (September 2016) [epub].

Dalm SU, Melis M, Emmering J, Kwekkeboom DJ, de Jong M. **Breast Cancer Imaging Using Radiolabelled Somatostatin Analogues.** Nucl Med Biol. 43(9):559-65 (2016)

Dalm SU, Nonnekens J, Doeswijk GN, de Blois E, van Gent DC, Konijnenberg MW, de Jong M. **Comparison of Therapeutic Response to Treatment with a ^{177}Lu-labeled Somatostatin Receptor Agonist and Antagonist in Preclinical Models.** J Nucl Med. 57(2):260-5 (2016)

Dalm SU, Sieuwerts AM, Look MP, Melis M, van Deurzen CH, Foekens JA, de Jong M, Martens JW. **Clinical Relevance of Targeting the Gastrin-releasing Peptide Receptor, Somatostatin Receptor 2, or Chemokine C-X-C Motif Receptor 4 in Breast Cancer for Imaging and Therapy.** J Nucl Med. 56(10):1487-93 (2015)

Dalm SU, Martens JW, Sieuwerts AM, van Deurzen CH, Koelwijn SJ, de Blois E, Maina T, Nock BA, Brunel L, Fehrents JA, Martinez J, de Jong M, Melis M. **In Vitro and In Vivo Application of Radiolabeled Gastrin-releasing Peptide Receptor Ligands in Breast Cancer.** J Nucl Med. 56(5):752-7 (2015)

Manuscripts Under Review

Dalm SU, Haeck J, Doeswijk GN, de Blois E, de Jong M, Deurzen CHM. **Short communication: SSTR-mediated Breast Cancer Imaging, Is There a Role for Radiolabeled SSTR Antagonists?** J Nucl Med, Submitted: September 2016

Dalm SU, Verzijlbergen JF, de Jong M. **Review: Targeted Nuclear Imaging of Breast Cancer.** Int. J. Mol. Sci, Submitted: September 2016

Other Publications

Martens-de Kemp SR, **Dalm SU**, Wijnolts FM, Brink A, Honeywell RJ, Peters GJ, Braakhuis BJ, Brakenhoff RH. **DNA-bound platinum is the Major Determinant of Cisplatin Sensitivity in Head and Neck Squamous Carcinoma Cells.** PLOS ONE. 8(4):e61555 (2013).

Conference presentations

Dalm SU, Bakker IL et al. **NeoBOMB1, a Novel GRP Analog, for Theranostic Use in Oncology.** Oral presentation delivered at the annual congress of European Association of Nuclear Medicine (EANM), Oct 2016, Barcelona, Spain.

Dalm SU, Schrijver WA et al. **Prospects of Targeting the Gastrin Releasing Peptide Receptor, the Chemokine C-X-C Motif Receptor 4 and the Somatostatin Receptor Subtype 2 in Primary Breast Cancer and Metastases.** Oral presentation delivered at the EANM, Oct 2016, Barcelona, Spain.

Dalm SU, Haeck J et al. **The Use of Somatostain Receptor Antagonists May Provide a Role for Receptor-mediated Nuclear Imaging and Therapy of Breast Cancer.** Oral presentation delivered at the EANM, Oct 2016, Barcelona, Spain). *Presentation was part of the Rapid Fire Session, a session dedicated to the top 10 abstracts within the M2M track.*

Dalm SU, Bakker IL et al. **^{68}Ga/^{177}Lu-NeoBOMB1, a Novel Radiolabeled GRPR Antagonsist for Theranostic Use.** Oral presentation delivered at the annual meeting of the Society of Nuclear Medicine and Molecular Imaging, June 2016, San Diego, USA.

Dalm SU, Schrijver WA et al. **Prospects of Targeting the Gastrin Releasing Peptide Receptor and the Somatostatin Receptor Subtype 2 in Primary Breast Cancer and Metastases.** Elevator Pitch and Poster presentation at the Pathology Days organized by the Dutch Pathology Society (NVVP), April 2016, Zeist, The Netherlands. *Second prize winner.*

Dalm SU, Nonnekens J et al. **Radiolabeled SSTR2 Agonist Versus Antagonist For Therapeutic Application.** Oral presentation delivered at the European Congress of Radiology, March 2016, Vienna, Austria.

Dalm SU, Doeswijk GN et al. **Preclinical Comparison of Therapeutic Response to Treatment with 177-Lutetium Labelled Somatostatin Receptor Agonists and Antagonists.** Oral presentation delivered at the EANM, Oct 2015, Hamburg, Germany.

Dalm SU, Sieuwerts AM et al. **Clinical Relevance of Targeting SSTR2, GRPR and CXCR4 with Radioligands for Imaging and Therapy in Breast Cancer.** Oral presentation delivered at the EANM, Oct 2015, Hamburg, Germany. *This work was mentioned in the congress highlights.*

Dalm SU. Preclinical Comparison of Therapeutic and Cellular Response to Treatment with Somatostatin Receptor Agonists and Antagonists. Oral presentation selected for the Young Investigators Meeting of the EANM, Vienna, Austria, July 2015.

Dalm SU, de Jong M et. al. **A Relevant In Vitro Model and In Vivo Mouse Model for Imaging and Therapy Using Radiolabeled GRP Analogues in Breast Cancer.** Oral presentation delivered at the EANM, Oct 2014, Gothenburg, Sweden.

Dalm SU, Sieuwerts AM et al. **GRP-R Expression in Breast Cancer As a Target for Nuclear Imaging and Therapy; Correlation with ER.** Oral presentation delivered at the EANM, Oct 2013, Lyon, France.

PhD Portfolio

Name PhD Student: Simone Dalm
Erasmus MC Departments: Radiology & Nuclear Medicine
Research School: Molecular Medicine
Promotor: Prof.dr. ir. M. de Jong
Co-promotors: Dr. J.W.M. Martens, Dr. C.H.M. van Deurzen

Courses	Year	ECTS
Radiation safety, level 5B	2012	1.0
Article 9 course (Laboratory animal science)	2012	4.0
Endnote	2013	0.3
Research Management for PhD Students	2014	0.6
Masterclass: Writing a competitive VENI proposal, Dutch NWO Talent Scheme	2016	0.3

Workshops	Year	ECTS
Molecular Medicine Day	2014	0.3
EANM Young investigator's Meeting	2015	1
Pathology days 2016, NVVP, Zeist	2016	1.25
NKRV workshop (Amsterdam and Rotterdam)	2014-2015	0.6
Nuclear Medicine Research Meetings	2012-2016	1
JNI Meetings	2012-2016	0.3
Pathology Meetings	2012-2016	0.3
Medical Oncology Research Meeting	2012-2016	0.3

International conferences	Year	ECTS
EANM Annual Congress 2013, Lyon France	2013	1.25
EANM Annual Congress 2014, Gothenburg, Sweden	2014	1.25
EANM Annual Congress 2015, Hamburg, Germany	2015	1.25
ECR Annual Congress 2016, Vienna, Austria	2016	1.25
SNMMI Annual Congress 2016, San Diego, USA	2016	1.25
EANM Annual Congress 2016, Barcelona, Spain	2016	1.25

Teaching activities and others tasks	Year	ECTS
Supervising trainees	2013-2014	10
Journal clubs Nuclear Medicine	2012-2016	1
Organizing committee Erasmus MC PhD day	2014-2015	0.5
Organizing committee Symposium "Novel Options for Cancer Imaging: Focus on Urological Tumors"	2016	0.3

Peer-review activities	Year	ECTS
Theranostics	2015-2016	0.3
Total		**30.85**

Dankwoord

"Unity is strength… where there is teamwork and collaboration, wonderful things can be achieved."- M. Stepanek

Dit proefschrift is het resultaat van hard werken, toewijding en passie voor het onderzoek. Het succesvol afronden van mijn PhD is een leerrijke en uitdagende ervaring geweest. Hetgeen niet mogelijk zou zijn zonder steun en hulp van velen. Hierbij wil ik van de gelegenheid gebruik maken om eenieder die mij gesteund heeft te bedanken.

Allereerst mijn promotor, Prof. dr. Marion de Jong. Beste Marion, bedankt voor de mogelijkheid om mijn promotie onderzoek binnen jouw preklinische groep te doen. Ik ben trots dat ik mag promoveren met jou als promotor en deel mag uitmaken van het preklinisch team van de afdeling Radiologie & Nucleaire Geneeskunde. Als pas afgestudeerde wetenschapper gaf jij mij de mogelijkheid om de nodige trainingen te volgen en mijzelf te ontplooien. Bedankt voor het vertrouwen, voor alle steun en motivatie. Ook wil ik je bedanken voor de persoonlijke gesprekken die soms nodig waren om mij te inspireren of om mij weer stevig met beide benen op de grond te zetten. Jij hebt mij tal van mogelijkheden gegeven — nu nog steeds — waar ik je enorm dankbaar voor ben. Ik heb veel van je geleerd en hoop nog heel veel van je te mogen leren.

Ik wil ook Dr. Carolien van Deurzen en Dr. John Martens, mijn co-promotoren, bedanken voor alle mogelijkheden, het vertrouwen en de steun die zij mij gegeven hebben. Mijn PhD project was een samenwerking tussen 3 afdelingen en de succesvolle afronding ervan zou niet mogelijk zijn zonder volledige inzet van alle 3 partijen. John, wij spreken elkaar niet op zeer regelmatige basis maar als ik ergens hulp bij nodig heb kan ik altijd bij jou terecht. Je weet mij altijd aan de juiste mensen te koppelen binnen jou afdeling om een experiment of vraagstuk op te lossen en dat heeft zijn vruchten geworpen. Carolien, wat heb jij mij veel geleerd over de pathologie van borstkanker, dank daarvoor! Het is heel fijn samenwerken met jou. Ik heb jou leren kennen als een gedisciplineerd en gedreven persoon, waar ik een voorbeeld aan neem. Ook dank voor alle fijne gesprekken die niet werk-gerelateerd waren.

Dr. Marleen Melis, beste Marleen zonder jou goede begeleiding in het eerste jaar van mijn PhD zou ik het proefschrift nooit zo goed hebben afgerond. Dank je wel voor alles wat jij mij geleerd hebt. Ik vind het bewonderingswaardig hoe jij je hart volgt en doet waar jij je goed bij voelt. Bedankt voor alle interesse die je desondanks je carriere-switch toont in mijn onderzoek en in mij als persoon.

Prof. dr. Fred Verzijlbergen en Prof. dr. Gabriel Krestin bedankt voor de mogelijkheid om mijn PhD project op de afdeling Radiologie & Nucleaire Geneeskunde te mogen uitvoeren. Prof. dr. Fred Verzijlbergen bedankt voor alle tijd die u heeft besteed aan het artikel dat wij samen hebben geschreven. Prof. dr. Grabiel Krestin bedankt voor het geloof en vertrouwen en de daaruit voortkomende mogelijkheid om mijn wetenschappelijke carrière voort te zetten op de afdeling.

Ik wil alle collega's bedanken van de afdeling Radiologie & Nucleaire Geneeskunde, de afdeling Pathologie en de afdeling Medische Oncologie voor alle hulp en een prettige werksfeer. In het bijzonder de collega's waar ik nauw mee heb samengewerkt:

Prof.dr. Dik Kwekkeboom bedankt voor alle tijd en moeite die u gestopt heeft in het lezen van mijn artikel en het geven van feedback.

Ingrid, Costanza, Sandra, Kristell, Hendrik, Tessa, Wouter en Daan bedankt voor het zijn van gezellige kamergenootjes, het bieden van een luisterend oor als het even niet mee zit en het meedenken wanneer dat nodig is. Bedankt voor de gezelligheid tijdens etentjes en borrels en voor het nooit opgeven met vragen of ik ook een koekje of chocolade wil ;-).

Gaby, Stuart, Linda en Saskia, dank jullie wel voor de hulp en het meedenken tijdens de experimenten en voor de gezelligheid in en buiten het lab. Gaby, bedankt dat ik altijd op je kan rekenen bij het uitvoeren van experimenten.

Mark, Monique, Joost, Jan, Sander, Marcel, Eric, Stefan en Julie bedankt voor de fijne werksfeer, de goede werk discussies, het fijne samenwerken en de gezelligheid tijdens borrels en andere uitjes. Mark, bedankt voor alle begeleiding en geduld rondom de dosimetrie vraagstukken en experimenten.

Ook de radiochemie groep, Erik, Rory, Ho Sze en Wout, wil ik bedanken voor de inspirerende overleggen, alle labelingen en de fijne werksfeer. Erik en Rory bedankt voor het klaarstaan en de flexibiliteit, vooral tijdens het NeoBOMB1 project heb ik veel aan jullie steun gehad.

Sally en Evelien, mijn 2 stagiares, bedankt voor jullie goede inzet, jullie positiviteit en voor alle hulp. Ik hoop dat ik jullie genoeg heb kunnen leren tijdens jullie stage, ik heb zeker ook van jullie geleerd.

Jaqueline, bedankt voor de gezelligheid en alle goede zorg tijdens o.a. de EANM.

Ton, super bedankt voor alle tijd en moeite die jij hebt gestoken in het maken van de mooie lay-out van dit proefschrift.

Van de afdeling Pathologie wil ik Hans bedanken voor het altijd klaarstaan. Vooral het laatste jaar heb ik vaak een beroep op jou gedaan voor het snijden van weefsel en immunokleuringen, hetgeen soms in korte tijd moest gebeuren. Ook Angelique wil ik bedanken voor al haar harde werk v.w.b. de microdissectie van tumorcellen.

Van de afdeling Medische Oncologie wil ik Anieta, Vanja, Michele en Maxime bedanken. Anieta, bedankt voor alles wat je mij geleerd hebt over mRNA expressie levels en alles wat daarmee gepaard gaat. Het is begonnen met een simpel experiment in een aantal cellijnen en na een overleg over mijn PhD project mede

door jou enthousiasme en steun uitgegroeid tot 2 grote projecten die wij met ondersteuning van onder andere Vanja, Michele en Maxime met succes hebben afgerond. Maxime, wat is het fijn samenwerken met jou! Mijn vele vragen en de complexiteit van het project was jou nooit teveel en elk overleg luisterde je weer vol interesse naar mijn ideeën en bedacht je nieuwe manieren om de data zo goed mogelijk te analyseren. Bedankt voor alle goede gesprekken over het rondreizen in Amerika en mijn toekomst perspectieven. Ik voelde mij altijd weer gerustgesteld en geïnspireerd na onze gesprekken.

Ik wil ook Willemijne en Wouter bedanken voor de fijne samenwerking. Ik ben trots op de artikelen die uit de samenwerkingen zijn gekomen. Ik wens jullie beiden het allerbeste in het vervolg van jullie carrière.

I also want to thank the international collaborators I worked with. Thea Maina and Berthold Nock thank you for all the fruitful discussions and your critical feedback that led to improvement of our manuscripts. Prof. dr. Helmut Maecke, thanks for providing us with the SSTR antagonist and for reading my abstract and manuscript. Thanks to Francesca Orlandi and Maurizio Mariani and all others from Advanced Accelerator Applications I worked with on the NeoBOMB1 study. Thank you for giving me the opportunity to attend the SNMMI in San Diego to present the study and for the financial support to print this thesis.

Het afronden van dit proefschrift zou niet mogelijk zijn geweest zonder de steun van mijn familie en vrienden. Ik geloof dat je het beste uit jezelf kan halen als je leven in balans is. De liefde en vreugde die mijn familie en vrienden mij geven speelt een belangrijke rol in mijn balans. Stuk voor stuk zijn jullie allemaal heel waardevol voor mij. Omdat er zoveel van jullie zijn, zal ik niet allemaal bij naam noemen maar ik wil jullie wel allemaal bedanken. Janaina en Chevaly die altijd heel bezorgd zijn als ik lange dagen werk of een stressvolle periode heb, mijn vriendinnengroep van het VWO die elke keer weer vragen hoe het met de muisjes gaat ;-), mijn lieve familie in Suriname die altijd geïnteresseerd is in mijn werk. En zo verder.

Lieve mama, waar moet ik beginnen... Jij bent mijn inspiratie! In mijn ogen ben jij superwoman, je bent super sterk en je kan alles aan. Bedankt voor de geweldige opvoeding die je mij, Jean-Patrice en Saviella hebt gegeven. Je staat altijd voor mij klaar en kent mij door en door. De discipline, het perfectionisme en de gedrevenheid die ik heb, heb ik niet van een vreemde. Je bent mijn voorbeeld.

Ik wil ook Cees en Tea, mijn schoonouders, bedanken voor hun attentheid en interesse in mijn onderzoek. Het is altijd heel fijn om te horen hoe trots jullie vertellen aan vrienden wat voor werk ik doe. Bedankt voor het geloof en vertrouwen in mij.

Jean-Patrice en Saviëlla bedankt voor het zijn van een geweldige broer en zus. Priscilla, ook al is onze band pas de laatste jaren sterker geworden, ik kan me geen leven meer zonder jou en je gezin voorstellen. Dank je wel voor alle leuke momenten samen. Anne-Greet en Marjon, far in distance but near at heart, bedankt voor jullie belangstelling en liefde.

Thorsten, Cybelle, Alexander-Jay, Connor, Kyan en Joshua bedankt voor het zijn van de geweldige kinderen die jullie zijn. Ik ben een hele trotse tante. Jullie weten altijd een lach op mijn gezicht te toveren. Jullie geven mij de motivatie om mijn dromen na te streven omdat ik graag een voorbeeld voor jullie ben.

Lieve Sadie, ik hoop ook voor jou een goed voorbeeld te zijn. Bedankt voor de acceptatie en het deel uitmaken van mijn leven.

Mijn paranimfen, Ingrid en Alexander. Lieve Ingrid, niet alleen mijn collega maar inmiddels kan ik je ook een vriendin noemen, wat ga ik je missen als je co-schappen gaat lopen. Wij zijn zo verschillend maar op een gekke manier klikt het daarom juist heel goed. Je bent een mooi mens, blijf in jezelf geloven en heb vertrouwen in je kunnen. Bedankt voor het zijn van een top collega. De lange avonden werken waren vaak dragelijker omdat we het samen deden. Je staat altijd klaar om mij te helpen met figuren en plaatjes en de mooie omslag en lay-out van dit proefschrift heb ik dan ook aan jou te danken. We hebben samen de YIM in Wenen, de EANM in Lyon en Hamburg en de SNMMI in San Diego mogen meemaken, bedankt voor de leuke tijd die we daar hebben gehad en de ondersteuning tijdens mijn presentaties. We hebben de afgelopen jaren veel met elkaar gedeeld, wat ik als heel fijn heb ervaren.

Alexander... mijn grote liefde, mijn steun en toeverlaat, mijn rots! Bedankt voor alle begrip en geduld de afgelopen 4 jaren. Je weet inmiddels meer van preklinisch onderzoek en nucleaire geneeskunde dan je ooit wilde weten. Bedankt voor alle keren dat je naar mijn presentaties wilde luisteren, de keren dat jij mij hielp als ik weer eens ongeduldig was omdat mijn tabellen en figuren niet zo mooi waren als ik wilde, de keren dat je met mij wakker bleef om mij te steunen omdat ik een deadline had, de keren dat jij al het huishouden op je nam omdat ik wekenlang tot laat in de avond op het werk zat en zo kan ik nog even doorgaan. Ik kan niet in woorden beschrijven hoe dankbaar ik daarvoor ben. Wij zijn een top team en met jou aan mijn zij ben ik de gelukkigste vrouw op aarde.

Voor alle mensen die ik vergeten ben of niet expliciet genoemd heb, er zijn zoveel mensen die de afgelopen jaren een positieve rol hebben gespeeld in mijn werk maar ook in mijn prive leven en daar ben ik enorm dankbaar voor!

Oma, dit boekje draag ik op aan jou! Voor de jaren waarin je mij en de rest van de kleinkinderen verzorgd hebt, voor de geweldige vrouw die jij was, voor de onvoorwaardelijke liefde die je ons gegeven hebt. Jij was immers mijn inspiratie om dit werk te gaan doen. Je bent niet meer bij ons op aarde, maar je leeft voor altijd door in ons hart.